

THE BEHAVIOUR OF THE REINFORCED CONCRETE
FLAT PLATE STRUCTURES
SUBJECTED TO VARIOUS COMBINATIONS OF
VERTICAL AND HORIZONTAL LOADS

by

A. Tuğrul Tankut

A thesis submitted for the degree of
Doctor of Philosophy
in the Faculty of Engineering
of the University of London

Concrete Structures and Technology
Civil Engineering Department
Imperial College of Science and Technology
London

November, 1969

ABSTRACT

The behaviour of reinforced concrete flat plate structures, subjected to various combinations of vertical and horizontal loads, was studied. Being mainly experimental, the investigation consisted of (i) The development and the design of the instrumentation systems to obtain the appropriate information; (ii) the observation of the behaviour at various stages and under various load combinations, and (iii) the evaluation of the experimental data which resulted in a suggestion for a method of analysis applicable to the design of structures of this particular type.

Two large scale test structures, consisting of a 21 ft. x 21 ft. and 4 in. thick plate supported on nine columns spaced at 10 ft. centres, were designed, instrumented and tested. The studies of the behaviour of these two test structures concentrated on two main aspects of the problem:

- i. The general flexural behaviour of the test structure, under various load combinations,
- ii. The local behaviour of various types of slab-column connections, with particular reference to the punching shear strength problem.

For both of the above aspects, various methods of analysis are applied; and compared with the experimental findings. A number of conclusions are drawn from these comparisons as well as from the observations. Some suggestions are also made for further research on the subject.

ACKNOWLEDGEMENTS

The work described in this thesis was carried out in the Concrete Structures and Technology Section of Civil Engineering Department, Imperial College, under the supervision of Prof. A. L. L. Baker. The author is grateful to Prof. Baker for his valuable supervision and guidance.

The technical guidance and assistance as well as moral support, tolerance and patience practiced by Dr. C. W. Yu throughout the work are sincerely appreciated.

Thanks are due to Mr. J. Newman for his help concerning the concrete mix design and related problems, and for correcting the language mistakes in the first draft of the thesis.

The author wishes to acknowledge Dr. C. Çıray for his valuable suggestion of using a hydraulic device for deflection measurements which eventually led to the "Hydraulic Deflection Measurement System" used in the experiments.

Thanks are extended to Messrs. N. N. Anis and U. Nahhas for their co-operation. The former analysed the column regions of the test structures by the method he has developed, and the latter allowed the author to use his comprehensive computer programme for the inelastic analysis of framed structures.

The help and co-operation of the laboratory technicians, with special reference to Messrs. S. Finch and H. Wilson, are to be mentioned.

The work was sponsored by the Construction Industries Research and Information Association, and the author was awarded a fellowship by the Central Treaty Organization during the course of the investigation. Sincere thanks are due to both institutions for their generosity.

CONTENTS

	Page
Abstract	2
Acknowledgements	3
Contents	4
Figures	6
Tables	8
1. Introduction	9
2. Review of Previous Work	11
3. Philosophy of the Project	22
4. Design of the Test Structures	31
4.1. Structural Analysis	32
4.2. Reinforced Concrete Design	35
4.3. Yield Line Analysis	42
4.4. Punching Shear Analysis	42
5. Instrumentation and Materials	44
5.1. Loading System	44
5.2. Reaction Measurement System	45
5.2.1. Design of the Reaction Dynamometers	46
5.2.2. Calibration of the Reaction Dynamometers	49
Calibration Theory for the Complete Dynamometer.	52
Mechanics of Calibration	57
5.3. Deflection Measurement System	58
5.4. Strain Measurement System	63
5.5. Materials	70
5.5.1. Concrete	70
5.5.2. Steel	73
6. Testing Procedures and Resultant Behaviour of the Test Structures	75
6.1. Tests Conducted on the Test Structure 1	75
6.1.1. Test 0 : Complete Instrumentation Check	75
6.1.2. Test 1 : Panel by Panel Loading Test	77
6.1.3. Test 2 : Check for Validity of Superposition	77
6.1.4. Test 3 : Crack Pattern Formation Test.	80
6.1.5. Test 4 : Testing to Failure	80
6.1.6. Test 5 : Individual Column Test.	84

	Page
6.2. Discussion of the Performance of the Test Structure 1 and Revision of the Design of the Test Structure 2	85
6.3. Tests Conducted on the Test Structure 2	87
6.3.1. Test 1 : Crack Pattern Formation Test	87
6.3.2. Test 2 : Check for Validity of Superposition	88
6.3.3. Test 3 : Testing to Failure	88
6.3.4. Test 4 : Individual Column Test	89
7. Analysis of the Experimental Results	91
7.1. Flexural Analysis	91
7.1.1. Strip Beams and Their Use in Flexural Analysis	97
7.1.2. Determination of the Distribution of Moments	100
7.1.3. Frame Analysis	105
Moment Approach	109
Deflection Approach	118
7.1.4. Proposed Design Method	122
7.2. Punching Shear Analysis	124
7.2.1. Design Recommendations	137
7.3. Deflections and Crack Width	138
8. Conclusions and Recommendations for Further Research	141
8.1. Conclusions	141
8.1.1. Conclusions on the Flexural Behaviour	141
8.1.2. Conclusions on the Shear Behaviour	142
8.1.3. Conclusions on the Performance of the Instrumentation	143
8.2. Recommendations for Further Research	144
8.2.1. Recommendations Concerning the Frame Analysis	144
8.2.2. Other Aspects to Consider	145
References	146
Appendices	
1. Moment and Deflection Distributions	150
2. Details of the Strip Beams	182
3. Punching Shear Formulae	188
3.1. Generalized Form of Moe Equations	188
3.2. Formulae for ACI-ASCE Joint Committee 426 Method	193

FIGURES

	Page
Fig. 1 - Geometry Considered by Nichols	13
Fig. 2 - Hillerborg's Stress Discontinuity Lines	13
Fig. 3 - Stress Discontinuity Lines to Fit Reinforcement Bands	13
Fig. 4 - Plans Considered for the Test Structures	23
Fig. 5 - Loading History Diagrams for the Principal Tests only.	23
Fig. 6 - Geometry of the Test Structures	24
Fig. 7 - Analyses with and without Upper Columns.	25
Fig. 8 - Panel by Panel Loading Test	28
Fig. 9 - The Frames Elastically Analysed.	33
Fig.10 - Moment Distribution over the Frames.	34
Fig.11 - Division and Designation of the Reinforcement Strips	34
Fig.12 - Reinforcement Spacing in the Test Structures	41
Fig.13 - Column Reinforcement Details	43
Fig.14 - Yield Line Patterns Considered	43
Fig.15 - Geometry of the Reaction Dynamometer	47
Fig.16 - Circuit Diagram for the Reaction Dynamometer Leg	47
Fig.17 - Assembly Drawing for the Reaction Dynamometer.	50
Fig.18 - Reaction Dynamometer Calibration Details	55
Fig.19 - Typical Load - Strain relationship for the Legs	56
Fig.20 - Reaction Dynamometer Calibration Frame	56
Fig.21.- Reaction Dynamometer Calibration Positions	56
Fig.22 - Deflection Measurement Unit	60
Fig.23 - Typical Deflection Record	60
Fig.24 - Two-Way Clinometer	62
Fig.25 - Location of Strain Gauges on Reinforcement in x-direction	64
Fig.26 - Location of Strain Gauges on Reinforcement in y-direction	65
Fig.27 - Location of Strain Gauges on Reinforcement Along a Section	66
Fig.28 - Strain Gauge Slot Details.	66

	Page
Fig. 29 - Location of Surface Strain Gauges on the Test Structure 1	68
Fig. 30 - Location of Surface Strain Gauges on the Test Structure 2	69
Fig. 31 - General View During the Casting Operation	71
Fig. 32 - General View of the Reinforcement Prior to Casting. . .	72
Fig. 33 - Applied Loading History Diagrams	76
Fig. 34 - Points Considered and Detailed Comparison Table	78
Fig. 35 - Supporting Frame for a Failed Column	83
Fig. 36 - Corrections for Column Reactions	83
Fig. 37 - Configurations for Individual Column Test	86
Fig. 38 - Data Analysis Scheme	92
Fig. 39 - Equal Deflection Contours for 2/31/13	94
Fig. 40 - Crack Patterns for the Test Structure 1	95
Fig. 41 - Crack Patterns for the Test Structure 2	96
Fig. 42 - Instrumentation of the Strip Beam	98
Fig. 43 - General View of the Strip Beam Testing Rig	98
Fig. 44 - Deflection Under Uniform Moment	98
Fig. 45 - Location of Demec Lines	98
Fig. 46 - Typical Moment-Steel Strain Relationship.	102
Fig. 47 - Variable Effective Beam Width	102
Fig. 48 - Equal M_x -contours for 2/31/13	103
Fig. 49 - Equal M_y -contours for 2/31/13	104
Fig. 50 - Variation of Flexural Rigidity.	108
Fig. 51 - Critical Sections for Frame Analysis.	110
Fig. 52 - Torsional Stress Transferring Sections.	117
Fig. 53 - Critical Sections for Uneven Loading.	117
Fig. 54 - Mid-panel deflections	120
Fig. 55 - Typical Internal Column Punching Cone	125
Fig. 56 - Typical Edge Column Punching Cone	126
Fig. 57 - Typical Corner Column Punching Cone	127
Fig. 58 - Idealized Load Deflection Relationship.	139
Figs. 59 to 87 - Equal Moment and Deflection Contours	153-181
Fig. 88 - Preliminary Strip Beams	183
Fig. 89 - Strip Beams Accompanying the Test Structure 1	184
Fig. 90 - Strip Beams Accompanying the Test Structure 2	185
Fig. 91 - Typical Flexural Relationships for Strip Beams (PB21) .	186
Fig. 92 - Critical Sections for Moe Method	190
Fig. 93 - Critical Sections for ACI-ASCE Joint Committee 426 Method	190

TABLES

	Page
Table 1 - Design Moments for the Reinforcement Strips	37
Table 2 - Reinforcement Computation for the Test Structure 1. . .	38
Table 3 - Reinforcement Computations for the Test Structure 2 . .	39
Table 4 - Measured Quantities to be Compared	78
Table 5 - "Panel by Panel Loading Test" Comparison Table	79
Table 6 - Comparison Table for "Check for Validity of Superposition Test"	81
Table 7 - Various Combinations of States of Cracking.	102
Table 8 - Experimental Values of Critical Moments	111
Table 9 - Variation of Critical Moments for the Test Structure 1.	112
Table 10 - Variation of Critical Moments for the Test Structure 2.	113
Table 11 - Sums of Squares of Differences for the Test Structure 1.	115
Table 12 - Sums of Squares of Differences for the Test Structure 2.	116
Table 13 - Variation of Critical Moments for Uneven Loading . . .	119
Table 14 - Sums of Squares of Differences for Uneven Loading. . .	119
Table 15 - Calculated Mid-panel Deflections	121
Table 16 - Design Coefficients for Variable Effective Beam Width.	123
Table 17 - Calculated and Measured Column Reactions	133
Table 18 - Apparent Load Factors.	134
Table 19 - Actual Load Factors	135
Table 20 - Results of Equilibrium and Compatibility Analysis. . .	136
Table 21 - Average V_p/\bar{V}_d Values	136
Table 22 - Column reactions for the Test Structure 1	151
Table 23 - Column Reactions for the Test Structure 2	152
Table 24 - Strip Beam Moment-Steel Strain Relationships	187
Table 25 - Expressions Required for ACI-ASCE Joint Committee 426 Method	194

C H A P T E R 1

INTRODUCTION

Flat Slab type structures consist of reinforced or prestressed floor slabs supported (without the aid of intermediate load transferring members, namely beams) by columns which may or may not have enlarged connections such as column capitals or drop panels. In design, such external stiffeners can sometimes be eliminated when the loads are relatively moderate; or in other words, they can be hidden in the column or in the slab. The resulting structure is called a FLAT PLATE. This is the particular type with which the present work is mainly concerned.

Flat Plate structures are being used more and more, mainly because of the architectural advantages they offer. Some of these structures do not have a structural core to provide stability. This type of structure must be designed to resist horizontal loads due to wind or earthquakes.

The majority of the work done on flat plate structures so far, is mainly concerned with the relatively simple case of internal panels under vertical load only. Therefore, the design of this type of structure, subjected to vertical load alone, can be carried out quite satisfactorily by various methods.

One of the most common methods of analysis is to consider the structure to be divided longitudinally and transversely into frames consisting of a row of columns and strips of slab between the panel centre-lines acting as beams. This method, without sufficient experimental evidence for its justification, is being used in practice, especially when the structure has to be designed for combined load.

The present investigation was planned to obtain information in this respect.

Two structures were tested. The choice of size, shape etc. of these test structures will be discussed later. After considering the time and facilities available, the following objectives were aimed for:

- i. The distribution of moments in two perpendicular directions at various stages of combined loading, to assess the way in which the structure resists the load.

- ii. The deflected shape at various stages of testing. This information together with that obtained from (i) will indicate the performance of the test structure under design load.
- iii. The crack pattern recorded from stage to stage, to see how realistic is the yield line analysis.
- iv. The strain, deformation and crack patterns near column regions, to investigate the behaviour of the connection with special regard to shear.
- v. Any possible recommendations for future codes of practice, to give a more realistic design procedure for this type of structure under combined loading.

Various aspects of the investigation are presented in this thesis in the following order:

Chapter 2 is devoted to the review of previous work on related subjects. This work is placed in two main categories; (i) work which deals with the flexural behaviour of flat plate type structures, and (ii) that which deals with the problem of punching shear strength of slabs.

In Chapter 3, the principles governing the design and the planning of the investigation are explained and discussed. The next chapter simply presents the design of the test structures. The highly sophisticated experimental side of the investigation required rather complicated systems of instrumentation. These systems as well as the materials used, are discussed in Chapter 5.

Chapter 6 explains the tests carried out on each test structure and the performance of the test structures during these tests. The chapter following is the backbone of the whole work. The methods of analysis of the experimental results are explained and discussed, and the proposed design methods are presented.

Chapter 8 is the closing chapter where the conclusions, drawn during the course of the work on various aspects of the problem, are listed. It is furthermore explained in that chapter that the present work is by no means the end of research on the subject, but it is just a modest start, and for further research some interesting avenues to explore are pointed out.

The text is followed by three appendices which may be useful for the interested reader, although they have been considered of secondary importance as far as the main text was concerned.

CHAPTER 2REVIEW OF PREVIOUS WORK

The following paragraph is quoted from Ref. 1:

"Centuries of construction with stone and timber preceded reinforced concrete. Consequently, just as the first motor cars were built to look like the horse-drawn carriages, the first reinforced concrete systems were conceived in the image of traditional types. In a timber structure, the planks carried the load to the joists, the joists to the girders, and the girders to the columns; so must they in a reinforced concrete structure. Hence the flat slab had to be invented rather than developed as one of the obvious applications of reinforced concrete."

So, the flat slab was treated as an invention when it was originated by C.A.P. Turner in 1902. Some engineers savagely resisted the idea while others were blindly in favour. Following the first flat slab built by Turner in 1906, many such structures came into existence, designed purely on the basis of the practical experience of the designer and the results of a few tests carried out on some of the existing flat slabs. These tests generally indicated much lower moments than would have been expected in corresponding slab and beam type structures. This fact caused a good deal of speculation in favour of the flat slab. However, the more conservative designers were not satisfied with the evidence produced, and they thought that the flat slab should still be designed to the conventional statical requirements. In 1910, A.B. McMillan illustrated the wild variation of the results of the various design methods, by comparing the amounts of reinforcement required for a certain practical case, by each of the known methods. The comparison dramatically showed 400 percent variation.

This controversy went on and on until Westergaard and Slater² published their comprehensive paper in 1921.

In 1914, J.R. Nichols³ suggested the following simple and straightforward analysis which formed the basis for most of the present codes of practice. For the case of an infinite number of uniformly loaded panels, he pointed out that the equilibrium conditions for one half of the panel indicate that the sum of positive and negative moments must be equal

to the total static moment. That is,

$$M_p + M_n = M_o = \frac{L_1 L_2 q}{2} \cdot \frac{L_1}{4} \dots \dots \dots (1)$$

where, M_p = total moment along panel centreline

M_n = total moment along column centreline

L_1 and L_2 = panel dimensions

q = uniform load per unit area

When the plate is supported on circular column heads of diameter D , the reaction can be assumed uniform around the periphery of the column head. Then for the geometry illustrated in Fig. 1, ignoring the twisting moments, Eq. 1 becomes

$$M_o = \frac{qL_2}{8} \left[L_1^2 + \frac{D^3}{3L_2} - \frac{4L_1 D}{\pi} \right] \dots \dots \dots (2)$$

For the usual dimensions used in flat slab structures Eq. 2 can be approximated closely by,

$$M_o = \frac{qL_2}{8} \left[L_1 - \frac{2D}{3} \right]^2 \dots \dots \dots (3)$$

This analysis was severely criticised by Turner and others for not taking into consideration the effect of the plate action.

This point is taken into account by the codes of practice, simply by changing the coefficient $\frac{1}{8}$ to $\frac{1}{10}$, 0.09 or 0.09F (F being $1.15 - \frac{D}{L}$, but not less than 1), without a comprehensive treatment. The question of justification for such a disregard of the considerations of statics, is discussed in detail by R. Taylor⁴.

Nichols' analysis could establish a basis for estimating the total static moment, but its distribution was not determined. The major work in this connection was published in 1921, by H.M. Westergaard and W.A. Slater². One of the main points shown in the above paper was the fact that the method previously used to calculate the moments from measured strains, was misleading. The linear moment-steel strain relationship which had been

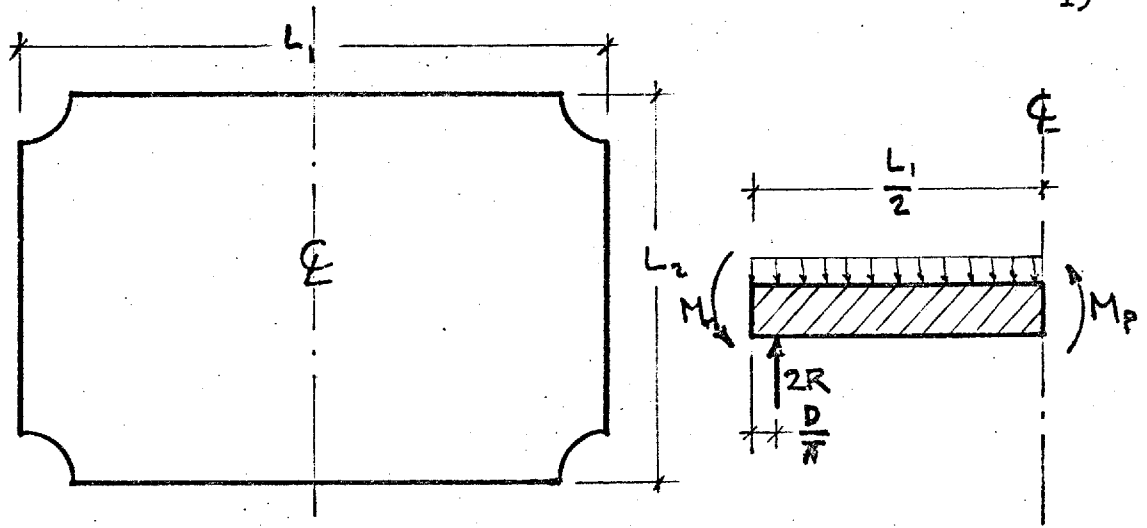


FIG. 1 - GEOMETRY CONSIDERED BY NICHOLS

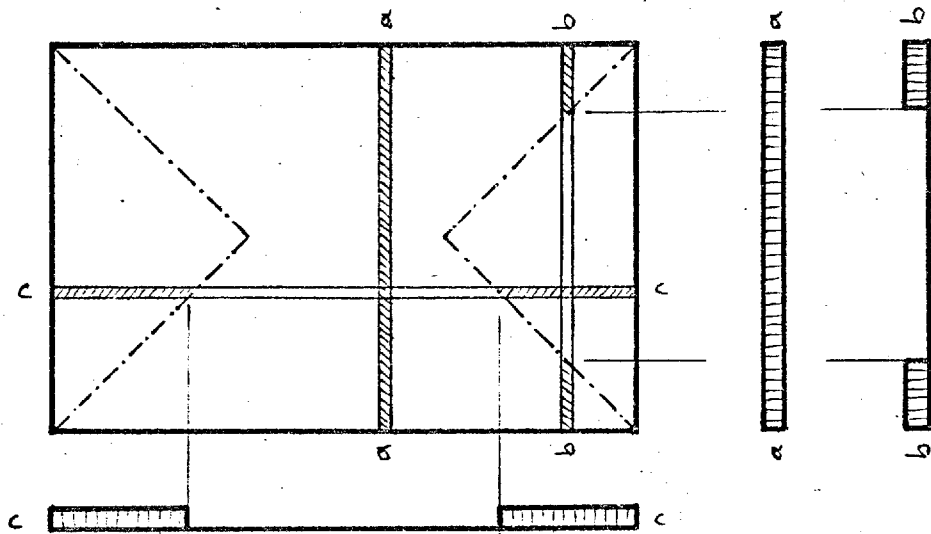


FIG. 2 - HILLERBORG'S STRESS DISCONTINUITY LINES

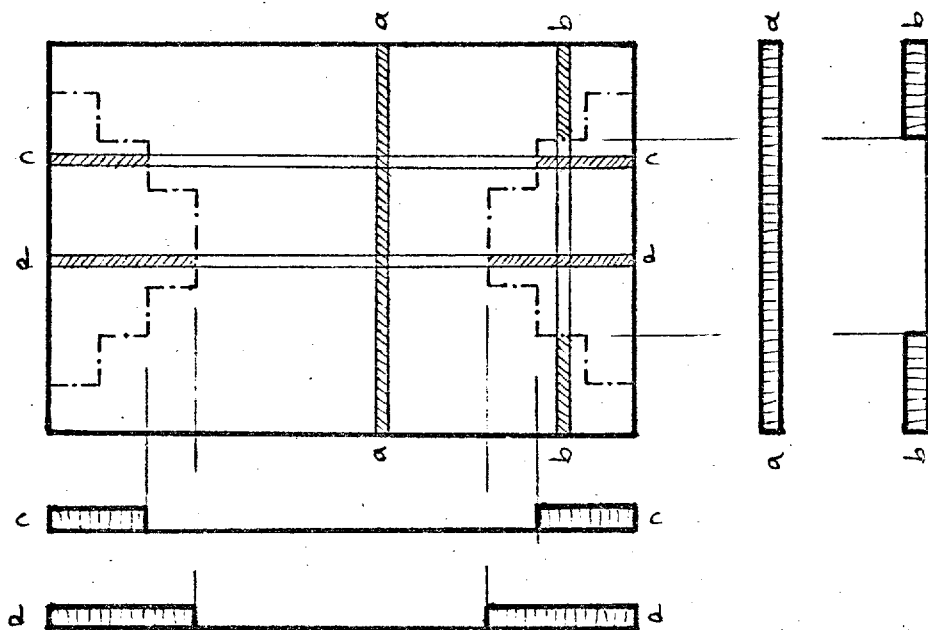


FIG. 3 - STRESS DISCONTINUITY LINES TO FIT REINFORCEMENT BANDS

used previously, gave only a fraction of the actual moment applied. This discrepancy was greatest in the pre-cracking zone and just after. This was the case in most of the previous tests since all the measurements were taken on real structures which could not be tested to loads far beyond cracking.⁽⁺⁾

On the other hand, Westergaard established a theoretical analysis to calculate the distribution of positive and negative moments throughout the slab when considered as an isotropic plate. His solution was checked by Slater by tests on reinforced concrete flat slabs. Their overall conclusion was that Nichols' analysis was in general sufficiently close to the experimental results; however, there were some indications that flat slabs had greater strength than expected.

With this information, the distribution coefficients were formulated, in the codes of practice, for the positive and negative moments at the column and the middle strips.

For the following forty years, various aspects of the flat slab were treated in a predominantly mathematical manner. Both V. Lewe and A. Nadai dealt with the problem of the deflection of an internal panel of an infinite slab on point supports, loaded with uniformly distributed vertical load, in a combined form of algebraic, trigonometric and hyperbolic series. The case of finite column area was studied by S. Woinowsky-Krieger, K. Frey as well as V. Lewe. But H. Marcus' numerical approach to these problems was more practical. The theory developed and published by J.E. Brothie in 1957, was more general and claimed to be applicable to any geometry with any type of loading and with any degree of fixity between slab and column. In this rather new and interesting approach, the slab was considered floating on a fictitious fluid of a density related to the stiffness of the slab. The solution which was in form of a Bessel function was given as influence coefficients in tabular form. Later, the ever increasing use of the computer encouraged the numerical approach to the problem. In this connection, A. Ang in 1959 developed a distribution procedure applying Newmark's plate analog concept, for the analysis of continuous rectangular flat slabs. At Imperial College, H.C. Chan⁵ studied the cases of one-panel, four-panels and infinite slabs on point supports and with finite column area, by finite difference method. Furthermore, he tested a full size one-panel flat plate and observed its behaviour under combined load, in support of his numerical work.

(+) Discussed in detail in Chapter 7.

In the early sixties, a comprehensive experimental investigation of this type of structure was carried out at the University of Illinois. G.T.Mayes, D.S.Hatcher and J.O.Jirsa under Professors M.A.Sözen and C.P.Siess each tested a quarter scale model of a nine-panel reinforced concrete flat slab floor. Different slab types were studied with each of these models; namely flat plate, flat slab, and one reinforced with welded wire mesh. The results obtained confirmed that the total moment in a panel can reasonably be estimated by Nichols' formula, and that the ultimate strength can closely be predicted by the yield line theory^{6,7,8}.

An interesting design approach for slabs in general was introduced by A. Hillerborg in 1960. Its appeal to the designer lies in its simplicity and accuracy, and the freedom of choice it provides in placing the reinforcement. The basic idea is to deliberately make the directions of reinforcement coincide with the principal moment directions in order to simplify the general equilibrium equation

$$\frac{\partial^2 M_x}{\partial x^2} + \frac{\partial^2 M_y}{\partial y^2} - 2 \frac{\partial^2 M_{xy}}{\partial x \partial y} = -p$$

into $\frac{\partial^2 M_x}{\partial x^2} = -\alpha p$ and

$$\frac{\partial^2 M_y}{\partial y^2} = -(1 - \alpha) p$$

where α is the proportion of load taken in strips in the x - direction, and $(1 - \alpha)$ in the y - direction. The value of α is taken to be either 0 or 1, in various regions formed by introducing lines of stress discontinuity chosen arbitrarily. This choice is in most cases guided by the elastic design experience of the designer. The application is illustrated in Fig. 2, by the loads to be considered in the design of each individual strip. Since the lines of stress discontinuity are arbitrarily chosen, it was suggested by R.H.Wood and G.S.T.Armer³⁹ that these lines can be chosen to fit the reinforcing bands (Fig. 3).

In the original form, this strip method was not applicable to the design of flat slabs. Later in 1964, Hillerborg published an advanced

strip method which treats in particular the case of slab supported on columns. In addition to the two types of elements considered in the simple strip method, another type of element is introduced; rectangular element dispersing load in two directions and supported at one corner. It is assumed to have no shear along its edges so that the moments acting along the edges can be considered maximum. The load on the element is assumed to be carried by complicated system of strips to the column at one corner. R.H.Wood and G.S.T.Armer⁹ very closely studied the method, and then stated that in spite of the fact that it requires violent discontinuities, the patterns of reinforcement it produces, are very satisfactory and reasonable.

The method was critically examined by Wood and Armer, and somewhat simpler alternatives for the design of flat slabs were suggested.

The work mentioned so far has been mainly concerned with the flexural behaviour of the flat slab, very little, if any, reference has been made to the problems of shear involved in the design of this type of structure. However, shear strength is a very critical, if not the most critical, aspect of the problem. In addition, it is the least known, and probably the most controversial.

The shear strength of slabs should have been a problem of interest even before the introduction of the concept of the flat slab, since it was involved in the design of reinforced concrete wall and column footings. But curiously enough, there is not a single investigation of the problem, reported before 1913, when A.N.Talbot⁹ published the results of his experimental investigation on wall and column footings. He computed the maximum shear stress v , caused by a loaded square area, using the formula,

$$v = \frac{V}{4(r + 2d_1)jd_1} \dots \dots \dots (4)$$

where V = shear force,

r = side length of loaded area,

d_1 = effective depth,

jd_1 = moment arm.

He also observed that the flexural reinforcement had some effect on the shear strength.

Later, O.Graf¹⁰ studied the problem. He used the formula,

$$v = \frac{V}{4rt} \dots \dots \dots (5)$$

where t = total thickness of the slab.

Although he suggested that the flexural cracking might have some influence on the shear strength, his formula implicitly indicated, by considering the total thickness instead of the effective depth, that this influence was not particularly significant. This view was somewhat supported by F.H.Sayani¹¹ of Imperial College in 1968. He studied the shear strength of beams with axial tension, and concluded that axial tension and therefore cracking did not have a significant effect on the shear strength within the practical range of loading, where interlocking of the aggregate could transfer the shearing stresses.

Another variation was suggested in 1946, by C. Forsell and A.Homberg. Assuming parabolic shear stress distribution, they employed the formula,

$$v = \frac{1.5V}{bt} \dots \dots \dots (6)$$

where b = length of critical section taken at a distance of $t/2$ from the edges of the loaded area.

In 1948, F.E.Richart published the results of his investigation on reinforced concrete footings. Later in 1953, E. Hognestad¹² re-evaluated the shear failures of footings reported by Richart to develop an ultimate shear stress formula in which he introduced the ratio

$$\phi_o = V_{\text{test}}/V_{\text{flex}}$$

Within the range of available information, he suggested the following expression for the ultimate shear strength,

$$\bar{v} = (0.035 + \frac{0.07}{\phi_o}) f'_c + 130 \text{ psi} \dots \dots \dots (7)$$

On the other hand, he thought that the maximum shear stress should be evaluated at the edge of the loaded area by,

$$\bar{v} = \frac{V}{\frac{7}{8} bd_1} \dots \dots \dots (8)$$

After testing a variety of slabs failing in shear, in co-operation with R.C.Hlstner¹³, he modified the ultimate shear strength equation into the following simpler form,

$$\bar{v} = 333 \text{ psi} + 0.046 f'_c / \phi_c \dots \dots \dots (9)$$

for slabs without shear reinforcement, and introduced,

$$\bar{v} = 333 \text{ psi} + 0.046 f'_c / \phi_o + \left(\frac{A_v f_y \sin \theta}{\frac{7}{8} bdf'_c} - 0.05 \right) f'_c \dots (10)$$

for slabs with shear reinforcement. These suggestions were accompanied by some rather disturbing conclusions. They found no effect on the ultimate shear strength due to concentration of the flexural reinforcement under the column. What is even more interesting; according to their results the eccentricity of the applied load did not seem to have any influence on the ultimate shear strength. (+)

In 1957, C.S.Whitney¹⁴ presented an ultimate shear strength theory with emphasis on the contribution of the ultimate resisting moment of the slab per unit width inside the "pyramid of rupture" which he defined as a frustrum of a cone or pyramid formed by 45° surfaces sloping from the column face. On the basis of analysis of previously reported data, he suggested the following ultimate shear strength expression,

$$\bar{v} = 100 \text{ psi} + 0.75 \frac{m_u}{d_1^2} \sqrt{\frac{d_1}{\phi_s}} \dots \dots \dots (11)$$

(+) The results of the present investigation contradict these conclusions. In Chapter 7, the problem is treated in detail.

where m_u = ultimate resisting moment of the slab per unit width, and
 l_s = shear span.

An entirely new approach to the problem of punching was developed by the Swedish school of thought, represented by H.Nylander, S.Kinnunen and J.L.Andersson^{15, 16, 17}. The "Compressed Conical Shell" concept was introduced by Nylander and Kinnunen¹⁵ in 1960. They established a theory for estimating the ultimate punching load by considering the equilibrium of this cone acted upon by the external forces and the stresses in the reinforcement and in the concrete. Various aspects of the problem, such as different types of flexural reinforcement and cases with shear reinforcement were studied (Ref. 16, 17) on the same basis. The shell concept is obviously not applicable to edge and corner columns where a closed ring can not be formed. So, Andersson¹⁸ abandoned the idea when he investigated the behaviour of edge columns in 1966, and developed another approach based on the superposition of torsional and direct shear stresses.

One of the recent major studies of the subject was published by J.Moe¹⁹ in 1961. His stress equation has the conventional general form of,

$$v = \frac{P}{bd_1} + \frac{\beta M}{W} \dots \dots \dots (12)$$

where β = coefficient defining the amount of external moment carried by internal shearing stresses, and

W = modulus of the resisting section at the face of the column.

The crucial contribution of the work is the ultimate shear strength equation which directly takes into consideration the effect of flexural reinforcement through the term V_{flex} . Based on the statistical analysis of information from his own tests and from some of the previously reported tests, he derived the expression,

$$\bar{v} = \frac{15 (1 - 0.075 \frac{r}{d_1})}{1 + 5.25 \frac{bd_1 \sqrt{f'_c}}{V_{flex}}} \cdot \sqrt{f'_c} \dots \dots \dots (13)$$

where V_{flex} has the same meaning defined by Hognestad, that is "the shear force at ultimate flexural capacity of the slab". However this term V_{flex} has continually been a source of controversy. It is easier to define than to calculate in actual cases, since various methods and assumptions may lead to a wide range of variation. The method is claimed to be applicable to edge and corner columns as well as internal ones⁽⁺⁾; but the results of the present work indicate that, for the cases of edge and corner columns, it is hopelessly unrealistic. Nevertheless, this situation may, to some extent, be explained by the manner in which V_{flex} was calculated; a different method might have given slightly more reasonable results. It was preferred to keep the same assumptions and the same method (Yield Line Theory) for all the cases treated. These and some other considerations make one tend to question the validity of Moe's ultimate shear strength equation. The same opinion can be traced in the report³⁵ of ACI-ASCE Joint Committee 326 (later 426) published in 1962. Although Moe's work was thoroughly considered in the above report, the simple form (from ACI 1956 Code),

$$\bar{v} = 4 \sqrt{f'_c} \dots \dots \dots (14)$$

of ultimate shear strength expression was recommended for design.

In a paper published in 1966, D.Yitzhaki²⁰ presented a different approach to establish a correlation between punching resistance and flexural strength. The effects of r/d_1 ratio and of the reinforcement strength pf_y on the punching strength were introduced by linear independent multipliers,

$$P_{pun} = 8(1 - \frac{q}{2}) d_1^2 (149.3 + 0.164 pf_y)(1 + \frac{r}{2d_1}) \dots \dots \dots (15)$$

where p = percentage of reinforcement, and

$$q = p \cdot \frac{f_{sy}}{f_{cu}}$$

(+) The information obtained in the present investigation was evaluated with the method suggested, and the results obtained were compared with experimental results in Chapter 7.

N.W.Hanson and J.M.Hanson²¹ reviewed the recent methods, in the light of their own tests, with special reference to the work of Moe and of the ACI-ASCE Joint Committee, from an interaction relationship point of view. They arrived at the conclusion that the ultimate strength design method recommended by ACI-ASCE Joint Committee 426, could give a good prediction of the strength of the slab-column connection if the moment reduction factor K was changed from 0.2 (original recommendation) to 0.4.

A theoretical method of analysis was suggested in 1967, by A.E.Long and D.Bond for the calculation of the punching load of flat slab structures with two-way flexural reinforcement and no shear reinforcement. The method is based on elastic thin plate theory considering a biaxial state of stress of concrete. An octahedral shear stress criterion of failure is used to find the failure stresses. Since the structural element is assumed to be elastic throughout, the approach is not entirely satisfactory method of analysis. Also, it does not have much value as a design tool being restricted only to the internal columns with axial load, and being rather complicated and impractical.

The latest work on the subject is being finalised by N.N.Anis and C.W.Yu²² at Imperial College. Their approach is directed towards a better understanding of the actual process of punching. Employing the "conical shell" concept, they have developed a theory on the basis of equilibrium and compatibility conditions. Some of the data obtained in the present investigation was evaluated using the above method and the results obtained are presented in Chapter 7.

As can easily be seen from the review of previous work, most of the research related to both principle aspects of the flat plate behaviour was conducted on either small scale or individual models. There are very few large scale complete prototypes tested. On none of these prototypes was the effect of horizontal loading systematically studied. Therefore, the need for a series of experimental investigations into the behaviour of flat slab type structures is quite obvious. This kind of work at the Imperial College was started by C.H.Chan who tested a large scale one panel flat plate. The present investigation can be considered as forming the next stage including two large scale four panel flat plate structures tested under various combinations of vertical and horizontal loading.

CHAPTER 3

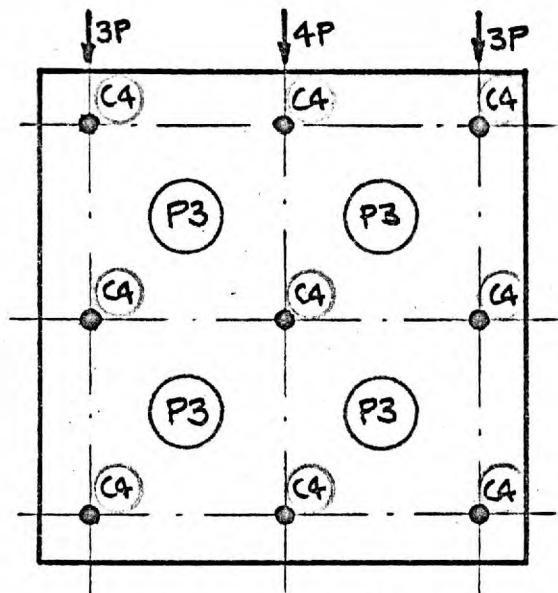
PHILOSOPHY OF THE PROJECT

The whole research project was based on the principle of constructing and testing structures to represent practical cases as realistically as possible. To this end, an attempt was made to choose the largest possible number of test structures to the largest possible scale and with the most realistic shape and dimensions, within the limitations of time, space and facilities available.

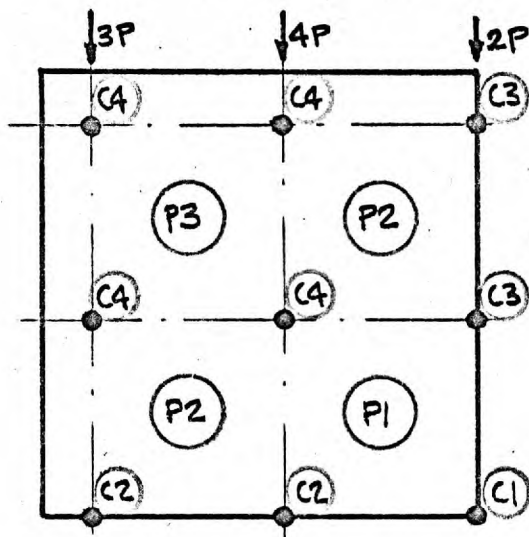
Considering the financial resources, the size of the project and the time required, it seemed reasonable to test two structures each consisting of four panels. Four panels were chosen since this is the minimum number of panels which can provide a number of combinations of various types of columns and panels. Three of these combinations (Fig.4) were considered. As this is one of the pilot research projects in the field, the one with the simplest geometry and symmetry (Fig.4C) was chosen.

Having decided on the number of panels, their size was determined solely by the space available in the laboratory which allowed a maximum size of 21 ft. x 21 ft., i.e. 10 ft. centre-to-centre column spacing. In practice a 20 ft. span length is quite common for this kind of structure. The test structures can thus be considered to represent common practical structures to approximately half scale. Therefore, all the dimensions and the load combinations were chosen accordingly. The test structures were intended to represent the third floor of a ten-storey building of common shape and dimensions, carrying 200 psf uniformly distributed vertical load, and 19 plf wind load which are the recommended values given by CP3,V. The final geometry of the test structures thus obtained is illustrated in Fig. 6. Considerations of the point of contraflexure being at mid-height and the intended scale of the test structures, would allow the 12 ft. high columns normally found in practice to be reduced to 3 ft. However, this latter dimension was further reduced by 2, so that the resultant relative stiffness ratio used in the equivalent frame method was similar to that of the actual structure considered. The results of the analysis (Fig. 7) show that this assumption is quite reasonable.

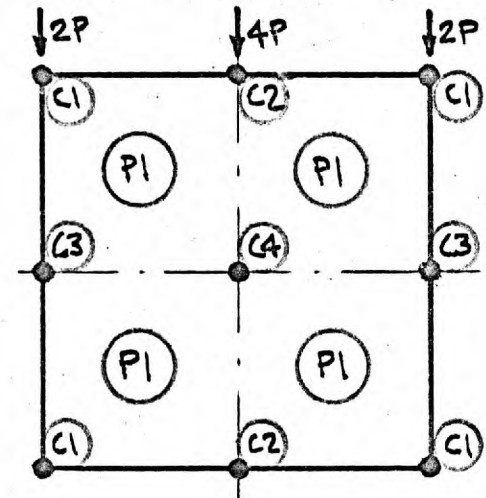
The choice of column sizes presented some difficulty. Due to the lack of a reliable method for assessing the shear strength of columns, the



a. SUGGESTION A (1,1)

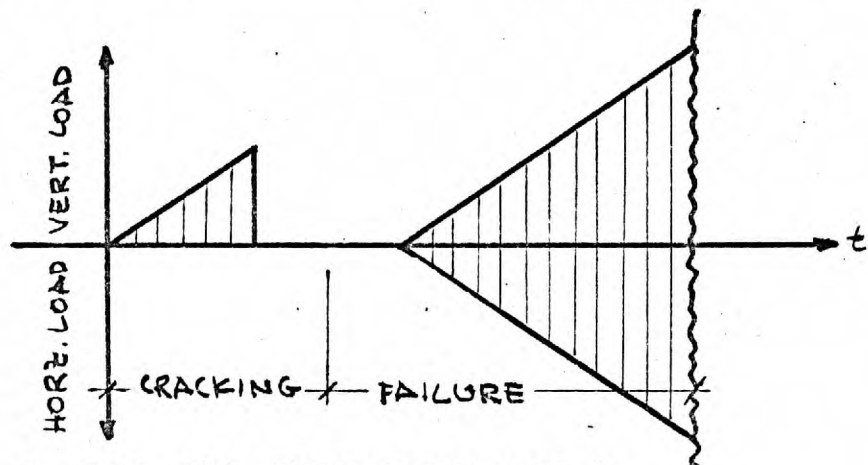


b. SUGGESTION B (3,4)

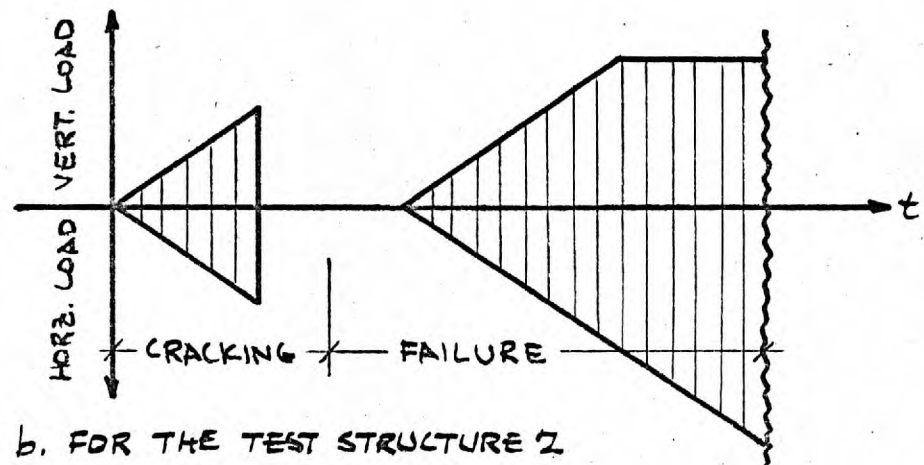


c. SUGGESTION C (1,4)

FIG. 4 - PLANS CONSIDERED FOR THE TEST STRUCTURES

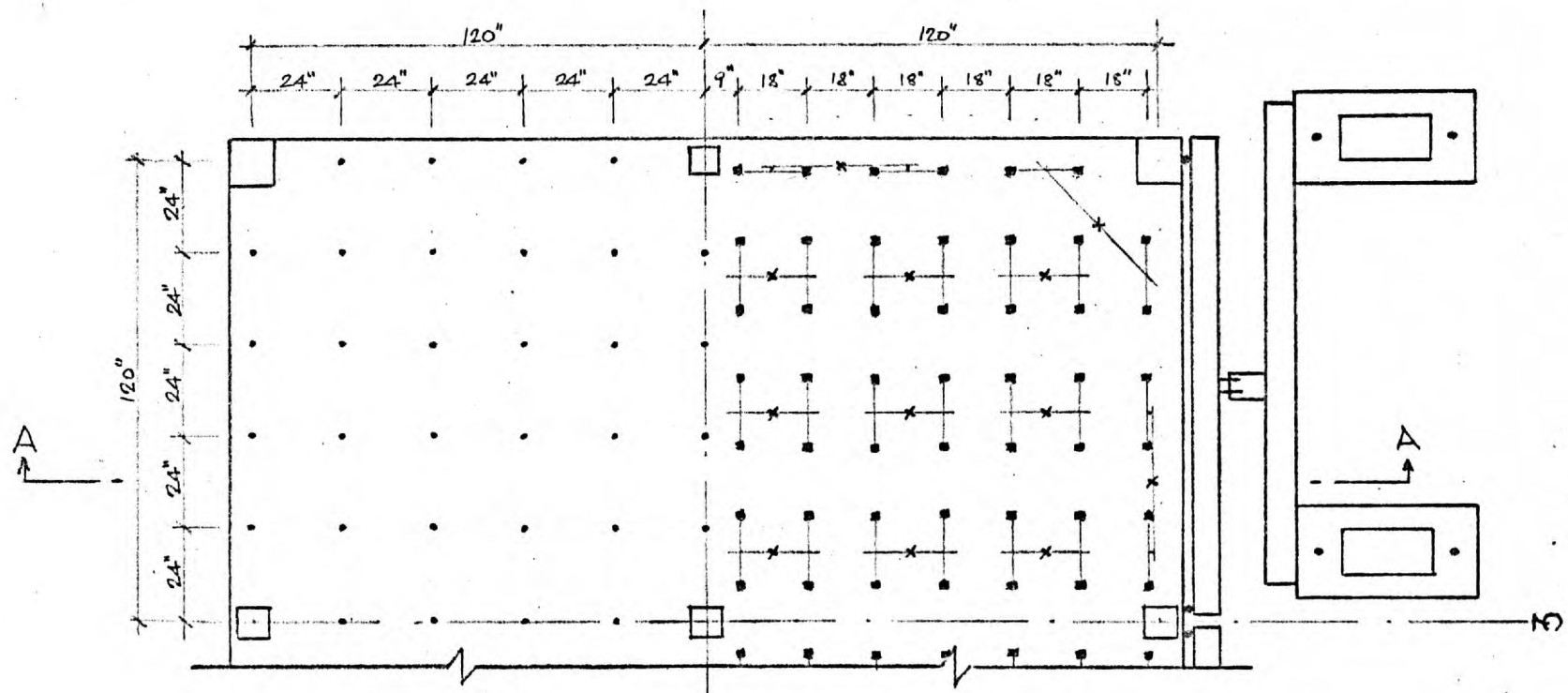


a. FOR THE TEST STRUCTURE 1

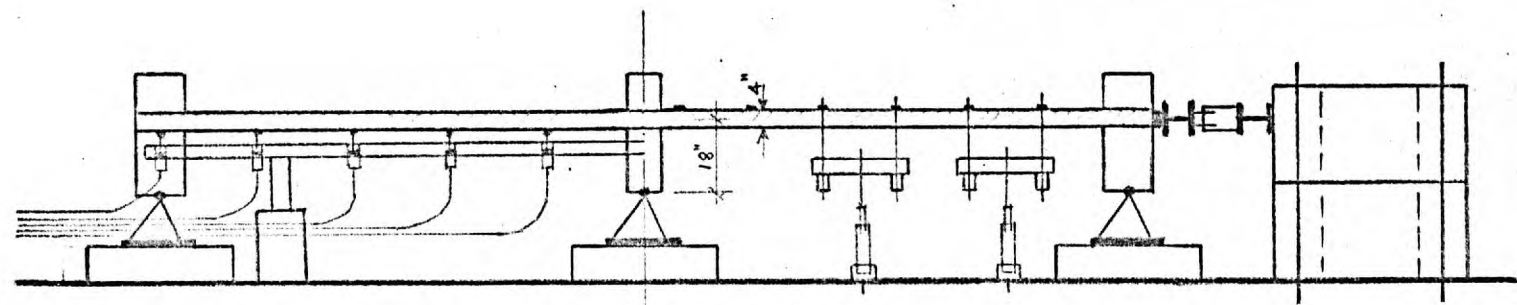


b. FOR THE TEST STRUCTURE 2

FIG. 5 - LOADING HISTORY DIAGRAMS FOR THE PRINCIPAL TESTS ONLY



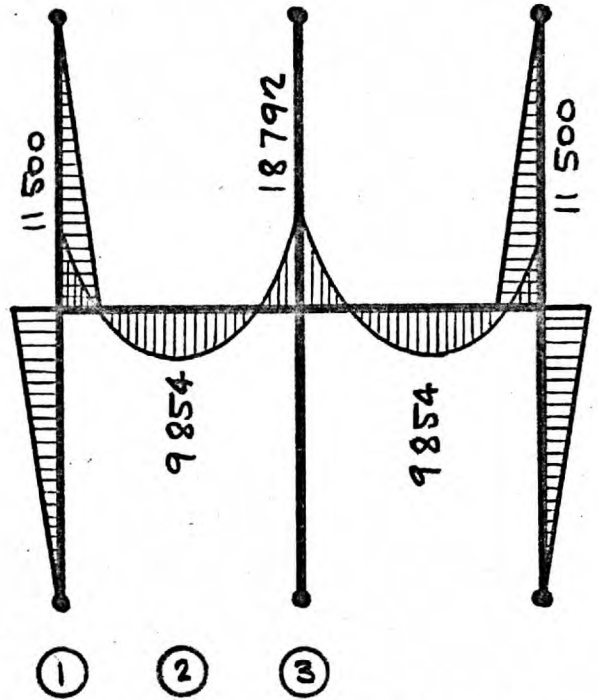
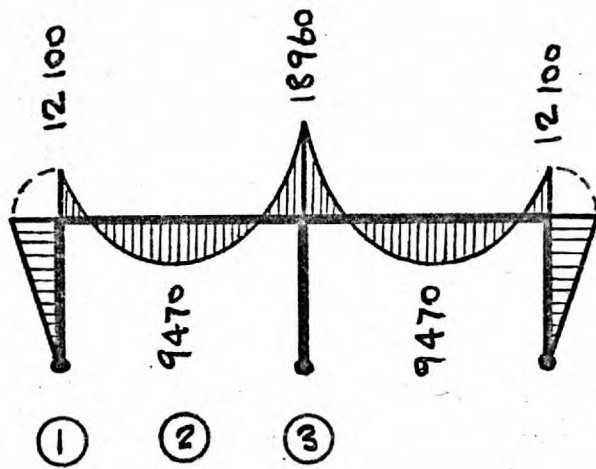
PLAN (S: 1/48)



A-A CROSS-SECTION (S: 1/48)

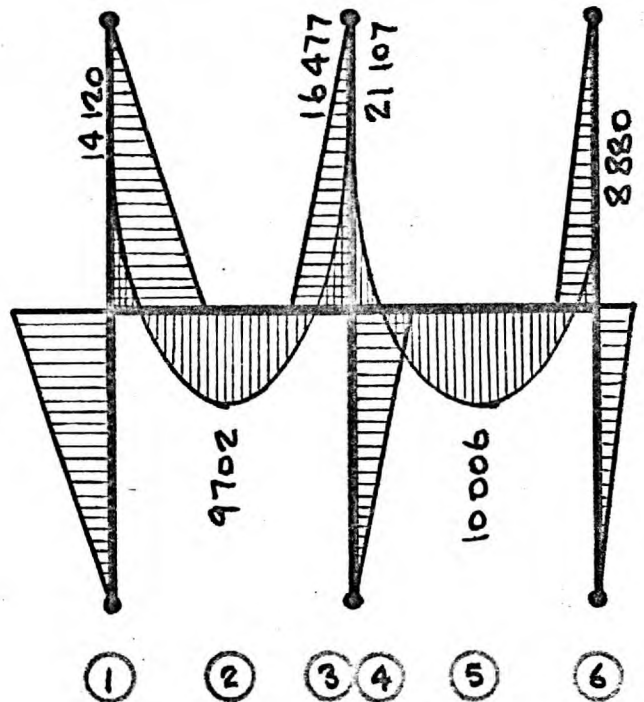
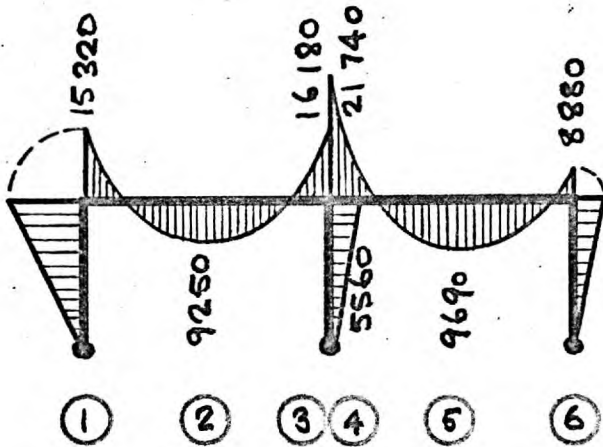
FIG. 6 - GEOMETRY OF THE TEST STRUCTURES SHOWING THE LOADING AND DEFLECTION MEASUREMENT SYSTEMS

FRAME F2



DIFFERENCES: $d_1 = 5.2\%$; $d_2 = 3.9\%$; $d_3 = 0.9\%$

FRAME F4



DIFFERENCES: $d_1 = 7.8\%$; $d_2 = 4.6\%$; $d_3 = 1.8\%$
 $d_4 = 3.0\%$; $d_5 = 3.1\%$; $d_6 = 0$

FIG. 7. COMPARISON OF ANALYSES WITH AND WITHOUT UPPER COLUMNS

British Code of Practice, CP 114 method was used as a guide. Other methods of analysis such as ACI and Moe's methods were then applied to check the shear strength of all columns. As a result, a larger size (12 in. x 12 in.) was chosen for corner columns, while the others were 8 in. x 8 in., in the hope that all columns would have a similar shear strength.

It is appreciated that it was impossible to ensure that the test structures would have the same strength in shear as in flexure. However investigation by all known applicable methods indicated that the test structures would be slightly weaker in shear than in flexure. This was the desired combination since the information required for studying the flexural performance can be obtained without failing the structure completely. On the other hand, information in respect of shear can only be obtained by complete failure of column regions.

Since the number of test structures has been limited to two as discussed above, the number and sequence of tests to be carried out on each test structure were very carefully studied. The object of the exercise is to investigate the performance of the structure, not only at the working loads, but also at the various combinations of higher loads. This requires information regarding the effects of various crack patterns, created by various loading combinations, on the overall behaviour of the test structure.

In general, there are two critical loading stages affecting the behaviour of the test structure:

1. The load at which the first crack pattern is formed. The tests indicate that this stage occurs between 1.25 and 1.50 times the design load.
2. The load at which the test structure fails either in flexure or in shear.

On the other hand, there are three combinations of loads which can be employed to obtain the above critical stages. Namely,

1. Uniformly distributed vertical load alone,
2. Combined vertical and horizontal loads,
3. Horizontal load alone.

All possible cases of loading history based on the above can be presented in a matrix form:

$$\begin{bmatrix} C_{11} & C_{12} & C_{13} \\ C_{21} & C_{22} & C_{23} \\ C_{31} & C_{32} & C_{33} \end{bmatrix}$$

where C_{ik} denotes the case where first crack pattern is formed by k th type of loading, and failure is caused by i th type of loading.

Each of these nine combinations were studied with respect to the practical cases they represent. The two which seemed the most useful, were C_{21} and C_{32} (Fig. 5). The former is the case where the first crack pattern is created by vertical load alone, and the failure is due to combined load. This represents the practical case where the structure is overloaded with gravity loads and a very high horizontal load (may be due to strong winds or earthquakes) is superimposed. In the latter case the test structure is cracked under combined load, and failure is obtained by increasing the horizontal load alone while the vertical load is kept constant at a certain level (1.5 times the design vertical load). This combination was chosen to study the behaviour of structures subjected to exceedingly high horizontal loads while they were already overloaded by gravity loads.

Each of the above cases was adopted for each of the test structures. However it was thought that it could be more beneficial if some additional tests of secondary importance were conducted on each test structure. The extent of loading and the location in the sequence of testing of these auxiliary tests were very carefully selected to minimize possible effects on the general behaviour of the test structures as far as the main tests were concerned. It is still, however, very difficult to be certain that the behaviour of the test structures was not affected. The question of these auxiliary tests being worth the doubts they caused, will be discussed in Chapter 6. As can be seen from the loading history diagrams (Fig. 33), two auxiliary tests were conducted on the test structure 1,

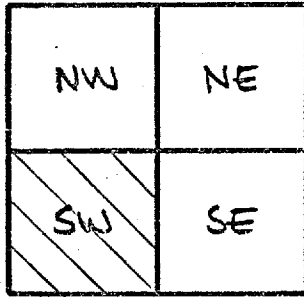
- i. Panel by panel loading and
- ii. Superposition check.

However, only the latter of these two auxiliary tests was carried out on the test structure 2, and to a lower extent.

The "Panel by panel loading test" consisted of three parts in which, respectively, one, two and three panels were loaded with uniformly distributed vertical load. Fig. 8 illustrates the patterns of loading and the comparisons intended.

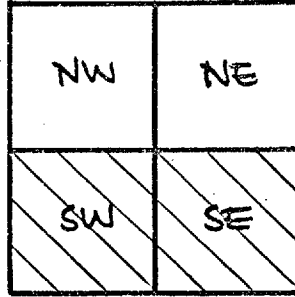
The "Superposition check" also consisted of three parts. The first was the loading of the whole slab with vertical load alone. In the second the applied horizontal load corresponded to the highest value of the

PART 1



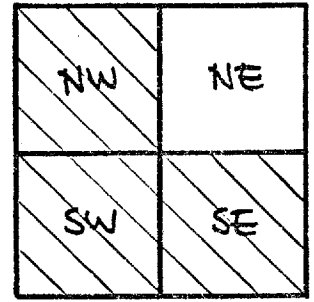
$$NW = \overline{SE} \quad (+)$$

PART 2



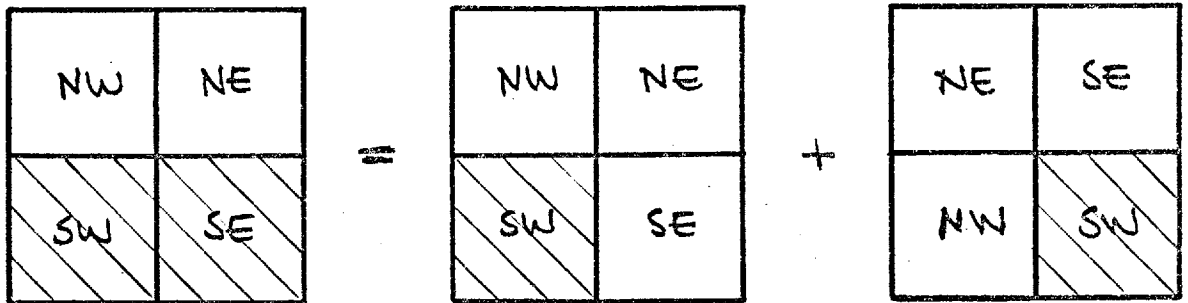
$$\begin{aligned} NW &= NE \\ SW &= SE \end{aligned}$$

PART 3



$$NW = \overline{SE}$$

a. PARTS OF THE "PANEL BY PANEL LOADING" TEST



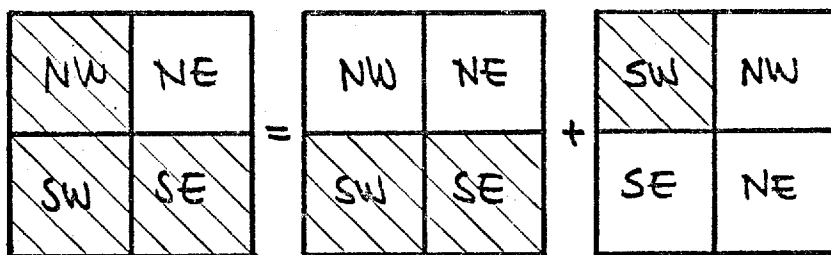
$$SW_2 = SW_1 + \overline{NW_1} \quad (+)$$

b. COMPARISON 1

FIG. 8 a. & b. - PANEL BY PANEL LOADING TEST

(*) BAR INDICATES THAT THE TWO COMPONENTS OF ANY QUANTITY IN THIS PANEL ARE TO BE INTERCHANGED

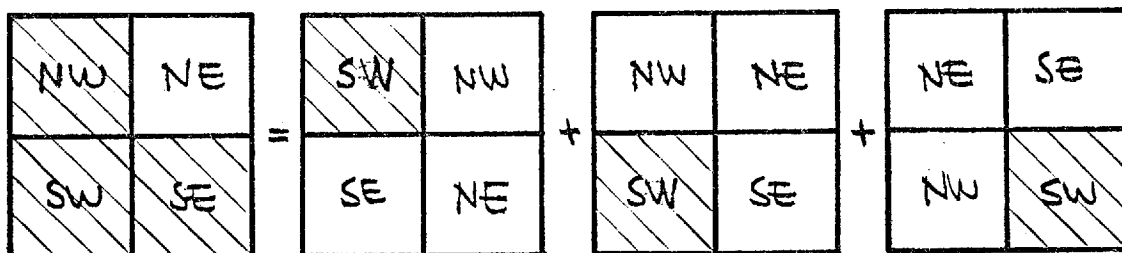
(+) SINCE ONLY THE WEST HALF WAS INSTRUMENTATED, THE OTHER PANELS CANNOT BE CONSIDERED IN COMPARISON



$$NW_3 = NW_2 + SW_1$$

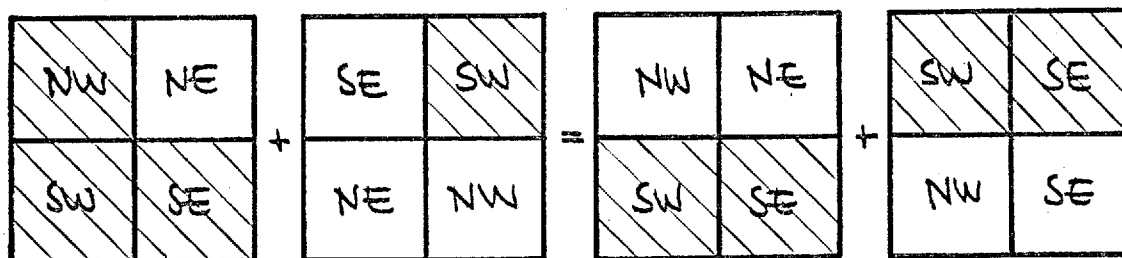
$$SW_3 = SW_2 + SE_1$$

c. COMPARISON 2



$$SW_3 = SW_1 + NW_1 + \overline{NW_1}$$

d. COMPARISON 3



$$NW_3 + NW_1 = NW_2 + SW_2$$

e. COMPARISON 4

FIG. 8 c.&d.&e. - PANEL BY PANEL LOADING TEST

vertical load in the previous part. The third part was a combined loading test. Both types of loads were applied proportionally to the same extent as the previous ones. This final part of the test was expected to produce effects on the test structure equivalent to the sum of the effects produced by the first and second parts.

CHAPTER 4DESIGN OF THE TEST STRUCTURES

The geometry of the test structures had been determined by a number of considerations related to the philosophy of the project. Having the geometry determined, the remaining information required for the process of design were:

- i. Loads to be considered, and
- ii. Properties of the materials to be used.

Consideration was given to the most common loads resisted by this type of structure. With the aid of the British Code CP 114, the design loads were calculated as follows:

- i. Uniformly distributed vertical load

Dead weight (including floor finish)	120 psf
Partitioning	20 psf
	<hr style="width: 100px; margin: 0 auto;"/>
	$g = 140$ psf
Live load	60 psf
	<hr style="width: 100px; margin: 0 auto;"/>
	$q = 200$ psf

- ii. Horizontal load - A rather high value (Exposure C, $V = 63$ mph) of wind load was chosen in the British Code CP3,V. The corresponding wind pressure was

$$p = 19 \text{ psf}$$

Considering the eighth floor from top, the equivalent uniformly distributed (per length) load was,

$$w = 7 \cdot \frac{1}{2} \cdot 12 \cdot 19 = 800 \text{ plf}$$

As far as the strength properties of the materials were concerned, it was desired to choose the most common values. For design purposes, the following properties were considered:

- i. High tensile strength steel with

$$f_{sy} = 60000 \text{ psi and}$$

$$E_s = 30 \cdot 10^6 \text{ psi, and}$$

ii. A concrete of

$$f_{cu} = 6000 \text{ psi and}$$

$$E_c = 3 \cdot 10^6 \text{ psi}$$

However some considerations related to the behaviour of the test structure 1 led to the use of mild steel in the test structure 2. The case was very carefully studied, and mild steel with the following properties was preferred:

$$f_{sy} = 40000 \text{ psi and}$$

$$E_s = 30 \cdot 10^6 \text{ psi}$$

Full details of the reasons for this choice are presented in Section 6.2 of Chapter 6.

4.1. STRUCTURAL ANALYSIS - For the structural analysis of flat plate structures, both the British (CP 114) and the American (ACI) codes of practice recommend two methods:

i. Empirical distribution of total moment

$$M = k q L_2 \left(L_1 - \frac{2D}{3} \right)^2$$

where $k =$ a coefficient $\left(\frac{1}{8} \text{ to } \frac{1}{10} \right)$

$q =$ uniformly distributed vertical load

$L_1 =$ longer span length

$L_2 =$ shorter span length

$D =$ diameter or equivalent diameter of the columns

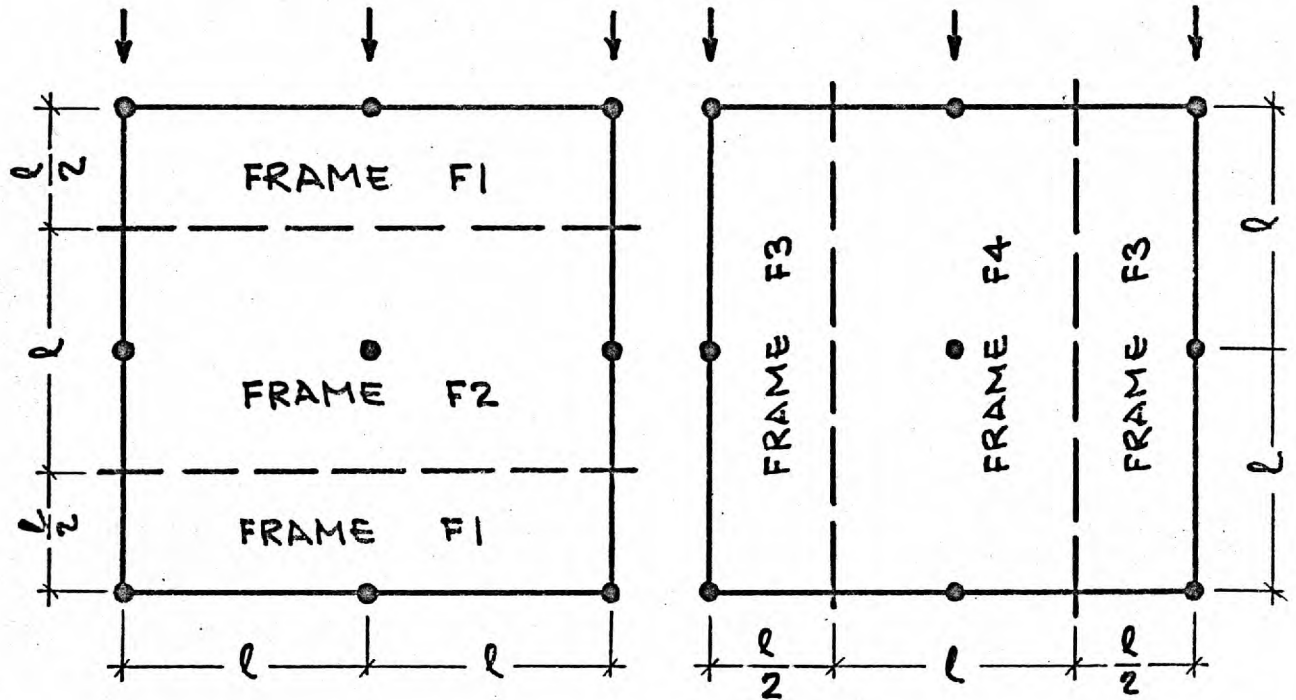
ii. In both directions, the elastic analysis of the frames formed by dividing the structure along panel centrelines.

For the analysis of the test structures, the latter method was chosen, since the effect of the horizontal load can be considered explicitly only in this method.

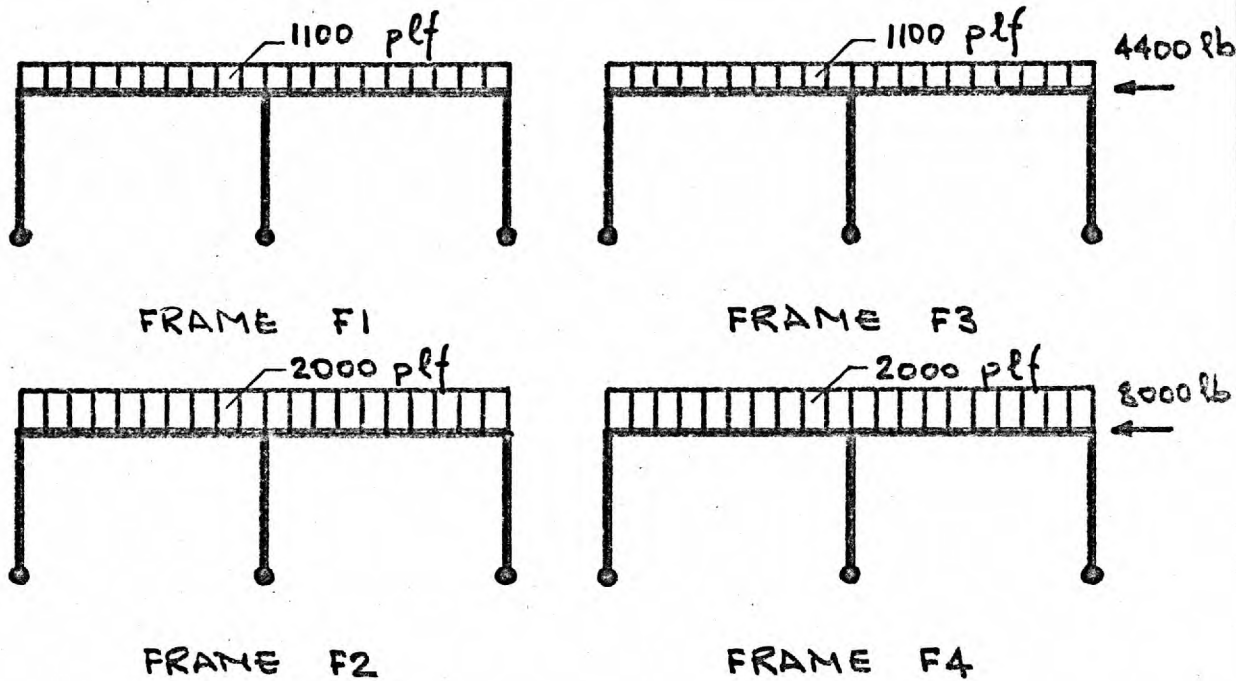
The frames were formed as recommended by the Code. Fig. 9 illustrates the division and designation of these frames.

The frames shown in Fig. 9, were elastically analysed, and the moment distributions were determined. These values are given in Fig. 10.

The reinforcement strips were also formed according to the code recommendations. The division and designation of these strips are shown



a. DIVISION AND DESIGNATION OF THE FRAMES



b. LOADS ON THE FRAMES

FIG. 9 . THE FRAMES ELASTICALLY ANALYSED

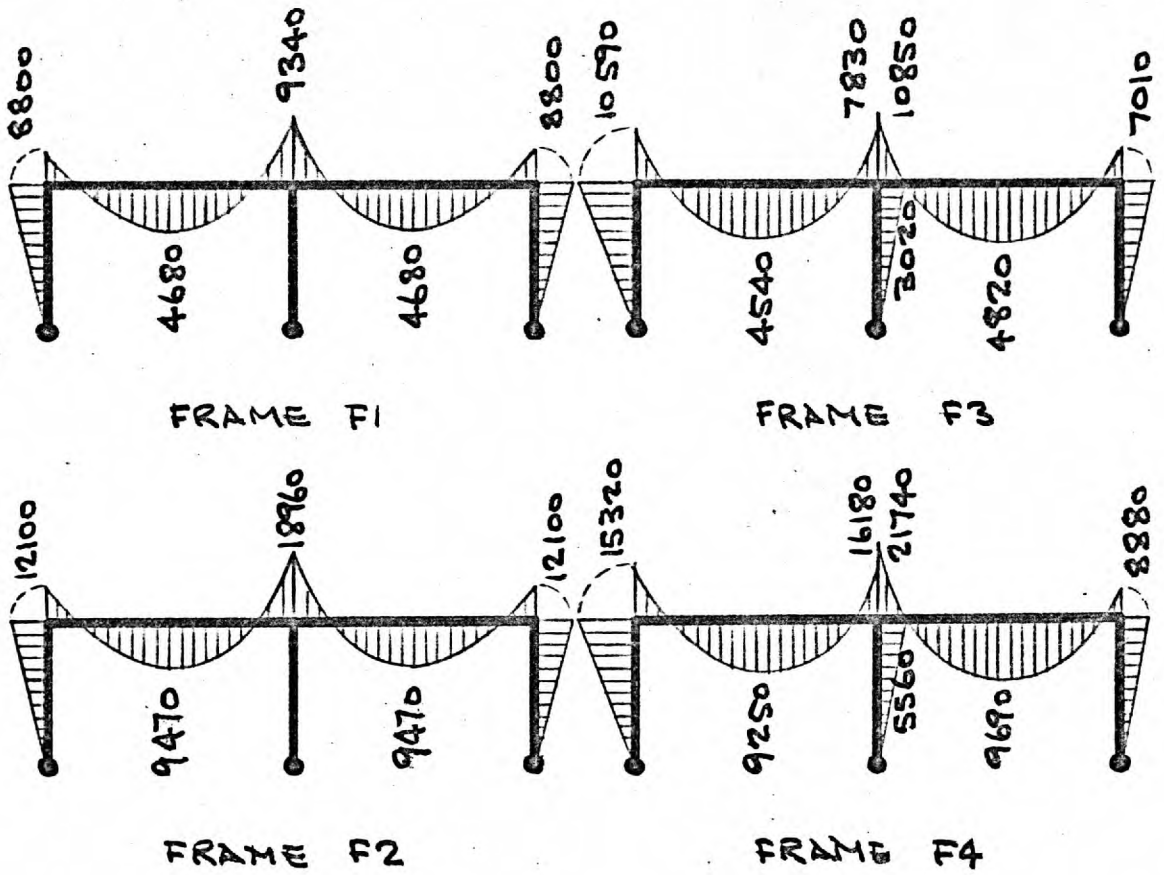


FIG. 10 - MOMENT DISTRIBUTION (IN ft.-lb) OVER THE FRAMES

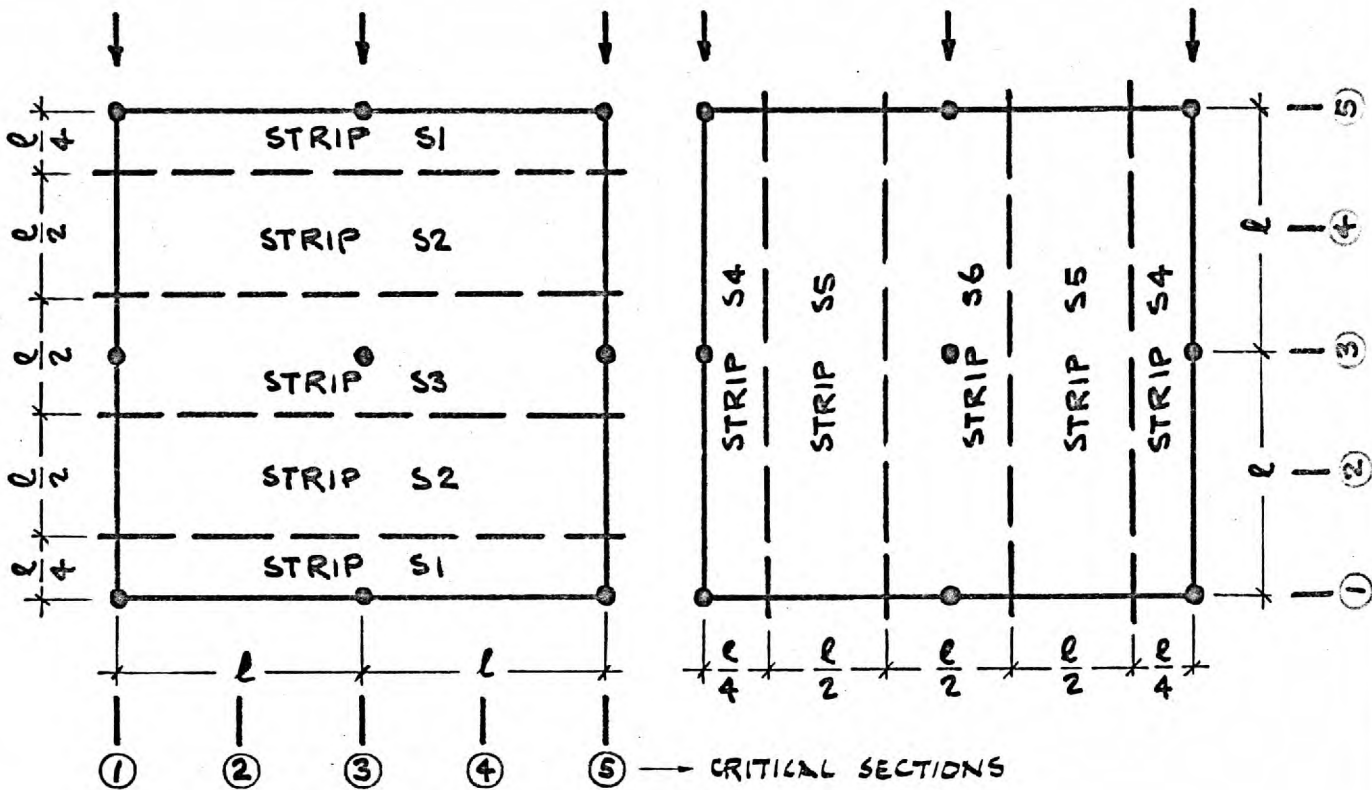


FIG. 11 - DIVISION AND DESIGNATION OF THE REINFORCEMENT STRIPS

in Fig. 11. Using the coefficients given in the code, the calculated moments were distributed to these reinforcement strips. The computations are given in Table 1.

The code, furthermore, requires that the sum of absolute values of the calculated moments in each panel to be not less than the total moment given for the Empirical Method, that is,

$$M_t = \frac{wL_2}{10} \left(L_1 - \frac{2D}{3} \right)^2$$

In this case,

$$M_t = \frac{200 \cdot 10}{10} \left(10 - \frac{2 \cdot 1}{3} \right)^2 = 17400 \text{ [ft-lb]}$$

On the other hand the sums of the calculated moments in each panel are:

In W-E direction

$$\begin{aligned} M_{NW}^T = M_{NE}^T = M_{SW}^T = M_{SE}^T &= 4680 + \frac{8800 + 9340}{2} + \frac{15530}{2} \\ &+ \frac{12100 + 18960}{4} = 29280 \text{ [ft-lb]} > M_t \end{aligned}$$

In N-S direction

$$\begin{aligned} M_{NW}^T = M_{NE}^T &= 4820 + \frac{7010 + 10850}{2} + \frac{9690}{2} + \frac{8880 + 21740}{4} \\ &= 26250 \text{ [ft-lb]} > M_t \end{aligned}$$

$$\begin{aligned} M_{SW}^T = M_{SE}^T &= 4540 + \frac{10590 + 7830}{2} + \frac{9250}{2} + \frac{15320 + 16180}{4} \\ &= 26250 \text{ [ft-lb]} > M_t \end{aligned}$$

Therefore, the above requirement was also satisfied.

4.2. REINFORCED CONCRETE DESIGN - Along each strip the highest positive and negative moments were chosen as design moments, and each strip was reinforced for these values. In order to avoid further complications, only two complete meshes were considered and short bars and bent-up bars were

not used. A standard size bar ($\frac{3}{8}$ in. dia.) was used throughout each slab. Each mesh provided two effective depths differing by one bar diameter. For optimum use of steel, the larger effective depth was considered in the more critical direction each time. This consideration resulted in precisely the same spacing of bars in both directions, for both top and bottom meshes.

The reinforcement was calculated by ACI ultimate design recommendation. Namely,

$$M_u = b d_1^2 q f_c (1 - 0.59 q) \quad \text{with } q = r \frac{f_{sy}}{f_c}$$

If a load factor ϕ is considered,

$$M_u = \phi M$$

Then, the ACI formula can be solved for A_s to obtain,

$$A_s = \frac{b}{1.18k} \left[d_1 - \sqrt{d_1^2 - 2.36 \frac{\phi M}{b f_c}} \right] \quad \text{where } k = \frac{f_{sy}}{f_c}$$

The above formula was used with appropriate material properties, to determine the spacing of $\frac{3}{8}$ in. bars in each strip. The computations are summarized in Tables 2 and 3. The material properties considered in these calculations are listed below:

For the test structure 1

$$f_{sy} = 60000 \text{ psi } (+)$$

$$f_c = 0.80 \cdot 6000 (+) = 4800 \text{ psi}$$

$$k = \frac{60000}{4800} = 12.5 \quad \text{and} \quad \phi = 2.0$$

$$a = 0.1104 \text{ sq. in. (area of one bar)}$$

$$\text{In W-E direction; } d_1 = 3.1875 \text{ in. and } d_1' = 2.8125 \text{ in.}$$

$$\text{In N-S direction; } d_1 = 2.8125 \text{ in. and } d_1' = 3.1875 \text{ in.}$$

$$\text{Then, } A_s = \frac{b}{1.18 \times 12.5} \left[d_1 - \sqrt{d_1^2 - \frac{2.36 \times 2.0}{4800} \times \frac{M}{b}} \right]$$

$$\text{or, } A_s = 0.0678b \left[d_1 - \sqrt{d_1^2 - 0.000984 \frac{M}{b}} \right]$$

STRIP	MOMENTS AT THE CRITICAL SECTIONS (*) [ft-lb]					DESIGN MOMENTS [in-lb]	
	1	2	3	4	5	M _{min}	M _{max}
S1	-0.75×8800 = -6600	0.55×4680 = 2570	-0.75×9340 = -7010	2570	-6600	-84120	30840
S2	$-0.25(8800 + \frac{1}{2} \times 12100)$ = -3715	$0.45(4680 + \frac{1}{2} \times 9470)$ = 4240	$-0.25(9340 + \frac{1}{2} \times 18960)$ = -4700	4240	-3715	-56400	50900
S3	-0.75×12100 = 9075	0.55×9470 = 5200	-0.75×18960 = -14200	5200	-9075	-170400	62500
S4	-0.75×10590 = -7940	0.55×4540 = 2500	-0.75×10850 = -8150	0.55×4820 = 2650	-0.75×7010 = -5260	-97800	31800
S5	$-0.25(10590 + \frac{1}{2} \times 15320)$ = -4560	$0.45(4540 + \frac{1}{2} \times 9250)$ = 4120	$-0.25(10850 + \frac{1}{2} \times 21740)$ = 5430	$0.45(4820 + \frac{1}{2} \times 9690)$ = 4350	$-0.25(7010 + \frac{1}{2} \times 8880)$ = -2860	-65160	52200
S6	-0.75×15320 = -11500	0.55×9250 = 5090	-0.75×21740 = -16330	0.55×9690 = 5320	-0.75×8880 = -6660	-195960	63840

TABLE 1 - DESIGN MOMENTS FOR THE REINFORCEMENT STRIPS

(*) REF. FIG. 11

STRIP	b	d _i	M	d _i ²	$\frac{.000984M}{b}$	$(\sqrt{d_i^2 - \dots})^2$	$\sqrt{d_i^2 - \dots}$	d _i - $\sqrt{d_i^2 - \dots}$	A _s	STEEL
	in	in	in-lb	in ²	in ²	in ²	in	in	in ²	3/8" HTS BARS
S1	36	3.1875	30 810	10.1602	0.842	9.318	3.053	0.135	0.330	4 @ 8 1/2"
S2	60	3.1875	50 900	10.1602	0.835	9.325	3.054	0.134	0.546	7 @ 8 1/2"
S3	60	3.1875	62 500	10.1602	1.025	9.135	3.022	0.166	0.677	7 @ 8 1/2"
S4	36	2.8125	31 800	7.9102	0.870	7.040	2.653	0.160	0.392	4 @ 8 1/2"
S5	60	2.8125	52 200	7.9102	0.856	7.054	2.656	0.157	0.640	7 @ 8 1/2"
S6	60	2.8125	63 810	7.9102	1.047	6.863	2.620	0.193	0.778	7 @ 8 1/2"

a. BOTTOM REINFORCEMENT

STRIP	b	d _i	-M	(d _i) ²	$\frac{.000984M}{b}$	$(\sqrt{d_i^2 - \dots})^2$	$\sqrt{d_i^2 - \dots}$	d _i - $\sqrt{d_i^2 - \dots}$	A _s	STEEL
	in	in	in-lb	in ²	in ²	in ²	in	in	in ²	3/8" HTS BARS
S1	36	2.8125	84 120	7.9102	2.300	5.610	2.370	0.443	1.085	7 @ 2 1/2" + 3 @ 5"
S2	60	2.8125	56 400	7.9102	0.925	6.985	2.644	0.169	0.688	7 @ 8 1/2"
S3	60	2.8125	170 400	7.9102	2.800	5.110	2.261	0.552	2.051	14 @ 2 1/2" + 4 @ 5"
S4	36	3.1875	97 800	10.1602	2.675	7.485	2.735	0.453	1.108	7 @ 2 1/2" + 3 @ 5"
S5	60	3.1875	65 160	10.1602	1.070	9.090	3.015	0.173	0.706	7 @ 8 1/2"
S6	60	3.1875	145 960	10.1602	3.210	6.950	2.636	0.552	2.051	14 @ 2 1/2" + 4 @ 5"

b. TOP REINFORCEMENT

TABLE 2 - REINFORCEMENT COMPUTATIONS FOR THE TEST STRUCTURE 1

STRIP	b	d _i	M	d _i ²	$\frac{.000787M}{b}$	$(\sqrt{d_i^2 - \dots})^2$	$\sqrt{d_i^2 - \dots}$	d _i - $\sqrt{d_i^2 - \dots}$	A _s	STEEL
	in	in	in-lb	in ²	in ²	in ²	in	in	in ²	3/8" MILD STEEL BARS
S1	36	3.1875	30 840	10.1602	0.6734	9.4863	3.080	0.108	0.330	4 @ 8 1/2"
S2	60	3.1875	50 900	10.1602	0.6681	9.4921	3.081	0.107	0.543	7 @ 8 1/2"
S3	60	3.1875	62 500	10.1602	0.8200	9.3402	3.056	0.132	0.671	7 @ 8 1/2"
S4	36	2.8125	31 800	7.9102	0.6944	7.2153	2.686	0.127	0.388	4 @ 8 1/2"
S5	60	2.8125	52 200	7.9102	0.6844	7.2258	2.688	0.125	0.636	7 @ 8 1/2"
S6	60	2.8125	63 840	7.9102	0.8370	7.0732	2.660	0.153	0.718	7 @ 8 1/2"

a. BOTTOM REINFORCEMENT

STRIP	b	d _i	-M	(d _i) ²	$\frac{.000787M}{b}$	$(\sqrt{d_i^2 - \dots})^2$	$\sqrt{d_i^2 - \dots}$	d _i - $\sqrt{d_i^2 - \dots}$	A _s	STEEL
	in	in	in-lb	in ²	in ²	in ²	in	in	in ²	3/8" MILD STEEL BARS
S1	36	2.8125	84 120	7.9102	1.8282	6.0720	2.464	0.349	1.065	10 @ 1 7/8" + 3 @ 4 1/2"
S2	60	2.8125	56 400	7.9102	0.7395	7.1707	2.678	0.135	0.687	7 @ 8 1/2"
S3	60	2.8125	170 400	7.9102	2.2341	5.6761	2.382	0.431	2.192	19 @ 1 7/8" + 4 @ 4 1/2"
S4	36	3.1875	97 800	10.1602	2.1311	8.0231	2.833	0.355	1.083	10 @ 1 7/8" + 3 @ 4 1/2"
S5	60	3.1875	65 160	10.1602	0.8543	9.3054	3.051	0.137	0.697	7 @ 8 1/2"
S6	60	3.1875	145 460	10.1602	2.5613	7.5401	2.755	0.433	2.202	19 @ 1 7/8" + 4 @ 4 1/2"

b. TOP REINFORCEMENT

TABLE 3 - REINFORCEMENT COMPUTATIONS FOR THE TEST STRUCTURE 2

For the test structure 2

$$f_{sy} = 48500 \text{ psi } (+)$$

$$f_c = 0.80 \times 6000 = 4800 \text{ psi } (+)$$

$$k = \frac{48500}{4800} \approx 10 \text{ and } \phi = 1.6$$

$$a = 0.1104 \text{ sq. in.}$$

In W-E direction; $d_1 = 3.1875 \text{ in.}$ and $d_1' = 2.8125 \text{ in.}$

In N-S direction; $d_1 = 2.8125 \text{ in.}$ and $d_1' = 3.1875 \text{ in.}$

$$\text{Then, } A_s = \frac{b}{1.18 \times 10} \left[d_1 - \sqrt{d_1^2 - \frac{2.36 \times 1.6}{4800} \times \frac{M}{b}} \right]$$

$$\text{Or, } A_s = 0.08475 b \left[d_1 - \sqrt{d_1^2 - 0.000787 \frac{M}{b}} \right]$$

The resulting cross sections for both test structures are shown in Fig. 12.

The design of the columns was not so critical as that of the slab, and attention was mostly concentrated on the behaviour of the slab as required by the philosophy behind the project. It was therefore thought that it would not matter if the columns were stronger than required as long as they provide a reasonable relative stiffness and reasonable sections to resist shear. Preliminary investigations using working load methods indicated that all the columns would be strong enough if they were reinforced with four high strength steel longitudinal bars of 1 in. diameter. Each column was then checked using an ultimate strength design method and each proved sufficiently strong.

However, the problem of bond presented some difficulties. Since the bars considered were not deformed and the columns were very short, it would not be possible to provide sufficient bond length. The solution to this problem was to use two U-shaped bars, instead of four individual ones, and to put them through the steel base plate and to fix them to the base by bolting. The details are shown in Fig. 13. The above method was not

(+) These are the values considered in design; later tests gave slightly different results as expected.

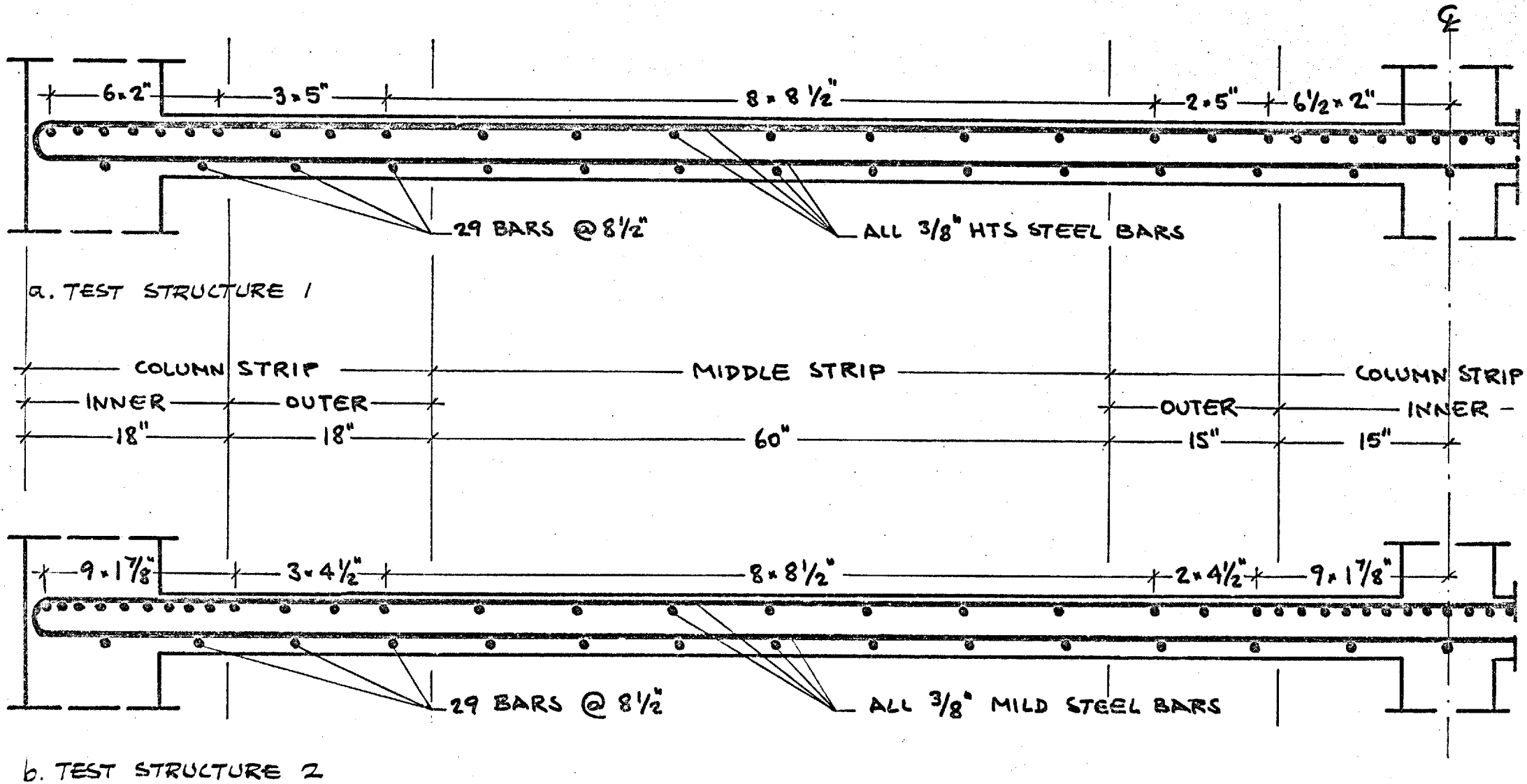


FIG. 12. REINFORCEMENT SPACING IN THE TEST STRUCTURES

satisfactory as it stood, since the radius of the bars would have caused a very unrealistic pattern of reinforcement in the slab-column connection. To overcome this problem, upper column stubs were introduced. In addition, they helped in obtaining more realistic behaviour in the test structure as far as the crack pattern was concerned, although they had no structural value.

4.3 YIELD LINE ANALYSIS - The designed test structures were then analysed by Yield Line Theory to estimate the overall flexural capacity of each test structure. Considering the geometry and the loading, the simple yield mechanism illustrated in Fig. 14a seemed likely. The mechanism consists of positive yield lines along panel centrelines perpendicular to the horizontal load direction, and negative yield lines along middle column centrelines and around far end columns. However, in a similar test, Dr. Chan⁵ had obtained a more complicated zig-zag yield line pattern (Fig. 14b). In this case, there are two parameters to be assumed, namely x and y , to determine the yield line pattern. A number of reasonable combinations of these parameters were considered. Each of these combinations and the simple yield mechanism were analysed, and the ultimate loads obtained for each of these patterns were compared. That obtained for the simple mechanism was:

$$(\text{Combined load})_{\text{ultimate}} = 2.15 (\text{Combined load})_{\text{design}}$$

The above seemed to be the smallest, and therefore the most likely. Indeed it was the one obtained in both test structures.

3.4. PUNCHING SHEAR ANALYSIS - As mentioned earlier in Chapter 2, very little attention has been focused on the problem of punching shear. A great deal is still unknown. Due to the absence of a reliable method for predicting the behaviour of the slab-column connections, for design purposes the simple nominal shear formula, as required by the version of the British Code (CP114), applying at that time, was used as a guide to check the strength of column regions. However at a later date the relevant code requirements were slightly altered. The new form is used in the analysis of experimental results. In Chapter 7, a number of various methods and their various combinations are explained, applied and compared, in addition to the British Code (CP114) method.

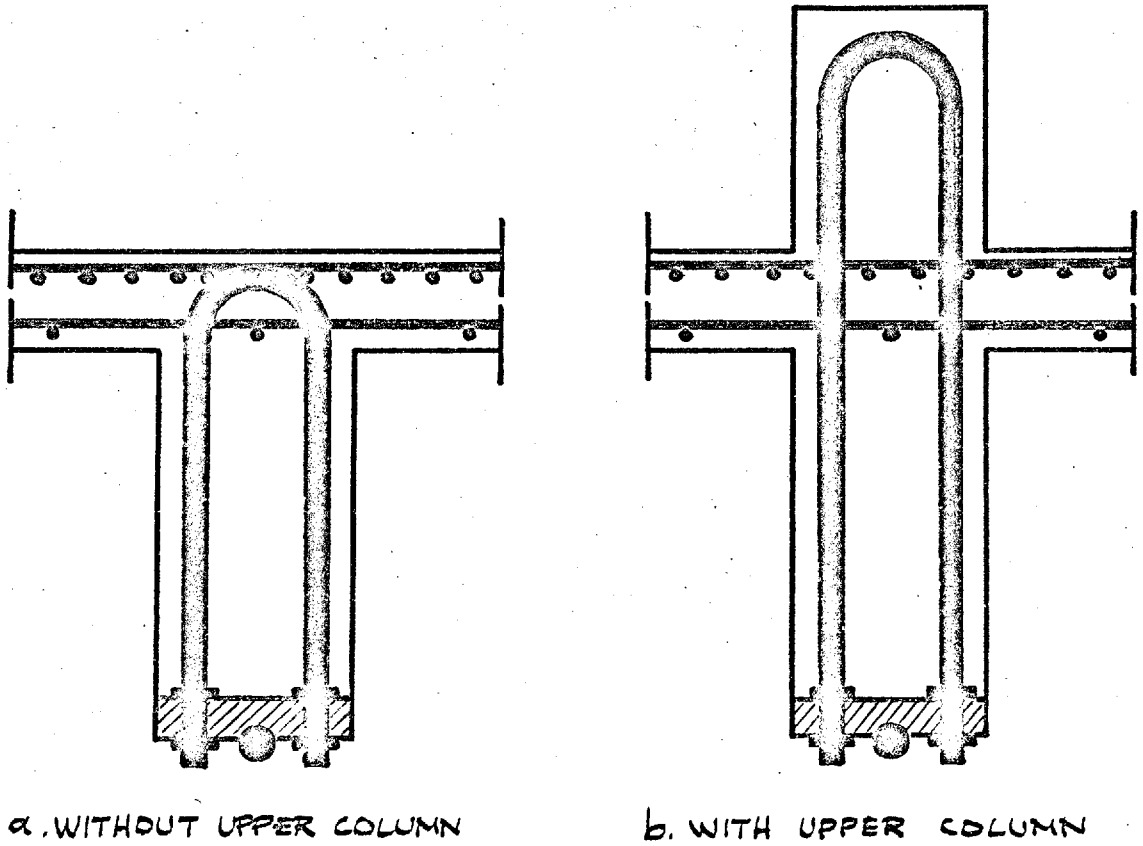


FIG. 13 - COLUMN REINFORCEMENT DETAILS

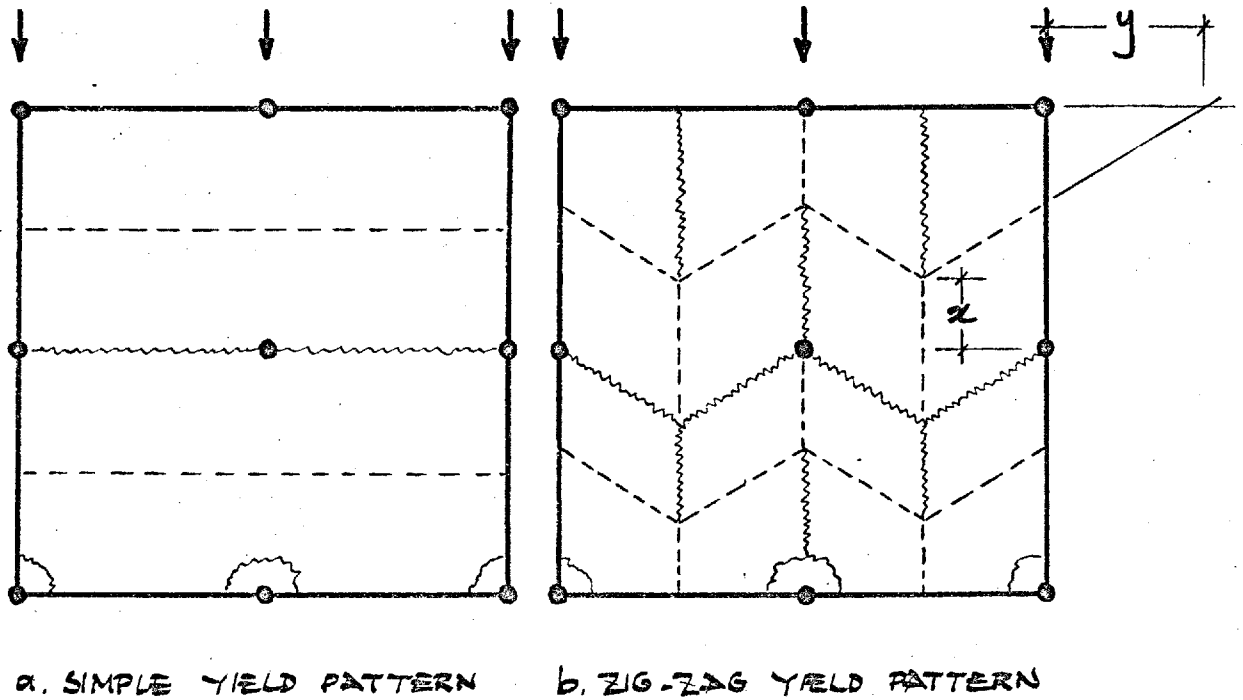


FIG. 14 - YIELD LINE PATTERNS CONSIDERED

CHAPTER 5

INSTRUMENTATION AND MATERIALS

Experimental investigations of this size are not very common. Considering their cost and the labour involved, it is obvious that a great deal of attention has to be paid to the instrumentation. On the one hand is the concern to get the maximum possible amount of information from each test; on the other are the financial limitations. Where instrumentation is in terms of hundreds of items, it is extremely important to consider the cost of each item, the amount of data to be recorded and processed, and the complexity of manufacture and maintenance of such a system. In the present investigation therefore, a considerable amount of effort was devoted to the design and the development of the instrumentation and experimentation techniques. For example, the newly developed hydraulic deflection measurement system saved a good deal of money and served the purpose very efficiently.

The principle behind the design of the instrumentation was to adopt a grid for each kind of instrumentation, which is fine enough to obtain a fair amount of information throughout the test structure, and yet not too fine to exceed the capacity of the instruments and man-power available. Considering the limitations concerning time, space, manpower, recording instruments, financial sources etc., the advantage of axial symmetry was taken; and only one half of each test structure was fully instrumented. However, a number of points in the other half were also instrumented to check that the behaviour remained symmetrical.

5.1. LOADING SYSTEM - To simulate uniformly distributed vertical load, concentrated loads were applied to the slab at 192 points uniformly spaced at 18 in. As schematically shown in Fig. 6 these loading points were arranged in groups of four by using a suitable system of simple beams made of steel box sections. 48 pull-type hydraulic jacks of 4 tonf. capacity and 6 in. ram travel, were employed to load these groups of four loading points. These hydraulic jacks were attached to the floor by hinges which allowed rotation as the test structure swayed under the horizontal load. The jacks were specially manufactured and were intended to be identical. The tests proved that their load-pressure characteristics were reasonably close, if not, identical. Besides, a number of calibrated pulling wires

were used in the tests on test structure 1, to check that the load applied by each of these jacks was reasonably the same.

As illustrated in Fig. 6, the horizontal load was applied by jacking against concrete blocks tied to the testing floor. Two symmetrically loaded simple beams applying equal reactions to the test structure at the end supports, were employed. Thus, the test structure was horizontally loaded with load P (variable) along the edge column centrelines and with load $2P$ along the central column centreline. As implied by the loading history diagrams, the horizontal load required for the test structure 1 was far less than that required for the test structure 2. It was therefore thought that if the high capacity jacks required for the test structure 2 were used for the other one, a considerable amount of error due to employing the very low loading range of jacks, might have been introduced. Therefore two different sets of jacks were used for each of the test structures. For the first one, only one push-type hydraulic jack of 20 tonf. capacity was used for each of the simple beams; but the horizontal load was applied by two 50 tonf. capacity jacks to each simple beam in the case of the test structure 2. The jacks used for horizontal loading were calibrated, and they were arranged so that the system applied a reasonably evenly distributed load.

To both of these loading systems, the pressure was applied by two Amsler pressure cabinets of 5500 psi capacity. The vertical loading jacks were connected to one of the pressure cabinets, through a pressure system which enabled panel by panel control of loading. That is, the jacks loading the same panel were connected together and controlled by use of a valve. The pressure system was designed to minimize the head loss differences among the jacks. Since the loading was gradual and very slow, the effect of head loss differences was, anyway, expected to be extremely small. Similarly, the horizontal loading jacks were connected to the other pressure cabinet through a pressure system which could be controlled by two valves, one for each half of the test structure.

5.2. REACTION MEASUREMENT SYSTEM - To measure the reactions at the bottom of each column, specially designed tripod-type reaction dynamometers were used. As explained in the previous chapters, the structural design of the test structures required the columns to be supported on moment-free supports. Therefore, the quantities to be measured at the bottom of each column were only the three components of the reaction. A tripod-type reaction dynamometer was sufficient to measure these, without introducing

more complicated systems. Efforts and attention were therefore concentrated on the design, manufacture and calibration of individual dynamometers.

5.2.1. DESIGN OF THE REACTION DYNAMOMETER - The idea of tripod-type reaction dynamometer is by no means a new one; it has been employed by at least two similar research projects (i.e. i. University of Illinois team, Ref. 6, 7, 8, and ii. Dr. Chan⁵ at Imperial College) before the present investigation. However, many points requiring improvement could be observed and special attention was paid to these points. For the sake of symmetry, simplicity and stability, a regular tetrahedron shape was chosen as the general form of the dynamometer. The column, which had a $1\frac{1}{2}$ " thick steel plate base, was supported on a $1\frac{1}{2}$ " diameter hardened steel ball bearing placed at the apex of the tetrahedron. Three legs formed the three sides and the base was made of 2" thick steel plate which was considered as infinitely rigid. The legs were attached to the base plate through foot units which were in turn bolted to the base. At the top of the dynamometer, the legs were connected together by a top unit upon which the ball bearing was placed. The legs were screwed into the top and foot units. This method of attachment allowed a slight movement which under the working loads was sufficient to enable the legs to be considered as pin jointed at both ends. The analysis of the dynamometer structure was therefore based on this assumption. Considering the geometry illustrated in Fig. 15, the flexibility analysis resulted in,

$$\begin{Bmatrix} P_x \\ P_y \\ P_z \end{Bmatrix} = \begin{bmatrix} K'_{1x} & K'_{2x} & K'_{3x} \\ K'_{1y} & K'_{2y} & K'_{3y} \\ K'_{1z} & K'_{2z} & K'_{3z} \end{bmatrix} \cdot \begin{Bmatrix} Q_1 \\ Q_2 \\ Q_3 \end{Bmatrix}$$

$$\text{or } \{P\} = [K'] \cdot \{Q\}$$

$$\text{where, } [K'] = \begin{bmatrix} 1/\sqrt{3} & -1/2\sqrt{3} & -1/2\sqrt{3} \\ 0 & -1/2 & 1/2 \\ \sqrt{2/3} & \sqrt{2/3} & \sqrt{2/3} \end{bmatrix}$$

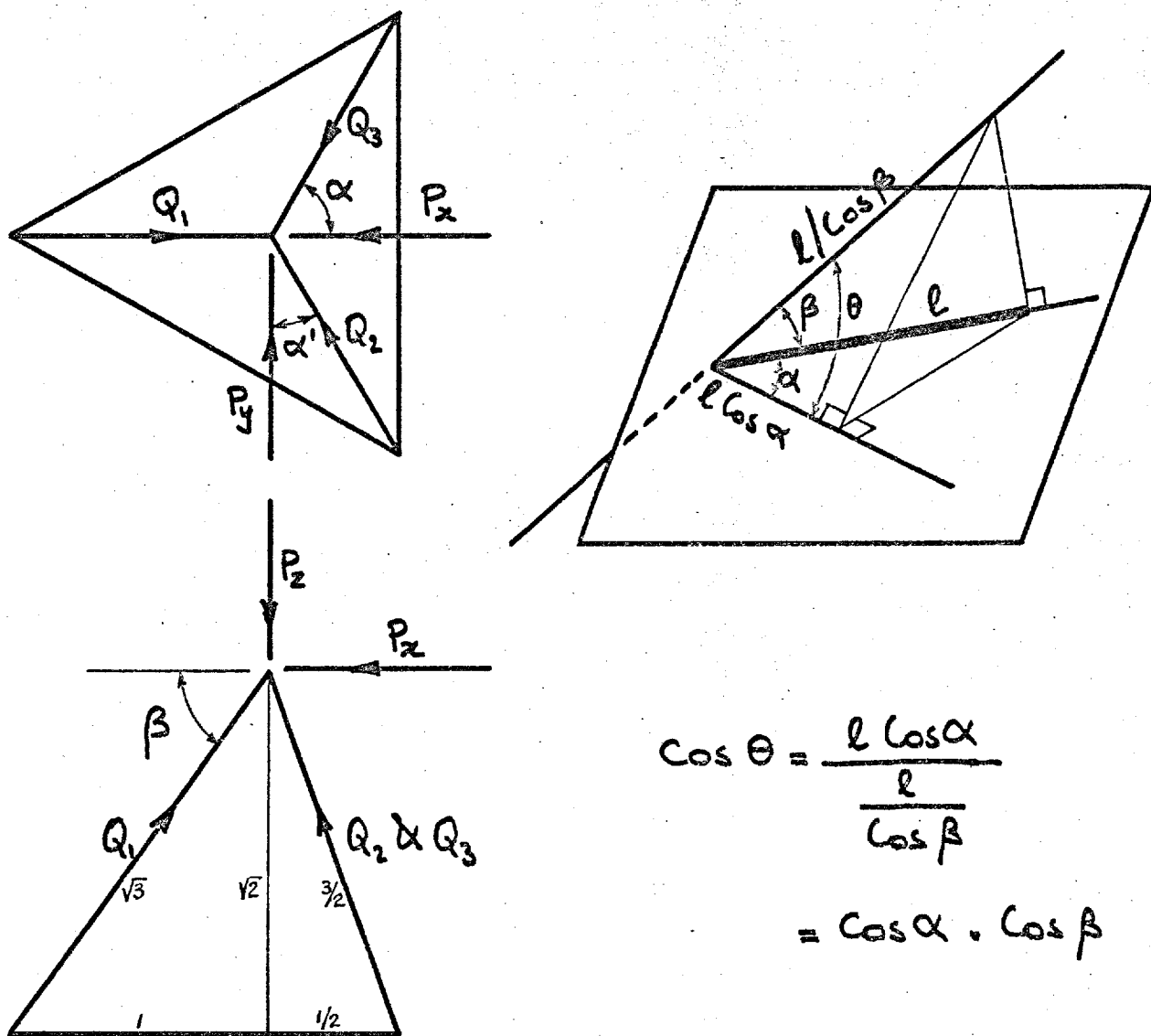


FIG. 15 - GEOMETRY OF THE REACTION DYNAMOMETER

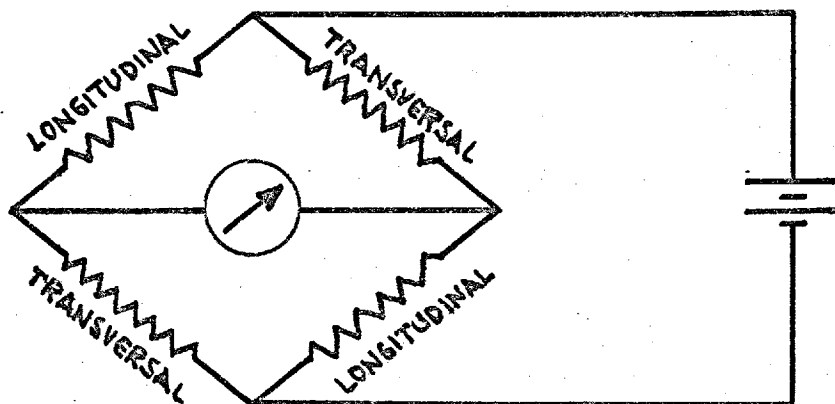


FIG. 16 - CIRCUIT DIAGRAM FOR THE REACTION DYNAMOMETER LEG

If a linear stress-strain relation is assumed for the material of which the legs were made,

$$\{Q\} = AE \{E\}$$

$$\text{or, } \{P\} = AE [K'] \cdot \{E\} = [K] \cdot \{E\}$$

where, A = cross-sectional area of the leg

E = modulus of elasticity for the material the legs were made of

The expected maximum reactions were already known from the structural analysis of the test structures. The only quantity to be determined was the maximum leg force expected in the most critical case. From the theoretical analysis of the dynamometer structure,

$$\{P\} = [K'] \cdot \{Q\}$$

$$\text{or } \{Q\} = [K']^{-1} \cdot \{P\}$$

So the theoretical $[K']$ -matrix was inverted and used to determine the leg forces from the components of the column reactions corresponding to the most critical cases. Then all the sections were designed for the maximum leg force calculated, considering the appropriate material properties.

The matrix $\{E\}$ is determined simply by measuring the strains on each leg. On the other hand the matrix $[K]$ represents the geometrical and material properties of the dynamometer. Once it is determined, the three components of the load applied at the apex of the dynamometer can be calculated by simply pre-multiplying the measured strains matrix $\{E\}$ by the matrix $[K]$. The calibration procedure to determine the matrix $[K]$ will be explained in detail in the next sub-section.

In both of the previous research projects which employed this kind of reaction dynamometer, the legs were welded to the top unit and the base plate. This welding inevitably introduced errors due to (i) the fixity of the ends, and (ii) the imperfections in geometry. The error due to the former was greatly reduced by the clearance of threads at the ends of the legs. On the other hand, lining-up errors could, to a considerable extent, be corrected by turning the legs which required adjustment. The top and bottom ends of the legs were machined to have right-handed and left-handed threads respectively. When the length of a particular leg required to be

increased or decreased to correct the geometry, it was simply turned to the left or right respectively. Before calibration each dynamometer was checked for geometry under very well defined loading conditions, imperfections were corrected, and the legs subsequently locked by tightening the locking screws at the foot of each leg. Since the foot units were separate units bolted down to the base plate, the assembling of the dynamometer was simple and straightforward.

Four strain gauges, two longitudinal and two transversal, were fixed on each leg. They were all Saunders-Roe foil gauges having a $\frac{1}{2}$ in. gauge length and a nominal resistance of 120 Ω . These gauges were fixed to the polished and cleaned leg surface with "Araldite" adhesive. The strain gauges were connected to form a wheatstone bridge which gives the maximum possible reading difference to reduce the errors of measurement to a minimum. The circuit they form is illustrated in Fig. 16. The wires from the four corners of the wheatstone bridge were connected to a set of 4 pin Belling-Lee sockets which were fixed on the dynamometer base. To record the strains of the dynamometers, a fifty-channel Peckel automatic strain recorder was used. The strain gauges on the legs were covered with Durapipe specially machined to prevent possible damage.

The detailed drawing used in the manufacture of these reaction dynamometers is given in Fig. 17.

5.2.2. CALIBRATION OF THE REACTION DYNAMOMETER. - The basic relation of the tripod-type reaction dynamometer analysis is,

$$\{P\} = [K] \cdot \{\epsilon\}$$

By "calibration" is meant the determination of the $[K]$ - matrix. As shown in the previous sub-section, the $[K]$ - matrix can be broken down into two parts,

$$[K] = E \cdot A [K']$$

where E is a material property

and $A [K']$ represents geometry.

In that sub-section, the $[K']$ - matrix was calculated theoretically.

Knowing the cross-sectional area of the leg only the value of E remained to be determined. Its approximate value was also known; however, for such a

sensitive instrument, obviously a higher degree of accuracy was required. Firstly, the value of the modulus of elasticity was measured for each individual leg and used to determine the $[K]$ -matrix. This consideration requires the equation

$$\begin{aligned} \{Q\} &= AE \{E\} && \text{to be replaced by} \\ \{Q\} &= \{AE E\} && \text{or,} \\ \begin{Bmatrix} Q_1 \\ Q_2 \\ Q_3 \end{Bmatrix} &= \begin{Bmatrix} (AE)_1 E_1 \\ (AE)_2 E_2 \\ (AE)_3 E_3 \end{Bmatrix} \end{aligned}$$

If this form of the $\{Q\}$ -matrix is substituted in the equation

$$\{P\} = [K'] \cdot \{Q\}, \text{ and}$$

then compared with the equation

$$\{P\} = [K] \cdot \{E\}$$

the $[K]$ -matrix can be expressed as,

$$[K] = \left[(AE)_1 \begin{Bmatrix} K'_{1x} \\ K'_{1y} \\ K'_{1z} \end{Bmatrix} \quad (AE)_2 \begin{Bmatrix} K'_{2x} \\ K'_{2y} \\ K'_{2z} \end{Bmatrix} \quad (AE)_3 \begin{Bmatrix} K'_{3x} \\ K'_{3y} \\ K'_{3z} \end{Bmatrix} \right]$$

Each leg was calibrated to determine the relation

$$Q_i = (AE)_i \cdot E_i$$

for that particular leg. Then, each column of the $[K']$ -matrix was multiplied by the appropriate value of $(AE)_i$ to obtain the $[K]$ -matrix

This method of determination of the $[K]$ -matrix was theoretically satisfactory. However, it was thought that a general calibration of the dynamometer as a whole should be more reliable, since corresponded to the real case and would probably include the effects of some other factors which could not be explicitly considered.

CALIBRATION THEORY FOR THE COMPLETE DYNAMOMETER. - The actual final calibration was carried out on each reaction dynamometer as a whole, and the $[K]$ -matrices were determined experimentally. The matrices obtained this way were then compared with the ones obtained by inserting the individual leg calibration results into the theoretical form of the $[K]$ -matrix. In all the cases they agreed very well.

To determine all the nine elements of the $[K]$ -matrix, it is theoretically sufficient to have three sets of strain readings corresponding to three different sets of known loading configurations:

<u>Conf.</u>	<u>Applied</u>			<u>Measured</u>		
1	P_{1x}	P_{1y}	P_{1z}	ϵ_{11}	ϵ_{12}	ϵ_{13}
2	P_{2x}	P_{2y}	P_{2z}	ϵ_{21}	ϵ_{22}	ϵ_{23}
3	P_{3x}	P_{3y}	P_{3z}	ϵ_{31}	ϵ_{32}	ϵ_{33}
	$\underbrace{\left\{ \begin{matrix} P_x \\ P_y \\ P_z \end{matrix} \right\}}_{[P]^T}$			$\underbrace{\left\{ \begin{matrix} \epsilon_{11} & \epsilon_{12} & \epsilon_{13} \\ \epsilon_{21} & \epsilon_{22} & \epsilon_{23} \\ \epsilon_{31} & \epsilon_{32} & \epsilon_{33} \end{matrix} \right\}}_{[E]}$		

If the basic relation is applied to each of these three cases,

$$\begin{aligned} \{P_1\} &= [K] \cdot \{\epsilon_1\} \\ \{P_2\} &= [K] \cdot \{\epsilon_2\} \\ \{P_3\} &= [K] \cdot \{\epsilon_3\} \end{aligned}$$

These three relations can be combined as,

$$\left(\begin{matrix} \{P_1\} \\ \{P_2\} \\ \{P_3\} \end{matrix} \right) = [K] \underbrace{\left(\begin{matrix} \{\epsilon_1\} \\ \{\epsilon_2\} \\ \{\epsilon_3\} \end{matrix} \right)}_{[E]^T}$$

On the other hand,

$$\left(\begin{matrix} \{P_1\} \\ \{P_2\} \\ \{P_3\} \end{matrix} \right)^T = \left(\begin{matrix} \{P_x\} \\ \{P_y\} \\ \{P_z\} \end{matrix} \right)$$

Therefore,

$$\left(\begin{matrix} \{P_x\} \\ \{P_y\} \\ \{P_z\} \end{matrix} \right) = [E] [K]^T$$

$$\text{Or} \quad [K]^T = [E]^{-1} \left(\begin{matrix} \{P_x\} \\ \{P_y\} \\ \{P_z\} \end{matrix} \right)$$

However, the degree of accuracy and reliability of the calibration statistically increases with the number of different loading configurations considered. Therefore five different configurations for each dynamometer were studied instead of three. The results were processed to obtain the best $[K]$ -matrix using the principle of least squares. It can easily be shown (Ref. 28, page 171) that the best n unknowns are determined, by the principle of least squares, from m ($m > n$) equations as explained below:

The problem is defined by,

$$\begin{matrix} L & \cdot & x & = & h \\ (m.n) & & (n.1) & & (m.1) \end{matrix}$$

If both sides are pre-multiplied by L^T

$$L^T L x = L^T h \quad \text{or} \quad x = (L^T L)^{-1} L^T h$$

The same principle can be applied to the problem of calibration,

$$\begin{matrix} [E] & [K]^T \\ L & x \end{matrix} = \begin{matrix} \left(\begin{matrix} \{P_x\} \\ \{P_y\} \\ \{P_z\} \end{matrix} \right) \\ h \end{matrix}$$

Then,

$$[K]^T = \left[[E]^T [E] \right]^{-1} [E]^T \left(\begin{matrix} \{P_x\} \\ \{P_y\} \\ \{P_z\} \end{matrix} \right)$$

If matrices $[A]$ and $[P]$ are defined as

$$[A] = \left[\left[[E]^T [E] \right]^{-1} [E]^T \right]^T$$

$$\text{and} \quad [P] = \left(\begin{matrix} \{P_x\} \\ \{P_y\} \\ \{P_z\} \end{matrix} \right)^T \quad \text{or}$$

$$= \left(\{P_1\} \{P_2\} \{P_3\} \right)$$

Then

$$[K] = [P] [A]$$

In this particular case n and m are 3 and 5 respectively. Therefore, $[P]$ is a (3.5) matrix, and $[A]$ is a (5.3) matrix. Consequently, their product $[K]$ is a (3.3) matrix.

As mentioned earlier, five different loading configurations were considered for the calibration of each dynamometer. In each case a load P was applied at the apex of the dynamometer in a particular direction which could be resolved into three known components. These configurations were:

<u>Conf.</u>	$\frac{P_z}{P}$	$\frac{P_x}{P}$	$\frac{P_y}{P}$
1	P	0	0
2	$\frac{\sqrt{3}}{2} P$	$\frac{1}{2} P$	0
3	$\frac{1}{\sqrt{2}} P$	$\frac{1}{\sqrt{2}} P$	0
4	$\frac{\sqrt{3}}{2} P$	0	$\frac{1}{2} P$
5	$\frac{1}{\sqrt{2}} P$	0	$\frac{1}{\sqrt{2}} P$

The mechanical details of calibration and the method of load application will be explained in the next paragraph.

For each of these configurations, the strain readings were recorded at a number of loading stages. The strains measured were then plotted against the load P , and a straight line was fitted to the strains of each leg by the least square method. A qualitative $P - \epsilon$ relationship is illustrated in Fig. 19. Then, strain values corresponding to $P = 1$ tonf. and the appropriate values of components of P were placed in the $[\epsilon]$ and $[P]$ -matrices respectively. Once all the five configurations were studied and the $[\epsilon]$ and $[P]$ -matrices were completed, the calibration matrix $[K]$ was calculated through the matrix operations explained above.

A comprehensive computer program was developed for the calibration of the reaction dynamometers. The measured strains and the corresponding load components, for both individual leg and general calibration cases,

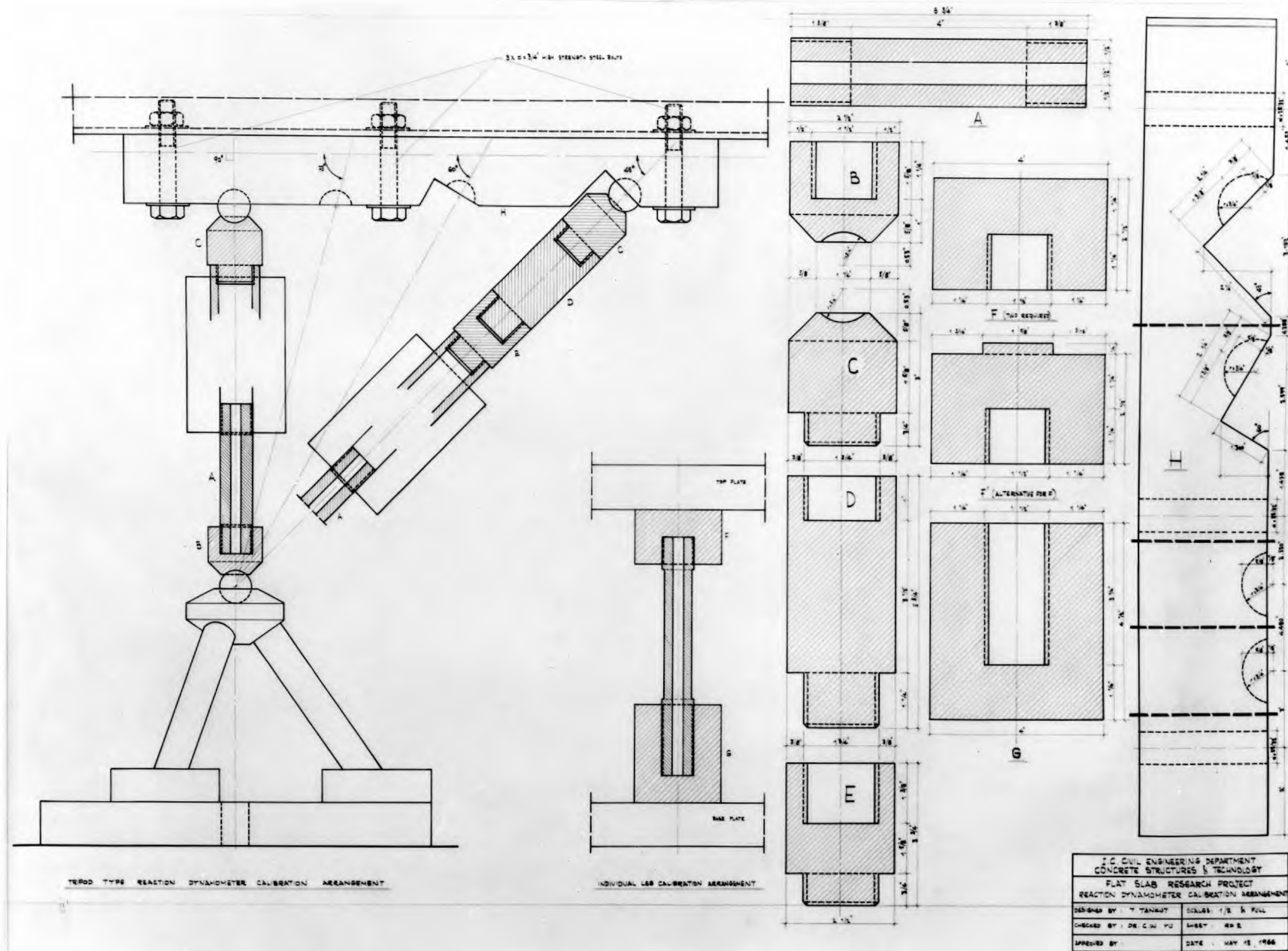


FIG. 18. REACTION DYNAMOMETER CALIBRATION DETAILS

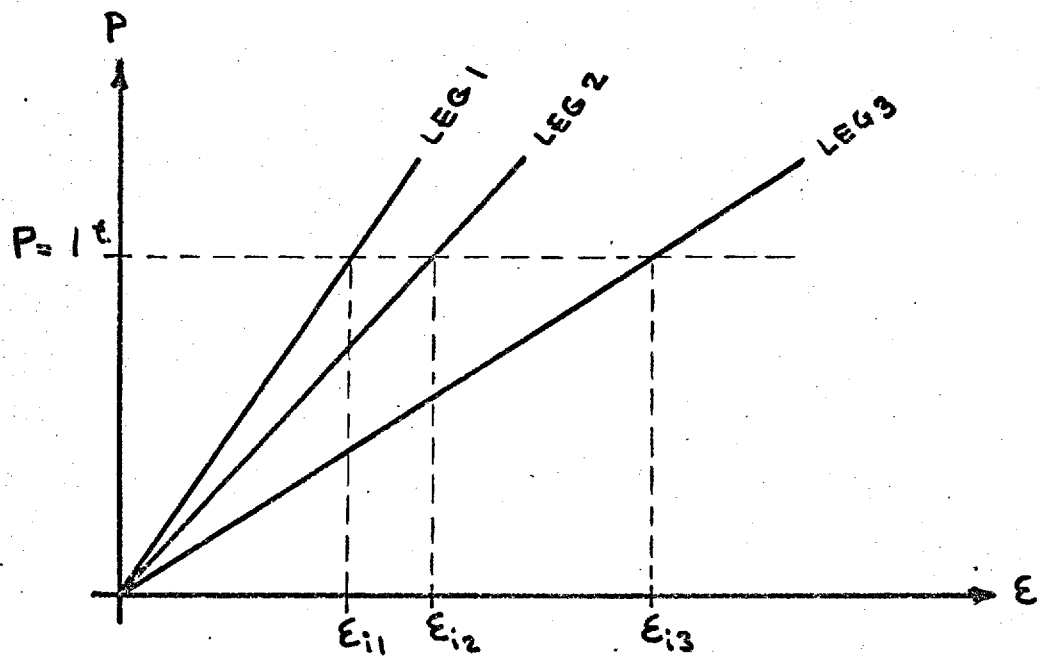


FIG. 19 - TYPICAL LOAD-STRAIN RELATIONSHIP FOR THE LEGS

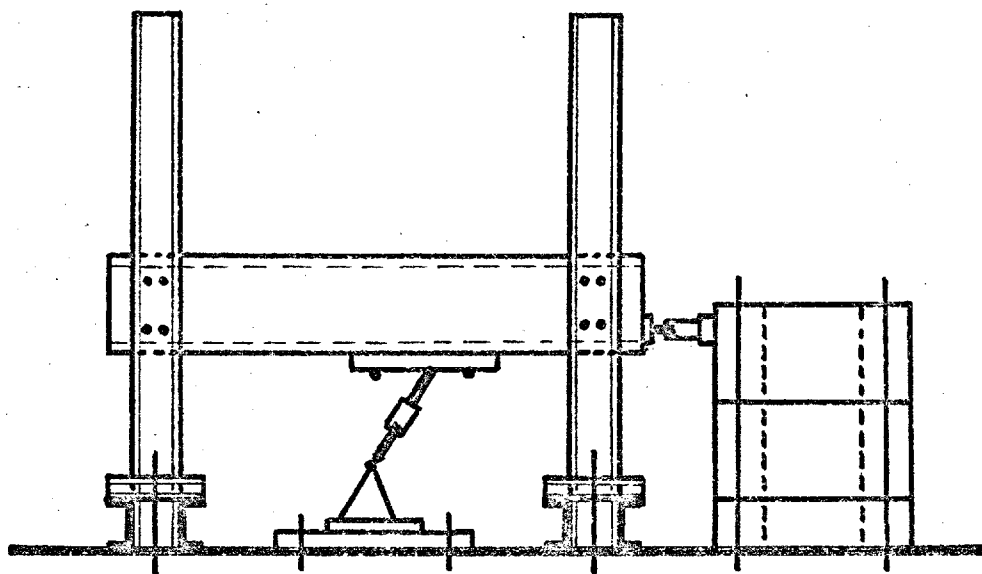
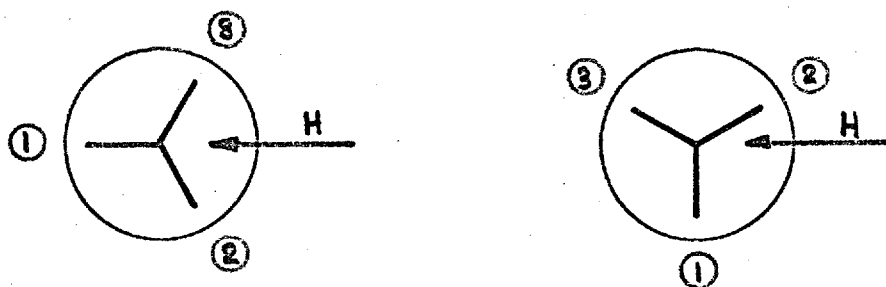


FIG. 20 - REACTION DYNAMOMETER CALIBRATION FRAME



a. POSITION 1

b. POSITION 2

FIG. 21 - REACTION DYNAMOMETER CALIBRATION POSITIONS

were fed into the computer. For the case of individual leg calibration, a straight line was fitted to the data for each leg, and the (AE) values were calculated. These values were then used to determine the theoretical $[K]$ -matrices. For the case of calibration as a whole, straight lines were fitted to the strain data to obtain the elements of the matrix $[\epsilon]$. Then the above explained matrix operations were carried out to calculate the experimental calibration matrices.

MECHANICS OF CALIBRATION - The individual calibration of the dynamometer legs was simple and straightforward. Two cylindrical steel blocks were manufactured to fit each end of a dynamometer leg as shown in detail in Fig. 18. It was then accurately placed in the 300 tonf. Amsler loading frame, and the strain readings were recorded at a number of loading stages. The calibration as a whole however required a much more elaborate system. The frame used for this purpose is schematically shown in Fig. 20 and the details are given in Fig. 18. As illustrated in these figures, a 30 tonf. capacity hydraulic jack, with a number of combinations of extension blocks, was used to apply the load at four different angles of inclination (90° , 75° , 60° , 45°) in the plane of the calibration frame.

Under the calibration frame, the dynamometer was bolted to a steel base, made of 15 in x 4 in. channel, fixed to the testing floor. This base had been prepared so that the dynamometer could be placed at various angles with respect to the calibration frame. The two positions used for the actual calibration are shown in Fig. 21. Considering these two positions, the loading configurations listed in the previous paragraph can be explained. Referring to the co-ordinate axes shown in Fig. 15,

<u>Conf.</u>	<u>Position</u>	<u>α</u>	<u>P_z</u>	<u>P_x</u>	<u>P_y</u>
1	1	90°	P	0	0
2	1	60°	$\frac{\sqrt{3}}{2} P$	$\frac{1}{2} P$	0
3	1	45°	$\frac{1}{\sqrt{2}} P$	$\frac{1}{\sqrt{2}} P$	0
4	2	60°	$\frac{\sqrt{3}}{2} P$	0	$\frac{1}{2} P$
5	2	45°	$\frac{1}{\sqrt{2}} P$	0	$\frac{1}{\sqrt{2}} P$

The pressure was applied to the hydraulic jack from an Amsler pressure cabinet, and the load P applied to the dynamometer was measured and adjusted by use of a pre-calibrated load cell.

5.3. DEFLECTION MEASUREMENT SYSTEM - A reasonably fine grid of deflection measurement points was essential to study the deformational behaviour of the test structure. Preliminary investigations showed that the grid would be reasonably satisfactory if the measurement points were spaced at 2 ft. centres. This meant more than 60 points over one half of the test structure. If dial gauges were used to measure the vertical deflections, three rather difficult problems would have to be faced:

- i. The time lapse between the first and the last readings. At least 20 to 30 minutes is required to take sixty or more such readings. That could have resulted in a considerable amount of creep.
- ii. At some points 4 to 6 inches of vertical deflection had been expected. The cost of so many dial gauges of this range of measurement would be considerable. Or otherwise resetting of smaller dial gauges could have caused enormous and dangerous practical problems.
- iii. If the dial gauge supporting system was designed to be placed over the test structure and independent of it, it would no doubt have introduced very difficult design problems due to the very long spans required.

The other alternative was the use of a level to measure the deflections by reading the scales fixed vertically at the measurement points on the test structure. In this case however, another source of error was to be faced in addition to the time lapse problem explained above. Due to the rotations of the measurement points, the scales would not remain vertical which might have caused a considerable amount of error in deflection readings.

There was of course another solution to all but one of the problems; the use of linear displacement transducers. They are sensitive enough; sixty of them can be recorded in 1 minute or so, provided that a recorder is available; there are a wide variety of sizes to choose from. But they cost £20 to £40 each; in other words, roughly £2000 was needed for the whole deflection measurement system.

Considering all these difficulties, a new system was developed. It was based on the simple principle of continuity. Ordinary plastic medical syringes which cost 10d. each were used as transducers. Through a plastic tube, the syringe was connected to a vertical glass tube, and filled with a coloured fluid. When the plunger of the syringe was pushed in, it displaced a volume of fluid which caused a change of fluid level in the glass tube in proportion to the ratio of cross-sectional areas of the syringe and the glass tube. Practically any magnification can be obtained in this manner by choosing suitable ratios of cross-sectional areas. In this particular case, 25 seemed to be reasonable and practical.

A supporting frame made of $1\frac{1}{2}$ in. x $2\frac{1}{2}$ in. steel box sections was placed under the slab and completely independent of the test structure. The syringes were fixed on this supporting frame so that the steel ball attached to the top of the plunger was just touching the underside of the slab. The details of the arrangement are clearly illustrated in Fig. 22. The spiral spring around the plunger ensured recovery and measurement of negative deflections.

The 67 glass tubes on the other end, were fixed in front of an illuminated box and arranged so that the deflected shape of each cross-section on the test structure could be seen immediately. At each loading stage, a photograph was taken of these tubes which clearly indicated the fluid levels. Thus the deflections of all the points were recorded automatically and simultaneously. A typical record of deflections is given in Fig. 23.

Of these 67 tubes, 65 were actual deflection measurements and the other two were used as reference tubes. The hydrostatic pressure applied by the fluid in the tubes was extremely small and therefore negligible, and the temperature and humidity were controlled in the laboratory. Nevertheless, it was thought that it would be wise to have two reference tubes having the same properties as the actual measurement systems but closed at the other ends. Each of these corresponded to the longest and shortest of the plastic tubes. Any deformation in the plastic tube due to pressure or temperature change should be the same in character in all of them and proportional to the length. If the changes in the two extreme cases were recorded, the intermediate ones could be corrected by simple proportioning.

The horizontal deflections, on the other hand, were simply measured with three dial gauges at the end of each column centre-line, in the horizontal load direction. They were supported by a frame made of scaffolding bars.

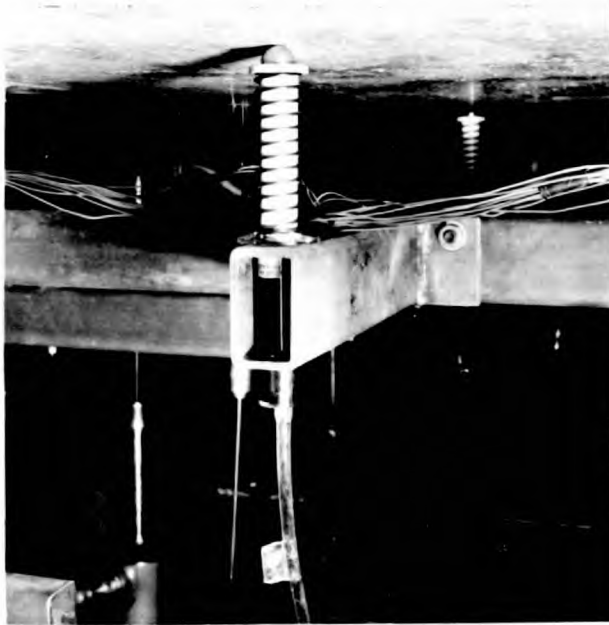


FIG. 22. DEFLECTION MEASUREMENT UNIT

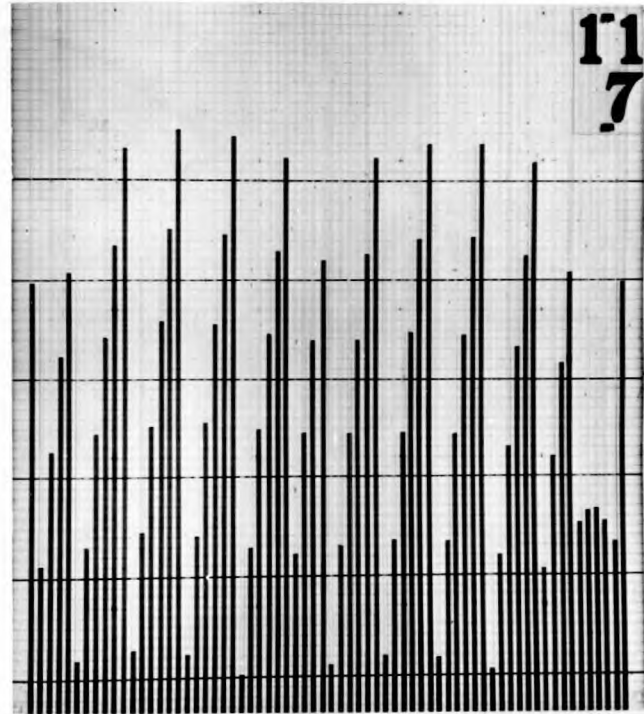


FIG. 23 - TYPICAL DEFLECTION RECORD

Clinometers were also used to record the rotation at certain parts of the test structures. However, the number of clinometers available in the laboratory was not sufficient to cover the whole test structure. Since they could measure the rotation in only one direction, two of them were required at each measurement point. Therefore this type of clinometer was not the ideal instrument to be used on two dimensional structures. A special two-way clinometer based on the suggestion of Prof. Baker was developed, and a prototype was manufactured with the intention of producing a sufficient number of them to cover the whole test structure. But due to some problems faced in preparing the prototype, it was anticipated that the manufacture of so many of them might take a considerable time and therefore might cause unjustified delay. However, the idea on which the design was based, will be explained below.

If a segment of sphere is filled with a fluid and a small air bubble is left inside, the container may be considered as a two-way spirit level. If it is graded to indicate the angle of rotation in two perpendicular directions, it becomes a two-way clinometer. Fig. 24 illustrates the design of the prototype. The practical requirements determined most of the dimensions:

$$\text{the diameter,} \quad d_{\text{practical}} = 6 \text{ inches}$$

$$\text{the rotation capacity,} \quad \theta_{\text{practical}} = \text{Arc Tan } \frac{1}{10}$$

$$\begin{aligned} \text{the spacing of the} \\ \text{division lines,} \quad s = 1 \text{ mm} = 0.04 \text{ in.} \end{aligned}$$

Referring to the geometry illustrated in Fig. 24,

$$r = \frac{d}{2 \sin \theta} \approx \frac{d}{2 \tan \theta} = \frac{6}{2 \times 0.1} = 30 \text{ in.}$$

$$x = r(1 - \cos \theta) = 30(1 - 0.995) = 0.15 \text{ in.}$$

Then the sensitivity is,

$$\Delta \theta = \frac{\frac{1}{2} \times s}{r} = \frac{0.02}{30} = 0.000667 \text{ rad.} \approx 2'$$

In the prototype, the base was made of an aluminium alloy. A circular glass sheet was cut spherically to the required geometry, and fixed on the base. It was then filled and sealed. A thin sheet of perspex on which the division lines had been marked, was fixed on top of the glass sheet. The instrument was placed at the measurement point with its axes parallel to

those of the test structure, and by using its three adjustable point supports it was adjusted so that the air bubble was right at the origin of the axes. As the point rotated under load, the air bubble moved from the origin. The components of this movement indicated the rotations along the corresponding axes. But unfortunately, in spite of all the efforts the size of the air bubble could not be controlled. If this problem can be solved, an ideal instrument for this kind of experiment can be designed based on this principle.

5.4. STRAIN MEASUREMENT SYSTEM - As explained in Chapter 7, a knowledge of the steel strains is essential to study the flexural behaviour of the test structure; similarly the concrete strains are very important for the investigation of the local behaviour of the slab-column junctions. Therefore a successful and satisfactorily comprehensive strain measurement system has an enormous value as far as the whole research project is concerned.

Despite the fact that the spacing of the reinforcement was somewhat different in the two test structures, it was possible to adopt exactly the same pattern for the steel strain measurement points. A grid of approximately 20 in. x 30 in. was chosen for steel strain measurement points in both directions. The pattern is shown in Figs. 25 and 26. In plan, all the strain gauges along a particular section seem to be on the same bar, but in fact some of them are on the bottom bar and some are on the top. This situation is illustrated in Fig. 27. Since the tension bars are expected to be further away from the neutral axis than the compression bars, higher strains and consequently higher sensitivity are expected from the strain gauges on the tension bars.

To measure the steel strains Saunders-Roe foil gauges having $\frac{1}{2}$ in. gauge length and a nominal resistance of 120 Ω , were used. They were fixed on the reinforcement with "Araldite 103" plus "Hardner 951", and water-proofed with "Gage Cote 5", a two part epoxy resin.

These strain gauges were not simply fixed on the surface of the bar, but they were placed in specially cut longitudinal slots. The shape and dimensions of these slots are shown in Fig. 28. Numerous tests had been carried out to compare the performance of the strain gauges placed in this kind of slot with that of strain gauges conventionally fixed to the surface. The results consistently indicated the following advantages of the slot gauges.

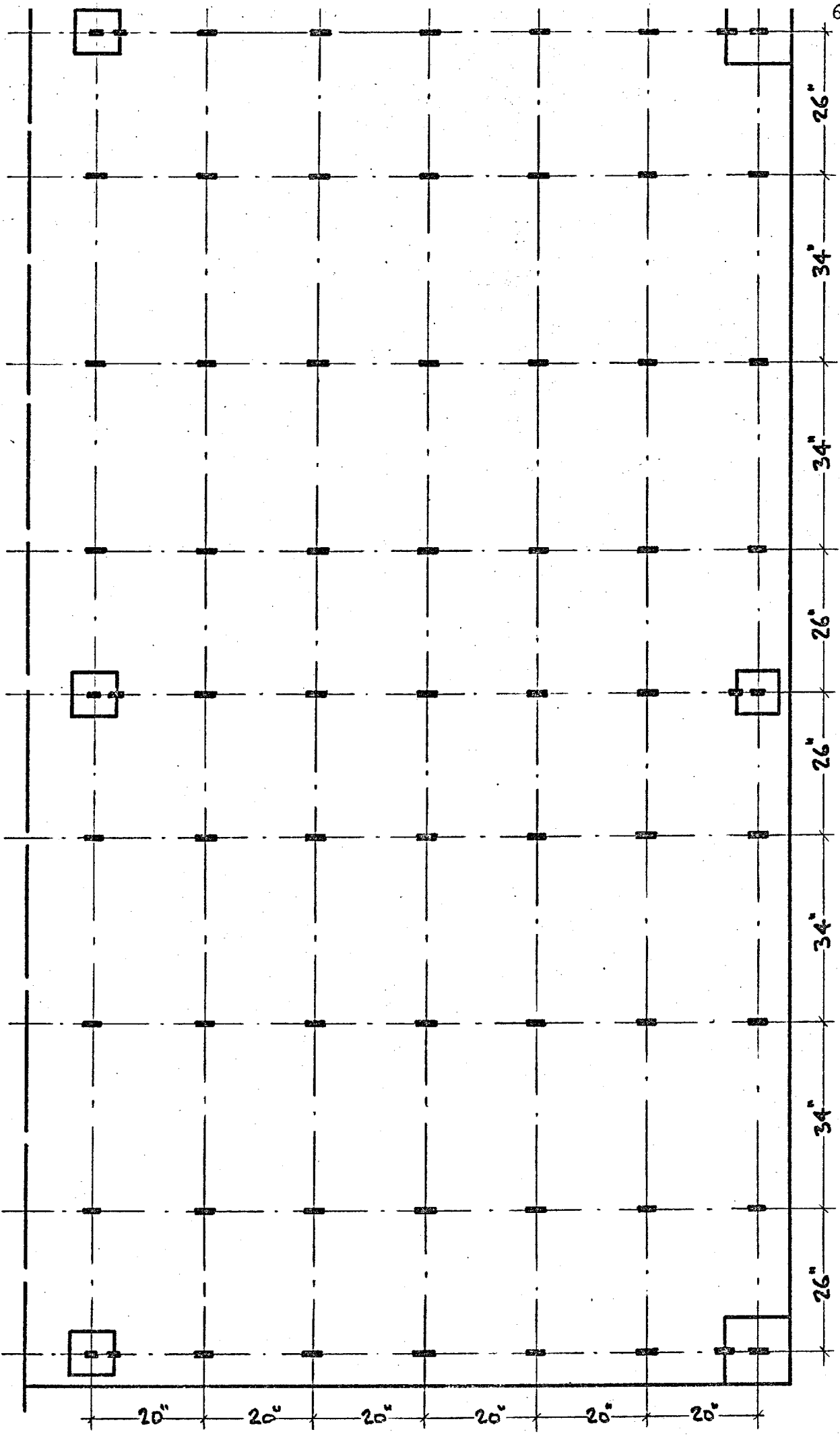


FIG. 25 - LOCATION OF STRAIN GAUGES ON REINFORCEMENT IN X-DIRECTION

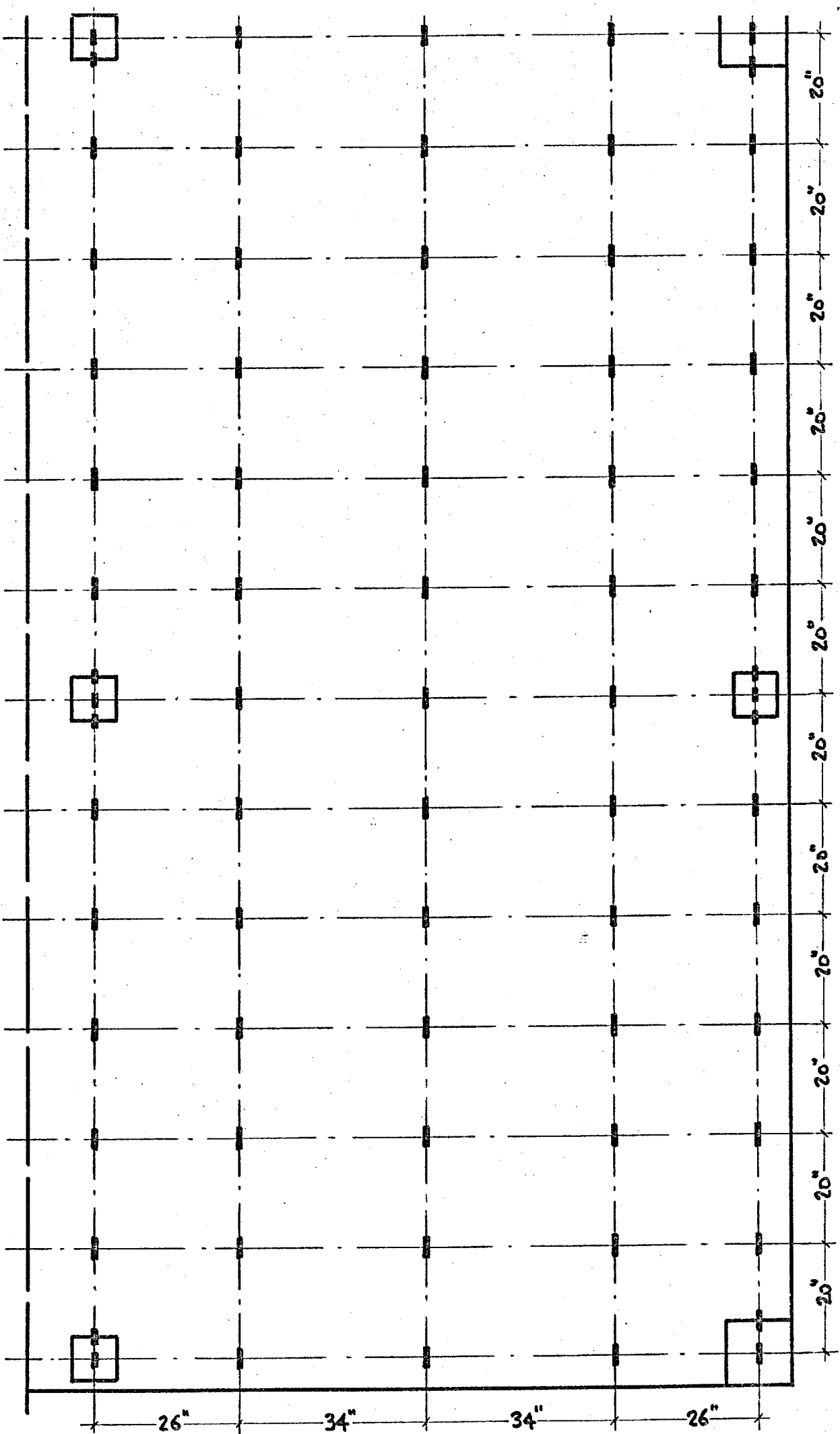


FIG. 26 . LOCATION OF STRAIN GAUGES ON REINFORCEMENT IN Y-DIRECTION

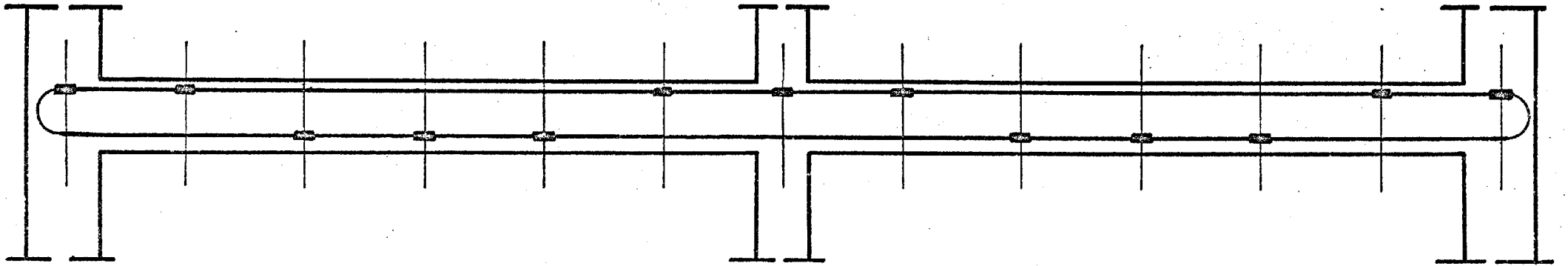


FIG. 27 - LOCATION OF STRAIN GAUGES ON REINFORCEMENT ALONG A SECTION

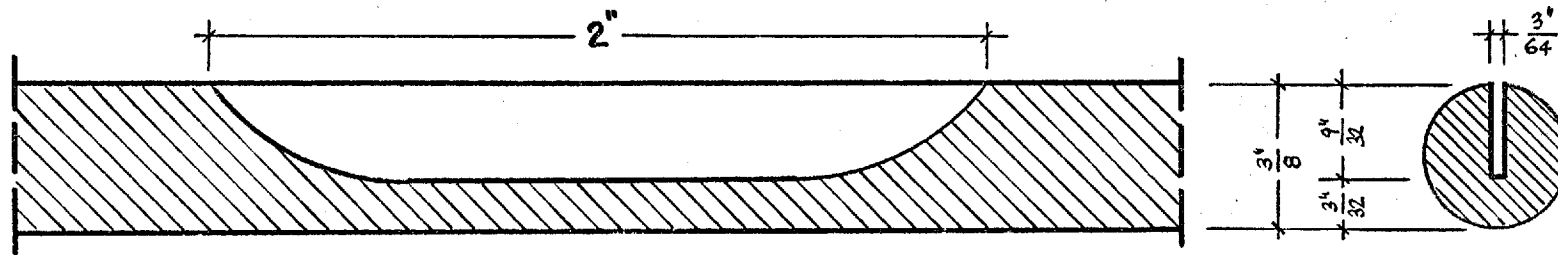


FIG. 28. STRAIN GAUGE SLOT DETAILS

- i. Smaller effects of eccentricity were expected and in fact, observed due to the strain gauge being positioned nearer the centroid of the cross-section than is the case for the surface gauge. In this sense, slot gauges can be considered as measuring the actual internal strains, instead of the peripheral strains measured by surface gauges.
- ii. Far better protection against external damage is provided by using slot gauges. A very good example of this was given by the unsuccessful first trial of casting the test structure 1. As explained in the following sub-section the concrete had to be removed after placing. This operation inevitably required a rather harsh handling of the reinforcement. When the strain gauges were checked at a later date, curiously enough, only two out of 163 gauges were found damaged.
- iii. Far better water-proofing is possible for slot gauges. The slots were filled with an epoxy resin after positioning the gauges; then the water-proofing material was applied. The tests had shown that the slot gauge was also superior to the surface gauge in this respect.

To measure the concrete strains around the column heads, a number of Tokyo Sokki wire gauges having 60 mm. gauge length and a nominal resistance of 120 Ω were used. The adhesive used to attach them was "PS Drug A plus Drug B" made and recommended by the manufacturer of the gauges.

The number of gauges and the pattern in which they were arranged, were different for the two test structures. For the test structure 1, 150 gauges were arranged in the pattern shown in Fig. 29. Along some comparatively more important sections rosettes were formed. Since each gauge was recorded separately, two members of a rosette indicated the tangential and the radial strains at that particular point as well as providing information for the determination of the principal strains and the principal directions. However, after testing the test structure 1, it was realised that some gauges nearer the column were required, and the rosettes were not so useful as had been expected. Therefore, the pattern was entirely changed for the next test structure. The new pattern which was composed of 116 strain gauges is illustrated in Fig. 30. In this case, T-shaped combinations were used, and the instrumentation was limited to comparatively more important sections.

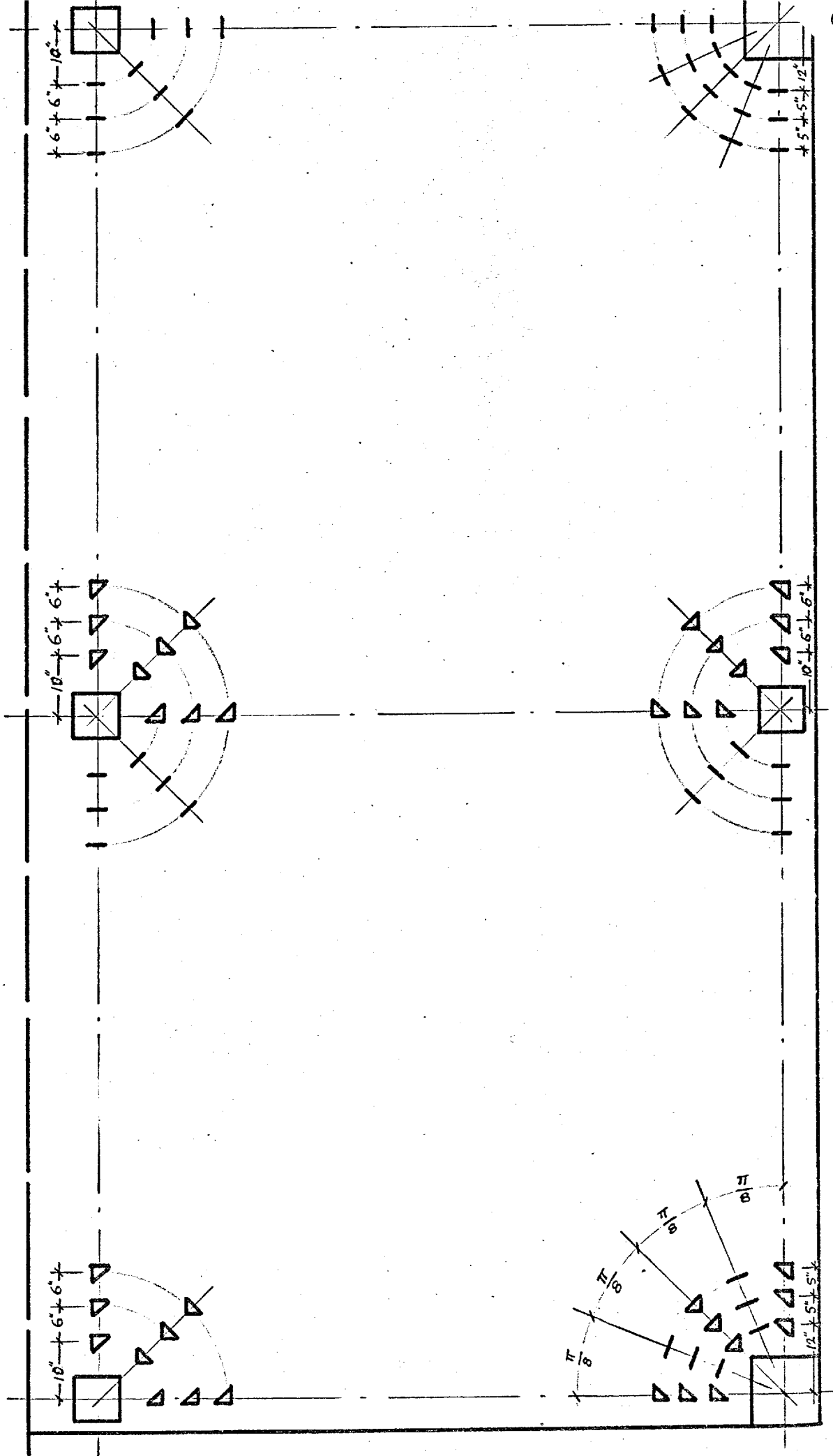


FIG. 29 . LOCATION OF SURFACE STRAIN GAUGES ON THE TEST STRUCTURE I

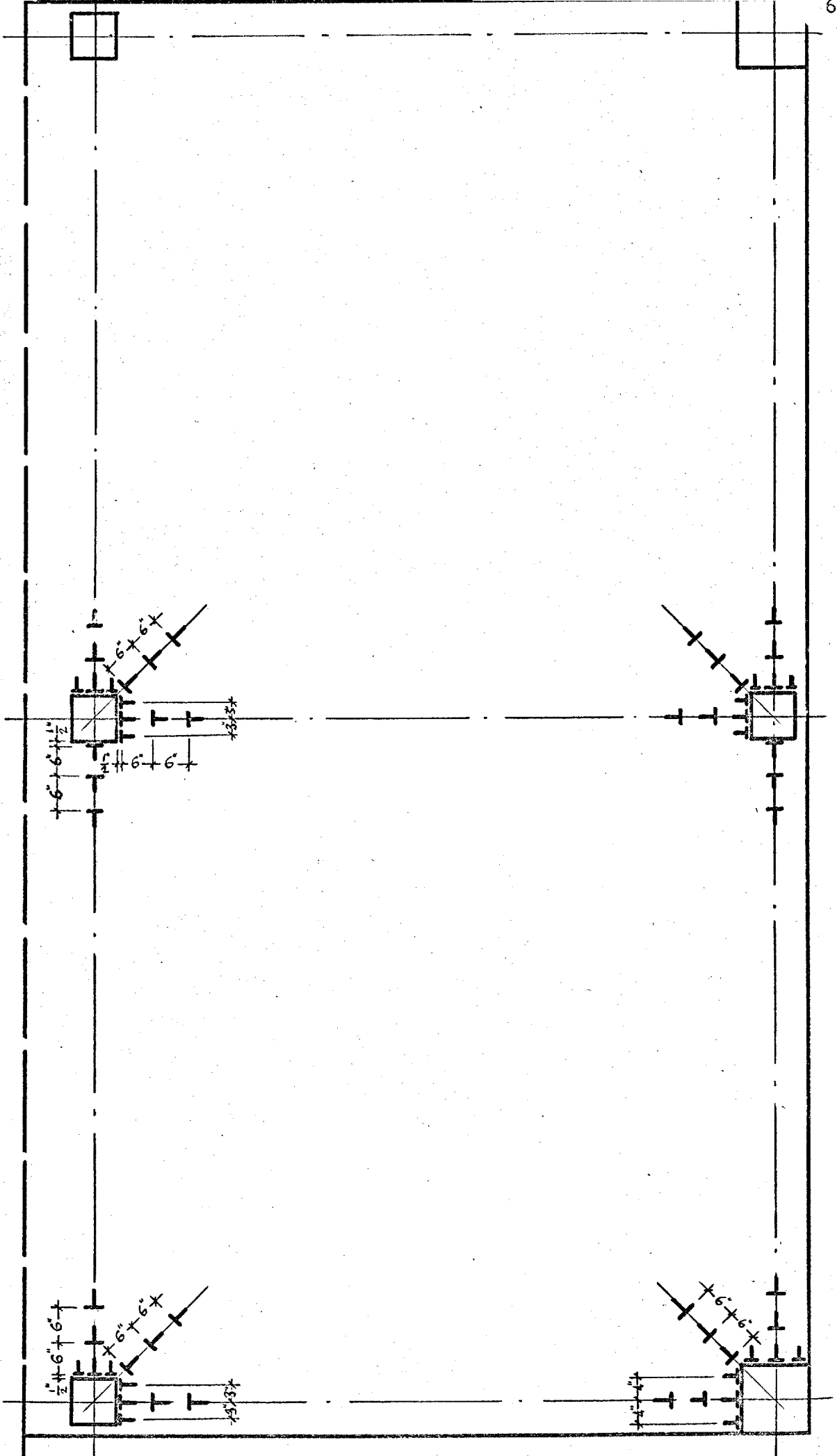


FIG. 30 . LOCATION OF SURFACE STRAIN GAUGES ON THE TEST STRUCTURE 2.

5.5. MATERIALS - When the number of specimens to be tested is limited, it is obviously best to keep unchanged as many parameters as possible. It was therefore desirable to have identical material properties for both of the test structures. This principle was reasonably satisfied for the concrete used for the test structures; but in the case of the reinforcement, some more important considerations led to the decision to use a different kind of steel in the test structure 2.

5.5.1. CONCRETE - Ready mixed concrete was used for both test structures. The mix was specially designed by Ready Mixed Concrete Ltd. to attain a cube strength of 6000 psi at 28 days. The mix was also designed for ease of placing and compacting. Approximately 8 cu.yd. of concrete had to be placed each time. By laboratory standards, this is a rather considerable amount. It took 3 to 4 hours for placement, compacting and screeding. Since only two separate mixes were used, a reasonable workability was needed for at least two hours after mixing. To ensure this, an initial slump of 3 to 4 in. and at least 1 in. slump at 3 hours were specified. Therefore the use of a retarder was inevitable. Before the casting of the test structure 1, the published data on retarders was studied in co-operation with Ready Mixed Concrete Ltd. From this data a suitable retarder was chosen and the amount required was determined. Some tests were carried out in the laboratories of Ready Mixed Concrete Ltd. These gave satisfactory results which led to the final decision concerning the material to be used, the casting date, etc. The initial tests on the casting day seemed satisfactory; therefore the casting was started. But 2 hours later, when more than half had already been placed, the concrete started to stiffen rapidly. By the time two thirds were in place, it was understood that the casting could not be completed. A group discussion on the spot resulted in the decision to reject the concrete before it was too late. A good deal of granulated sugar was spread over the concrete in place and some water was added. With the invaluable efforts of the technicians and the students, the concrete was removed and the formwork and the reinforcement cleaned. It took over a month to prepare for another casting. The accelerating effect of the so called retarder was studied and unsatisfactorily explained by Ready Mixed Concrete Ltd. by a probable chemical reaction between the retarder and the dry mix before the water was added. After this unpleasant experience, most of the retarders available in this country were comprehensively tested; one was chosen and it was made sure that exactly the same procedure would be followed in preparing the actual mix as in the



FIG. 31 . GENERAL VIEW DURING THE CASTING OPERATION

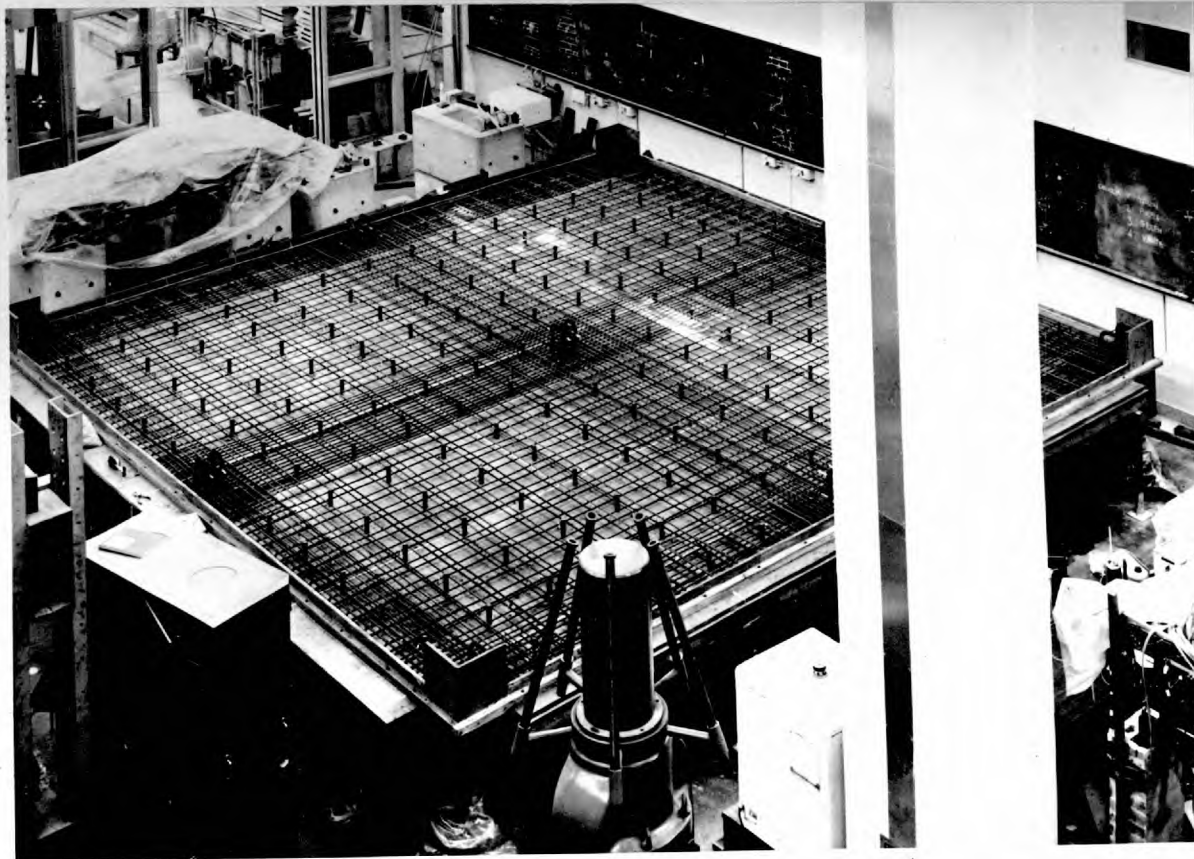


FIG. 32 . GENERAL VIEW OF THE REINFORCEMENT PRIOR TO CASTING

test mixes. As a result of this investigation, the next trial was successful; both of the test structures were cast without any serious difficulty. Together with each test structure, six strip beams, sixteen cubes, eight cylinders and eight 4" x 4" x 20" prisms were cast.

Here, it must be mentioned that the screeding of a slab of these dimensions, with the accuracy required by research standards presented some difficulty. A large screeding board was designed for this purpose. It was hung on one of the cranes with specially designed spiral springs so that it was not too heavy to handle and was heavy enough to serve the purpose. The result obtained was $\pm \frac{1}{8}$ in. on the slab thickness, and it was regarded as satisfactory.

When the casting was completed, a curing compound (Febcure Super 90) was sprayed over the exposed slab surface to prevent shrinkage cracks. A couple of hours later, when the concrete had reasonably stiffened, the structure was covered with wet hessian, and a layer of polythene was spread on top to reduce the evaporation to a minimum. However, the hessian was wetted every other day up to the 28th day after casting. The strip beams were cured in exactly the same manner. The control specimens were stripped on the 7th day and then immersed in water at 20°C.

When the specimens were tested, the following average material properties were obtained:

$$\begin{aligned} \text{For the test structure 1; } f_{cu} &= 6200 \text{ psi} \\ E_c &= 4.62 \times 10^6 \text{ psi} \end{aligned}$$

$$\begin{aligned} \text{For the test structure 2; } f_{cu} &= 6700 \text{ psi} \\ E_c &= 5.80 \times 10^6 \text{ psi} \end{aligned}$$

The values obtained were considered satisfactorily close to the specified ones.

5.5.2. STEEL - The reinforcement in the test structure 1, consisted of $\frac{3}{8}$ in. diameter deformed bars of high tensile strength steel. Its trade name is "Norhite 60" indicating a guaranteed 60000 psi yield strength. This type of steel has a well defined yield point and a high ductility. The deformations on the bars were in the form of longitudinal and transversal ribs providing good bond strength and crack control properties. A number of specimens were tested and the average values of yielding stress and modulus

of elasticity given below, were obtained:

$$f_y = 58600 \text{ psi}$$
$$E_s = 24.44 \times 10^6 \text{ psi}$$

On the other hand, mild steel bars of the same standard size were used for the test structure 2. These were plain bars with 40,000 psi guaranteed yield strength. The tests conducted on a number of specimens gave the following average values:

$$f_y = 44900 \text{ psi}$$
$$E_s = 26.67 \times 10^6 \text{ psi}$$

For the column reinforcement in both of the test structures, 1 in. diameter plain bars of 60000 psi high strength steel were used. This material was not tested to obtain very accurate values, because the strength of the columns, as explained in Chapter 3, was not at all critical. On the other hand, these bars were annealed for bending to the required U-shape; their properties would therefore have been affected by this process.

CHAPTER 6

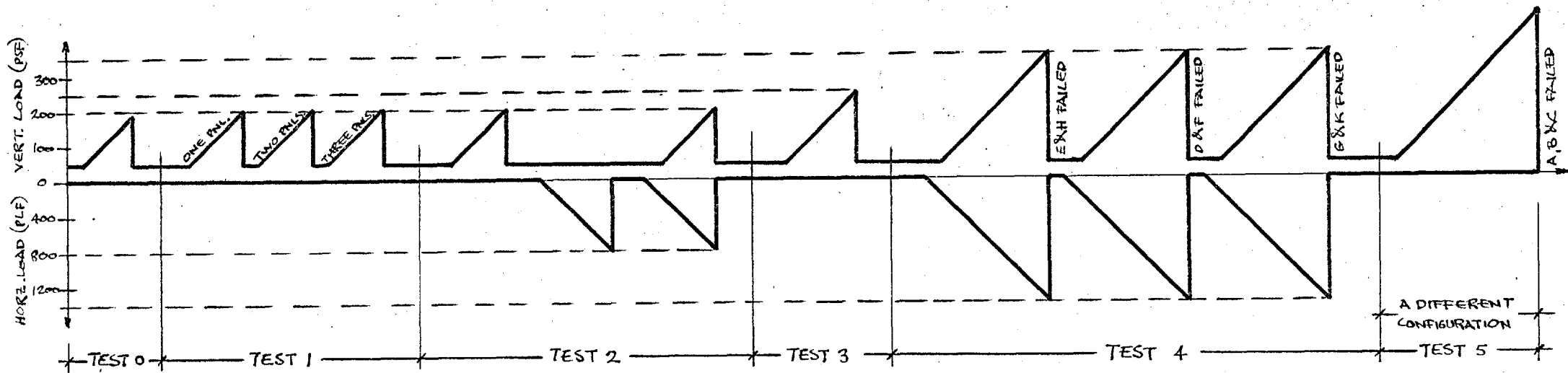
TESTING PROCEDURES AND RESULTANT BEHAVIOUR OF THE TEST STRUCTURES

Outlines of the tests conducted on each test structure were briefly explained in Chapter 3 where the loading history diagrams were first introduced. In the present chapter, each test carried out on each test structure, and the performance of the test structure during these tests are explained in detail. The actual applied loading history diagrams (Fig. 3.3) were much more complicated than the ones presented in Chapter 3. In other words, not only were the principal tests carried out, but also a number of auxiliary tests were conducted on each test structure.

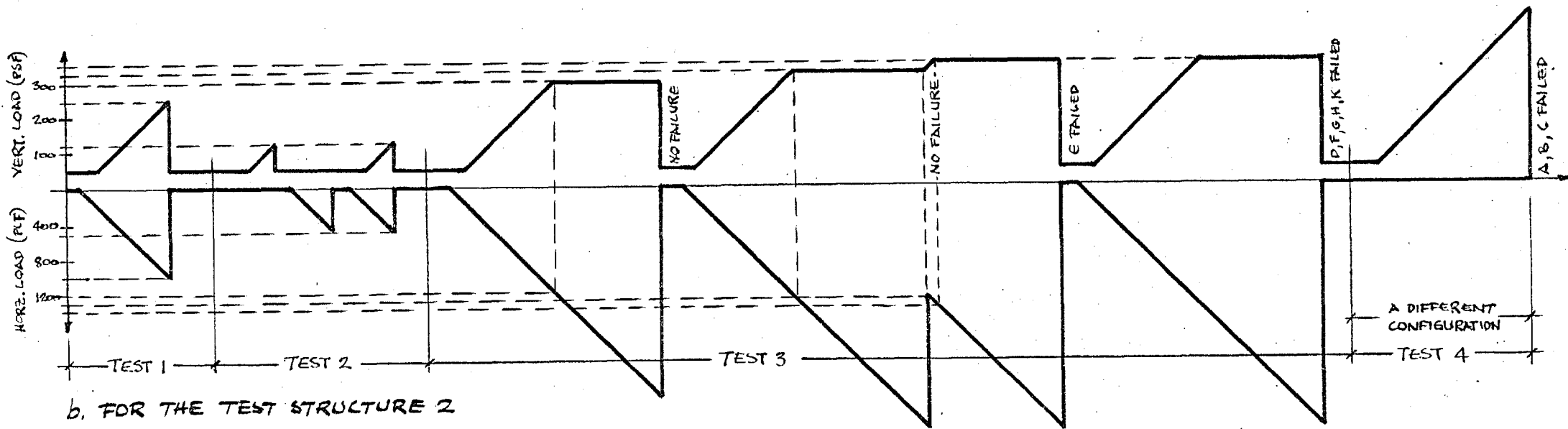
6.1. TESTS CONDUCTED ON THE TEST STRUCTURE 1 - Being the first one to be tested, the test structure 1 underwent a larger number of tests than the test structure 2. The performance of the instrumentation systems as well as the behaviour of the test structure itself had to be tested. Apart from one or two minor modifications required during the tests, the intended testing plan was followed. The actual applied sequence of loading is illustrated in Fig. 33a.

6.1.1. TEST 0: COMPLETE INSTRUMENTATION CHECK - The purpose of this test was to see whether each item of the whole system would work as planned. Only the vertical load was applied up to nearly the design vertical load. Every single part of the instrumentation was employed to its full capacity. All the systems seemed to be working satisfactorily, and in addition it was seen that only two skilled persons could carry out all the experiments except at the critical stages. Later the data from the reaction dynamometers and the load cells were evaluated and compared with the applied load. This comparison indicated that the applied pressure had not quite produced the loads intended. Therefore, the pressure-load relationship for the loading system was revised before proceeding any further.

Starting from the dead weight which was one quarter of the design vertical load, the load was applied in increments of approximately one eighth of the design vertical load. Visible cracking started at about 0.6 times the design vertical load; negative moment cracks appeared around the



a. FOR THE TEST STRUCTURE 1



b. FOR THE TEST STRUCTURE 2

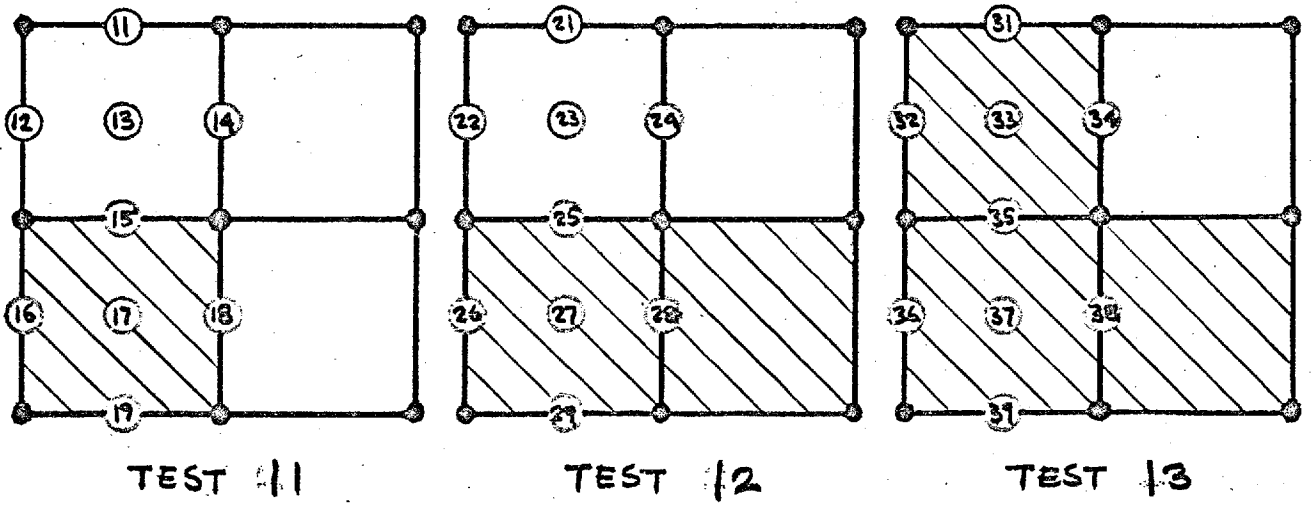
FIG. 33 - APPLIED LOADING HISTORY DIAGRAMS FOR THE TEST STRUCTURES

columns mostly at the root of the upper columns. Some diagonal and some radial negative moment cracks were added to these at the last stage of the test when the load reached approximately 0.9 times the design load. Besides these local cracks around the columns, a continuous negative moment crack along the BEH column centre-line and two continuous positive moment cracks along the panel centre-lines in the E-W direction appeared at this last stage. The moment distributions and the deflection surface as well as the reactions of this stage are presented in Appendix 1.

6.1.2. TEST 1: PANEL BY PANEL LOADING TEST - This test was intended to investigate the influence of partial loading on the behaviour of the structure, and at the same time to see whether individually loaded panels could be superimposed. The test consisted of three parts with one, two and three panels loaded respectively. In each part only the vertical load was applied up to the design vertical load with increments of one eighth of the design vertical load. Based on the comparisons explained in Chapter 3 (Fig. 8), the extent of reliability of superposition was studied. To this end, nine critical points (Fig. 34) were chosen; the two components of the bending moment and the deflection were determined at each of these points (Table 4), and the quantities obtained were compared with the corresponding appropriate quantities (Table 5). The study showed that the effects of partial loads can be superimposed within the limits of working loads. In general, differences of less than 10% were noticed.

Another observation confirmed the anticipated behaviour under repeated loading. It was thought that such loading would cause additional cracking which in turn would reduce the flexural rigidity, thus causing higher deflections. From this point of view, the idea of having "Panel by Panel Loading" tests before the principal tests, may be criticised. One cannot be certain that this kind of unsymmetrical loading would not have affected the behaviour of the test structure during the later tests. However, the results obtained from the later tests indicate that the symmetry of the behaviour had not been considerably disturbed. Especially at the stages above the design load, the influence of previous unsymmetrical repeated loading decreased as the loading increased.

6.1.3. TEST 2: CHECK FOR VALIDITY OF SUPERPOSITION - This test was the last auxiliary test before the main tests. It consisted of three parts; in the first part the vertical load alone was applied over the whole slab, in the second part the test structure was loaded with only the horizontal load, the last part was a combined loading test. In all of the above parts



PT.	COMP. 1	COMP. 2A	COMP. 2B	COMP. 3	COMP. 4
1	$25 = 15 + \overline{14}$	$31 = 21 + \overline{16}$	$35 = 25 + 15$	$35 = 15 + 15 + \overline{14}$	$31 + \overline{12} = 21 + 29$
2	$26 = 16 + \overline{11}$	$32 = 22 + \overline{19}$	$36 = 26 + 12$	$36 = 12 + 16 + \overline{11}$	$32 + \overline{11} = 22 + 26$
3	$27 = 17 + \overline{13}$	$33 = 23 + \overline{17}$	$37 = 27 + 13$	$37 = 13 + 17 + \overline{13}$	$33 + \overline{13} = 23 + 27$
4	$28 = 18 + \overline{15}$	$34 = 24 + \overline{15}$	$38 = 28 + 14$	$38 = 14 + 18 + \overline{15}$	$34 + \overline{15} = 24 + 28$
5	$29 = 19 + \overline{12}$	$35 = 25 + \overline{18}$	$39 = 29 + 11$	$39 = 11 + 19 + \overline{12}$	$35 + \overline{14} = 25 + 25$

FIG. 34 - POINTS CONSIDERED AND DETAILED COMPARISON TABLE (*)

QUANT.	TEST	Pt. 1	Pt. 2	Pt. 3	Pt. 4	Pt. 5	Pt. 6	Pt. 7	Pt. 8	Pt. 9
δ	11	0	-5	0	-6	47	72	132	51	72
	12	-11	-7	-6	-10	42	86	158	145	64
	13	93	70	139	39	122	67	165	140	68
M_x	11	0	20	360	-220	1200	-200	1340	-1020	1260
	12	0	0	400	-560	1360	-200	1250	-1200	1120
	13	1360	-80	1560	-1200	2020	-120	1400	-1400	1250
M_y	11	0	0	-150	0	-720	1160	1100	1280	-80
	12	0	0	-100	0	-1050	1100	1350	1580	-20
	13	-80	1450	1050	1420	-1700	1200	1250	1450	-60

TABLE 4 - MEASURED QUANTITIES TO BE COMPARED

(*) BAR INDICATES THAT THE COMPONENTS ARE TO BE INTERCHANGED

COMP.	δ			M_z			M_y		
	LHS	RHS	DIFF.	LHS.	RHS	DIFF.	LHS	RHS	DIFF.
11	42	41	-1	1360	1200	-160	-1050	-940	-110
12	86	72	-14	-200	-200	0	1100	1160	60
13	158	132	-26	1250	1190	-60	1350	1460	110
14	145	98	-47	-1200	-1740	540	1580	2480	900
15	64	67	3	1120	1260	140	-20	-60	40
2A1	93	61	-22	1360	1160	-200	-80	-200	120
2A2	70	65	-5	-80	-80	0	1450	1260	-190
2A3	139	126	-13	1560	1500	-60	1050	1240	190
2A4	39	37	-2	-1200	-1280	80	1420	1200	-220
2A5	122	93	-29	2020	2640	620	-1700	-2070	370
2B1	122	89	-33	2020	2560	540	-1700	-1770	70
2B2	67	81	14	-120	-180	60	1200	1100	-100
2B3	165	158	7	1400	1610	210	1250	1200	-50
2B4	140	139	-1	-1400	-1420	20	1450	1580	130
2B5	68	64	-4	1250	1120	-130	-60	-20	-40
31	122	88	-34	2020	2400	380	-1700	-1660	-40
32	67	67	0	-120	-180	60	1200	1160	-40
33	165	132	-33	1400	1550	150	1250	1310	60
34	140	92	-48	-1400	-1960	560	1450	2480	1030
35	68	67	-1	1250	1260	10	-60	-60	0
41	88	53	-35	1360	1120	-240	-80	-20	-40
42	70	79	9	-80	-200	120	1450	1100	-350
43	139	152	13	1410	1650	240	1410	1250	-160
44	86	135	49	-1920	1760	-160	2620	1580	-1040
45	116	84	-32	2020	2720	700	-1920	2100	180
AVR. DIFF.	-11 %			+10 %			+3 %		

TABLE 5 - "PANEL BY PANEL LOADING TEST" COMPARISON TABLE

the load was increased in steps of one eighth of the design load up to the full design load. The purpose was to study the effects of vertical and horizontal loads applied (i) separately, and (ii) together, and to check whether the same results can be obtained simply by adding the results of separate loading tests to obtain those of combined loading. To this end, the same points on the test structure were chosen as in the case of "Panel by Panel Loading" test; the two components of the bending moment and the deflections were determined and compared in Table 6. The table shows that the effects of the vertical and horizontal loads can be superimposed to an acceptable degree of approximation. Another fact which has already been mentioned in the discussion of the "Panel by Panel Loading" test was reconfirmed; repeated loading caused more cracking and consequently more deflections. An average 12% difference in deflections indicates that deflections were greater during the third and last part of the test, than those obtained by adding the results of the preceding two parts. Here it must be noted that the average difference observed during this test is very close to that observed during "Panel by Panel Loading" test.

6.1.4. TEST 3: CRACK PATTERN FORMATION TEST - This test was the first phase of the main testing. It was intended to create a pronounced crack pattern under vertical load only. The test structure had already cracked during the previous tests; however, the loading had never exceeded the design load. So, the cracking which had already taken place was regarded as "Normal Cracking" and it was assumed not to have changed the behaviour of the test structure. The cracking induced by this particular test was, in that sense, more important; it was regarded as "Overcracking" which might affect the behaviour of the test structure.

The vertical load alone was applied in the usual manner. Up to the design vertical load, there was very little change in the crack pattern. Two more loading stages beyond the design vertical load were chosen. A noticeable increase in both the number of cracks and the crack width occurred at these stages (Fig. 40). Although the test structure did not seem too weak to resist further load increments, it was decided to stop the test at this stage to avoid the risk of possible excessive local damage which might impair the subsequent tests, as the shear strength of the column regions could not be precisely estimated.

6.1.5. TEST 4: TESTING TO FAILURE - This test was the last and most important phase of the main testing programme. It was not as simple as had been planned since the test structure was weaker in shear than in

QUANT.	TEST	Pt. 1	Pt. 2	Pt. 3	Pt. 4	Pt. 5	Pt. 6	Pt. 7	Pt. 8	Pt. 9	AVR. DIFF.
δ	21	63	64	132	102	108	65	151	114	62	12%
	22	-3	-5	-3	-3	-5	-15	-12	-10	-3	
	23	67	69	144	110	115	63	162	120	63	
	23-(21+22)	7	10	15	11	12	13	23	16	4	
M_x	21	1280	-40	1650	-1520	1700	-100	1600	-1650	1400	-3%
	22	0	0	0	0	0	0	0	0	0	
	23	1300	-20	1600	-1500	1600	-150	1600	-1600	1250	
	23-(21+22)	20	-20	-50	-20	-100	50	0	-50	-150	
M_y	21	-20	1200	1450	1260	-1560	1300	1450	1600	0	5%
	22	0	-100	0	0	0	-100	0	-60	0	
	23	-80	1300	1400	1350	-1700	1400	1500	1500	40	
	23-(21+22)	60	200	-50	90	140	100	50	-100	40	

TABLE 6. COMPARISON TABLE FOR "CHECK FOR VALIDITY OF SUPERPOSITION TEST"

flexure, and the shear strength of each type of column region was different. To discard the test structure after having one column region failed, would have been a considerable waste. Therefore the test was performed in three parts which resulted in the failure of six of the column regions.

Before the first part of this test took place the test structure was cracked but otherwise undamaged. The combined load was applied in increments of one eighth of the design combined load. At the first load stage, only an increment of the horizontal load which corresponded to the dead weight of the test structure, was applied. Then both types of load were increased proportionally. Between 1.00 and 1.25 times the design combined load, a number of new cracks appeared which caused wider crack bands, without changing the outlines of the crack pattern. A considerable increase in crack width, especially of the cracks around the internal column, was observed between 1.25 and 1.50 times the design combined load. The next loading stage had been planned at 1.75 which could not be reached since the internal column (E) and the far end edge column (H) punched through at approximately 1.62 times the design load. In order to prevent the rest of the test structure from becoming badly damaged, the loads were rapidly removed without taking a set of readings which in any case would not be reliable.

To be able to continue testing so that the undamaged parts of the test structure could be used, a method of supporting the failed columns, was developed. Steel frames were designed which could be fixed to the slab using the loading holes around the columns, and braced against the column bases. Details of one of these frames, designed for an edge column, is given in Fig. 35. These frames can be regarded as column capitals since they serve the same purpose of increasing the length of the critical shear section. They can be criticised for having changed the flexural properties including effective span length, stiffness etc. This criticism is no doubt true. However, at this stage, it was already very clearly understood that the local strength of the column regions was more critical than the overall flexural strength. Therefore it was thought that some error in the study of the flexural behaviour could be accepted for the sake of having more possibilities of studying the local behaviour. As far as the study of the flexural behaviour is concerned, the test structure had become, in any case, less useful and reliable after failure of first column region.

After reinforcing the failed columns as explained above, the second part of the test was carried out. The combined load was applied again keeping the ratio of vertical to horizontal loads constant. But

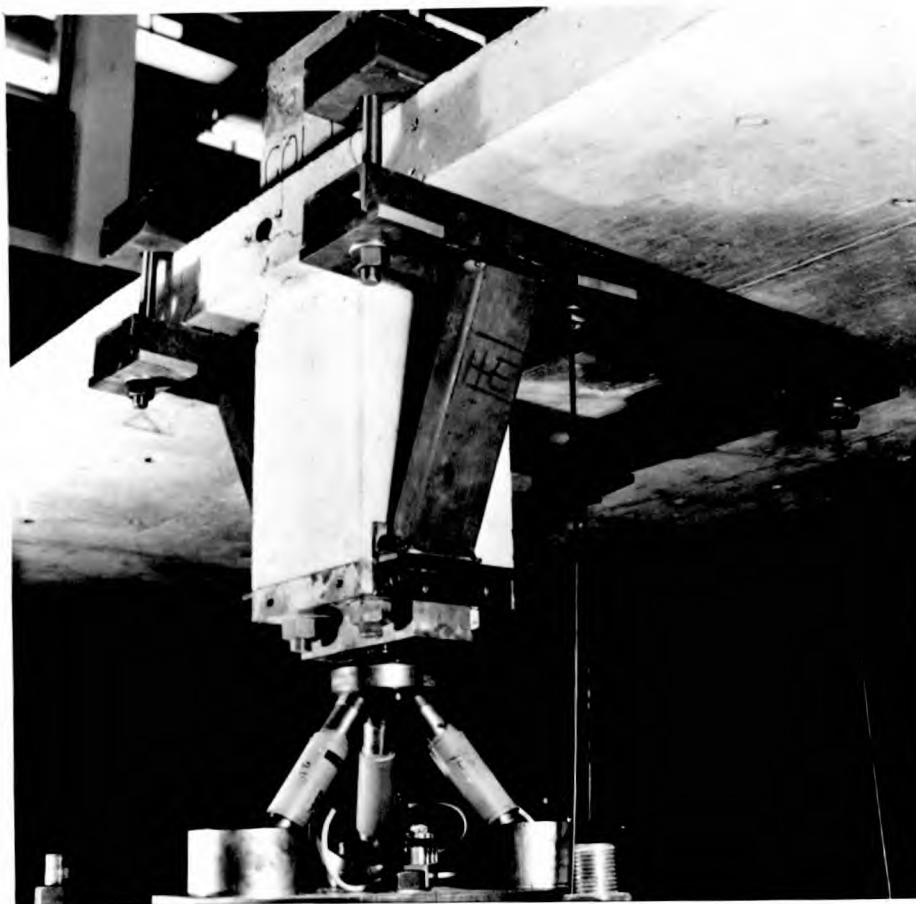


FIG. 35. DETAILS OF A SUPPORTING FRAME FOR A FAILED COLUMN

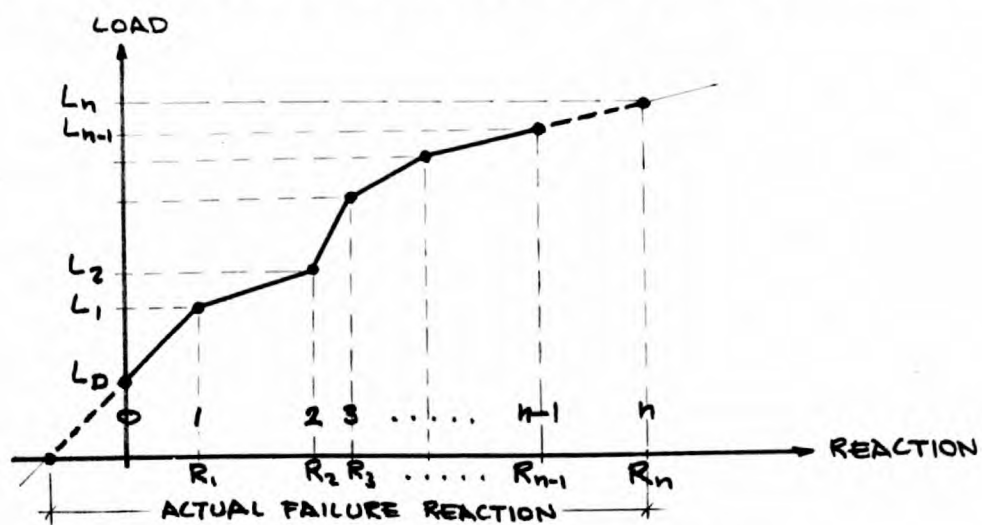


FIG. 36. CORRECTIONS FOR COLUMN REACTIONS

instead of loading incrementally, the load was applied without interruption up to 1.50 times the design load when the first set of readings was taken. After that stage, the load was increased in steps of one eighth or, towards the end, one sixteenth of the design load. During the course of this test the number of cracks considerably increased, and the deflection exceeded the value obtained at the corresponding load stages of the previous tests. At approximately 1.75 times the design load, two symmetrical edge column regions (D and F) punched through. The load was rapidly removed. The test structure was then prepared for the next loading, by strengthening the failed columns in the way previously described.

The third part of the test was more or less a repetition of the second part. The combined load was applied proportionally, and additional cracks and more deflections obtained. At a load slightly higher than the failure load for the two edge columns, approximately 1.80 times the design load, two far end corner columns failed. After strengthening these columns with steel frames, another attempt was made to induce failure in the columns on the less critical side of the test structure (A, B and C). But this could not be achieved, since the internal column again failed in shear forming a second and larger punching cone.

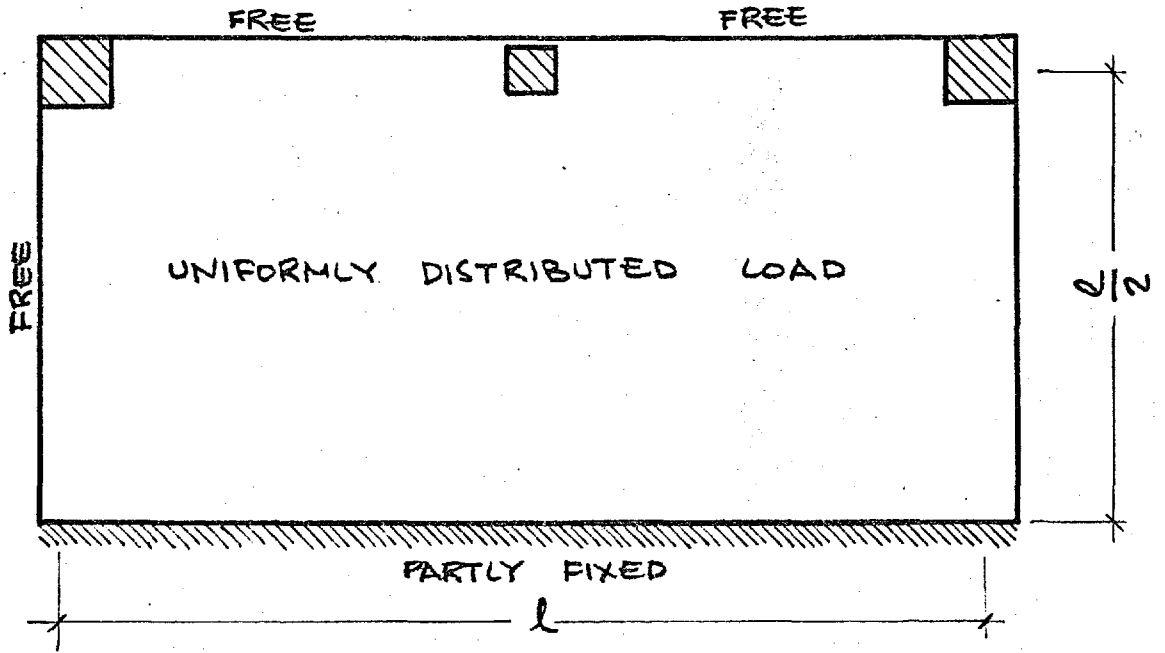
The actual column reactions at the punching load were obviously vitally important for the study of punching shear strength of the column regions. On the other hand it was quite impossible to measure the reaction at failure, since the failure was instantaneous which relieved the load suddenly. Therefore approximate punching reaction was estimated from the adjacent loading stage. The same problem existed also due to impossibility of measuring the dead weight reactions. A similar correction was applied in this case. Both corrections are illustrated by the qualitative, and exaggerated, load-reaction relationship of Fig. 36.

6.1.6. TEST 5: INDIVIDUAL COLUMN TEST - This test was a kind of "post mortem". The expected information had already been obtained from the tests already performed, but it was thought that the remaining three columns might provide some additional useful data; if not on the behaviour of the test structure, at least on the punching shear strength of these column regions. Most of the work on this particular subject has, in fact, been carried out on similar isolated models.

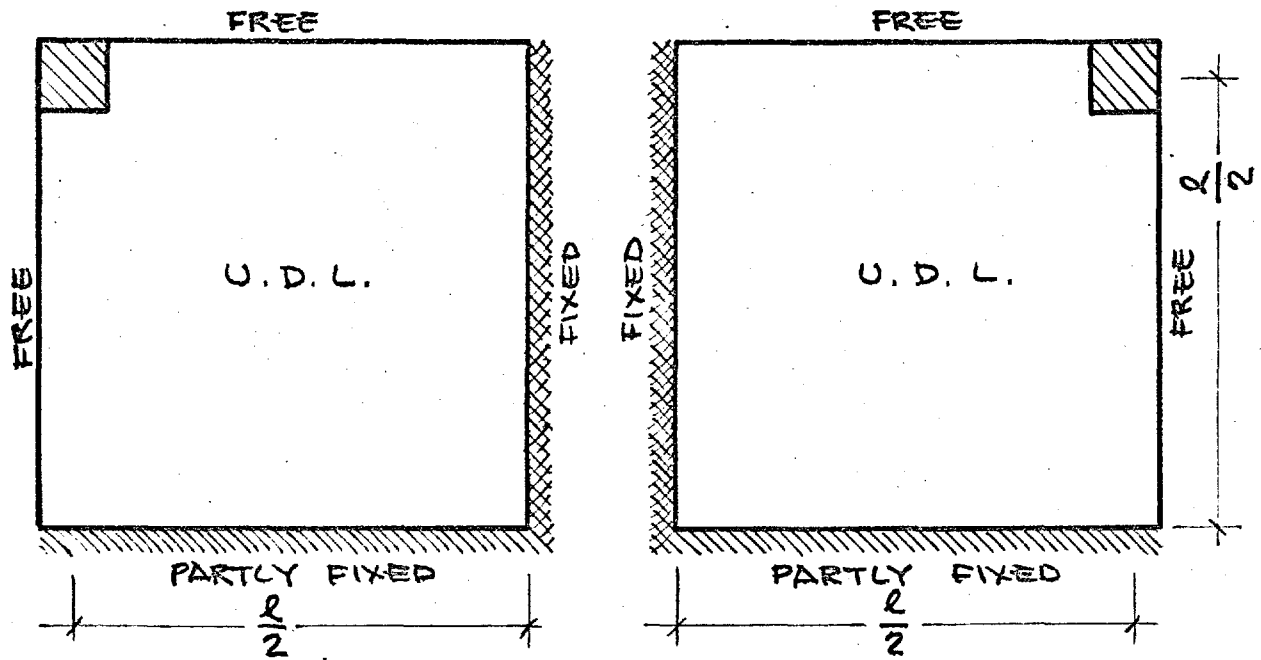
A number of adjustable props which had been previously used to support the formwork, were fixed along the column centre-line in the E-W direction. The configuration formed in this manner was entirely different

from the original, yet it was considered perfectly acceptable for studying the local behaviour. This configuration and the one used in the second part of this test are illustrated in Fig. 37. Uniformly distributed vertical load was then applied and the reactions of these three columns and the deflections in this half of the test structure were recorded. When the edge column (B) failed, another row of props along the N-S direction column centre-line was introduced, thus forming another configuration (Fig. 37b). Again only the vertical uniform load was applied until the corner columns (A and C) failed in shear. After modifying the measured reactions by the corrections explained in the subsection above, the failure reactions were used in punching shear studies.

6.2. DISCUSSION OF THE PERFORMANCE OF THE TEST STRUCTURE 1 AND REVISION OF THE DESIGN OF THE TEST STRUCTURE 2 - As already explained in Chapter 3, in the design of the test structures all the columns were intended to have approximately the same strength, and each test structure, as a whole, was intended to be slightly weaker in shear than in flexure. In the test structure 1 which had been reinforced with high tensile strength steel, shear failures occurred between 1.6 and 1.9 times the design load, while the flexural failure was anticipated to lie between 2.2 and 2.4 times the design load. The difference between the two sets of values was larger than expected. This amount of difference was not desirable, since it restricted the range of loading where the general flexural behaviour was studied. It was therefore decided that this gap should, somehow, be reduced for the test structure 2. Changing the dimensions was not desirable since it would have restricted the comparisons between the behaviour of the two test structures and would also have introduced many complications in the practical as well as theoretical side of the work. If the column sizes were altered, then the stiffness ratios would not remain realistic, and if the slab thickness was increased then the flexural strength as well as the shear strength would increase, probably at a faster rate. So, the reinforcement seemed to be the only factor which could be redesigned to achieve the purpose of having a test structure either stronger in shear or weaker in flexure than the test structure 1. The information available on the shear strength of slabs was reviewed and the requirements of the code were reconsidered. As a result, the use of mild steel instead of high tensile strength steel was suggested. The analyses by the available methods showed that this modification should produce the desired effect. Using various sizes of mild steel bars a number of reinforcement patterns, all satisfying the design requirements, were formed, and compared as regards the practical problems they may present as



a. FIRST PART



b. SECOND PART

FIG. 37 - CONFIGURATIONS FOR "INDIVIDUAL COLUMN TEST"

well as their shear and flexural strength. The combination presented in Chapter 4 was finally decided upon. The pattern of reinforcement was not very different from that of the test structure 1 except slightly more closely spaced top bars in the column strips. Therefore very little effect was anticipated on the behaviour due to the difference in reinforcement pattern. As will be explained in the next section, irrespective of the strength of the steel used, the required increase in the shear strength was obtained by the use of mild steel, while the flexural strength remained more or less unchanged. This fact tends to indicate that the contribution of flexural steel to the shear strength is mainly controlled by the amount of steel and not by the strength of steel. This conclusion may be extended to the recommendation of the use of mild steel to achieve better economy in this type of structure.

6.3. TESTS CONDUCTED ON THE TEST STRUCTURE 2 - The testing of this test structure was easier and more straightforward as a result of the experience gained from the test structure 1. Since the instrumentation systems had been working perfectly well, there was no need for a full scale instrumentation check test. The testing therefore started with those concerned with the behaviour of the test structure itself. In the light of the observed performance of the test structure 1, the extent of loading of auxiliary tests and their locations in the sequence of testing had to be reconsidered, and some small alterations were made. The repeated unsymmetrical loading had proved to affect the symmetrical behaviour of the test structure at least up to the maximum applied load. This type of testing was therefore excluded from the loading programme. On the other hand, it was found more desirable to carry out the first phase of the main testing, namely the "Crack Pattern Formation" test, when the test structure was undamaged. The "Check for Validity of Superposition" test which followed was not expected to have a significant influence on the behaviour of the previously cracked test structure since its maximum applied load was less than that of the "Crack Pattern Formation" test.

6.3.1. TEST 1: CRACK PATTERN FORMATION TEST - As in the case of Test 3 of the test structure 1, the idea behind this test was to create the first crack pattern under a prescribed type of loading which in this case was combined loading. Firstly an increment of horizontal load corresponding to the dead weight was applied alone. From this stage on, the test structure was loaded with proportionally increasing combined load. At appropriate load levels complete sets of readings were taken and the crack pattern was marked

and recorded. In general, the behaviour remained quite symmetrical and consistent during the whole test. First visible cracks appeared at approximately 0.75 times the design load along the more critical faces of the internal and far end columns. A considerable increase in the number of cracks around the middle and far end columns was noticed at 1.125 times the design load. At the last stage of the test, when the load reached 1.25 times the design load, diagonal and radial cracks appeared around the above mentioned columns in addition to the existing mostly tangential cracks. The rest of the column regions, namely the columns on the horizontal load side, remained uncracked. At the critical positive moment regions, only one almost continuous crack appeared along each of the panel centre-lines in the W-E direction, at the last loading stage of the test.

6.3.2. TEST 2: CHECK FOR VALIDITY OF SUPERPOSITION - The information expected from the auxiliary tests had already been satisfactorily obtained from the test structure 1. On the other hand, it was particularly desired to ensure that the behaviour of this test structure would not be affected by the tests of secondary importance. These considerations led to the decision of having the "Check for Validity of Superposition" test with loads not exceeding 0.60 times the design load. The testing was rather simple and straightforward and it did not present any difficulty. The performance was up to expectations and none of the three parts of the test caused any additional cracking. But, when the data obtained in this test was analysed, it was discovered that this relatively small magnitude of loading was not sufficient for obtaining accurate information. The results of this particular test were not considered successful and therefore excluded from the analysis of the experimental results.

6.3.3. TEST 3: TESTING TO FAILURE - This test structure was intended to fail under increasing horizontal load, after having been cracked by combined load. A horizontal load test to failure would not be at all realistic, and would present a number of very difficult practical problems. As discussed in Chapter 3, this test was planned with a reasonably high constant vertical load and a horizontal load which would steadily be increased beyond the maximum proportional load until the test structure failed. The test consisted of three parts as illustrated in Fig. 33b.

In the first part, the loading was proportionally applied up to 1.50 times the design combined load in the usual manner. The loading up to this critical stage resulted in one or two almost continuous negative moment

cracks along the column centre-lines in both directions and a few continuous positive moment cracks along the panel centre-lines at the bottom face of the test slab. The vertical load was kept constant at this level and in the following load stages only the horizontal load was increased. When the horizontal load reached 3.75 times the design horizontal load, there was no sign of failure; neither in shear nor in flexure. The load was removed, and it was decided to increase the maximum proportional load to 1.625 in the next cycle.

The second part was carried out in a similar manner to that described above, but with a maximum proportional load of 1.625 times the design combined load. The test structure seemed no weaker than before when the horizontal load reached 3.50 times the design horizontal load. The maximum proportional load was again thought to be insufficient. However, relieving the loads altogether and introducing a new cycle did not appear very desirable since repeated loading was expected to cause additional cracking. Therefore, only the horizontal load was decreased to the maximum proportional load level, and an increment of combined loading was applied to raise the maximum proportional load level to 1.75. Then the horizontal load was steadily increased until the internal column (E) punched through at 3.50 times the design horizontal load. The loading was rapidly removed to prevent any further unwanted damage.

The failed column region was strengthened with a steel frame braced against the column, as described in Section 6.1. Then the third part of the test was carried out to observe the behaviour of the rest of the test structure. In this part, the critical load was again chosen as 1.75 times the design combined load. Once this level was reached by proportionally increasing the combined load, the horizontal load alone was gradually increased up to 3.50 at which stage all five of the remaining critical (middle and far end) column regions (D, F, G, H and K) simultaneously failed in shear. It must be noted that the combination of failure load was nearly the same for these columns as for the internal column; the latter being slightly weaker.

6.3.4. TEST 4 - INDIVIDUAL COLUMN TEST - With the same considerations explained and discussed in Section 6.1, the remaining three undamaged columns were tested to failure under uniformly distributed vertical load over the north half of the slab. The boundary conditions had been altered by fixing a number of props along the column centre-line in the E-W direction. The configuration formed is illustrated in Fig. 37a. Unlike

the corresponding test on the test structure 1, all the three column regions simultaneously failed when the vertical load was approximately 2.45 times the design vertical load.

The failure reactions measured on each of the columns were modified by the two corrections explained in Section 6.1, before they were used in the study of the local behaviour of the column regions for this particular test structure.

CHAPTER 7

ANALYSIS OF THE EXPERIMENTAL RESULTS

The test structures, as explained in Chapter 5, were rather heavily instrumented. Hundreds of readings were taken at each loading stage. However, most of the recording was automatically done; the conducting of the experiments, most of the time, required no more than two persons. This ease of testing resulted in a huge collection of data. The data processing was, therefore, a rather long and complicated task.

The analysis was channelled mainly in two lines; (i) Flexural behaviour of the test structure as a whole, and (ii) Local behaviour of the slab-column connections, as implied by the philosophy of the project.

A general idea of the data analysis is given in a schematic form in Fig. 38. Each item and each operation shown in that chart is explained in the following sections. The data processed was obtained from three sources:

- i. The main test structures - The recorded data consisted of loads applied, reactions, deflections, steel and concrete strains and crack patterns.
- ii. The strip beams - Six strip beams were cast and tested together with each test structure. These beams were essential for the flexural analysis. In the tests conducted on these strip beams, loads applied, deflections, steel strains, rotations and concrete strains were measured and recorded.
- iii. The material specimens - The properties of the materials used were determined by testing a number of cubes, cylinders, prisms and steel specimens. The main properties determined were the strength and the modulus of elasticity of each material.

7.1. FLEXURAL ANALYSIS - Although it is the comparatively better known aspect of the problem, the flexural behaviour of this kind of structure has not yet been clearly understood. Most of the past investigations were limited to rather simple cases and were based on idealizations and assumptions which were strongly influenced by the past experience of the engineer on framed structures. However unfortunate, it is admitted that the latter criticism is to a certain extent true for the present

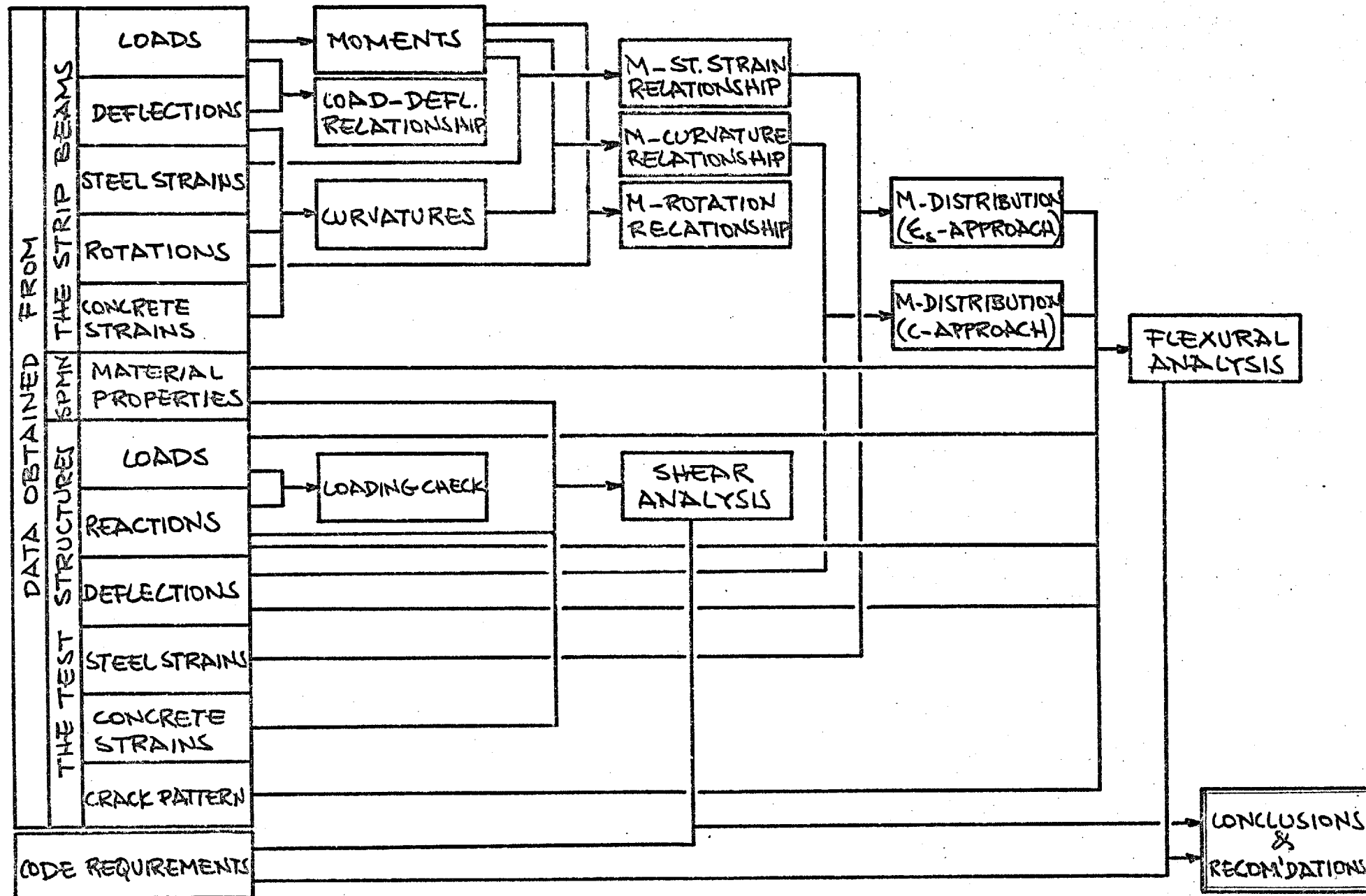


FIG. 38 - DATA ANALYSIS SCHEME

investigation as well. With the aim of obtaining a better understanding of, and a better insight into the flexural behaviour, the following phenomena were studied:

- i. The distribution of moments in two perpendicular directions at various stages of combined loading.
- ii. The deflected shape at various stages of testing.
- iii. The crack pattern observed on the top and bottom faces of the test slab at various loading stages.

The determinations of the deflected shape and the crack pattern were rather straightforward; the recordings of the former were evaluated and then plotted in form of equal deflection contours in plan (An example of this is given in Fig. 39, and a set is presented in Appendix 1.), and the latter was recorded from stage to stage with a suitable colour convention. The final form of the crack patterns are given in Figs. 40 and 41. Due to the printing difficulties, the colour convention could not be shown in these figures. The determination of the moment distribution, however, required a rather elaborate analysis. This analysis was based on the assumption that the behaviour of each point of the test slab can be simulated by a beam having the same properties in one direction as the point considered. At the yield stage, this assumption coincides with the square yield criterion. This assumption is obviously vulnerable to criticism for being unrealistic when suggesting the use of uniaxial state of stress and strain as a measure for biaxial state of stress and strain. As far as the concrete (that is the material which really undergoes biaxial state of stress) stresses and strains are concerned, the criticism is, no doubt, true. However, only the steel strains are essential for the analysis proposed. Since the reinforcement in such structures consists of individual bars which take only longitudinal uniaxial stresses, it is perfectly reasonable to consider the steel strain in a particular point of a particular bar is caused purely by the component of the external effects applied at that particular point along the direction of that particular bar. On the other hand, the influence of the change of concrete stress-strain relationship on the moment arm is relatively small. Therefore, the steel strain is quite a realistic measure of the applied moment. If the relationship between the external moment and the steel strain is known, the applied moment can be determined from the measured steel strain. To determine this relationship as well as the moment-rotation and the moment curvature relationships, a beam having the same properties in one direction as the point under consideration, can be used. This beam can be tested

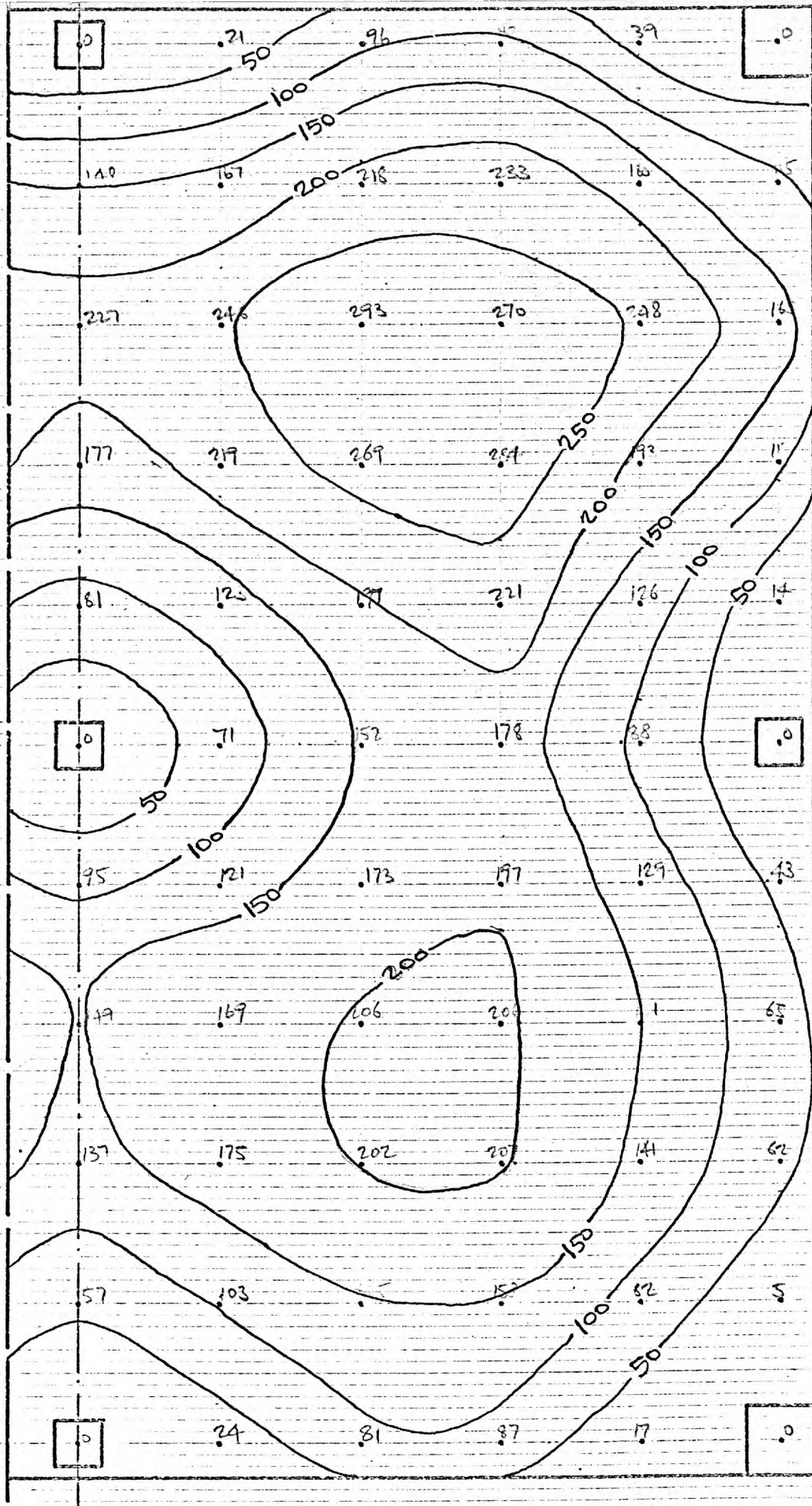
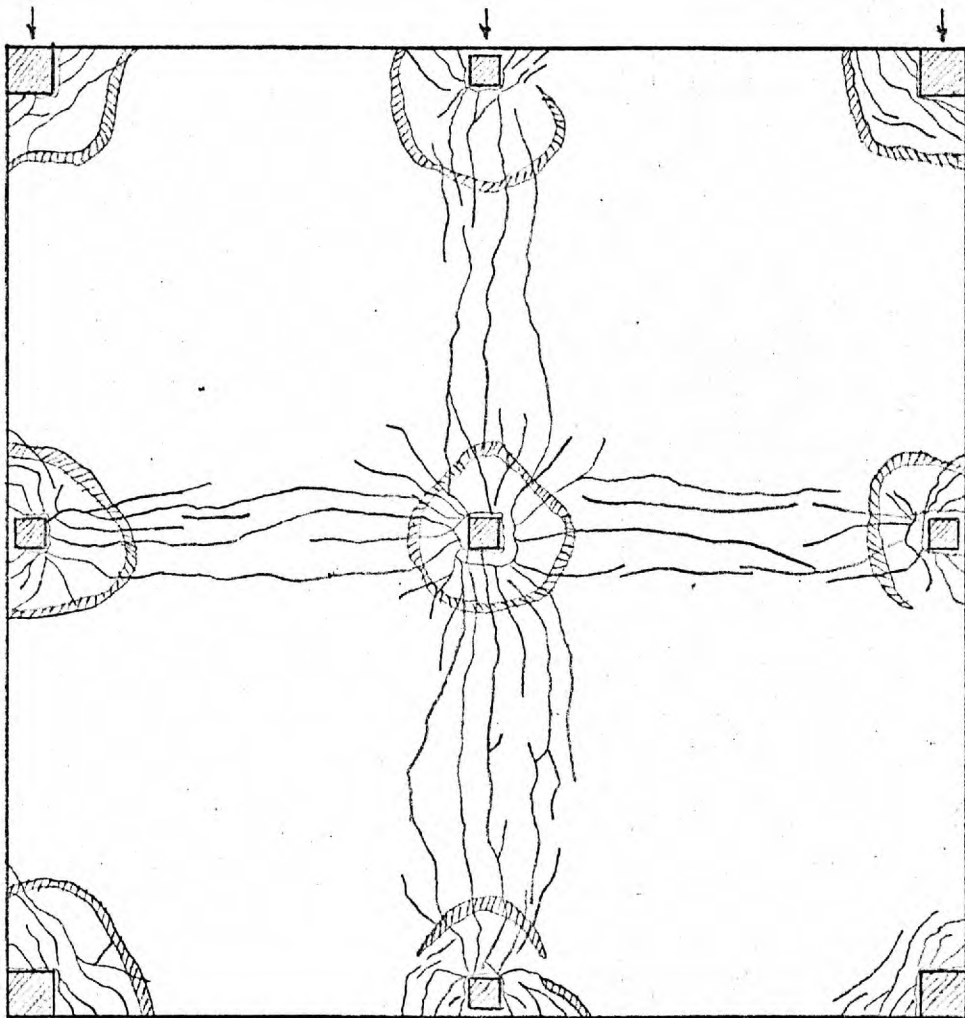
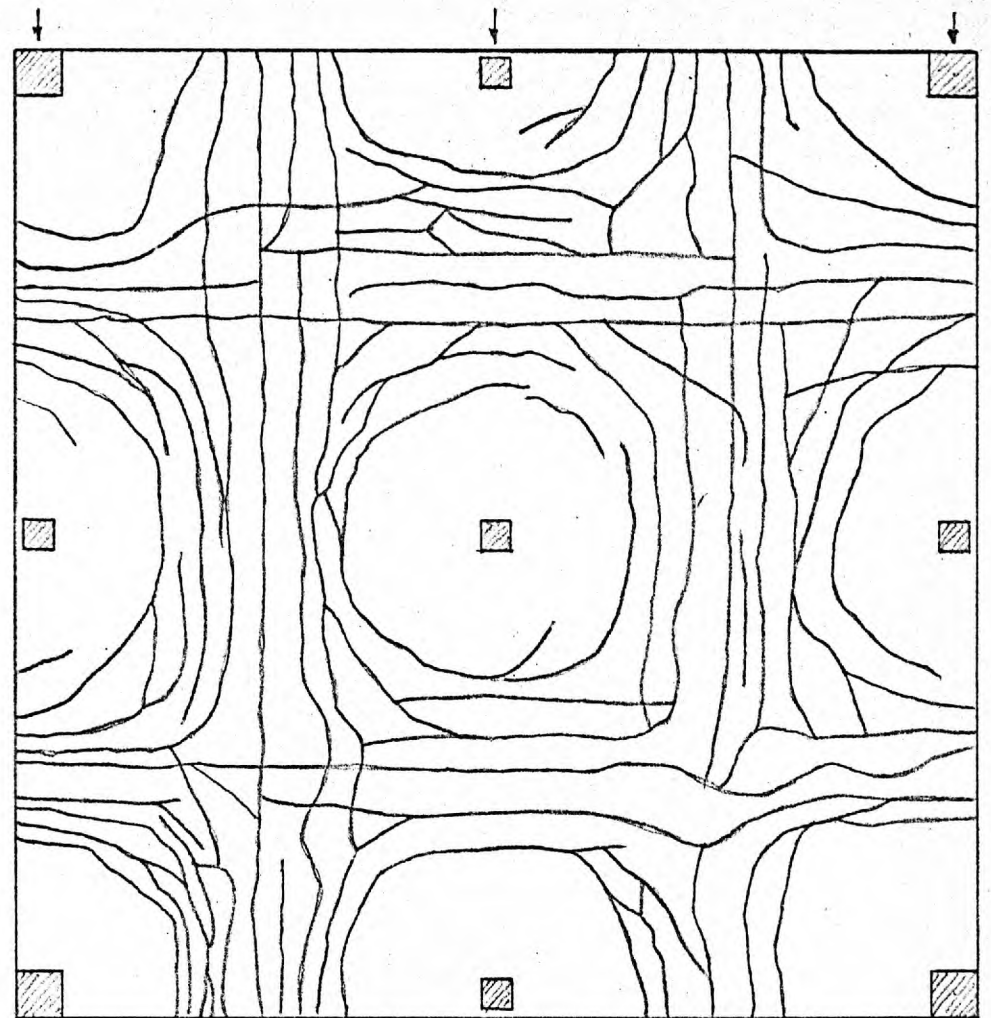


FIG. 39. EQUAL DEFLECTION CONTOURS FOR LDG. STG. 2/31/13

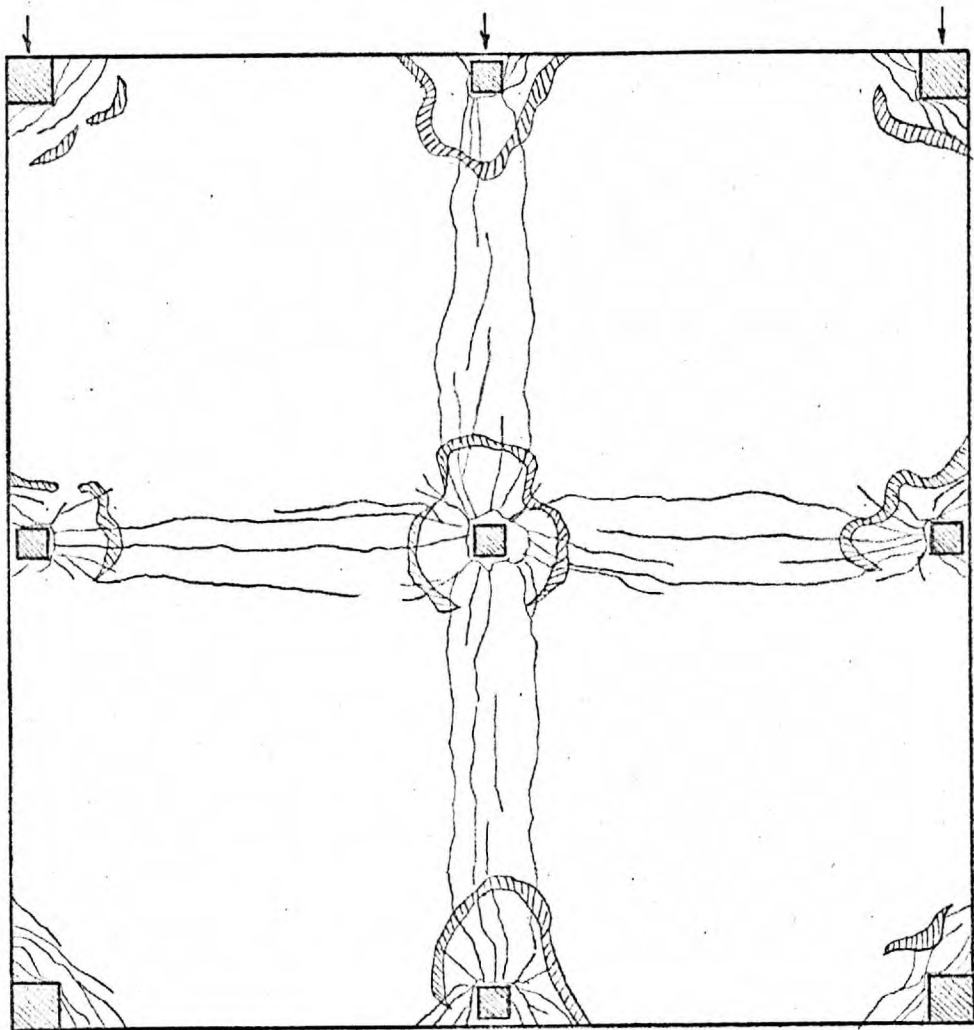


a. TOP

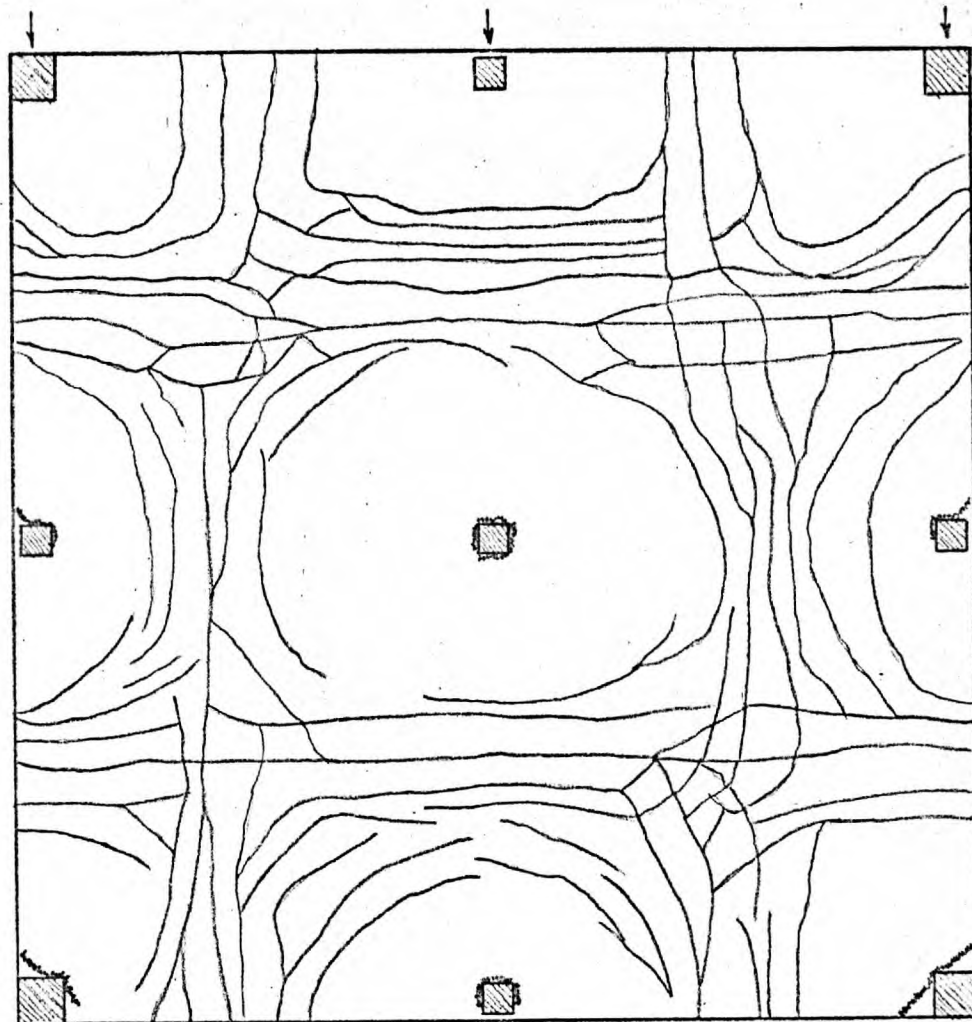


b. BOTTOM

FIG. 40- TOP AND BOTTOM CRACK PATTERNS FOR THE TEST STRUCTURE I



a. TOP



b. BOTTOM

FIG. 41 - TOP AND BOTTOM CRACK PATTERNS FOR THE TEST STRUCTURE 2

under very well defined conditions of statics so that the moment applied is definitely known and the steel strains and the other information can be directly measured to obtain the relationships required. In the present investigation, six such strip beams representing various parts of the test structure, were cast together with each test structure and tested as simply supported beams.

7.1.1. STRIP BEAMS AND THEIR USE IN FLEXURAL ANALYSIS - During the reinforced concrete design of the test structures, it was tried to standardize the spacing of the bars as far as possible. As a result of this effort, only three different spacing of bars were used in each test structure ($2\frac{1}{2}$ in., 5 in., $8\frac{1}{2}$ in. in the test structure 1; and $1\frac{7}{8}$ in., $4\frac{1}{2}$ in., $8\frac{1}{2}$ in. in the test structure 2). Due to one bar diameter difference in the effective depth between the bars of two perpendicular directions, each of these spacings had to be considered twice with two different effective depths. Therefore for each test structure, six strip beams were considered to represent all the sections of the test slab. The compression reinforcement was another parameter to be considered. Since all of these sections were under-reinforced, a considerable difference was not expected in the flexural behaviour of a strip beam, due to the difference in the compression reinforcement. However to study this problem as well as the problem of standard beam width, eight more strip beams were designed and tested. The results verified the assumption that the compression reinforcement would not considerably affect the flexural behaviour of these strip beams, therefore six strip beams were decided to be sufficient. On the other hand, the use of standard steel moulds available in the laboratory, could not provide the exact beam width required. The effect of having a slightly different beam width was studied on the preliminary strip beams mentioned above. On the basis of the results obtained, some correction factors were calculated and used to modify the results of the actual strip beams.

The geometry and the instrumentation of the strip beams are illustrated in Fig. 42, and a general view of the strip beam testing rig is presented in Fig. 43. On each strip beam, four clinometers, three dial gauges, four pairs of 8 in. Demec Gauges on either side, a load cell and two or three steel strain gauges in the constant moment region were used. The measured deflections and steel strains were directly plotted against the measured loads and the moments respectively. The sum of the rotations of clinometers 1 and 4, was taken as the total rotation of the beam for

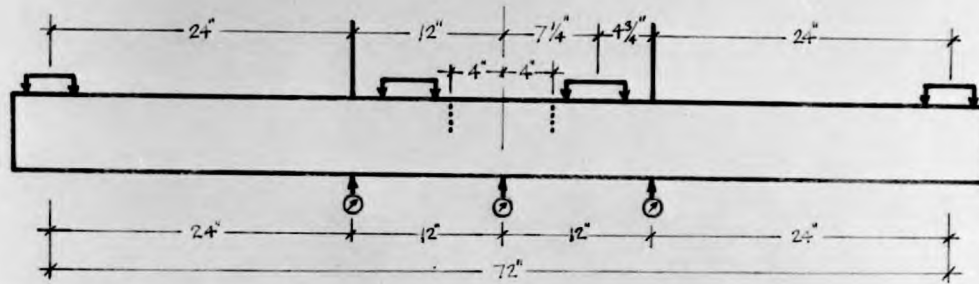


FIG. 42. INSTRUMENTATION OF THE STRIP BEAM



FIG. 43. GENERAL VIEW OF THE STRIP BEAM TESTING RIG

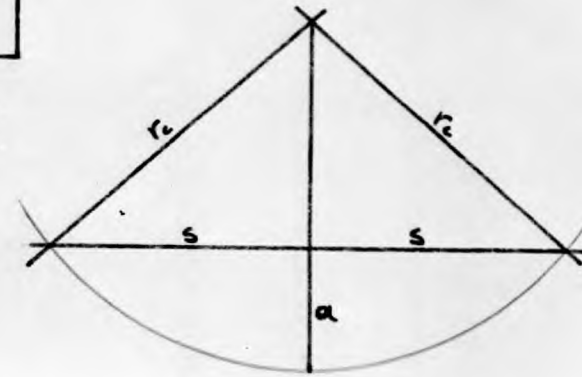


FIG. 44. DEFLECTION UNDER UNIFORM MOMENT

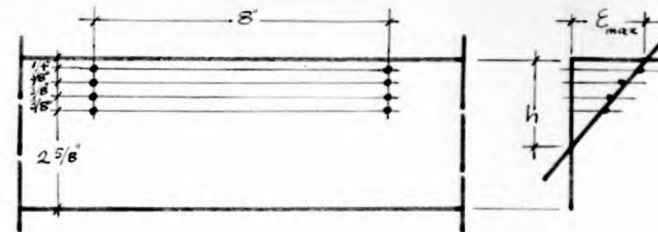


FIG. 45. LOCATION OF DEMEC LINES

determination of M- θ relationship. The curvatures were calculated in three different ways:

- i. From Demec Gauges - The Demec lines were concentrated in the upper half of the beam, and linear strain distribution was assumed in the compression zone. A straight line was statistically fitted to the measured strains, and the strain in the outermost fibre and the neutral axis depth were calculated (Fig. 45). Then, the curvature is given by,

$$c = \frac{\epsilon_{\max}}{h}$$

- ii. From the clinometers 2 and 3 - These clinometers were within the limits of constant moment region where constant curvature was expected. The curvature could therefore be calculated, as rotation per unit length, by

$$c = \frac{\theta_2 + \theta_3}{d}$$

where d = distance between the two clinometers.

- iii. From the dial gauges - In the constant moment region, the deflection was supposed to be circular. From Fig. 44,

$$r_c^2 = s^2 + (r_c - a)^2$$

$$\text{Then, } r_c = \frac{s^2 + a^2}{2a}$$

$$\text{or, } c = \frac{1}{r_c} = \frac{2a}{s^2 + a^2}$$

$$\text{where } a = \delta_2 - \frac{\delta_1 + \delta_3}{2} \quad \text{and}$$

s = spacing of the dial gauges.

The moment-curvature relationship determined on the basis of these three different approaches were in very good agreement with each other, for all the twenty strip beams tested.

All of the relationships studied, namely (i) Load-Deflection, (ii) Moment-Steel strain, (iii) Moment-Curvature, and (iv) Moment-Rotation relationships displayed a rather consistent common pattern. In each case, this pattern could be idealized by a set of three straight lines, first corresponding to the pre-cracking stage, second corresponding to the post-cracking stage, and the last corresponding to the yielding.

A special attention was paid to the Moment-Steel strain relationship since it was one of the most essential elements of the flexural analysis. The study of a number of cases, indicated that this relationship can be idealized as illustrated in Fig. 46. The actual curve followed in a particular loading is controlled by the state of the particular cross-section at the time of that particular loading. However, the limits of the variation can be determined by the two limiting cases; the case of first loading, and the case of fully cracked section. In the former case, the curve followed can be idealized by the straight lines 1, 2 and 3; on the other hand the path defined by the straight lines 4 and 3 is expected to be followed in the latter case. Therefore all the intermediate cases are expected to lie in the shaded triangle.

Various cracking patterns studied led to the consideration of two extreme cases; the gradual cracking, idealized by the straight line 2, and the instant complete cracking, idealized by the straight lines 5 and 4. In some cases, the observed curve tends to follow one of these limiting paths, but it always lies within the limits.

The relationships explained above were determined as accurately as possible for each of the strip beams. They are then employed for the determination of the distribution of bending moments from the measured quantities. To this end, two attempts were made through (i) Steel strain and (ii) Curvature approaches.

7.1.2. DETERMINATION OF MOMENT DISTRIBUTION - In the steel strain approach, moment-steel strain relationships determined by the strip beams were used. For each section, the appropriate strip beam was chosen, and the bending moment at each point of the section was calculated by obtaining the corresponding moment on the moment-steel strain relationship for the steel strain measured at the point under consideration. A computer program was written (i) to study all the previous stages to determine the state of the section at the time of the particular test, thus (ii) to choose the appropriate set of straight lines to define the likely path, and (iii) to calculate, on this basis, the bending moment corresponding to the steel strain recorded.

The operation (i) was based on the assumption of instant cracking which might in some cases be misleading. Therefore the upper and the lower limits were also calculated at each point so that the most reasonable bending moment distribution could be obtained.

Once the moments were determined at discrete points, moment distribution curves along each section where the steel strains were measured, were produced. Then these curves were summarised in form of equal moment contours plotted in plan. A set of these equal moment contours are presented in Appendix 1; however a typical one of each of M_x and M_y distribution contours are shown in Figs. 48 and 49.

An immediate observation from these equal moment contours is that the null moment line near the edge runs almost parallel to the edge when the deflections are comparatively high. This indicates negative moment in the transverse direction over the edge strip. When the deflections are not so high, the null moment line runs around the columns, giving positive moment in the transverse direction over the edge strip. This observation clearly indicates that moment transfer through torsion is not significant when the structure is not cracked very much and the deflections are not so high. However, its contribution increases as the cracking and the deflection increases.

To check the results obtained using this approach another method was developed employing the curvature approach. The vertical deflections of the test slab had been measured over a grid system. To determine the moment distribution along a certain section, the deflection profile of the section was considered. A polynomial curve of either type

$$y = a_0 + a_1x + a_2x^2 + a_3x^3 + \dots \quad \text{or type}$$

$$y = a_0 + a_1x^2 + a_2x^4 + a_3x^6 + \dots$$

was statistically fitted to the deflection data along the particular section. Theoretically, the curvature is given by,

$$C = y'' \left[1 + (y')^2 \right]^{-\frac{3}{2}}$$

where y' and y'' are the first and the second derivatives of y respectively. The curvature at a number of points along the section was calculated using this equation. Then these values of curvature were used to determine the bending moments by using the moment-curvature relationship obtained from the corresponding strip beam. A computer program was written to realize this

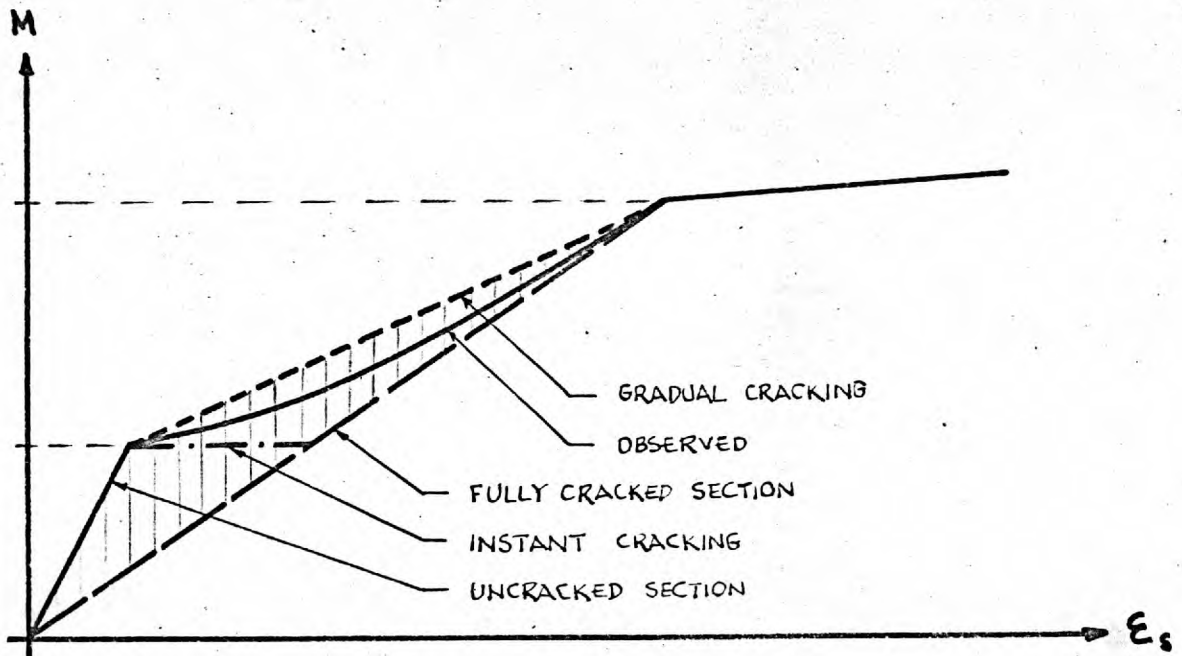


FIG. 46 - TYPICAL MOMENT - STEEL STRAIN RELATIONSHIP

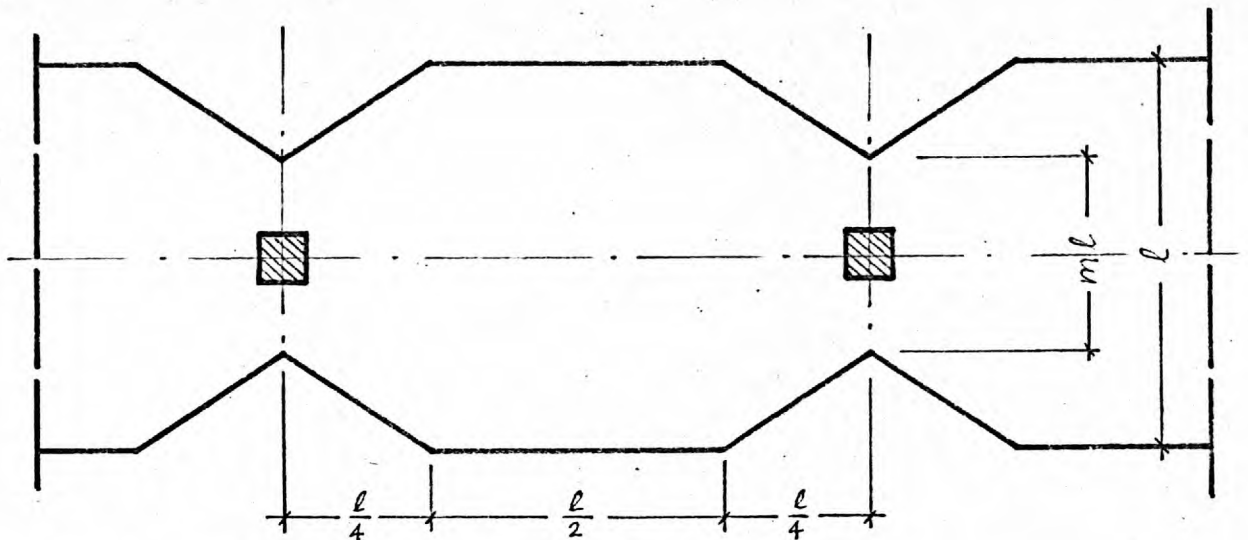


FIG. 47 - VARIABLE EFFECTIVE BEAM WIDTH

ASSUMED STATE	M_A	M_{AC}^o	M_{CA}	M_{CD}	M_{CE}	M_{CE}^o	M_E	$\sum d_i^2$
EXPERIMENTAL	7658	12000	17400	4035	13365	12000	10850	—
CRKD. BEAM UNCRD. COL.	9281	11551	17617	5840	11777	11391	15441	30 111
CRKD. BEAM CRKD. COL.	9606	11462	17470	5873	11597	11335	15733	35 271
UNCRD. BEAM UNCRD. COL.	10631	9412	20546	5670	14876	9082	16961	76 249

TABLE 7 - VARIOUS COMBINATIONS OF ASSUMED STATES OF CRACKING

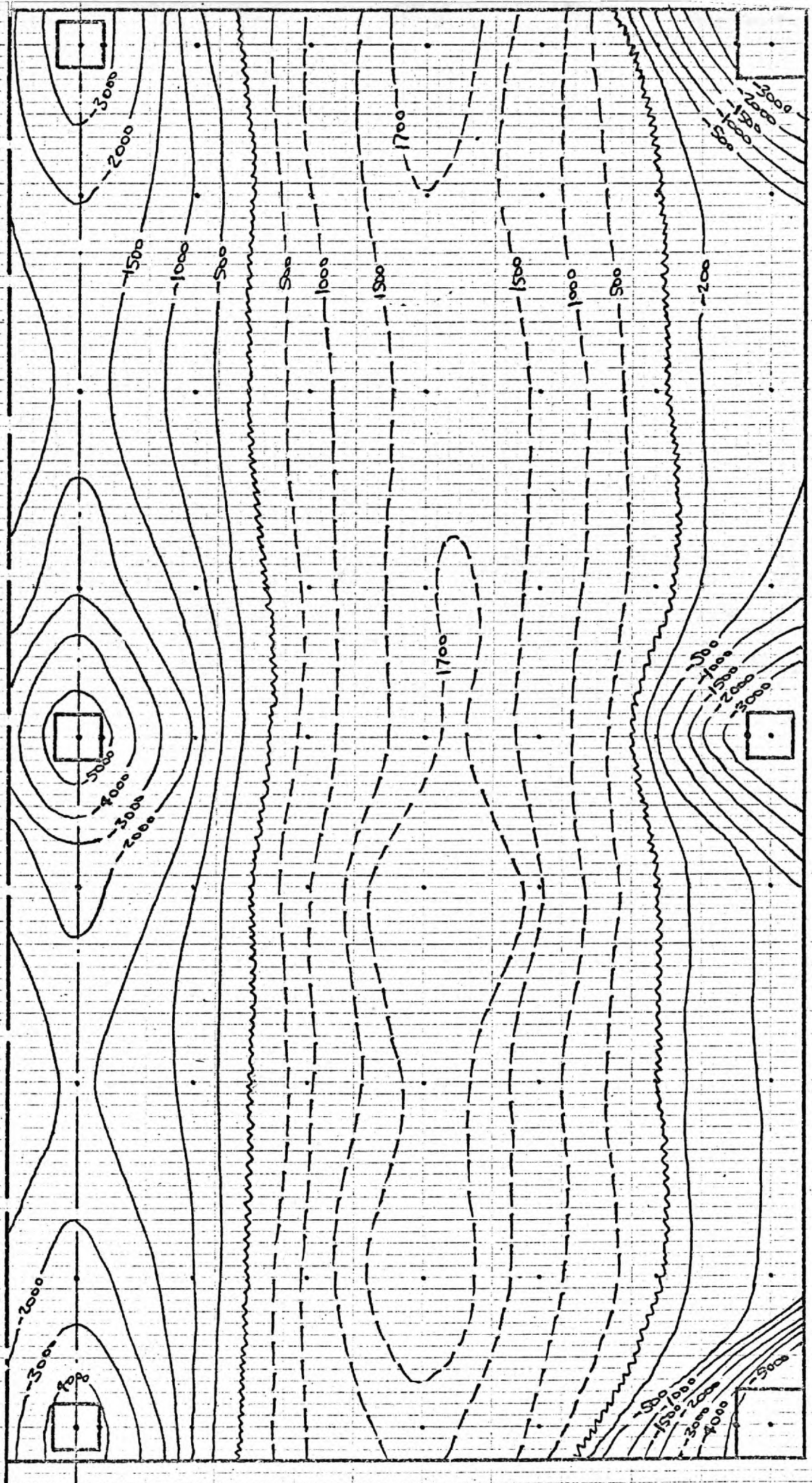


FIG. 48 - EQUAL MOMENT (M_x) CONTOURS FOR LGS. STG. 2/31/13

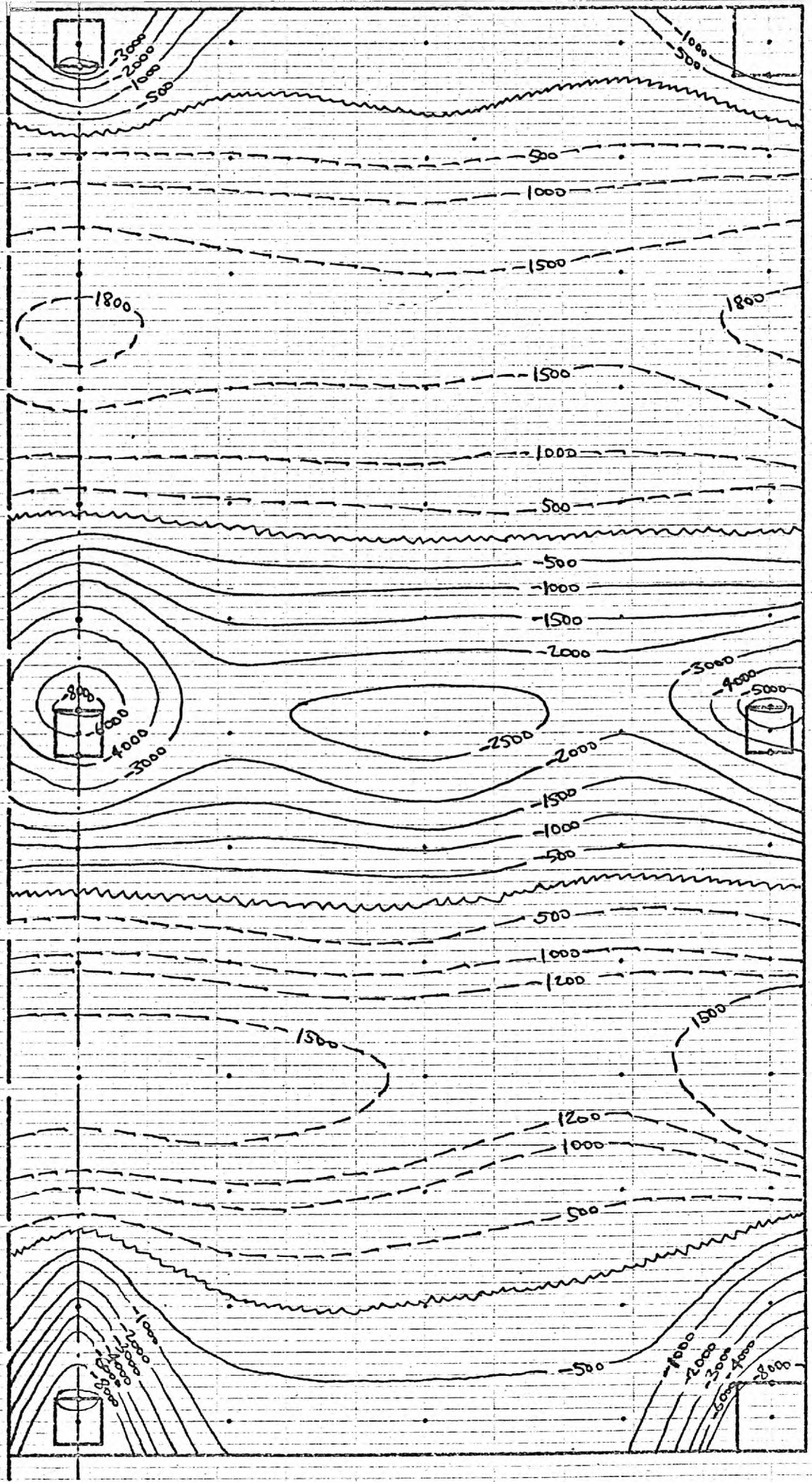


FIG. 49. EQUAL MOMENT (M_y) CONTOURS FOR LDG. STG. 2/31/13

method of analysis. However, the results obtained by this approach were not very successful, in spite of all the efforts. The failure of this approach can be explained by:

- i. The over-sensitive character of the polynomial curve - A slight experimental error may cause the polynomial change the curvature wildly at that point. The use of polynomials of smaller degree might have solved this problem, but they could not provide the accuracy required, and,
- ii. The difficulty in defining the boundary conditions - The boundary conditions are well defined only in the case of sections through the columns where, the deflection $y = 0$, and the rotation, $y' =$ measured value

$$\text{i.e. } y' = \frac{\text{measured horizontal deflection}}{\text{column height}}$$

In the other cases, the boundary conditions cannot be reasonably defined for certain.

7.1.3. FRAME ANALYSIS - Considering that the Empirical Design Method is no more than a rule of thumb method, the Frame Method is the more reasonable of the two design methods recommended by the Code. However one can, even purely by common sense, tell that a frame with beams usually 12 to 18 times wider than its columns cannot be realistic. This consideration had led to the concept of "effective width" in one of the previous works. On purely theoretical grounds, it was concluded by Chan⁵ that for an internal square panel in an infinite slab subjected to combined load, the effective width to be assumed in the elastic frame analysis should be 45 and 55 percent of the span width for the cases where the column size is approximately $\frac{1}{12}$ and $\frac{1}{16}$ of the span width respectively. His analysis was based on the comparison of the rotation in the slab with the rotation obtained from simple beam theory.

This idea of constant effective width was, no doubt, an improvement. But the observations of the behaviour of the present test structures inspired that the part of the slab actually contributing to the frame action has a varying width, and therefore it would be far more realistic to consider a small effective width across the columns and a large one at the middle of the spans. The idea was reinforced by the Principal Moment Trajectories obtained by elastic analysis for a ten-panel flat plate, presented by Reimann³⁴ in his doctoral thesis.

Once the concept of "Variable Effective Width" was found reasonable after serious considerations, the question remaining was to find out the variation, and to make it easily applicable to design problems. A review of the moment distribution contours suggested that in the middle half of the span, almost the full width was effectively used; and the variation took place in the end quarters of the span. For the sake of simplicity, the effective width across the columns was assumed to be a fraction of the total width, and the variation was assumed to be linear. These considerations are illustrated in Fig. 47. As a matter of fact, the effective width across the columns is not affected only by the total width, but also by the column size. Therefore it would have been more reasonable to express this width in terms of both, i.e. as

$$w_o = m_1 \ell + n_1 a$$

However, this expression would have unnecessarily complicated the analysis a lot. On the other hand, the ratio of column size to span length does not vary very much; the most common values used in practice lie between $\frac{1}{12}$ and $\frac{1}{18}$. Therefore an average value of $\frac{1}{15}$ can be assumed more or less true for all the practical cases. Then, the column size can be expressed in terms of span length and thus the effective width across the columns can be expressed in terms of span length alone, i.e.

$$w_o = m \ell \quad \text{where} \quad m = m_1 + \frac{n_1}{15}$$

So, the problem was reduced to determination of the coefficient m from the experimental results.

Observations of the performance of the test structures indicated that it would be very realistic if the flexural rigidities of the beams were based on cracked sections while the columns were assumed uncracked. This thought was supported by the cases numerically studied. The following example illustrates the case clearly. The frame F4, which is the most general, of the test structure 2 was analysed by assuming (i) cracked beams and uncracked columns, (ii) cracked beams and columns, and (iii) uncracked beams and columns. The results obtained for each case are compared with the experimental results obtained in "Normal Cracking" loading stage in Table 7. The sums of the squares of the differences from the experimental values clearly show that the combination adopted for the analysis, namely "Cracked Beam, Uncracked Column" is the most realistic and most reliable of them all.

However the results of "Cracked Beam, Cracked Column" combination are not too bad either; they are only slightly less reliable than those of the former while the results of the third combination, "Uncracked Beam, Uncracked Column" are wildly different from the measured values.

Furthermore flexural rigidities for the cracked beam sections were calculated on the basis of limit analysis. In other words the value of (EI) for each section was calculated from the design charts compiled at Imperial College considering the sectional and material properties, instead of using constant values of E and I separately. Points of contraflexure were assumed at $l/4$ from the column centres, and (EI) values were accordingly determined for the middle half span and the end quarters. Fig. 50 illustrates these idealized sectional properties. The flexural rigidity coefficients for each of the test structures, taken from the design charts are given along the line called (EI) . As a matter of coincidence, the ratio of span and support region flexural rigidity coefficients are the same for both test structures. The (EI) value for the middle half of the beam for the test structure 2 was taken as unity by defining $(EI)_0 = 25 b d_1^3 \bar{\sigma}_b^+$. Then the geometrical variation was combined with the variation of flexural rigidity to obtain the combined variation which formed the basis for the calculation of the stiffness and carry-over factors and the fixed end moments used in the frame analysis.

Three loading stages from each test structure were chosen as a basis for this analysis. These loading stages were:

- i. Design combined load applied when the test structure had not been loaded many times before. Therefore this stage is named "Normal Cracking".
- ii. Design combined load applied after a number of tests had already been carried out on the test structure, and considerable cracking had already taken place. This stage is called "Overcracking".
- iii. The highest proportional combined load applied just before the failure. The test structure had already been severely cracked before this loading stage. That is why this stage is named "Severe Cracking". In order to make this loading stage comparable with the others as well as the theoretical ones, the moments and the deflections measured at this stage were reduced by the ratio of the design combined load to the actual applied combined load. For comparison purposes, this approximation was found to be satisfactory in giving a general qualitative picture of the

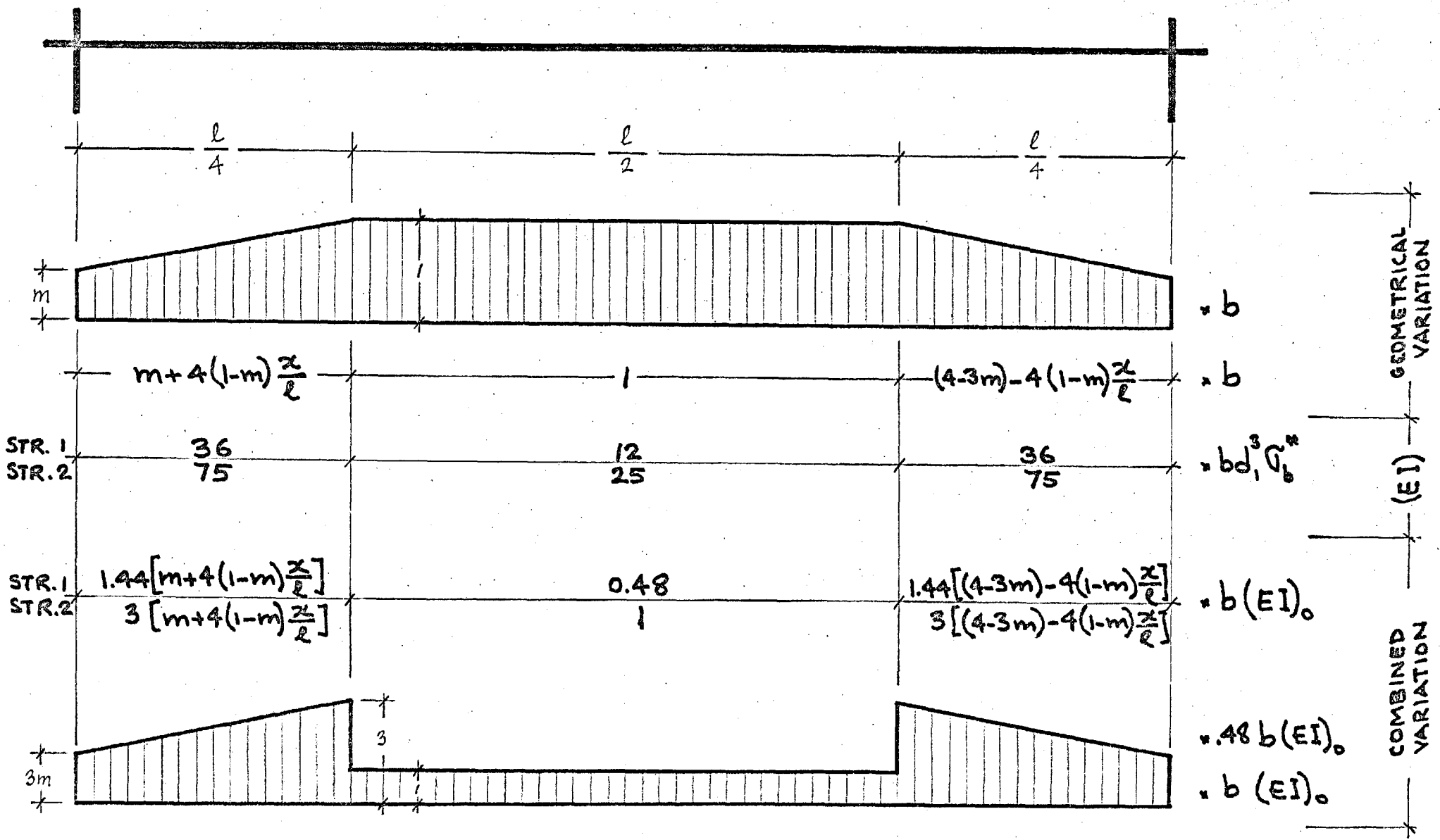


FIG. 50 - VARIATION OF FLEXURAL RIGIDITY ALONG A BEAM OF VARIABLE EFFECTIVE WIDTH

behaviour of the test structure at such a late loading stage. As far as the design recommendations are concerned, the previous two stages, especially the "Normal Cracking", are essential since these are the likely cases to take place during the lifetime of the structure being designed. Therefore, more importance was paid to these two stages than the "Severe Cracking" when the design recommendations were considered.

Two criteria were considered to determine the coefficient m which defines the effective width over the columns; (i) the total moments along the critical sections of each frame, and (ii) the mid-panel deflections. The results of both approaches were in agreement. Especially, the results of the former were very reasonable, consistent, well defined and therefore reliable.

MOMENT APPROACH - Seven critical sections on each frame were chosen for comparison. These sections are shown in Fig. 51. At each of these sections, the total moment measured was calculated by integration from the moment distribution contours for each loading stage considered. These calculations were based on the frame division as recommended by the code and used in the design of the test structures. The moments at the critical sections of each frame are listed in Table 8.

Each frame was analysed with beams of variable width for eight values of the coefficient m from 1 to $\frac{1}{10}$. The results of these analyses are summarised in Tables 9 and 10. These frame analyses with variable beam width were done by using a special version of a comprehensive computer program developed by U. Nahhas³⁶ for inelastic analysis of framed structures, based on the regular stiffness or displacement approach. The stiffness and carry-over factors and the fixed end moments were calculated for each value of the coefficient m and fed into the program. These values are tabulated for easy reference of the designer and are presented in the sub-section of "Proposed Design Method".

For determination of the best value of the coefficient m for each frame at each loading stage, the concept of least squares was used. The differences between the experimental and analytical values of the bending moments at the critical sections, were calculated, squared and added together for each case. The value of the coefficient m corresponding to the smallest sum of squares of differences was accepted to be the best for that particular case. It can be thought at this point that the second or even the third best m -value could have been chosen if they were on the safe

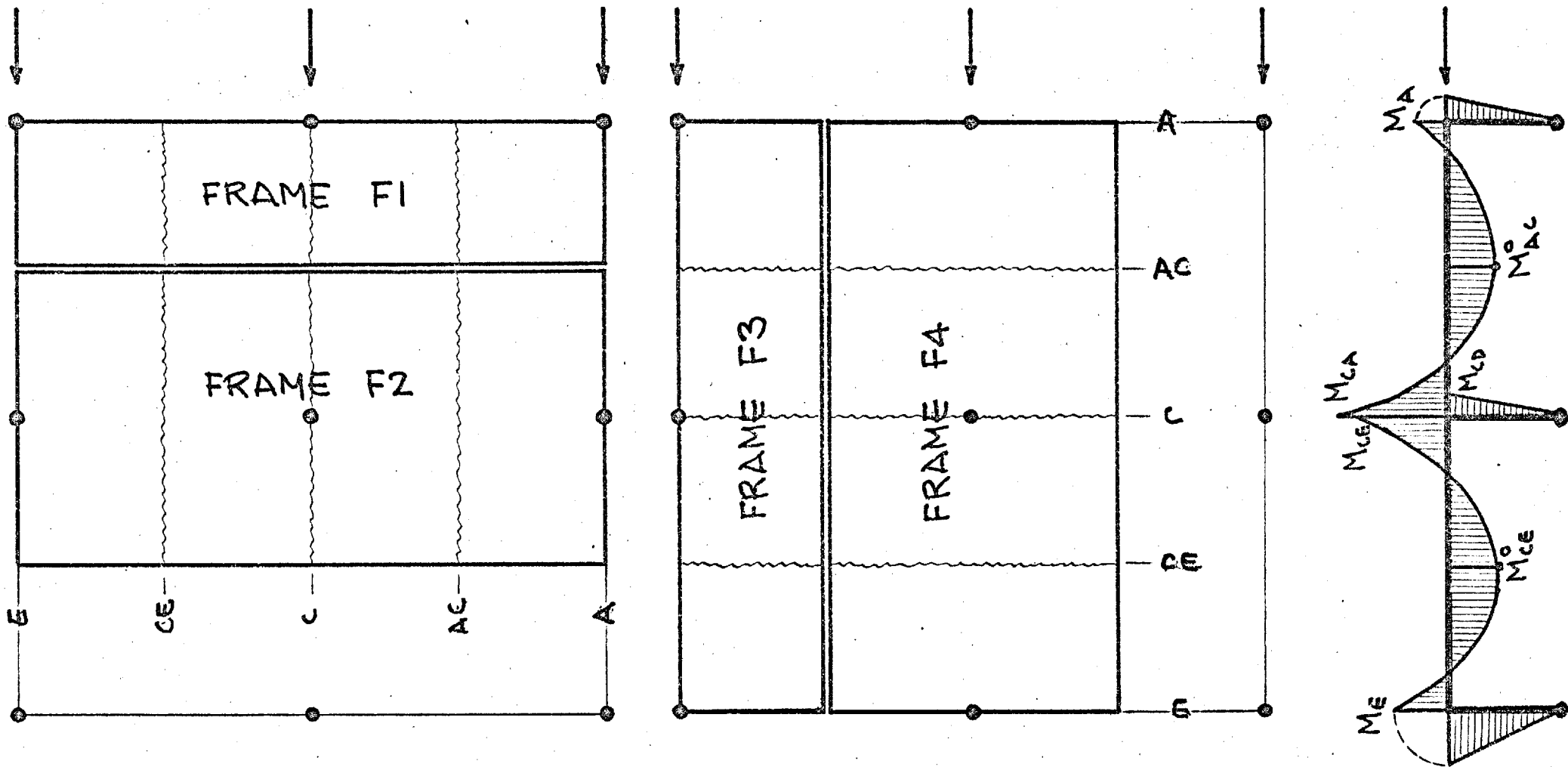


FIG. 51 - CRITICAL SECTIONS CONSIDERED FOR THE STUDY OF FRAME ANALYSIS

FRAME	METHOD	CRITICAL MOMENTS (*) (ft-lb)								
		M_A	M_{AC}^0	M_{CA}	M_{CD}	M_{CE}	M_{CE}^0	M_E		
FRAME F1	CP14	EMPR.	4 820	4 540	5 860	0	5 860	4 540	4 820	
	CP14	FRAME	8 800	4 680	9 340	0	9 340	4 680	8 800	
	EXP. 1	1/23/7		5 513	7 700	8 698	272	8 426	7 700	5 980
		1/41/7		6 650	10 100	10 167	179	9 988	10 100	6 396
		1/42/11		6 332	8 475	12 400	240	12 160	8 475	6 739
	EXP. 2	2/11/7		5 312	7 425	8 220	284	7 936	7 425	5 971
2/31/2			5 700	7 700	10 229	203	10 026	7 700	6 400	
2/33/8			6 398	5 243	10 155	66	10 089	5 243	6 927	
FRAME F2	CP14	EMPR.	9 640	9 080	11 720	0	11 720	9 080	9 640	
	CP14	FRAME	12 100	9 470	18 960	0	18 960	9 470	12 100	
	EXP. 1	1/23/7		9 700	14 717	17 167	228	16 939	14 717	9 300
		1/41/7		10 420	19 860	19 650	189	19 461	19 860	9 975
		1/42/11		10 932	16 000	24 583	260	24 323	16 000	10 153
	EXP. 2	2/11/7		8 864	14 000	18 238	272	17 966	14 000	8 931
2/31/2			9 516	14 000	22 660	404	22 256	14 000	10 070	
2/33/8			10 286	12 367	19 143	23	19 120	12 367	10 657	
FRAME F3	CP14	EMPR.	4 820	4 540	5 860	0	5 860	4 540	4 820	
	CP14	FRAME	7 010	4 820	10 850	3 020	7 830	4 540	10 590	
	EXP. 1	1/23/7		3 220	6 600	9 800	3 100	6 700	6 233	7 500
		1/41/7		4 085	7 333	13 330	3 064	10 266	7 333	9 213
		1/42/11		3 902	6 600	14 764	3 612	11 152	7 333	9 376
	EXP. 2	2/11/7		3 578	7 217	9 410	2 660	6 750	6 541	8 285
2/31/2			4 214	7 700	12 010	3 869	8 141	7 057	8 988	
2/33/8			4 351	5 657	9 583	4 048	5 535	5 657	9 550	
FRAME F4	CP14	EMPR.	9 640	9 080	11 720	0	11 720	9 080	9 640	
	CP14	FRAME	8 880	9 690	21 740	5 560	16 180	9 250	15 320	
	EXP. 1	1/23/7		6 858	12 000	19 318	5 010	14 308	12 000	11 750
		1/41/7		6 227	14 000	26 250	4 765	21 485	14 000	12 580
		1/42/11		7 736	12 900	23 610	4 536	19 074	13 330	12 256
	EXP. 2	2/11/7		7 658	12 000	17 400	4 035	13 365	12 000	10 850
2/31/2			8 000	14 000	23 420	4 395	19 025	13 960	11 928	
2/33/8			8 343	10 286	17 429	4 088	13 341	11 257	12 243	

TABLE B. EXPERIMENTAL VALUES OF CRITICAL MOMENTS

(*) REF. FIG. 51

FRAME	M	CRITICAL MOMENTS ^(*) (ft-lb)						
		M _A	M _{AC} ^o	M _{CA}	M _{CD}	M _{CE}	M _{CE} ^o	M _E
FRAME #1	1	10 406	2 947	11 200	0	11 200	2 947	10 406
	1/2	8 876	4 622	9 381	0	9 381	4 622	8 876
	1/3	8 100	5 455	8 490	0	8 490	5 455	8 100
	1/4	7 430	6 161	7 748	0	7 748	6 161	7 430
	1/5	6 499	7 124	6 754	0	6 754	7 124	6 499
	1/6	6 358	7 267	6 591	0	6 591	7 276	6 358
	1/8	5 550	8 109	5 732	0	5 732	8 109	5 550
	1/10	4 921	8 755	5 070	0	5 070	8 755	4 921
FRAME #2	1	13 891	6 226	23 658	0	23 658	6 226	13 891
	1/2	12 581	9 126	19 168	0	19 168	9 126	12 581
	1/3	11 819	10 563	17 056	0	17 056	10 563	11 819
	1/4	11 045	11 781	15 394	0	15 394	11 781	11 045
	1/5	9 786	13 449	13 316	0	13 316	13 449	9 786
	1/6	9 667	13 707	12 920	0	12 920	13 707	9 667
	1/8	8 556	15 151	11 143	0	11 143	15 151	8 556
	1/10	7 660	16 270	9 800	0	9 800	16 270	7 660
FRAME #3	1	8 805	3 048	12 600	2 800	9 800	2 847	12 006
	1/2	7 284	4 714	10 789	2 816	7 913	4 530	10 468
	1/3	6 513	5 542	9 903	2 826	7 077	5 368	9 687
	1/4	5 847	6 245	9 164	2 832	6 332	6 077	9 014
	1/5	4 918	7 205	8 172	2 837	5 335	7 043	8 080
	1/6	4 779	7 355	8 012	2 842	5 170	7 196	7 938
	1/8	3 974	8 185	7 156	2 848	4 308	8 033	7 126
	1/10	3 347	8 828	6 497	2 853	3 644	8 681	6 495
FRAME #4	1	10 711	6 406	26 478	5 640	20 838	6 046	17 071
	1/2	9 414	9 293	22 001	5 666	16 355	8 959	15 748
	1/3	8 660	10 722	19 897	5 682	14 215	10 404	14 978
	1/4	7 892	11 934	18 241	5 693	12 548	11 627	14 199
	1/5	6 636	13 599	16 166	5 701	10 465	13 300	12 935
	1/6	6 522	13 852	15 774	5 709	10 065	13 561	12 813
	1/8	5 415	15 291	14 003	5 719	8 284	15 010	11 696
	1/10	4 524	16 406	12 664	5 727	6 937	16 133	10 797

TABLE 9. VARIATION OF CRITICAL MOMENTS FOR THE TEST STRUCTURE 1 WITH M

(*) REF. FIG. 51

FRAME	M	CRITICAL MOMENTS (*) (ft-lb)						
		M_A	M_{AC}^o	M_{CA}	M_{CD}	M_{CE}	M_{CE}^o	M_E
FRAME F1	1	10 650	2 905	11 040	0	11 040	2 905	10 650
	1/2	9 038	4 589	9 285	0	9 285	4 589	9 038
	1/3	8 229	5 426	8 419	0	8 419	5 426	8 229
	1/4	7 537	6 136	7 692	0	7 692	6 136	7 537
	1/5	6 586	7 103	6 709	0	6 709	7 103	6 586
	1/6	6 438	7 256	6 551	0	6 551	7 256	6 438
	1/8	5 613	8 093	5 702	0	5 702	8 093	5 613
	1/10	4 974	8 740	5 046	0	5 046	8 740	4 974
FRAME F2	1	16 440	5 786	21 988	0	21 988	5 786	16 440
	1/2	14 438	8 748	18 066	0	18 066	8 748	14 438
	1/3	13 358	10 222	16 199	0	16 199	10 222	13 358
	1/4	12 361	11 471	14 697	0	14 697	11 471	12 361
	1/5	10 876	13 183	12 759	0	12 759	13 183	10 876
	1/6	10 689	13 448	12 415	0	12 415	13 448	10 689
	1/8	9 389	14 930	10 751	0	10 751	14 930	9 389
	1/10	8 362	16 078	9 483	0	9 483	16 078	8 362
FRAME F3	1	9 100	2 955	12 490	2 900	9 590	2 855	12 200
	1/2	7 492	4 635	10 739	2 908	7 831	4 543	10 584
	1/3	6 685	5 470	9 875	2 913	6 962	5 383	9 772
	1/4	5 995	6 178	9 150	2 917	6 233	6 094	9 079
	1/5	5 045	7 143	8 169	2 919	5 250	7 062	8 126
	1/6	4 899	7 295	8 012	2 921	5 091	7 216	7 978
	1/8	4 076	8 130	7 164	2 924	4 240	8 055	7 151
	1/10	3 437	8 777	6 510	2 927	3 583	8 704	6 510
FRAME F4	1	13 344	5 882	24 893	5 809	19 084	5 691	19 535
	1/2	11 350	8 836	20 978	5 825	15 153	8 661	17 525
	1/3	10 275	10 305	19 116	5 833	13 283	10 138	16 441
	1/4	9 281	11 551	17 617	5 840	11 777	11 391	15 441
	1/5	7 798	13 261	15 681	5 844	9 837	13 105	13 953
	1/6	7 613	13 524	15 339	5 849	9 490	13 373	13 764
	1/8	6 316	15 003	13 679	5 855	7 824	14 858	12 461
	1/10	5 291	16 149	12 412	5 858	6 554	16 007	11 432

TABLE 10 - VARIATION OF CRITICAL MOMENTS FOR THE TEST STRUCTURE 2 WITH M

(*) REF. FIG. 51

side. The variations of the critical moments, however, are not the same; some may increase with increasing m -value while the others decrease. Therefore, the m -value producing the smallest sum of squares of differences was generally found really the best. In all the cases the differences corresponding to the best m -value are anyway reasonably small.

The sums of squares of differences for each frame at each loading stage are given in Tables 11 and 12. When these tables are studied the following points can be observed:

- i. In the case of "Normal Cracking", the coefficient m is consistently $\frac{1}{4}$ and $\frac{1}{5}$ for internal and edge frames respectively. The best m is very well defined.
- ii. In the case of "Overcracking", less consistency is observed. The coefficient m is approximately $\frac{1}{3}$ and $\frac{1}{4}$ for internal and edge frames respectively.
- iii. In the case of "Severe Cracking", the consistency is still less, and the coefficient m is still higher, $\frac{1}{3}$ for both kinds.
- iv. To sum up, it can be said that as the degree of cracking increases, the behaviour of the structure increasingly deviates from the frame behaviour, and the yield line pattern commences to form. This is clearly indicated by (i) decreasing consistency, and (ii) increasing sums of squares of differences.
- v. Although not very consistently, the general tendency of the parameter m is to increase as the cracking becomes worse. This phenomenon can be explained by stress transfer or re-distribution. Along a section over a column, the effective width increases as additional cracking releases the stress at the points near the column and causes points further away to take the torsional stresses. Referring to Fig. 52, a considerable part of the stress transfer through torsion takes place in sections near column face before the formation of cracks. Once the sections 1 are cracked, the stress is transferred to sections 2, then to sections 3 as the cracking increases.

So far the analysis was based on evenly loaded frames. In practice, one often gets uneven loading; therefore a method cannot be considered complete without considering such cases. The information obtained from "Panel by Panel Loading Test" was found extremely useful in this respect. The third part of the test with three panels loaded, was chosen as a basis. Referring to Fig. 53, three frames with various

STATE	m	FRAME F1	FRAME F2	FRAME F3	FRAME F4
NORMAL CRACKING (1/23/7)	1	102 592 940	270 529 505	93 117 961	204 205 002
	1/2	40 097 251	90 608 110	34 461 631	50 830 224
	1/3	21 388 363	45 424 948	17 722 221	18 517 862
	1/4	11 138 349	27 676 780	9 955 430	11 934 260
	1/5	8 553 813	31 467 554	8 824 507	30 881 544
	1/6	9 097 119	36 417 332	9 724 127	38 378 872
	1/8	16 649 607	72 173 160	19 236 521	87 016 428
	1/10	28 197 099	116 964 812	32 292 796	141 971 736
OVER CRACKING (1/41/7)	1	135 086 528	432 869 403	69 384 422	162 446 507
	1/2	72 118 822	242 252 563	38 300 630	113 149 025
	1/3	53 264 540	190 774 537	35 159 460	112 736 018
	1/4	43 610 200	166 765 753	38 791 261	160 168 105
	1/5	39 885 928	160 555 821	53 049 316	224 947 659
	1/6	45 208 886	164 493 993	56 426 138	241 410 051
	1/8	47 668 680	191 348 158	79 246 490	329 293 107
	1/10	58 981 290	229 146 167	102 569 591	413 566 967
SEVERE CRACKING (1/42/11)	1	93 581 133	213 984 847	74 226 873	139 819 478
	1/2	57 624 725	159 081 987	50 584 475	58 493 740
	1/3	52 033 545	172 216 881	52 747 373	60 277 786
	1/4	53 556 725	200 640 717	60 818 430	80 386 436
	1/5	64 895 643	262 630 145	81 054 575	133 045 784
	1/6	67 857 369	278 473 697	85 392 495	146 684 616
	1/8	88 132 165	364 050 987	113 375 605	224 357 960
	1/10	109 507 445	446 589 051	140 678 708	301 529 016

TABLE II - SUMS OF SQUARES OF DIFFERENCES FOR THE TEST STRUCTURE I

STATE	m	FRAME F1	FRAME F2	FRAME F3	FRAME F4
NORMAL CRACKING (2/11/7)	1	108 915 957	279 033 417	95 180 549	276 992 312
	1/2	42 410 039	116 672 001	34 259 831	98 549 434
	1/3	21 953 001	75 694727	16 582 769	50 632 223
	1/4	11 144 999	60 084 617	8 152 593	30 110 750
	1/5	6 077 975	66 372 421	6 311 449	35 727 181
	1/6	6 327 529	71 825 511	7 075 805	35 255 068
	1/8	12 522 949	110 400 567	16 074 037	69 443 380
	1/10	23 073 735	157 897 231	28 793 853	113 804 857
OVER CRACKING (2/31/2)	1	90 276 176	224 144 892	77 630 731	224 875 676
	1/2	38 939 356	137 296 668	31 636 956	120 295 854
	1/3	25 982 992	70 778 769	21 357 875	107 366 327
	1/4	21 484 664	146 845 454	19 150 463	114 875 830
	1/5	24 966 508	192 220 240	25 757 541	151 829 641
	1/6	26 584 878	204 337 020	27 897 967	162 424 712
	1/8	40 167 750	276 562 212	44 169 059	227 413 440
	1/10	56 428 850	349 831 222	62 529 479	295 235 381
SEVERE CRACKING (2/33/8)	1	44 564 703	174 253 905	70 939 087	220 214 023
	1/2	13 689 025	60 000 761	21 128 069	64 679 203
	1/3	11 265 695	43 134 54	9 016 703	28 502 708
	1/4	15 080 653	48 145 247	5 340 841	18 276 173
	1/5	30 374 497	82 946 079	10 046 895	33 903 910
	1/6	33 855 675	92 741 421	11 820 319	40 107 863
	1/8	57 667 155	156 016 725	26 448 921	86 995 621
	1/10	81 838 089	222 630 801	71 415 848	141 276 252

TABLE 12. SUMS OF SQUARES OF DIFFERENCES FOR THE TEST STRUCTURE 2

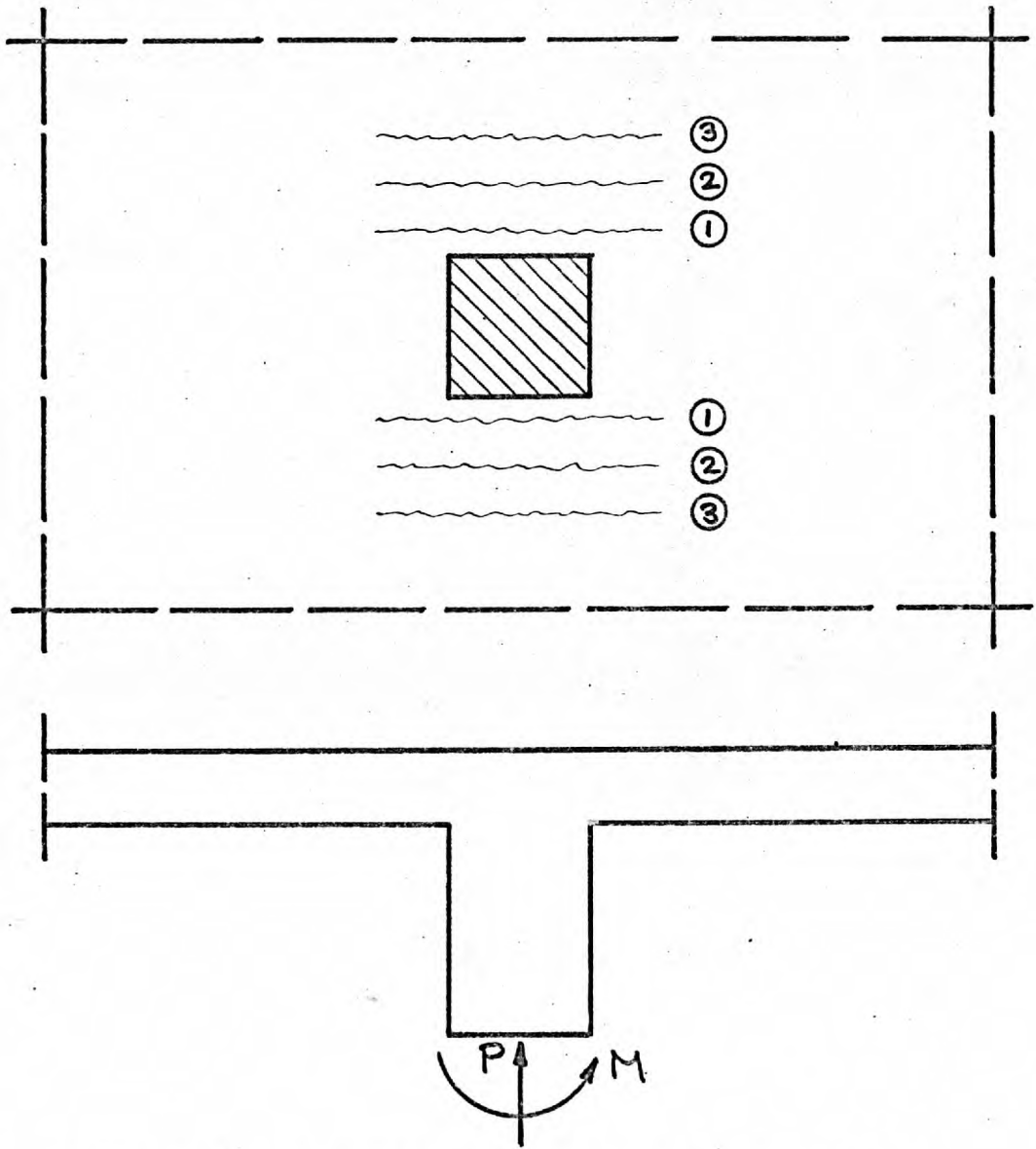


FIG. 52. TORSIONAL STRESS TRANSFERING SECTIONS

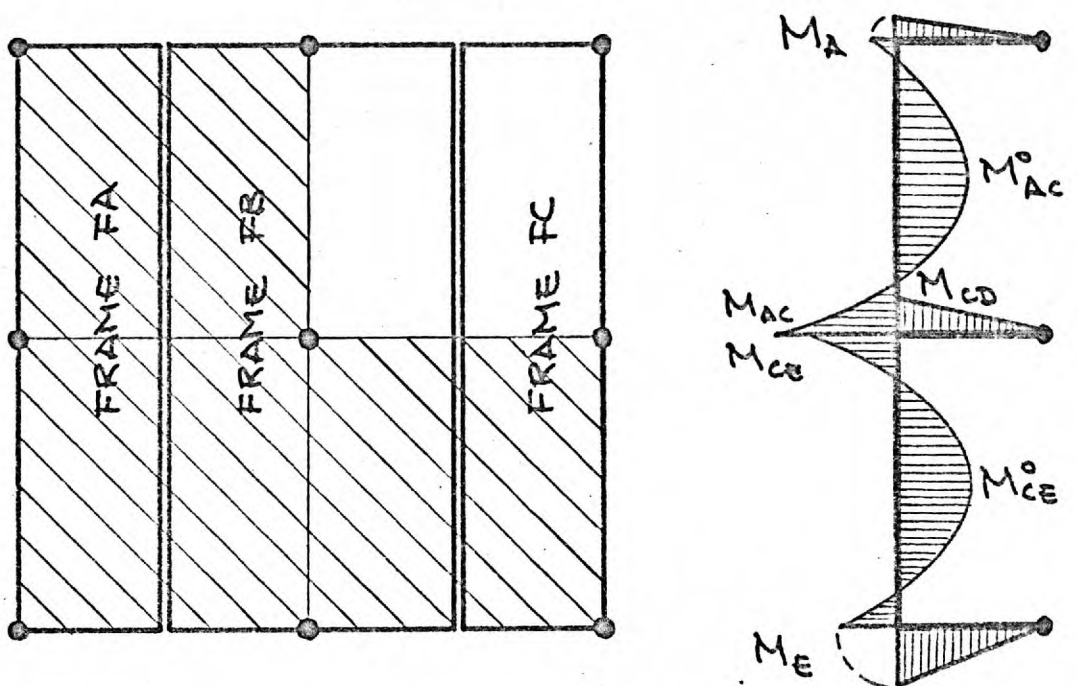


FIG. 53. CRITICAL SECTIONS FOR UNEVEN LOADING FRAME ANALYSIS.

combinations of loading were formed: Frame FA is an edge frame carrying evenly distributed vertical load; the load on the two spans of the internal frame FB are not equal; however, they are not very different (5 to 8) either; the frame FC, on the other hand, carries very different (1 to 4) loads over its two spans. In other words, the loading becomes more and more uneven from FA to FC. Each of these frames were elastically analysed for eight various values of the coefficient m from 1 to $\frac{1}{10}$, and the resulting moments at the critical sections were listed in Table 13 together with those obtained from the analysis of "Panel by Panel Loading Test" data. These critical section moments were compared one by one with the corresponding experimental value. The sums of squares of differences for each frame were then tabulated in Table 14. This last table shows that the best m values found from the analysis of evenly loaded frames, apply to the cases of uneven loads as well. One thing, however, must be pointed out that as the loading becomes more and more uneven, the best value of m becomes less and less defined.

DEFLECTION APPROACH - The same principle as the one used for moment approach, was applied. The mid-panel deflections were calculated for various values of the coefficient m , and compared with the measured deflections. The best m was then chosen on the basis of least squares.

The calculation of the mid-panel deflections from the frame analysis involved a higher degree of approximation. Therefore, this approach could not be as reliable as the moment approach. The results were, therefore, weighed accordingly. However, it served as a further check on the results of the moment approach, and provided additional confidence by giving rather reasonable results in agreement with those of the former.

Theoretically, a beam is a one dimensional element. Therefore, the deflection at a particular section is assumed to be constant along the width. This obviously cannot be true for the hypothetical beam which in fact is a part of a slab. However, it was thought that the order of error should be the same for all calculations corresponding to various values of m . Since the comparison was more important than the quantities themselves, the approach was justified as an approximation.

The consideration is illustrated in Fig. 54, and the results are given in Table 15.

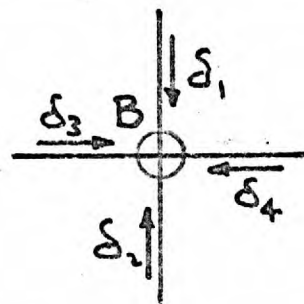
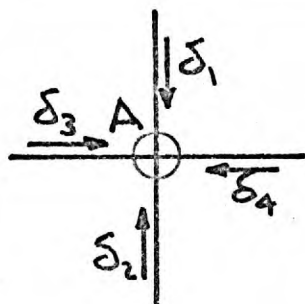
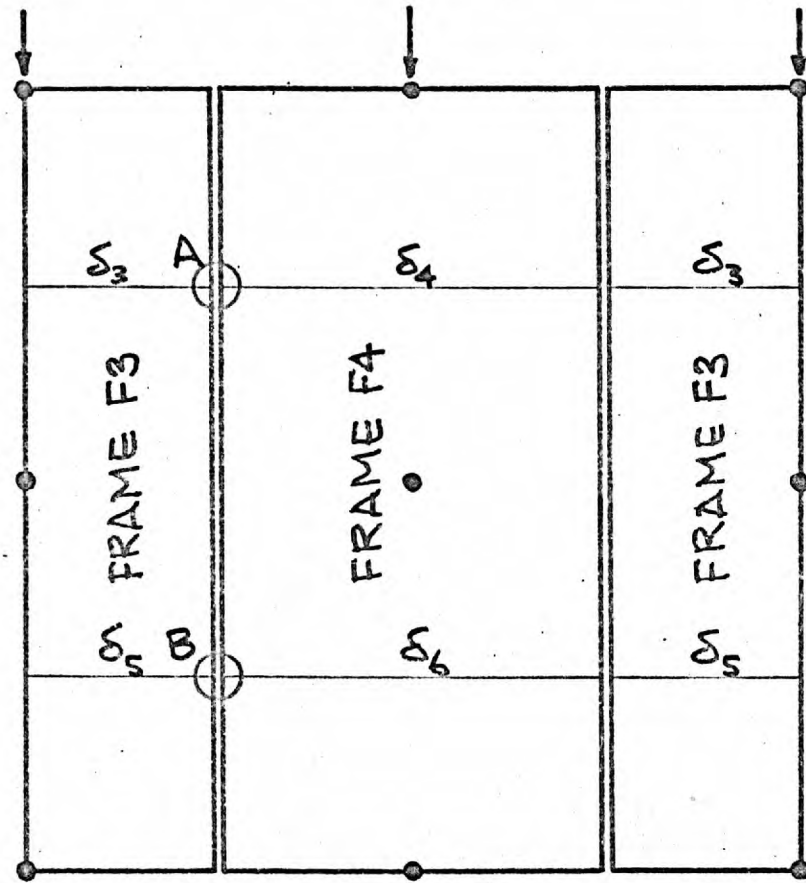
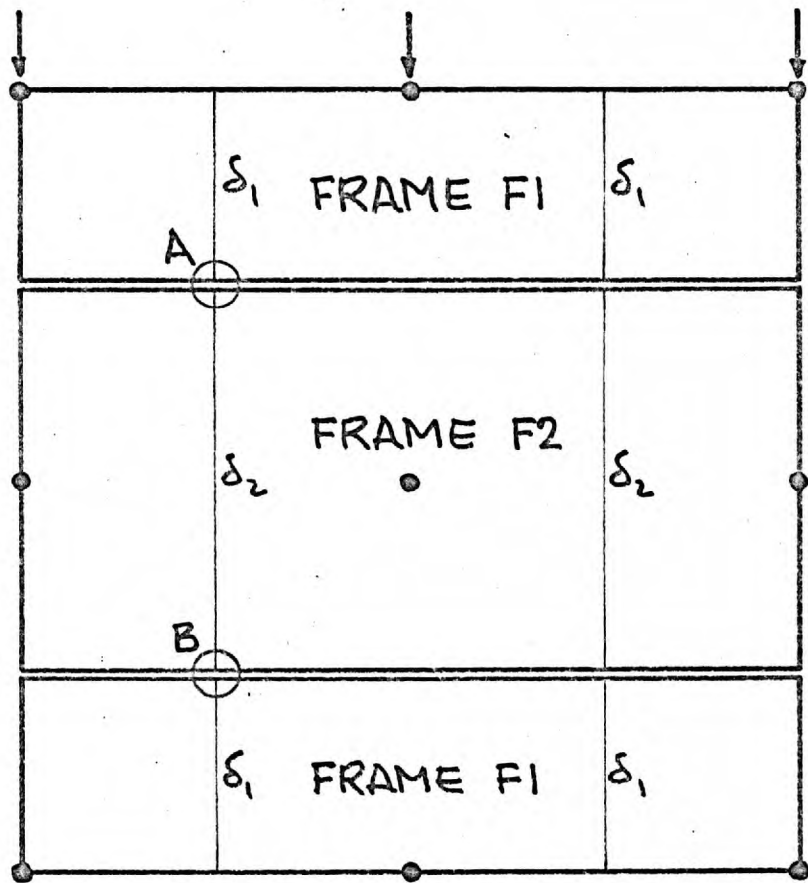
The best value of m determined this way is $\frac{1}{5}$. But it is not as well defined as that of the moment approach. As can be seen in the table, there is not much difference between the values corresponding to $\frac{1}{4}$ and $\frac{1}{5}$.

FRAME	m	CRITICAL MOMENTS (ft.-lb)						
		M _A	M _{AL} ^o	M _{CA}	M _{CD}	M _{CE}	M _{CE} ^o	M _E
A F L W Z A F R A M E	1	10 406	2 947	11 200	0	11 200	2 947	10 406
	1/2	8 876	4 622	9 381	0	9 381	4 622	8 876
	1/3	8 100	5 455	8 490	0	8 490	5 455	8 100
	1/4	7 430	6 161	7 748	0	7 748	6 161	7 430
	1/5	6 499	7 142	6 754	0	6 754	7 142	6 499
	1/6	6 358	7 276	6 591	0	6 591	7 276	6 358
	1/8	5 550	8 109	5 732	0	5 732	8 109	5 550
	1/10	4 921	8 755	5 070	0	5 070	8 755	4 921
	EXP.	5 690	6 600	7 050	1 470	8 520	6 350	5 910
B F L W Z A F R A M E	1	8 244	3 413	16 180	6 085	22 265	6 703	14 329
	1/2	7 611	5 338	12 963	5 222	18 185	9 491	12 833
	1/3	7 210	6 288	11 465	4 787	16 252	10 876	11 996
	1/4	6 770	7 088	10 304	4 408	14 712	12 055	11 179
	1/5	6 017	8 174	8 885	3 868	12 753	13 681	9 885
	1/6	5 958	8 346	8 600	3 794	12 394	13 927	9 752
	1/8	5 289	9 285	7 391	3 325	10 716	15 335	8 614
	1/10	4 745	10 011	6 484	2 957	9 441	16 428	7 703
	EXP.	4 430	6 650	11 950	4 960	16 910	12 500	8 640
C F L W Z A F R A M E	1	2 750	438	3 250	7 500	10 750	3 250	10 250
	1/2	2 358	922	2 674	6 379	9 053	4 856	8 736
	1/3	2 153	1 163	2 397	5 819	8 216	5 656	7 972
	1/4	1 975	1 364	2 173	5 339	7 512	6 338	7 313
	1/5	1 727	1 631	1 886	4 670	6 556	7 274	6 397
	1/6	1 689	1 676	1 834	4 571	6 405	7 418	6 260
	1/8	1 473	1 908	1 587	3 992	5 579	8 228	5 465
	1/10	1 304	2 087	1 398	3 542	4 940	8 857	4 847
	EXP.	45	170	4 800	4 530	9 380	8 250	6 220

TABLE 13 - VARIATION OF CRITICAL MOMENTS FOR UNEVEN LOADING

m	FRAME FA	FRAME FB	FRAME FC
1	93 945 290	138 829 245	61 435 549
1/2	34 182 002	41 195 873	31 628 171
1/3	16 951 650	22 457 674	23 892 479
1/4	8 810 530	20 131 771	20 967 563
1/5	7 289 702	35 653 269	22 422 022
1/6	8 054 002	41 446 429	23 312 458
1/8	17 191 330	77 542 349	30 747 051
1/10	31 347 172	117 377 825	39 883 692

TABLE 14 - SUMS OF SQUARES OF DIFFERENCES FOR UNEVEN LDG.



$$\delta_A = \frac{1}{4} (\delta_1 + \delta_2 + \delta_3 + \delta_4)$$

$$\delta_B = \frac{1}{4} (\delta_1 + \delta_2 + \delta_5 + \delta_6)$$

FIG. 54. MID-PANEL DEFLECTIONS OBTAINED FROM THE FRAME ANALYSIS

m	δ_1	δ_2	δ_3	δ_4	δ_5	δ_6	$\delta_1 - \delta_A$	$\delta_2 - \delta_A$	$\delta_3 - \delta_A$	$\delta_4 - \delta_A$	$\delta_1 - \delta_B$	$\delta_2 - \delta_B$	$\delta_3 - \delta_B$	$\delta_4 - \delta_B$	$\sum d_i^2$
1	239	503	338	608	139	397	84	348	183	453	69	333	-31	227	534 999
1/2	199	429	319	565	78	307	44	274	164	410	29	259	-92	137	367 163
1/3	182	403	318	550	46	258	27	248	163	395	12	233	-124	88	322 380
1/4	149	355	297	515	0	194	-6	200	142	360	-21	185	-170	24	253 942
1/5	62	244	221	416	-97	72	-93	89	66	261	-108	74	-267	242	236 040
1/6	57	253	241	434	-94	71	-98	98	86	279	-113	83	-264	241	251 880
1/8	-2	156	181	354	-184	-42	-157	1	26	199	-172	-14	-354	212	264 967
1/10	-70	70	124	281	-265	-141	-225	-85	-31	126	-240	-100	-435	311	428 233

OL. FOR THE TEST STRUCTURE 1 ($\delta_A = 0.155$ in. AND $\delta_B = 0.170$ in. MEASURED IN 1/23/7)

m	δ_1	δ_2	δ_3	δ_4	δ_5	δ_6	$\delta_1 - \delta_A$	$\delta_2 - \delta_A$	$\delta_3 - \delta_A$	$\delta_4 - \delta_A$	$\delta_1 - \delta_B$	$\delta_2 - \delta_B$	$\delta_3 - \delta_B$	$\delta_4 - \delta_B$	$\sum d_i^2$
1	122	320	242	451	1	188	20	218	140	349	40	238	-81	106	265 366
1/2	101	275	257	445	-54	105	-1	173	155	343	19	193	-136	23	228 066
1/3	93	253	272	450	-87	57	-9	151	170	348	11	171	-169	-25	231 434
1/4	77	225	276	445	-123	6	-25	123	174	343	-5	143	-205	-76	231 954
1/5	34	165	250	401	-182	-72	-68	63	148	299	-48	83	-264	-154	222 503
1/6	40	168	270	420	-190	-85	-69	66	168	318	-42	86	-272	-167	248 581
1/8	3	115	257	394	-251	-164	-99	13	155	292	-79	33	-333	-246	279 994
1/10	-30	69	243	369	-303	-231	-132	-33	141	267	-112	-13	-385	-313	368 590

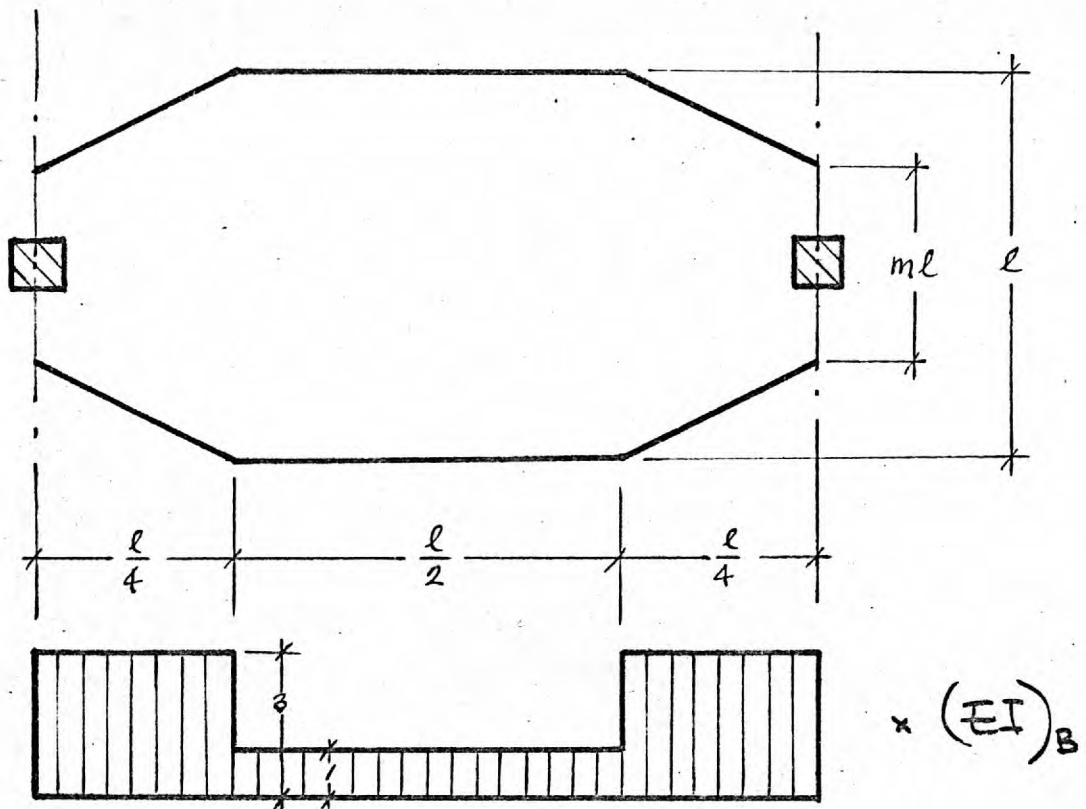
b. FOR THE TEST STRUCTURE 2 ($\delta_A = 0.102$ in. AND $\delta_B = 0.082$ in. MEASURED IN 2/11/7)

TABLE 15. CALCULATED MID-PANEL DEFLECTIONS AND COMPARISON WITH THE MEASURED VALUES

The same values had been obtained by the moment approach for various kinds of frames. So, the deflection approach confirms the results of the former, in spite of its being more approximate.

7.1.4. PROPOSED DESIGN METHOD - If the results of the flexural analysis of the experimental evidence obtained from the two test structures are reconsidered from the designer's point of view, the following points attract the attention:

- i. The flat plate type structures should be designed as continuous frames. But,
- ii. The beams of these frames should be considered fully cracked and the columns uncracked. The combination of cracked beams and cracked columns is acceptable; but the beams should never be considered uncracked. And,
- iii. The effective beam width should be considered varying, instead of the full constant width suggested by the codes of practice. Based on the information obtained from a limited number of test structures, the variation illustrated in Fig. 47 was found very reasonable. Since the variation suggested is linear, it does not introduce much complication; the stiffness coefficients, carry-over factors and the fixed end moments corresponding to three different rates of variation are given in Table 16, for the easy reference of the designer. Having these values in hand, most of the methods of structural analysis can be applied to the frames considered, without any difficulty. For the ordinary design purposes, the effective beam width variation coefficient m can be recommended as $\frac{1}{5}$ for the edge frames and $\frac{1}{4}$ for the internal frames. However, $\frac{1}{4}$ can be used rather satisfactorily for both kinds. These values are recommended considering that a practical structure will perform in a state similar to the "Normal Cracking" state of the analysis of the experimental results of the present investigation. On the other hand, in the design of some structures, economy considerations may justify slightly higher deflections. For such structures, $m = \frac{1}{3}$ instead of $\frac{1}{4}$ should be considered more realistic. In any case, it must never be forgotten that these coefficients are recommended for the beams where the ratio of the cracked section flexural rigidity corresponding to the negative moment region to that of the positive moment region is around 3.0 which is considered rather common for the practical structures.



$$S_A = S_B = \frac{2(EI)_B}{l} \times K_{AA} \quad \text{AND} \quad M_{FA} = -M_{FB} = K_F \times w l^2$$

WHERE $(EI)_B$ IS THE CRACKED SECTION FLEXURAL RIGIDITY FOR THE POSITIVE MOMENT REGION
 $(EI)_T$ IS THE CRACKED SECTION FLEXURAL RIGIDITY FOR THE NEGATIVE MOMENT REGION

$\frac{(EI)_T}{(EI)_B}$	m	$K_{AA} = K_{BB}$	$C_{AB} = C_{BA}$	K_F
3.0	$\frac{1}{3}$	5.82962	0.55687	0.075913
	$\frac{1}{4}$	5.26955	0.53031	0.069435
	$\frac{1}{5}$	4.89104	0.51046	0.060612

TABLE 16. DESIGN COEFFICIENTS FOR VARIABLE EFFECTIVE BEAM WIDTH

- iv. The moments obtained at the critical sections by the modified frame analysis suggested above, should be distributed between column and middle strips by the coefficients recommended by the British Code of Practice CP 114. The requirements of this code on the placement of the calculated reinforcement seem to be rather reasonable and satisfactory. In other words, since the whole argument is based on the results obtained from the two test structures designed according to this code, it is rather essential to follow its recommendations on apportionment of the moments and on the reinforcement spacing in order to be sure of the design coefficients suggested in this thesis.
- v. Last but not least, the designer should not be misled by this concept of varying effective beam width. The geometry suggested this way is a fictitious mathematical model which serves the purpose of determining the moments at the critical sections as realistically as possible. Once the critical section moments are determined, this concept must not interfere with the design of the sections.

7.2. SHEAR ANALYSIS - One of the important conclusions of the present investigation is that the punching problem is generally more critical than the problem of flexure in flat-plate type structures without shear reinforcement, designed for practical load combinations. This opinion was recently reinforced by the interaction relationships in this kind of slab-column connections studied by N. N. Anis²². They indicate that in the cases of eccentricity less than three times the column size, the punching problem is more critical, and for larger eccentricities flexure becomes the controlling factor. Since in practical cases, the eccentricity is in general less than that critical value, the punching failure mostly precedes the flexural one.

The physical mechanism of punching is rather complicated and it has not been clearly understood yet. There are so many factors influencing the behaviour that none of the available methods can satisfactorily apply; each one of them is restricted in one respect or another.

The two test structures had 18 columns of various realistic types subjected to various realistic load combinations. The punching cone details of typical three of these are given in Figs. 55, 56 and 57, and the calculated as well as measured column reactions for each case are listed in Table 17. It was thought that these 18 columns could form a very good basis

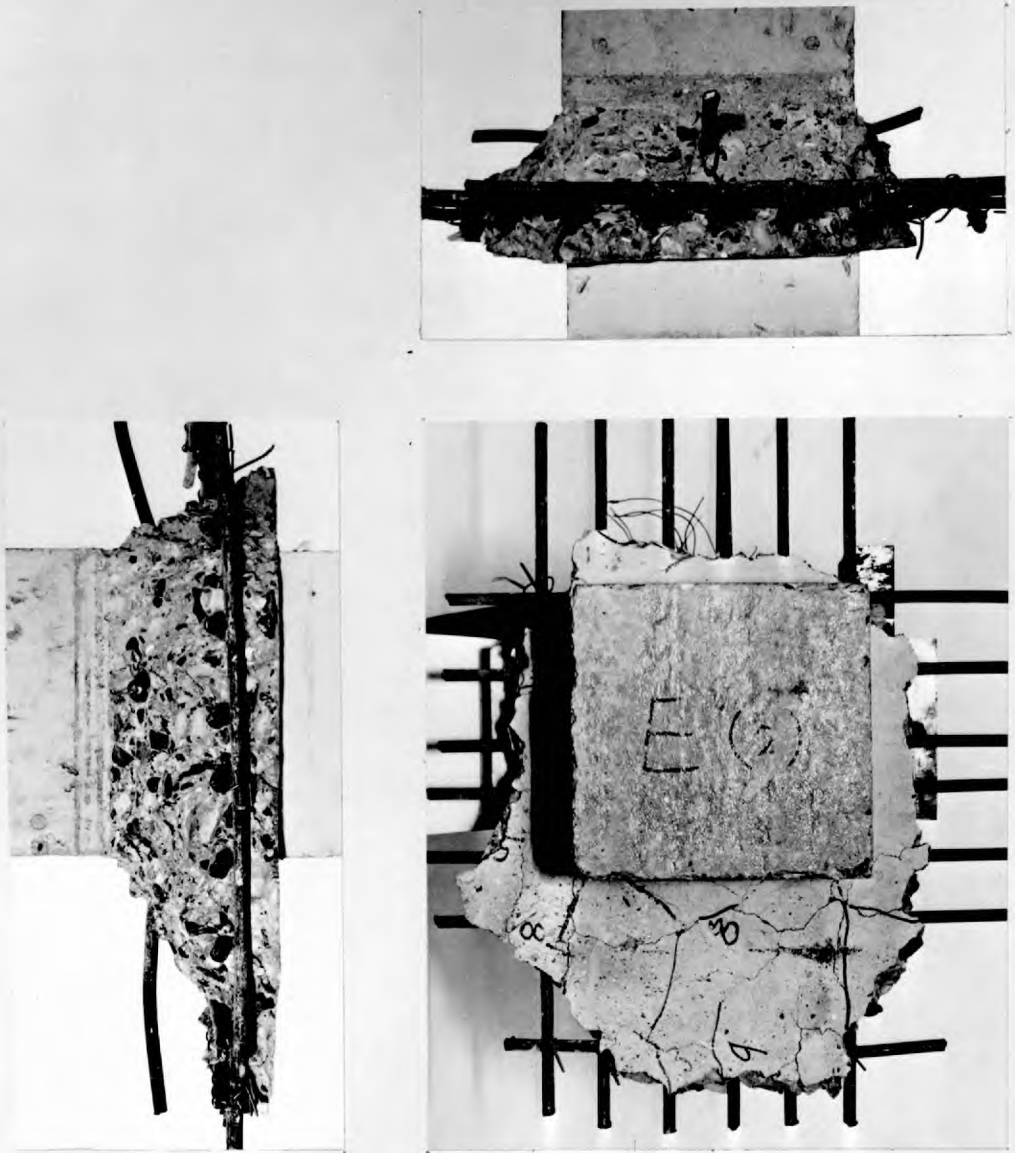


FIG. 55 - TYPICAL INTERNAL COLUMN PUNCHING CONE

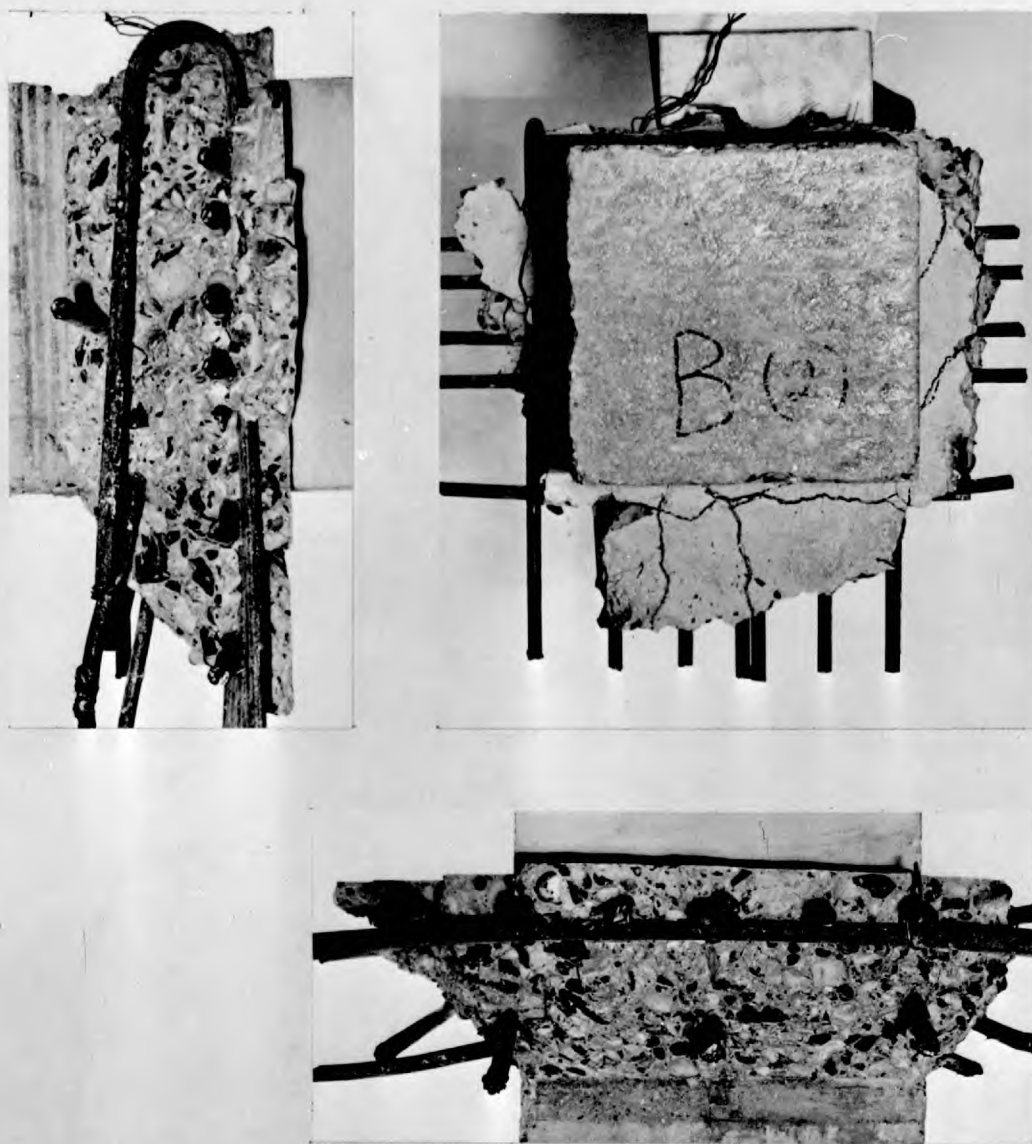


FIG. 56 - TYPICAL EDGE COLUMN PUNCHING CONE

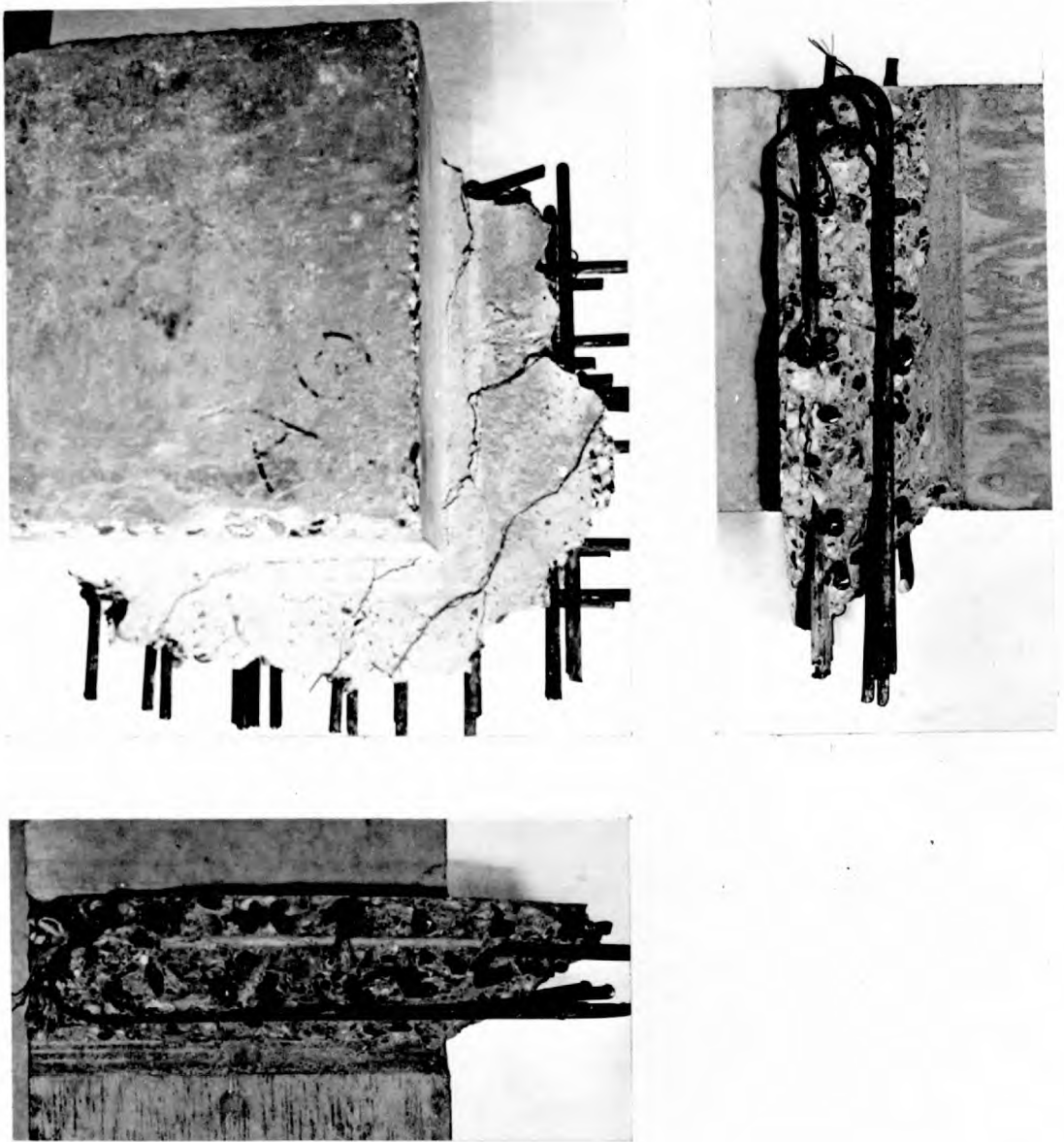


FIG. 57 - TYPICAL CORNER COLUMN PUNCHING CONE

for a comparison of various methods. In the present investigation, the attention was concentrated on the results of the available methods compared with the experimental values, rather than on their nature. The methods considered in this study were:

- i. British Code CP 114 method - The nominal shear stress is calculated at a distance from the column face equal to half the overall depth of the slab, by

$$v = \frac{V}{b_o n_1 d_1} \quad \text{where}$$

V = total shear force,

b_o = critical section length, and

$n_1 d_1$ = resistance moment arm.

The value of the calculated v should not exceed the allowable shear stress given by the code for the quality of concrete used. In nominal shear stress calculation, the effect of the moment in the column is not taken into account, and neither is the contribution of the flexural reinforcement to the shear strength. However, the proposed draft British Code gives the allowable shear stress in accordance with the percentage of flexural reinforcement as well as the concrete strength.

- ii. American Concrete Institute Building Code Method - The way the nominal shear stress is obtained, is slightly different from CP 114 method. It is given by

$$v = \frac{V}{b_o d_1} \quad \text{where}$$

b_o is calculated at a distance from the column face equal to half the effective depth of the slab, and the effective depth d_1 is considered instead of the resistance moment arm ($n_1 d_1$). The allowable shear stress is again given in terms of solely the cylinder strength of the concrete used. Obviously, both of the criticisms mentioned for British Code method are valid for this method as well.

- iii. Method proposed by J. Moe - This method is intended to take into consideration the effect of the moment in the column, in shear stress calculation, and the contribution of the flexural

reinforcement to the shear strength through the term V_{flex} . This method is therefore more realistic and should be more reliable than the two mentioned above, for the internal columns. However, it is not as realistic for the edge and corner columns as it is for the internal ones, simply because the determination of the coefficients was based on the test results which mainly consisted of internal columns. The shear stress formula given in the book (Ref. 19) had been derived for the case of internal column and therefore was not applicable to the other kinds. The generalized form of these equations for various column types were derived on the same basis, and used in the calculations required for the present investigation. The derivation of these equations are presented in Appendix 3. On the other hand the shear strength is given by,

$$\bar{v} = \frac{15 \left(1 - 0.075 \frac{r}{d_1}\right) \sqrt{f'_c}}{1 + 5.25 \frac{b_o d_1 \sqrt{f'_c}}{V_{flex}}} \quad \text{where}$$

r = column size,

f'_c = cylinder strength of concrete,

b_o = length of critical section calculated at the column face,

V_{flex} = shear force at ultimate flexural capacity.

The determination of V_{flex} presents some difficulty. In this investigation, it is calculated on the basis of yield line theory. For each case considered in this investigation, various yield line patterns corresponding to (i) local flexural failure, and (ii) overall flexural failure, were considered. The local flexural failure seemed to be more likely in the cases of edge and corner columns, and the overall flexural failure in the cases of internal columns.

- iv. Method recommended by ACI-ASCE Joint Committee 426 - This method considers the critical section at a distance $d_1/2$ from the column face, and assumes that the vertical shear stresses are constant across the critical sections parallel to the axis of torsion and vary linearly on the other two critical sections perpendicular to the axis of torsion. It is further assumed that the law of

superposition applies so that the shear stress can be computed by

$$v = \frac{V}{b_o d_1} + K_x \frac{M_x}{J_x} C_x + K_y \frac{M_y}{J_y} C_y \quad \text{where}$$

M_x and M_y = total joint moments along x and y directions respectively,

J_x and J_y = corresponding polar moments of inertia of the critical peripheral section about its centroidal axes,

C_x and C_y = corresponding outermost fibre distances from the centroidal axes of the critical peripheral section,

b_o = length of the critical peripheral section,

d_1 = effective depth,

K_x and K_y = reduction factors on the corresponding total moments to obtain the moment transferred by torsional shear stresses. These were found to be 0.2 on the basis of limited test data considered by the committee. However, at a later date, it was suggested by Hanson and Hanson²¹ that 0.4 would be a more realistic value. The expressions for polar moments of inertia for various types of columns were given in Appendix 3, in the form they were used in computations.

As far as the shear strength is concerned, this method accepts a very similar form as that of the ACI Building Code method.

That is

$$\bar{v} = 4 \sqrt{f'_c}$$

The contribution of the flexural reinforcement to the shear strength is again omitted. The method was applied to the cases dealt with twice; once with $K_x = K_y = 0.2$ as suggested by the committee, and once with $K_x = K_y = 0.4$ as suggested by Hanson and Hanson.

- v. A combination of the ACI-ASCE Joint Committee 426 and Moe's methods - The method recommended by the Committee 426 seemed to be quite satisfactory as far as the shear stress was concerned, but as

explained above it did not explicitly consider the effect of the flexural reinforcement in the strength equation. A combination of the stress part of this method with the strength part of Moe's method, which explicitly considers the flexural reinforcement, seemed to be reasonable. This combination is also included in the analysis with $K_x = K_y = 0.4$ as well as $K_x = K_y = 0.2$.

- vi. The Equilibrium and Compatibility Analysis - This approach has been developed by N. N. Anis and C. W. Yu, considering the compatibility of strains and equilibrium of forces in the failure region, to establish a relationship between the ultimate load and sectional properties of the slab-column connection. The basic criterion of failure is assumed to be the crushing of concrete under biaxial compression⁽⁺⁾, and consequently the steel is considered not to have yielded. The compatibility is based on the rotation around the neutral axis at the root of the shear crack, of the rigid body bounded by (i) the shear crack, (ii) the radial cracks, and (iii) the line of contraflexure. It is considered that the variation of shear stress distribution due to the column moment is linear, and it is superposed on the uniform peripheral shear stress distribution caused by the axial load. Four equilibrium equations; three at failure, one at cracking, and one compatibility equation are formed and solved for five unknowns including the ultimate shear capacity P_{ult} and the geometrical properties. The contribution of the dovel effect to the ultimate shear capacity is separately calculated and added to the value formerly obtained. The method is applicable to edge and corner columns as well as the internal ones. Since the equations are rather complicated, the method is not very suitable for hand calculations and the use of computer is essential for the time being. However, recent progress has indicated that the equations may be put in the form of charts or tables for easy reference of the designer.

The analysis is basically the comparison of the results of the methods explained above applied to the 18 columns of the two test structures, evaluated for:

- i. The reactions obtained by elastic analysis of the frames at the design load,

(+) Biaxial compression stress envelopes developed by G. W. D. Vile.³⁷

- ii. The reactions measured at the design load, and
- iii. The reactions measured at punching.

These reactions are tabulated in Table 17.

A detailed comparison of the results is given in Tables 18 and 19. In these tables the following notations are used:

- v_d = Maximum shear stress calculated with the design load reactions (either measured or from the elastic analysis)
- v_p = Maximum shear stress calculated from measured punching reactions
- \bar{v} = Allowable design shear stress as recommended by the code
- \bar{v}_d = Ultimate shear strength calculated with design load reactions from elastic analysis
- ϕ = Safety factor implicitly considered by the code.

In these tables, the criterion is the comparison of apparent and actual load factors which are defined as,

$$\text{Apparent LF} = \frac{\bar{v}}{v_{dc}} \phi \quad (\text{In case of } \bar{v} \text{ is given})$$

$$\text{Or} \quad = \frac{\bar{v}_d}{v_{dc}} \quad (\text{In case of } \bar{v}_d \text{ is given})$$

$$\text{Actual LF} = \frac{v_p}{v_{dm}}$$

Due to its different nature the results of the equilibrium and compatibility analysis are not included in these tables; instead they are presented in Table 20 where calculated ultimate shear capacity P_{uc} is compared with the measured punching load P_{um} for each column.

The study of these three tables gives a good insight to the problem and an idea of the efficiency and consistency of each method considered. However, Table 21 gives a general view of the picture. The tabulated values are the average ratios of observed ultimate stress to the calculated ultimate strength (expressed in terms of stress), i.e. v_p/\bar{v}_d for the first seven methods, and the average ratios of measured punching load to the calculated ultimate shear capacity, i.e. P_{um}/P_{uc} for the equilibrium and compatibility analysis.

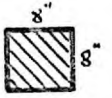
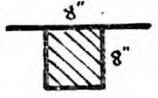
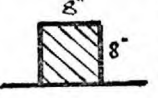
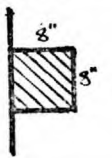
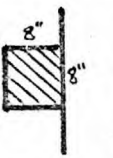
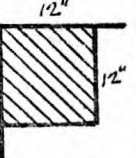
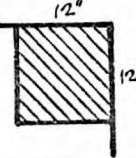
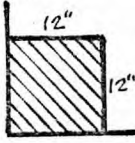
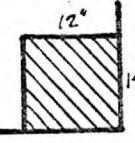
COLUMN	TYPE		INTERNAL	EDGE (\perp)		EDGE (\parallel)		CORNER			
	NAME		E	B	H	D	F	A	C	G	K
	SHAPE										
CAL'D AT DES. LD.	STR. 1	V (lb)	21 372	11 108	11 108	11 108	11 108	5 446	5 446	5 776	5 776
		M _x (in.-lb)	0	0	0	145 200	145 200	105 600	105 600	105 600	105 600
		M _y (in.-lb)	66 720	106 560	183 840	36 240	36 240	84 120	84 120	127 080	127 080
	STR. 2	V	21 372	11 108	11 108	11 108	11 108	5 446	5 446	5 776	5 776
		M _x	0	0	0	145 200	145 200	105 600	105 600	105 600	105 600
		M _y	66 720	106 560	183 840	36 240	36 240	84 120	84 120	127 080	127 080
MEAS'D AT DES. LD.	STR. 1	V	22 100	8 720	9 970	10 460	9 850	4 500	4 200	4 900	5 140
		M _x	27 400	6 200	320	116 400	111 600	70 200	68 200	62 100	75 300
		M _y	60 120	82 300	141 000	40 480	33 900	40 900	36 400	104 200	75 800
	STR. 2	V	23 108	10 220	10 450	10 360	10 380	4 470	3 920	4 460	5 260
		M _x	4 840	4 000	4 920	114 200	120 840	75 880	78 540	60 920	75 120
		M _y	53 950	96 040	143 140	46 500	46 370	50 720	50 400	111 200	104 510
MEAS'D AT PUN'G.	STR. 1	V	37 000	19 750	17 050	16 650	16 650	10 750	10 450	12 100	12 150
		M _x	7 700	3 500	7 950	99 000	99 000	150 800	119 000	196 000	207 500
		M _y	103 900	218 800	240 000	51 200	51 200	121 700	103 000	312 500	299 000
	STR. 2	V	41 760	27 100	16 760	17 960	17 930	10 980	13 210	9 230	10 400
		M _x	1 050	200	4 000	182 650	192 250	226 900	221 800	115 960	127 900
		M _y	176 200	336 000	174 400	148 100	141 700	204 340	231 300	239 900	233 450

TABLE 17 - CALCULATED AND MEASURED COLUMN REACTIONS AT THE DESIGN LOAD AND PUNCHING

COLUMN TYPE & SIZE		WITH CALCULATED REACTIONS AT THE DESIGN LOAD																Z Z J J D D
		CALCULATED MAX. & ALLOWABLE (psi)				CALCULATED MAX. & CALCULATED ULT. (psi)					APPARENT LOAD FACTORS							
		CP 114		ACI		MOE		ACI-ASCE 426			CP 114	ACI	MOE	ACI-ASCE 426		426 + MOE		
		V_d	\bar{V}	V_d	\bar{V}	V_d	\bar{V}_M	V_{2d}	V_{4d}	\bar{V}_{426}	\bar{V}/V_d	\bar{V}/V_d	\bar{V}_M	\bar{V}_{426}	\bar{V}_{426}	\bar{V}_M	\bar{V}_M	
									x (SF IMPLIED BY THE CODE)		V_d	V_{2d}	V_{4d}	V_{2d}	V_{4d}			
INT. (8"x8")	E1	148	130	162	143	309	487	189	216	286	0.88	0.88	1.58	1.52	1.33	3.04	2.66	E1
	E2	148	130	162	143	309	409	189	216	286	0.88	0.88	1.33	1.52	1.33	2.87	2.51	E2
EDGE (-) (8"x8")	B1	118	130	109	143	339	358	164	219	286	1.10	1.31	1.06	1.75	1.30	2.18	1.86	B1
	B2	118	130	109	143	339	307	164	219	286	1.10	1.31	0.91	1.75	1.30	1.87	1.40	B2
	H1	118	130	109	143	473	358	204	299	286	1.10	1.31	0.76	1.40	0.96	1.76	1.20	H1
	H2	118	130	109	143	473	307	204	299	286	1.10	1.31	0.65	1.40	0.96	1.50	1.03	H2
EDGE (I) (8"x8")	D1	118	130	109	143	460	358	200	291	286	1.10	1.31	0.78	1.43	0.98	1.79	1.23	D1
	D2	118	130	109	143	460	307	200	291	286	1.10	1.31	0.67	1.43	0.98	1.54	1.06	D2
	F1	118	130	109	143	460	358	200	291	286	1.10	1.31	0.78	1.43	0.98	1.79	1.23	F1
	F2	118	130	109	143	460	307	200	291	286	1.10	1.31	0.67	1.43	0.98	1.54	1.06	F2
CORNER (12"x12")	A1	79	130	71	143	508	130	144	220	286	1.64	2.01	0.26	1.99	1.30	0.90	0.59	A1
	A2	79	130	71	143	508	112	144	220	286	1.64	2.01	0.22	1.99	1.30	0.78	0.51	A2
	C1	79	130	71	143	508	130	144	220	286	1.64	2.01	0.26	1.99	1.30	0.90	0.59	C1
	C2	79	130	71	143	508	112	144	220	286	1.64	2.01	0.22	1.99	1.30	0.78	0.51	C2
	G1	79	130	71	143	606	129	165	258	286	1.64	2.01	0.21	1.74	1.11	0.78	0.50	G1
	G2	79	130	71	143	606	111	165	258	286	1.64	2.01	0.18	1.74	1.11	0.67	0.43	G2
	K1	79	130	71	143	606	129	165	258	286	1.64	2.01	0.21	1.74	1.11	0.78	0.50	K1
	K2	79	130	71	143	606	111	165	258	286	1.64	2.01	0.18	1.74	1.11	0.67	0.43	K2

TABLE 18 - APPARENT LOAD FACTORS BASED ON CALCULATED REACTIONS AT THE DESIGN LOAD

COLUMN TYPE & SIZE		WITH MEASURED REACTIONS AT PUNCHING AND AT THE DESIGN LOAD																		Z X Y C O O
		MAX. AT THE DESIGN LOAD & MAX. AT PUNCHING (psi)										ACTUAL LOAD FACTORS								
		CP 114		ACI		MOE		426 (0.2)		426 (0.4)		CP114	ACI	MOE	426		426+MOE			
		V_d	V_p	V_d	V_p	V_d	V_p	V_d	V_p	V_d	V_p	$\frac{V_p}{V_d}$	$\frac{V_p}{V_d}$	$\frac{V_p}{V_d}$	$\frac{V_{.2p}}{V_{.2d}}$	$\frac{V_{.4p}}{V_{.4d}}$	$\frac{V_{.2p}}{V_{.2d}}$	$\frac{V_{.4p}}{V_{.4d}}$		
I. Z (8"x8")	E1	153	294	168	280	312	531	193	325	219	370	1.92	1.68	1.70	1.68	1.69	1.68	1.69	E1	
	E2	160	331	175	316	317	679	199	391	223	466	2.06	1.81	2.14	1.96	2.08	1.96	2.08	E2	
EDGE (+) (8"x8")	B1	92	209	85	194	273	660	131	308	175	422	2.27	2.26	2.42	2.35	2.41	2.35	2.41	B1	
	B2	108	287	100	266	316	960	152	440	203	613	2.66	2.65	3.03	2.89	3.02	2.89	3.02	B2	
	H1	105	181	98	167	384	665	171	295	244	422	1.72	1.71	1.73	1.73	1.73	1.73	1.73	H1	
	H2	111	178	102	164	402	542	179	337	255	509	1.60	1.60	1.35	1.88	2.00	1.88	2.00	H2	
EDGE (//) (8"x8")	D1	111	176	103	163	408	480	181	293	259	422	1.58	1.59	1.08	1.62	1.63	1.62	1.63	D1	
	D2	109	190	101	176	426	782	182	461	261	745	1.74	1.73	1.88	2.53	2.86	2.53	2.86	D2	
	F1	104	176	103	163	382	480	165	293	232	422	1.69	1.69	1.25	1.78	1.82	1.78	1.82	F1	
	F2	110	190	102	176	406	793	185	453	268	750	1.73	1.73	1.95	2.45	2.80	2.45	2.80	F2	
CORNER (12"x12")	A1	61	148	56	133	250	603	100	243	145	352	2.42	2.39	2.42	2.43	2.43	2.43	2.43	A1	
	A2	61	150	55	136	269	751	105	309	157	380	2.46	2.44	2.79	2.95	2.42	2.95	2.42	A2	
	C1	57	142	52	129	233	525	94	222	136	315	2.49	2.52	2.25	2.36	2.32	2.36	2.32	C1	
	C2	53	180	48	163	261	799	100	248	151	532	3.40	3.36	3.06	2.48	3.52	2.48	3.52	C2	
	G1	67	165	60	149	834	958	127	353	262	557	2.46	2.48	2.87	2.78	2.12	2.78	2.12	G1	
	G2	61	125	55	114	332	622	124	260	193	407	2.05	2.05	1.88	2.09	2.11	2.09	2.11	G2	
	K1	70	166	63	150	317	957	123	354	184	557	2.37	2.37	3.02	2.88	3.02	2.88	3.02	K1	
	K2	71	142	65	128	359	646	137	277	209	426	2.00	1.97	1.80	2.02	2.03	2.02	2.03	K2	

TABLE 19 - ACTUAL LOAD FACTORS BASED ON MEASURED REACTION AT PUNCHING AND DESIGN LOAD

COL.	P_{uc}	P_{um}	$\frac{P_{um}}{P_{uc}}$	COL.	P_{uc}	P_{um}	$\frac{P_{um}}{P_{uc}}$
E1	34 600	37 000	1.07	E2	37 300	41 760	1.12
B1	14 900	19 750	1.32	B2	16 000	27 100	—
H1	14 200	17 050	1.20	H2	16 900	16 760	0.99
D1	17 300	16 650	0.96	D2	14 500	17 960	1.24
F1	17 300	16 650	0.96	F2	16 000	17 930	1.12
A1	11 870	10 750	0.91	A2	12 700	10 980	0.86
C1	13 700	10 450	0.76	C2	12 800	13 210	1.03
G1	10 800	12 100	1.12	G2	11 700	9 230	0.79
K1	10 900	12 150	1.12	K2	10 600	10 400	0.98

TABLE 20. RESULTS OF EQUILIBRIUM AND COMPATIBILITY ANALYSIS

COLUMN TYPE	CP 114	ACI	MOE	ACI-ASCE (0.2)	ACI-ASCE (0.4)	COMM. MOE (0.2)	COMM. MOE (0.4)	EQLB. COMPT. ANLS.
INTERNAL	1.20	1.04	1.35	1.25	1.46	0.64	0.75	1.10
EDGE	0.76	0.64	2.04	1.25	1.88	1.08	1.58	1.12
CORNER	0.59	0.48	6.04	1.02	1.53	2.33	3.63	0.95

TABLE 21. AVERAGE $\frac{U_P}{U_R}$ VALUES (MEASURED / CALCULATED)

From these tables, it is evident that both British CP 114 and American Concrete Institute Building Code methods are very unsatisfactory and very unsafe for edge and corner columns. The allowable stress values are being revised in the proposed draft British Code. The new form is a considerable improvement. It was found approximately 20 percent safer than the version presently in use, when applied to the test structures of present investigation. However, it is still not very consistent for various column types. Considering the values, given in Table 21 for CP 114, increased by 20 percent, it is found that the internal columns are too safe and corner columns are still unsafe, while the edge columns are reasonable.

Moe's method predicted the strength of the internal columns reasonably well, but was far too conservative for the edge and corner columns. The ACI-ASCE Joint Committee 426 method appears to be fairly satisfactory; it is reasonably consistent for $K_x = K_y = 0.4$ as well as $K_x = K_y = 0.2$, however 0.4 gives rather conservative estimates while the results obtained by 0.2 are more realistic. The combination of this method with Moe's, shows a very similar pattern as Moe's method itself. This fact leads to the conclusion that Moe's stress equations agree with that of ACI-ASCE Joint Committee 426. What causes the discrepancy for edge and corner columns is Moe's strength equation.

The results of the Equilibrium and Compatibility Analysis appear to be rather satisfactory; internal and edge columns are generally on the safe side, and the corner columns are slightly unsafe.

7.2.1. DESIGN RECOMMENDATIONS - The states of stress around the various types of slab-column connections subjected to various combinations of loads have not been clearly understood yet. Most of the available methods to estimate the punching shear strength of the connection, approach the problem from the practical side. In this respect, the Equilibrium and Compatibility Analysis is a promising attempt to understand the real behaviour of the various types of connections. However, in the present form it does not appeal to the designer since it consists of rather complicated equations and the use of computer is essential.

Judging the methods by the results obtained on the 18 columns of various types of the two test structures, ACI-ASCE Joint Committee 426 Method seems to be the one which appeals to the designer most. It is rather simple and straightforward as well as being a quite satisfactory measure of the punching shear strength of the slabs having practical sectional properties.

In Appendix 3, the formula suggested by the committee is elaborated by addition of a third term representing a second component of the unbalanced column moment. The expressions needed for determination of each term are listed in tabular form in the same appendix for easy reference.

Some designers may find the method suggested by J. Moe more attractive, since this method explicitly considers the contribution of the flexural reinforcement to the punching shear strength. The results obtained in the present investigation indicate that this method can be recommended for internal columns, but it should not be applied to the edge and corner columns.

7.3. DEFLECTIONS AND CRACK WIDTH - For each principal test, the measured mid-panel deflections were plotted against the applied load (in terms of the design load). Both of the two sets of curves corresponding to each test structure displayed rather a similar pattern. For the early tests on each test structure, the load deflection curve could be simplified by two straight lines each corresponding to the pre-cracking and post-cracking loads respectively. In the later tests, the change in the slopes of these two straight lines became smaller. In the very late tests, the whole range could be idealized with a single straight line. These last forms of the relationship for the two test structures were very close. Therefore, the idealized load-deflection relationship given in Fig. 58, is intended to represent both test structures.

In the proposed draft British Code, the allowable deflection is given by,

$$\delta_{\text{allw}} = \frac{\text{Span length}}{250}$$

On the other hand, the additional deflection due to long term effects was accepted to be equal to the instantaneous deflection. Therefore, the allowable deflection was reduced by 2, to obtain 0.240 in. This value was found to correspond to exactly the design combined load on the idealized relationship determined from the test results. As explained in Chapter 6, in some of the tests carried out on the test structure 2, the vertical load was kept at a certain level while the horizontal load was increased. This phenomenon can be illustrated, on the load-deflection curves, by branching lines. In various tests, the branches corresponding to the horizontal load were found nearly parallel each time. It was, therefore, considered rather reasonable to draw parallel lines from the points corresponding to various

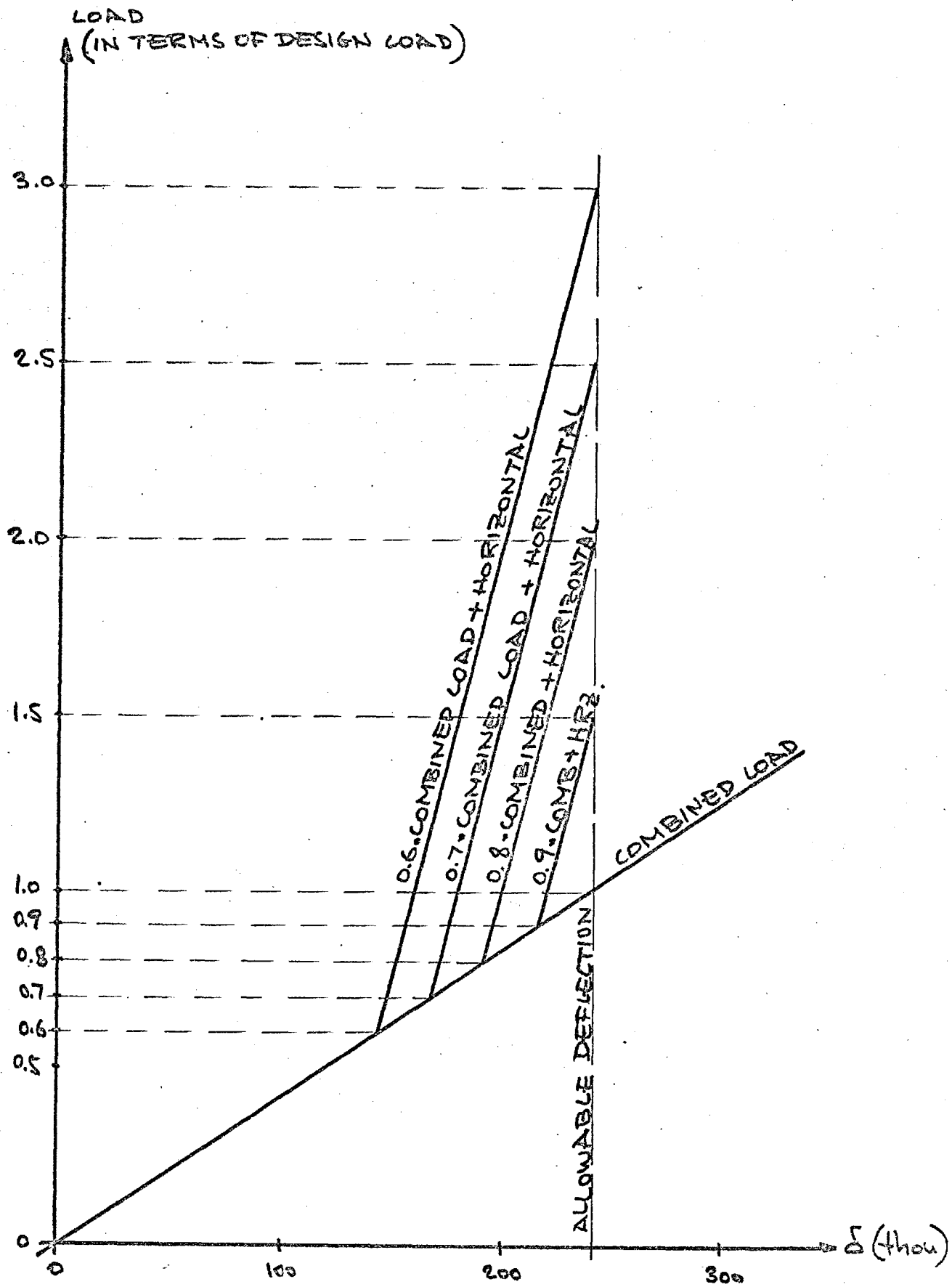


FIG. 58. IDEALIZED LOAD-DEFLECTION RELATIONSHIP

loading combinations, to estimate the horizontal load to cause the maximum allowable deflection, when the combined load has already reached a certain level. For example, referring Fig. 58, 1.5 times the design horizontal load is expected to cause the maximum allowable deflection, if the vertical load is kept constant at 0.9 times the design vertical load level.

On the other hand, the width of the widest crack observed on the test structure 2, was measured and recorded from time to time during the tests. The observations on this matter can be summarized as:

- i. The first visible cracks were recorded at approximately 0.7 times the design load.
- ii. The proposed draft British Code gives the allowable crack width as

$$w_{\text{allw}} = 0.3 \text{ mm.} = 0.012 \text{ in.}$$

This value was reached when the load was approximately 1.2 to 1.4 times the design combined load. In other words, this requirement of the code is in general automatically satisfied for the design loads.

- iii. Repeated loads caused wider and irreversible (which did not close after the removal of the load) cracks, as expected.
- iv. The crack width prior to the punching failure was measured as 0.075 in., that is more than six times the maximum allowable crack width.

CHAPTER 8

CONCLUSIONS AND RECOMMENDATIONS

FOR FURTHER RESEARCH

Various aspects of the present investigation have been presented in the previous chapters. The major conclusions drawn from various sources of information at various stages of the work, are summarised in this last chapter. Most of these conclusions encourage, some even require, further research on the subject. During the course of the work, a number of directions for investigation, were contemplated. However, the limitations of time and instrumentation allowed only some of them to be realised. The remaining directions and the improvements they promise are pointed out in the "Recommendations for Further Research" section.

8.1. CONCLUSIONS - On several occasions, it has already been mentioned that the attention was concentrated on the two aspects of the problem; (i) the general flexural behaviour, and (ii) the local behaviour of the slab-column connections. The conclusions are therefore classified into groups corresponding to each of these two aspects. However, since a great deal of effort was devoted to the development of the instrumentation systems, another group was formed to present the conclusions drawn from the observations concerning the behaviour and performance of the instrumentation systems.

8.1.1. CONCLUSIONS ON THE FLEXURAL BEHAVIOUR -

1. Under usual loading combinations, flexure is, in general, the less critical aspect of the design of flat plate type structures.
2. The yield line analysis is quite a good measure of flexural strength of this type of structure. Since punching failures preceded the flexural failure in the present investigation, well defined yield line patterns could not be obtained. However, the steel strains across the expected yield lines were consistently higher than those across the cracks in the other direction. The difference increased as the testing progressed. It is therefore assumed that the expected yield mechanism would form if the load could be sufficiently increased.

3. The deflections and crack width were found complying with the requirements of the proposed draft British code.
4. The modified frame analysis based on the concept of "Variable effective beam width" appears to be sufficiently realistic and very practical. It has also proved to be realistic even for the cases of frames with uneven loading.
5. The effective beam width over the columns increases as the cracking progresses. This can be explained by further sections taking part in stress transfer through torsion.
6. The null moment lines running around the columns for small deflections, and running parallel to the edge when the deflections are comparatively high, appear to indicate that moment transfer through torsion is not significant when the structure is not badly cracked and the deflections are not so high. However, its contribution increases as the cracking and the deflections progress.
7. The most realistic results are obtained from the frame analysis when the beams are assumed to be cracked and the columns uncracked. The combination of cracked beams and cracked columns is acceptable; but the beams should never be considered uncracked.
8. The internal column, in general, took more load than that predicted by the elastic analysis recommended by the code.
9. Progressive cracking of the slab resulted in a further increase in the internal column reaction and a decrease in those of the edge columns.

8.1.2. CONCLUSIONS ON THE SHEAR BEHAVIOUR -

1. As mentioned in the preceding sub-section, under usual load combinations, punching shear is generally the more critical aspect of the design of flat plate type structures. Besides, the physical mechanism of punching is very complicated, and it has not been clearly understood yet. None of the available methods for assessing the punching shear strength, can satisfactorily consider all the factors influencing the behaviour. However,
2. The method recommended by the ACI-ASCE Joint Committee 426 is the most consistent and practical among the available methods.

3. The equilibrium and compatibility analysis appears to be able to explain some aspects of the punching phenomenon and rather satisfactory as far as the results are concerned; however, in the present form, it is not very practical for design purposes.
4. The methods recommended by the British (CP 114) and American Concrete Institute codes are very unrealistic and unsafe for edge and corner columns. On the other hand, due to the underestimated internal column reactions obtained by the elastic analysis recommended by the code (Ref. Sub-section 8.1.1), even the punching shear strength of an internal column region cannot be satisfactorily estimated.
5. The proposed draft British code includes some improvements; the effect of flexural reinforcement on the shear strength is somehow taken into consideration. However, the method of maximum shear stress calculation remains unchanged and unsatisfactory; the effect of unbalanced column moment is still neglected.
6. As discussed in Section 6.2., the contribution of the flexural reinforcement to the punching shear strength is mainly controlled by the amount of steel and not by the steel strength.
7. The last conclusion may be extended to the recommendation of the use of mild steel to achieve better economy in the design of this type of structure.

8.1.3. CONCLUSIONS ON THE PERFORMANCE OF THE INSTRUMENTATION -

1. The specially designed tripod-type reaction dynamometers performed very satisfactorily. They proved to be superior to all such dynamometers previously used, in the following respects:
 - i. The method of attachment of the legs allowed a slight movement which, under the working loads, was sufficient to enable the legs to be considered pin jointed at the ends.
 - ii. The right-handed and left-handed threads at the ends of the legs, enabled the imperfections of geometry to be corrected.
 - iii. The method of calibration was very realistic.
2. The newly developed hydraulic deflection measurement system served the purpose very efficiently.
 - i. The system enables practically any number of readings to be recorded simultaneously. 67 readings were taken at each load stage without any difficulty.

- ii. Practically any degree of sensitivity can be obtained to a reasonable accuracy. In the present investigation, readings were taken up to 0.002 in.
 - iii. Expensive data recording instruments are not required. Any camera can do the job.
 - iv. The cost is incomparable. The syringes used in the present work which cost 10d. each could have been replaced by linear displacement transducers which cost £20 to £40 each.
3. The slot gauges proved to be superior to the conventional surface gauges in the following respects:
- i. Smaller effects of eccentricity were observed since the strain gauge was positioned very near the centroid of the cross-section.
 - ii. They provide far better protection against external damage.
 - iii. Far better water-proofing is possible for this type of gauge.
4. The two-way clinometer introduced in Section 5.3. can be developed to obtain an ideal instrument for this kind of experiment.

8.2. RECOMMENDATIONS FOR FURTHER RESEARCH - A very important conclusion of the present work is that more, much more research is required on the subject. For example, the introduction of the concept of "Variable effective beam width" is a very promising approach; but it requires to be elaborated. This process naturally depends on more experimental reliable data. On the other hand, the punching shear problem has not yet been clearly understood, although it is vitally important for the design of column footings as well as the flat plate structures.

The recommendations concerning the frame analysis are presented in a separate sub-section, and all the others are listed in another.

8.2.1. RECOMMENDATIONS CONCERNING THE FRAME ANALYSIS.

1. Various geometry of effective width variation should be considered, to check the efficiency of the proposed modified frame analysis.
2. A number of cases with various $\frac{(EI)_T}{(EI)_B}$ ratios (the ratio of the cracked section flexural rigidity corresponding to top reinforcement and that corresponding to the bottom reinforcement) should be studied.

3. Then, the coefficient m could be split into two parts, each representing the geometrical variation and the flexural rigidity ratio.
4. Thus, comprehensive design charts and tables could be prepared.

8.2.2. OTHER ASPECTS TO CONSIDER -

1. The effect of the loading history on the behaviour of this type of structure should be thoroughly studied. Since, more than one parameter had to be varied in the present investigation, definite conclusions could not be drawn in this respect, although it had been originally intended as one of the objectives.
2. The structures of various geometry with various numbers of panels should be tested. The geometry of the plan B of Fig. 4 is considered very suitable for a similar investigation. It is capable of providing information for the study of three different types of panels and four different types of columns, without introducing much complication. It is particularly recommended for an investigation which may be carried out in the Concrete Structures and Technology Department of Imperial College, since all the instrumentation (from the formwork, to the hydraulic deflection measurement system) used in the present work is preserved and can be used for such an experiment with some very small alterations.
3. Test structures of this kind should somehow be elevated (e.g. They can be supported on concrete blocks.) to provide enough space underneath for a person to stand and walk around. In the present investigation, crack marking has been sheer agony.

REFERENCES

1. Mete A. SOZEN and Chester P. SIESS, "Investigation of Multiple-Panel Reinforced Concrete Floor Slabs"; ACI Journal August 1963, pp.999-1027.
2. H. M. WESTERGAARD and W. A. SLATER, "Moments and Stresses in Slabs"; ACI Proceedings V.17, 1921, pp.415-538.
3. J. R. NICHOLS, "Statical Limitations Upon the Steel Requirement in Reinforced Concrete Flat Slab Floors"; ASCE Transactions V.77, 1914, pp.1670-1736.
4. R. TAYLOR, "Flat-Slab Design, Background to the Code of Practice Recommendations"; Concrete Feb. 1967, pp.67-69.
5. H. C. CHAN, "The Interaction Between Slab and Columns in Flat Slab Construction"; Ph.D. thesis submitted to the University of London, Imperial College, June 1965.
6. G. T. MAYES, M. A. SOZEN and C. P. SIESS, "Tests on a Quarter-Scale Model of Multiple-Panel Reinforced Concrete Flat Plate Floor"; University of Illinois, Structural Research Series No: 181, September 1959.
7. D. S. HATCHER, M. A. SOZEN and C. P. SIESS, "A Study of Tests on A Flat Plate and A Flat Slab"; University of Illinois, Structural Research Series No: 217, July 1961.
8. J. O. JIRSA, M. A. SOZEN and C. P. SIESS, "An Experimental Study of A Flat Slab Floor Reinforced With Welded Wire Fabric"; University of Illinois, Structural Research Series No: 249, June 1962.
9. A. N. TALBOT, "Reinforced Concrete Wall Footings and Column Footings"; University of Illinois Engineering Experiment Station Bulletin No: 67, March 1913.
10. O. GRAF, "Tests of Reinforced Concrete Slabs under Concentrated Load Applied Near One Support"; Deutscher Ausschuss für Eisenbeton, Heft 73, 1933.

11. F. H. N. SAYANI, "Influence of Axial Tension on the Shear Strength of Reinforced Concrete Beams", M. Phil. thesis submitted to the University of London, Imperial College, July 1968.
12. E. HOGNESTAD, "Shearing Strength of Reinforced Concrete Column Footings"; ACI Journal, November 1953.
13. R. C. ELSTNER and E. HOGNESTAD, "Shearing Strength of Reinforced Concrete Slabs"; ACI Journal, July 1956.
14. C. S. WHITNEY, "Ultimate Shear Strength of Reinforced Concrete Flat Slabs, Footings, Beams, and Frame Members without Shear Reinforcement"; ACI Journal October 1957, pp. 265-298.
15. S. KINNUNEN and H. NYLANDER, "Punching of Concrete Slabs Without Shear Reinforcement"; Transactions of the Royal Institute of Technology No: 158, Stockholm, 1963.
16. S. KINNUNEN, "Punching of Concrete Slabs With Two-Way Reinforcement"; Transactions of the Royal Institute of Technology No: 198, Stockholm 1963.
17. Jan L. ANDERSSON, "Punching of Concrete Slabs With Shear Reinforcement"; Transactions of the Royal Institute of Technology No: 212, Stockholm, 1963.
18. Jan L. ANDERSSON, "Punching of Slabs Supported on Columns at Free Edges"; Royal Institute of Technology, Stockholm 1966.
19. J. MOE, "Shearing Strength of Reinforced Concrete Slabs and Footings Under Concentrated Loads"; PCA Development Department Bulletin D47, 1961.
20. D. YITZHAKI, "Punching Strength of Reinforced Concrete Slabs"; ACI Journal May 1966, pp. 527-542.
21. N. W. HANSON and J. M. HANSON, "Shear and Moment Transfer Between Concrete Slabs and Columns"; PCA Journal January 1968, pp. 2-16.

22. N. N. ANIS, "Shear Strength of Reinforced Concrete Flat Slabs Without Shear Reinforcement"; Ph. D. thesis to be submitted to the University of London, Imperial College
23. A. KLEINLOGEL, "Rigid Frame Formulas", Frederick Ungar Publishing Co. New York, 1958.
24. K. W. JOHANSEN, "Yield Line Theory"; Cement and Concrete Association, 1962.
25. R. H. WOOD, "Plastic and Elastic Design of Slabs and Plates"; Thames and Hudson, 1961.
26. S. TIMOSHENKO and S. WOINOWSKY-KRIEGER, "Theory of Plates and Shells", Mc.Graw Hill, New York, 1959.
27. P. M. FERGUSON, "Reinforced Concrete Fundamentals"; John Wiley & Sons, New York, 1963.
28. D. R. HARTREE, "Numerical Analysis"; Clarendon Press, Oxford, 1952.
29. "ACI Standard Building Code Requirements for Reinforced Concrete (ACI 318-63)"; American Concrete Institute Publication.
30. "CP 114 (1957): The Structural Use of Reinforced Concrete in Buildings"; The Council for Codes of Practice, British Standards Institution, 1957.
31. "CP 114 (1965): The Structural Use of Reinforced Concrete in Buildings"; The Council for Codes of Practice, British Standards Institution, 1965.
32. A. E. LONG and D. BOND, "Punching Failure of Reinforced Concrete Slabs"; The Institution of Civil Engineers Proceedings May 1967, pp. 109-135.
33. M. W. KWIECINSKI, "Some Tests on the Yield Criterion for a Reinforced Slab"; Research Report No: C/R/23/65, University of Wales, 1965.

34. H. REIMANN, "Zur Bemessung von dünnen Plattendecken auf Stützen ohne Kopf gegen Durchstanzen", Doctoral thesis, Otto Graf Institut, Stuttgart, 1963.
35. ACI-ASCE Committee 326 (426); "Shear and Diagonal Tension", ACI Journal, January, February and March 1962.
36. U. NAHRAS, "The Inelastic Behaviour of Reinforced Concrete Sway Frames"; Ph. D. thesis to be submitted to the University of London, Imperial College.
37. G. W. D. VILE, "Behaviour of Concrete Under Simple and Combined Stresses"; Ph. D. thesis submitted to the University of London Imperial College, 1965.
38. A. HILLERBORG, "Strimlemetoden"; Svenska Riksbyggen, Stockholm, 1959. See also "Strip Method for Slabs on Columns, L-shaped Plates etc." translated by F. A. BLAKEY, Commonwealth Scientific and Industrial Research Organisation, Melbourne, 1964.
39. R. H. WOOD and G. S. T. ARMER, "The Theory of the Strip Method for Design of Slabs"; The Institution of Civil Engineers Proceedings October 1968, pp. 285-312.
40. G. S. T. ARMER, "Ultimate Load Tests of Slabs Designed by the Strip Method"; The Institution of the Civil Engineers Proceedings October 1968, pp. 313-331.
41. A. HILLERBORG, "A Plastic Theory for the Design of Reinforced Concrete Slabs"; Proceedings, 6th Congress, Int. Ass. Brit. Structural Engineering, Stockholm, 1960.
42. J. YARNELL, "Resistance Strain Gauges"; Electronic Engineering Publication, August 1951.

A P P E N D I X 1MOMENT AND DEFLECTION DISTRIBUTIONS

The tests conducted on each test structure and the data obtained at various loading stages of each test are explained in Chapter 6 in detail. The method of analysis and the results thus obtained are discussed in Chapter 7 at length. However, it is thought that the outcome of the data analysis at a number of important loading stages should be presented so that some further conclusions may be drawn by the interested and capable reader. Ten loading stages are chosen from the complete set analysed, and equal moment (both M_x and M_y) and equal deflection contours corresponding to each of these stages are given in the following pages. Tables 22 and 23 show the applied loads and the measured reactions at the loading stages considered for each test structure.

LDG. STAGES		1/01/7	1/13/7	1/23/7	1/41/7	1/41/11
VRT. LOAD		$0.92 V_d$	V_d	V_d	V_d	$1.50 V_d$
HRZ. LOAD		—	—	H_d	H_d	$1.50 H_d$
A	z	1.813	2.194	2.003	2.690	3.120
	x	-1.531	-1.847	-1.741	-2.274	-3.132
	y	1.462	1.722	1.014	1.374	1.750
B	z	3.769	2.170	3.893	4.680	6.379
	x	0.036	1.414	-0.154	-0.029	0.035
	y	2.207	1.332	2.041	1.853	3.454
C	z	1.733	-0.207	1.863	1.897	3.034
	x	1.454	0.045	1.691	1.831	3.064
	y	1.440	0.013	0.903	1.058	1.735
D	z	3.970	4.645	4.668	4.751	1.283
	x	-2.334	-2.799	-2.888	-3.101	-4.880
	y	0.174	0.468	-1.005	-0.990	-1.718
E	z	8.191	6.793	9.856	9.959	15.296
	x	-0.070	1.443	-0.069	-0.056	-0.116
	y	0.030	1.486	-1.491	-1.418	-2.025
F	z	3.936	2.208	4.391	4.494	6.788
	x	2.198	1.453	2.767	2.969	4.532
	y	0.138	1.389	-0.841	-0.834	-1.507
G	z	1.628	1.955	2.167	2.183	3.348
	x	-1.324	-1.597	-1.540	-1.685	-2.521
	y	-1.543	-1.785	-2.585	-2.712	-4.068
H	z	3.475	4.264	4.449	4.521	6.676
	x	0.044	0.264	0.067	0.077	0.180
	y	-2.194	-2.637	-3.494	-3.744	-5.472
K	z	1.682	2.161	2.296	2.336	3.517
	x	1.606	1.917	1.818	1.976	2.953
	y	-1.566	-1.888	-2.650	-2.272	-4.304

TABLE 22 - COLUMN REACTIONS FOR THE TEST STRUCTURE I

LDS. STAGES		2/11/7	2/31/11	2/32/2	2/32/8	2/32/11
VRT. LOAD		V_d	1.50 V_d	1.625 V_d	1.75 V_d	1.75 V_d
HRS. LOAD		H_d	3.75 H_d	1.625 H_d	1.75 H_d	2.50 H_d
A	z	1.921	2.810	3.329	3.644	3.649
	x	-1.683	-3.029	-3.362	-3.621	-3.724
	y	1.068	0.190	1.809	2.220	1.691
B	z	4.668	6.385	7.466	8.259	8.177
	x	-0.152	-0.046	-0.056	-0.067	-0.043
	y	2.279	1.781	3.831	4.345	3.810
C	z	1.776	2.381	2.948	3.338	3.238
	x	1.610	3.115	3.441	3.756	3.809
	y	1.062	0.336	1.941	2.312	1.760
D	z	4.777	7.037	7.717	8.453	8.433
	x	-2.638	-4.336	-4.946	-5.357	-5.355
	y	-0.785	-3.982	-2.288	-2.009	-2.848
E	z	10.163	15.779	17.023	18.545	18.530
	x	-0.081	-0.020	-0.017	-0.012	0.004
	y	-1.201	-5.027	-2.565	-2.129	-3.088
F	z	4.747	6.991	7.678	8.378	8.354
	x	2.658	4.606	5.166	5.550	5.594
	y	-0.797	-4.110	-2.373	-2.207	-2.952
G	z	2.004	3.689	3.642	3.941	4.076
	x	-1.479	-2.279	-2.773	-3.043	-2.958
	y	-2.515	-5.764	-4.941	-5.035	-5.577
H	z	4.779	7.498	7.706	8.358	8.414
	x	0.017	0.020	-0.016	-0.002	0.044
	y	-3.229	-6.972	-6.323	-6.378	-6.876
K	z	2.256	4.126	4.031	4.320	4.447
	x	1.944	2.826	3.218	3.459	3.446
	y	-2.416	-5.684	-4.810	-4.912	-5.395

TABLE 23 - COLUMN REACTIONS FOR THE TEST STRUCTURE 2

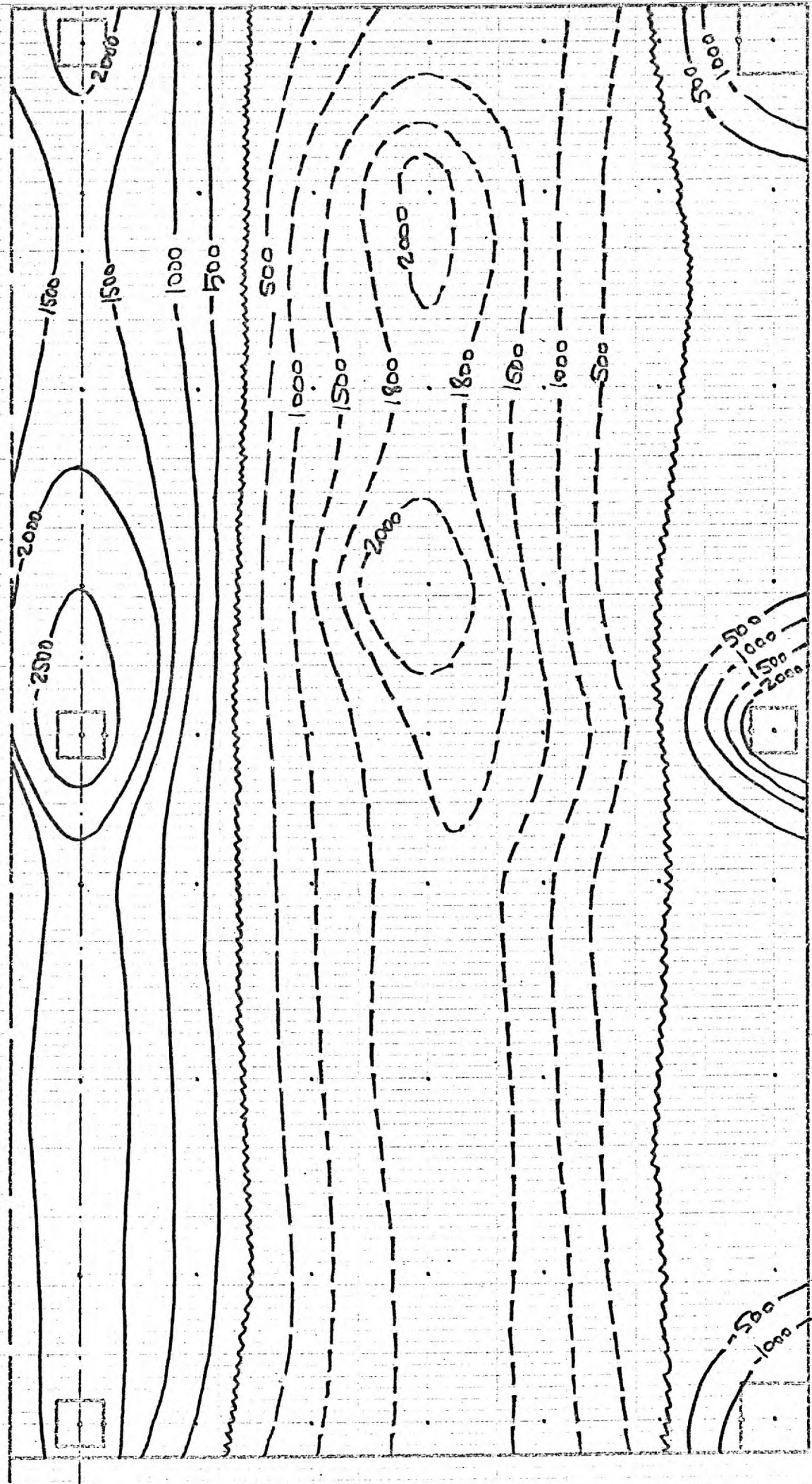


FIG. 59 - EQUAL MOMENT (M_x) CONTOURS FOR 1/01/7

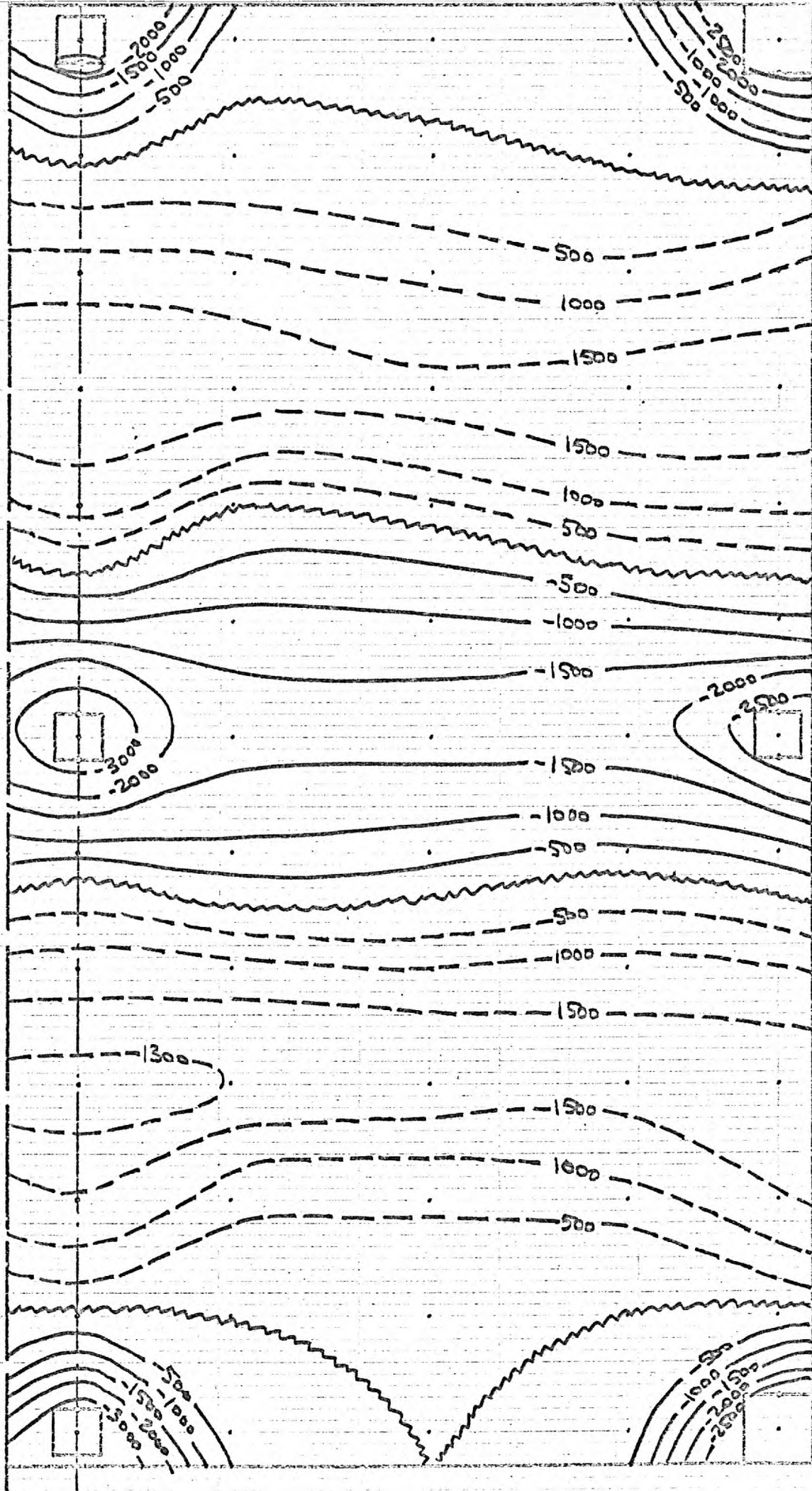


FIG. 60 - EQUAL MOMENT (M_y) CONTOURS FOR 1/01/7

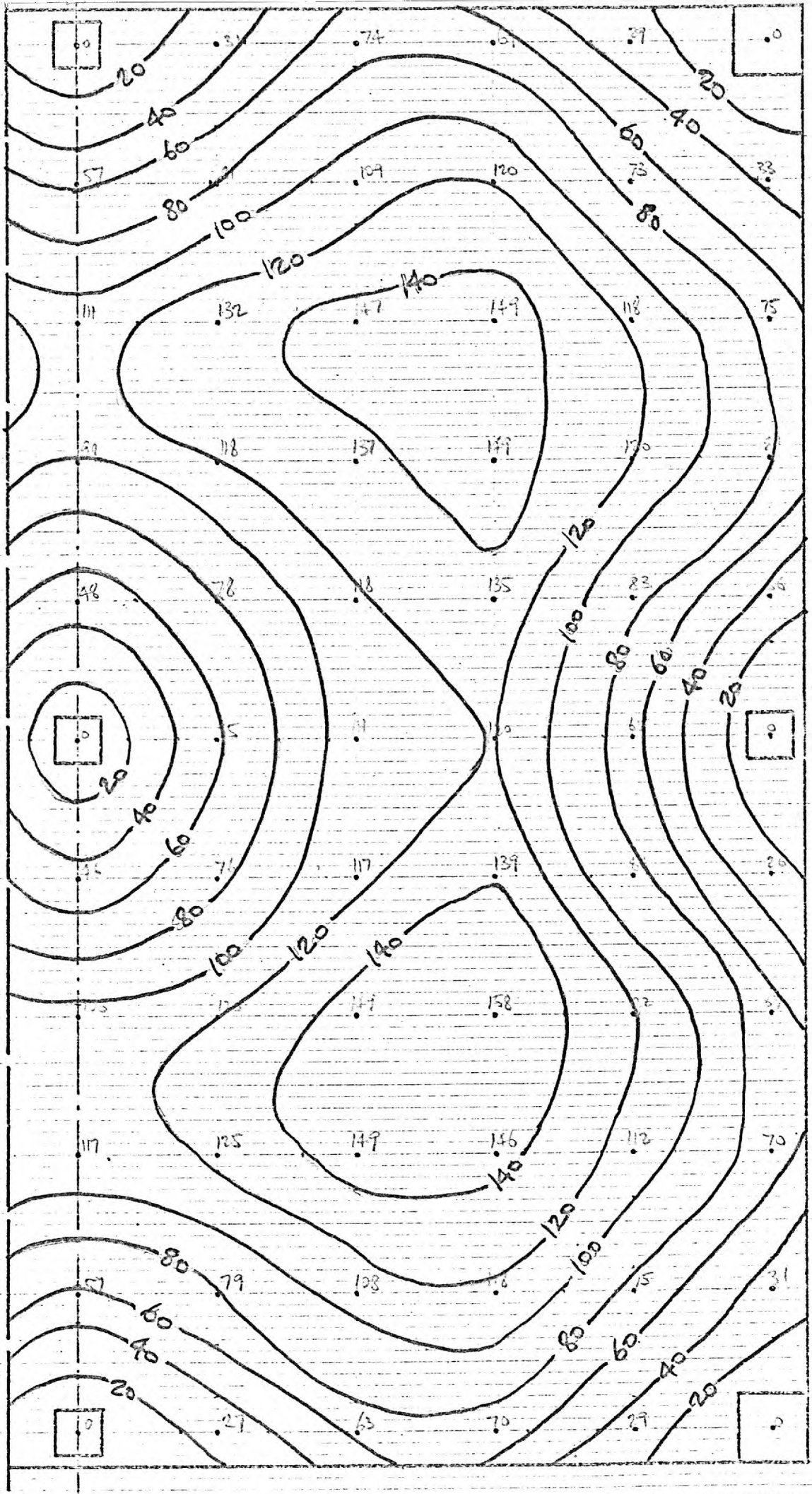


FIG. 61 - EQUAL DEFLECTION CONTOURS FOR 1/01/7

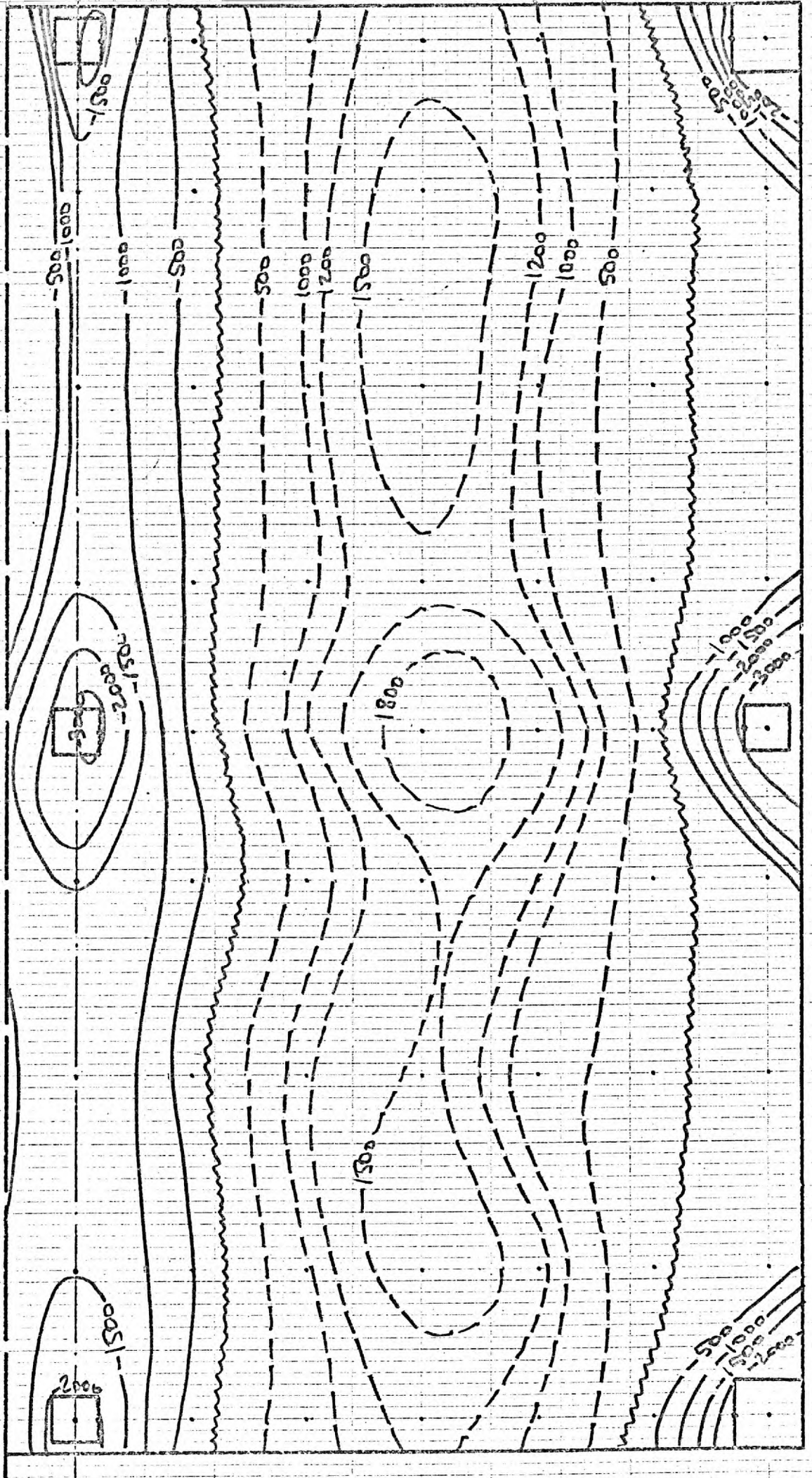


FIG. 62. EQUAL MOMENT (M_x) CONTOURS FOR 1/13/7

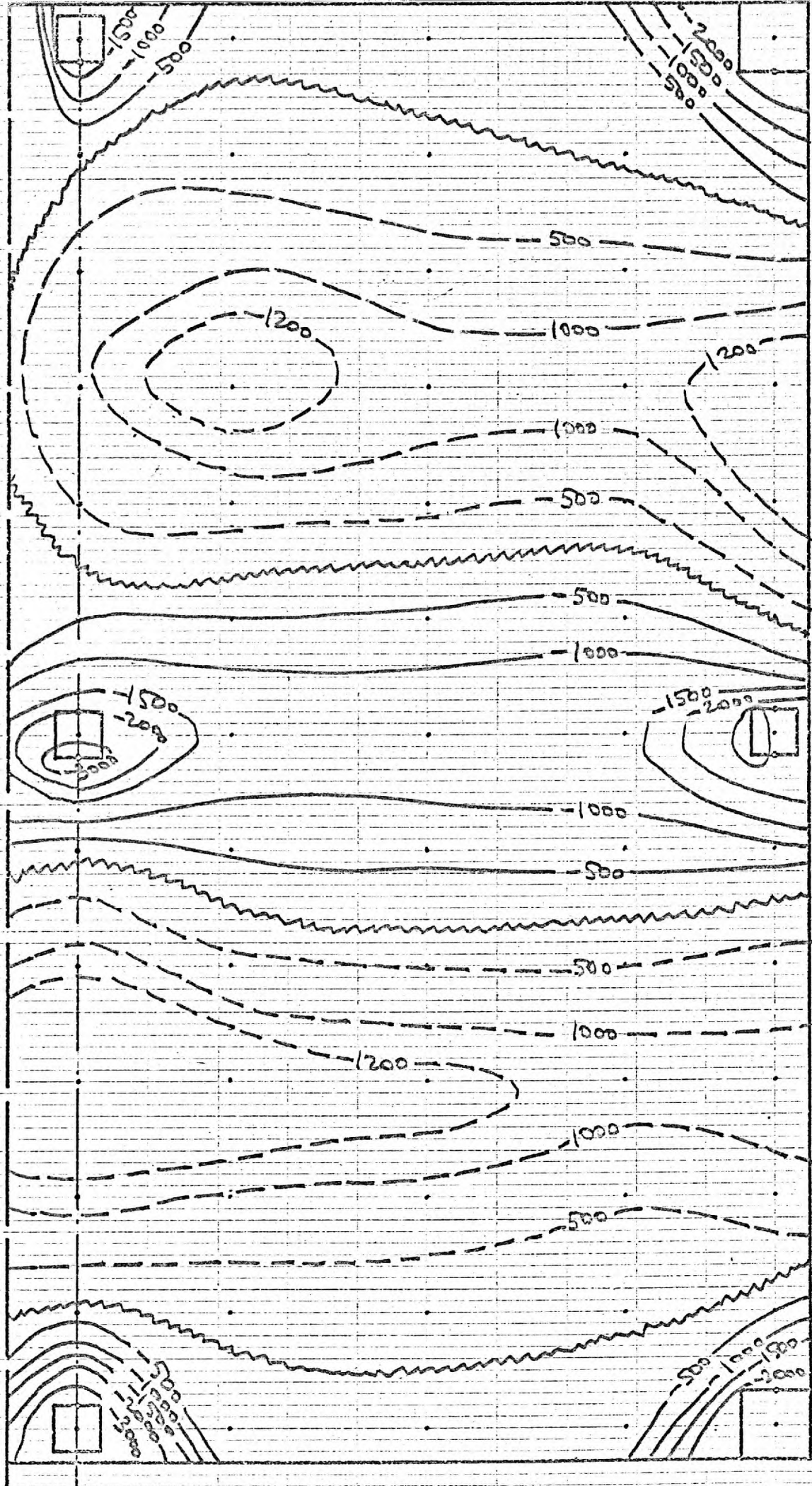


FIG. 63. EQUAL MOMENT (M_y) CONTOURS FOR 1/13/7

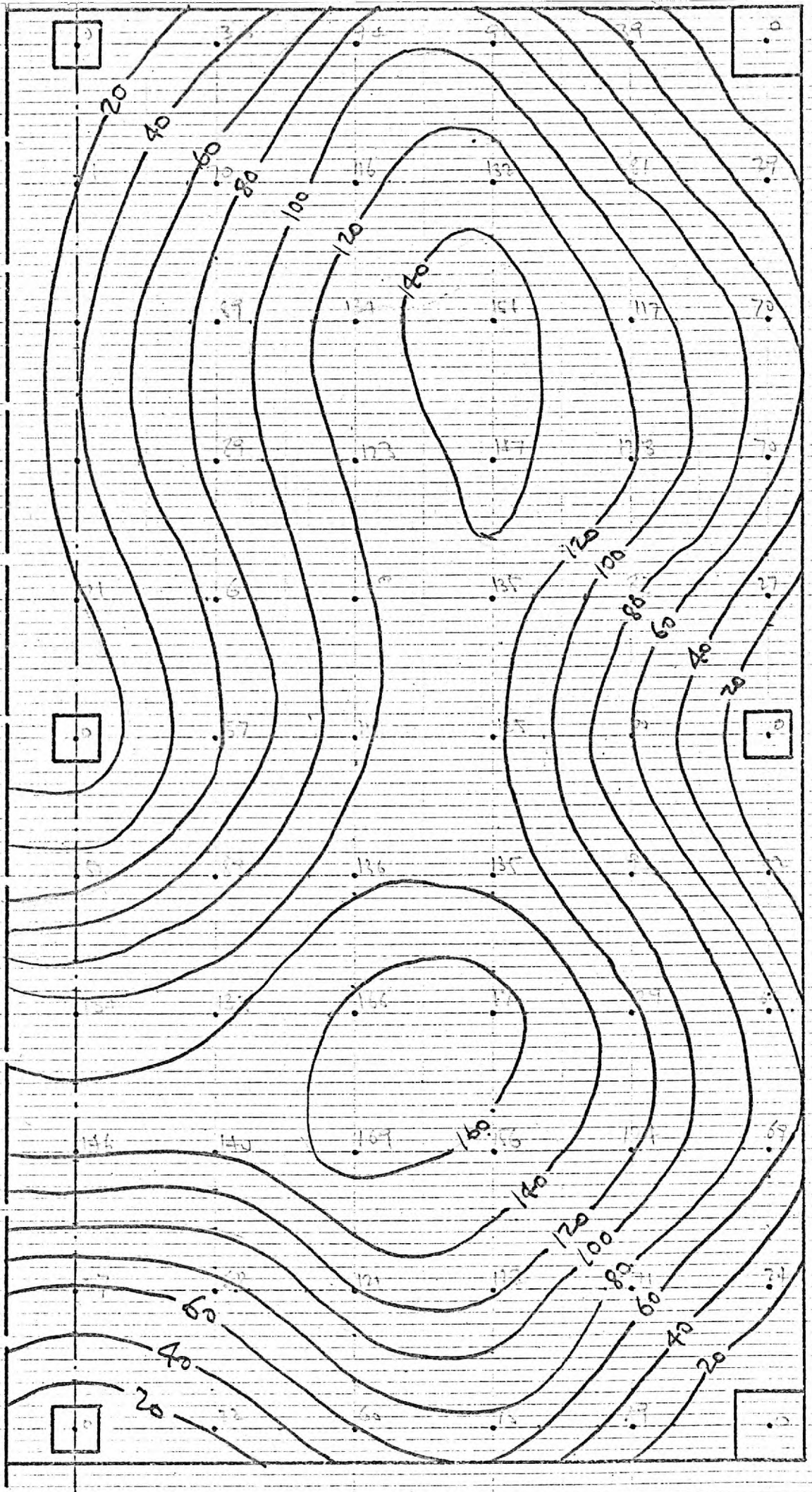


FIG. 64 - EQUAL DEFLECTION CONTOURS FOR 1/13/7

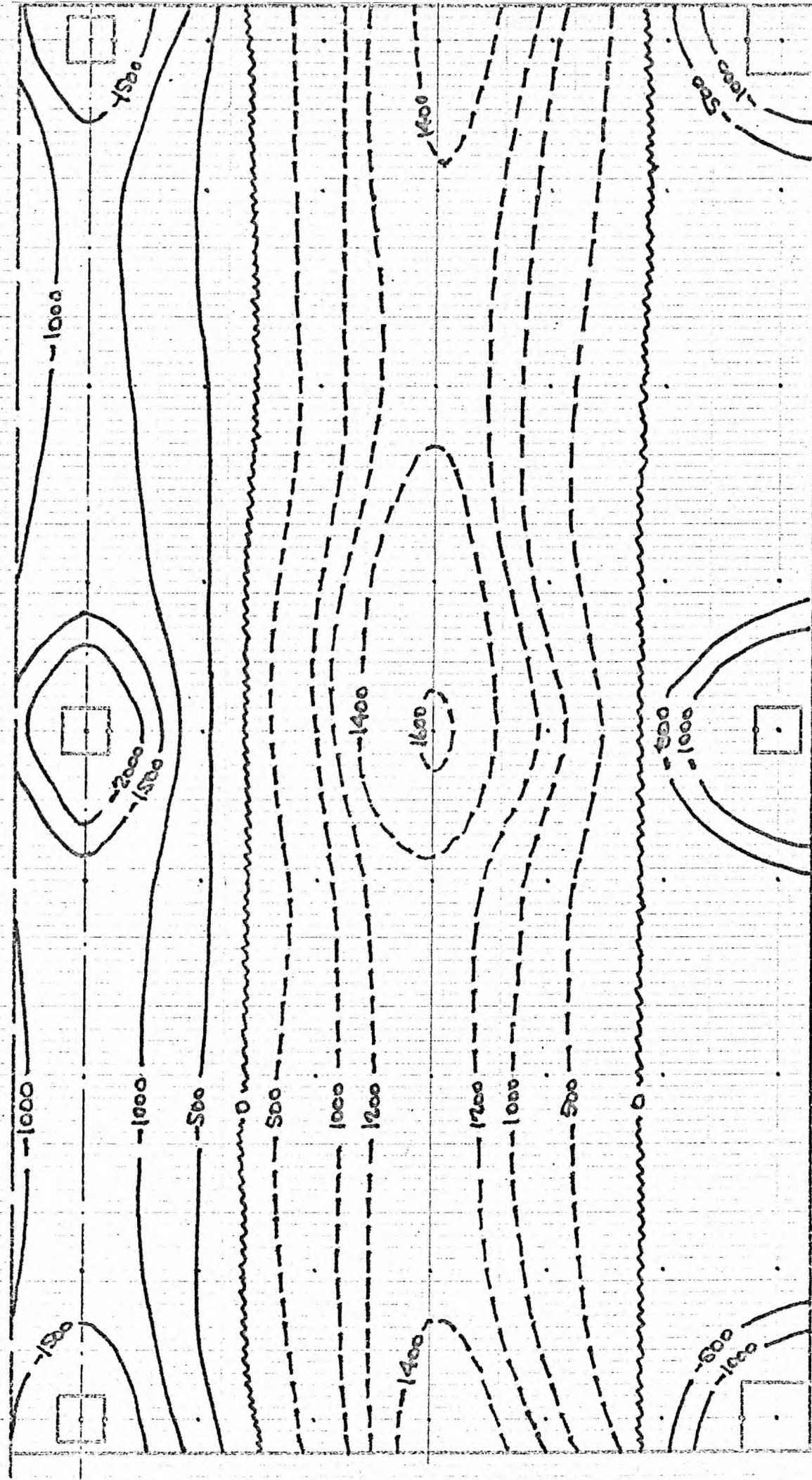


FIG. 65. EQUAL MOMENT (M_x) CONTOURS FOR 1/23/7

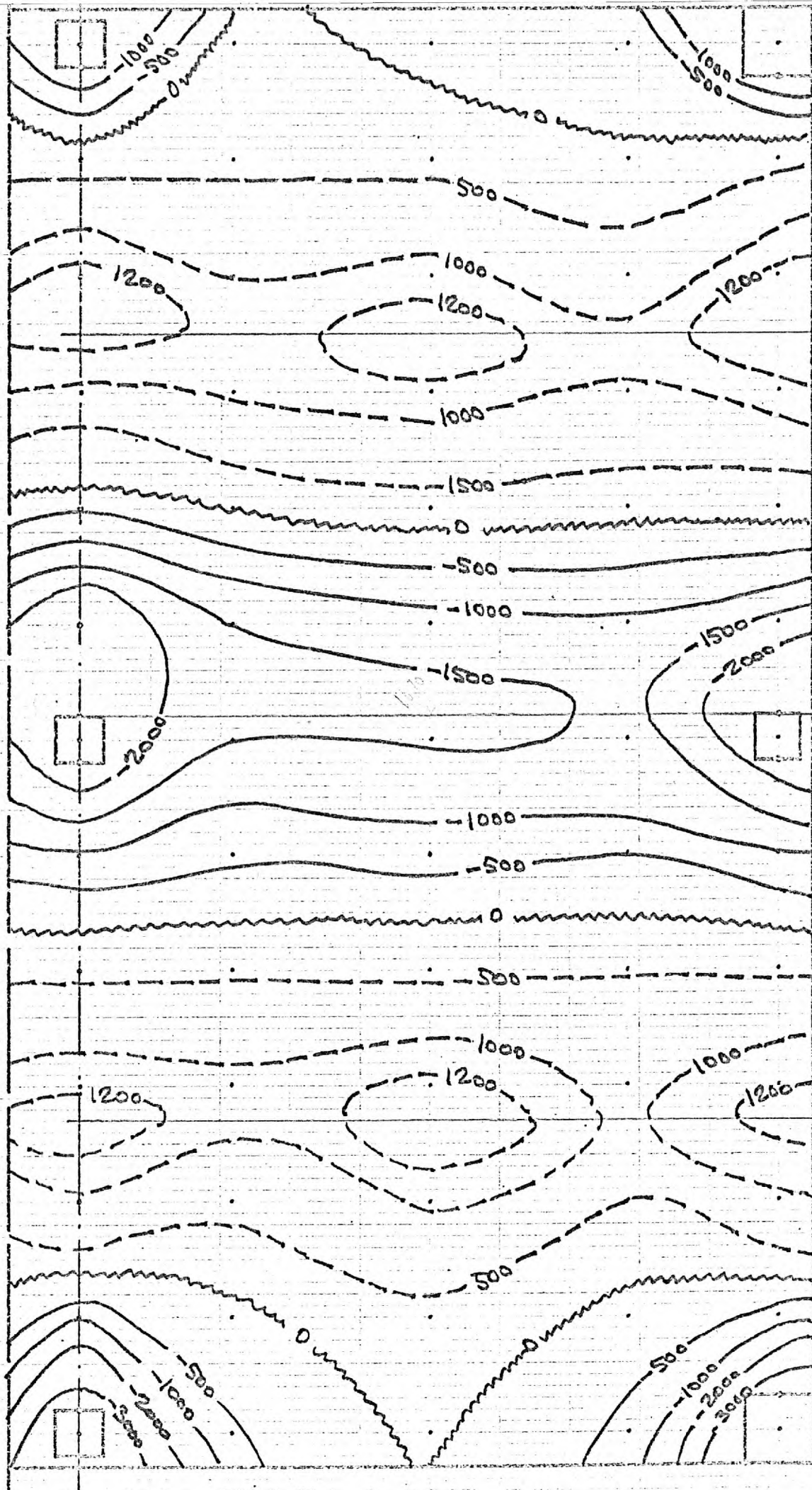


FIG. 66 - EQUAL MOMENT (M_y) CONTOURS FOR 1/23/7

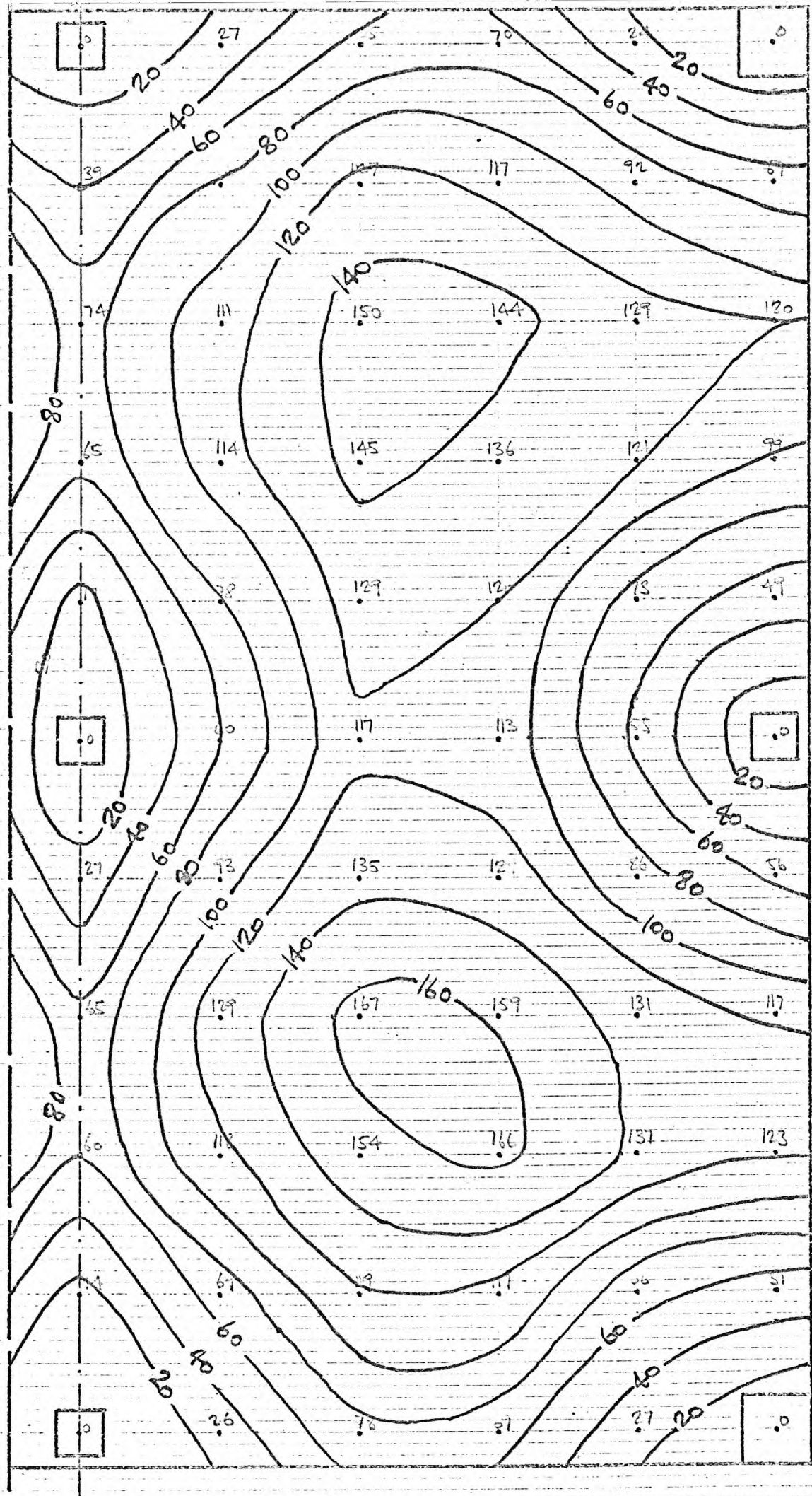


FIG. 67. EQUAL DEFLECTION CONTOURS FOR 1/23/7

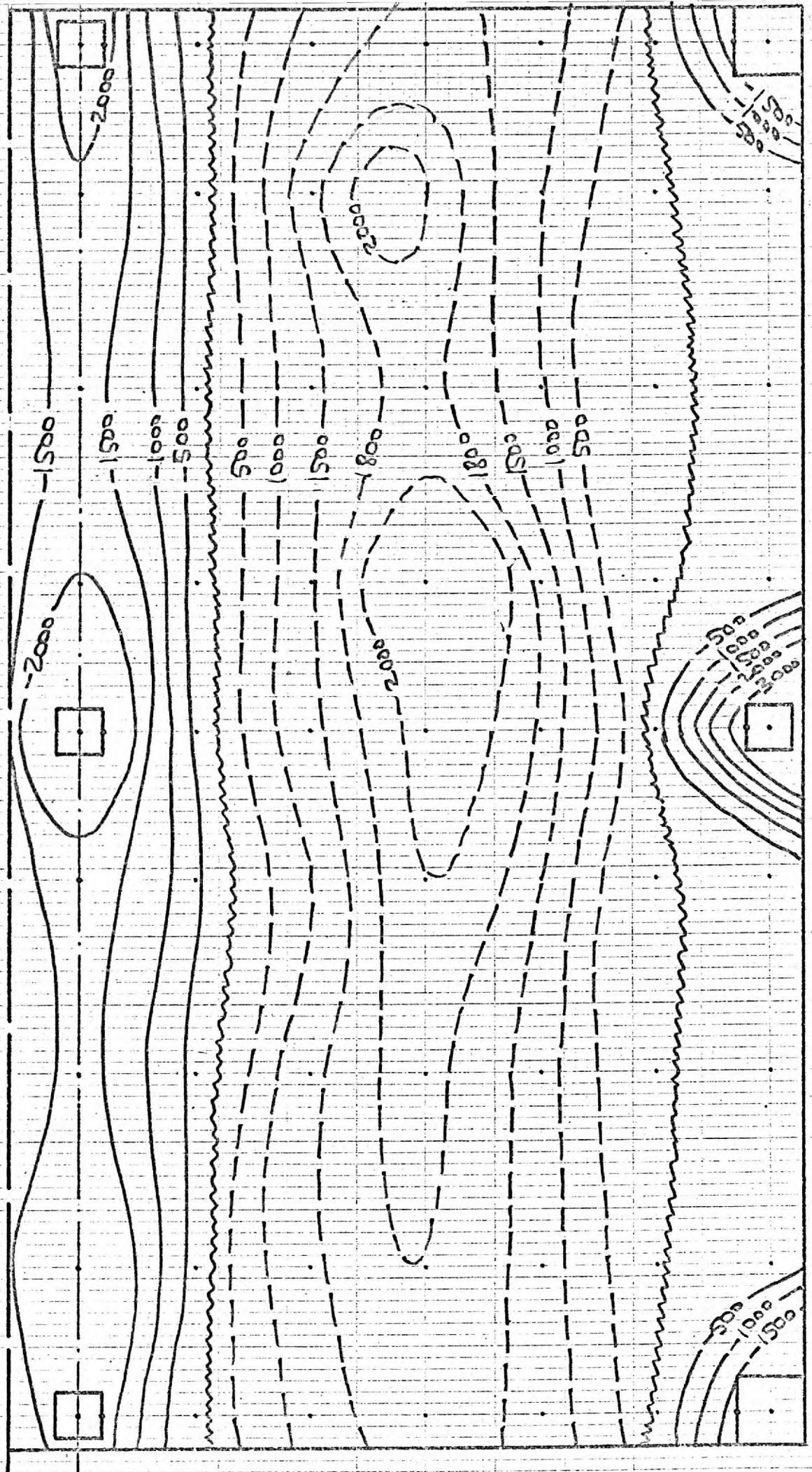


FIG. 68. EQUAL MOMENT (M_x) CONTOURS FOR $1/41/7$

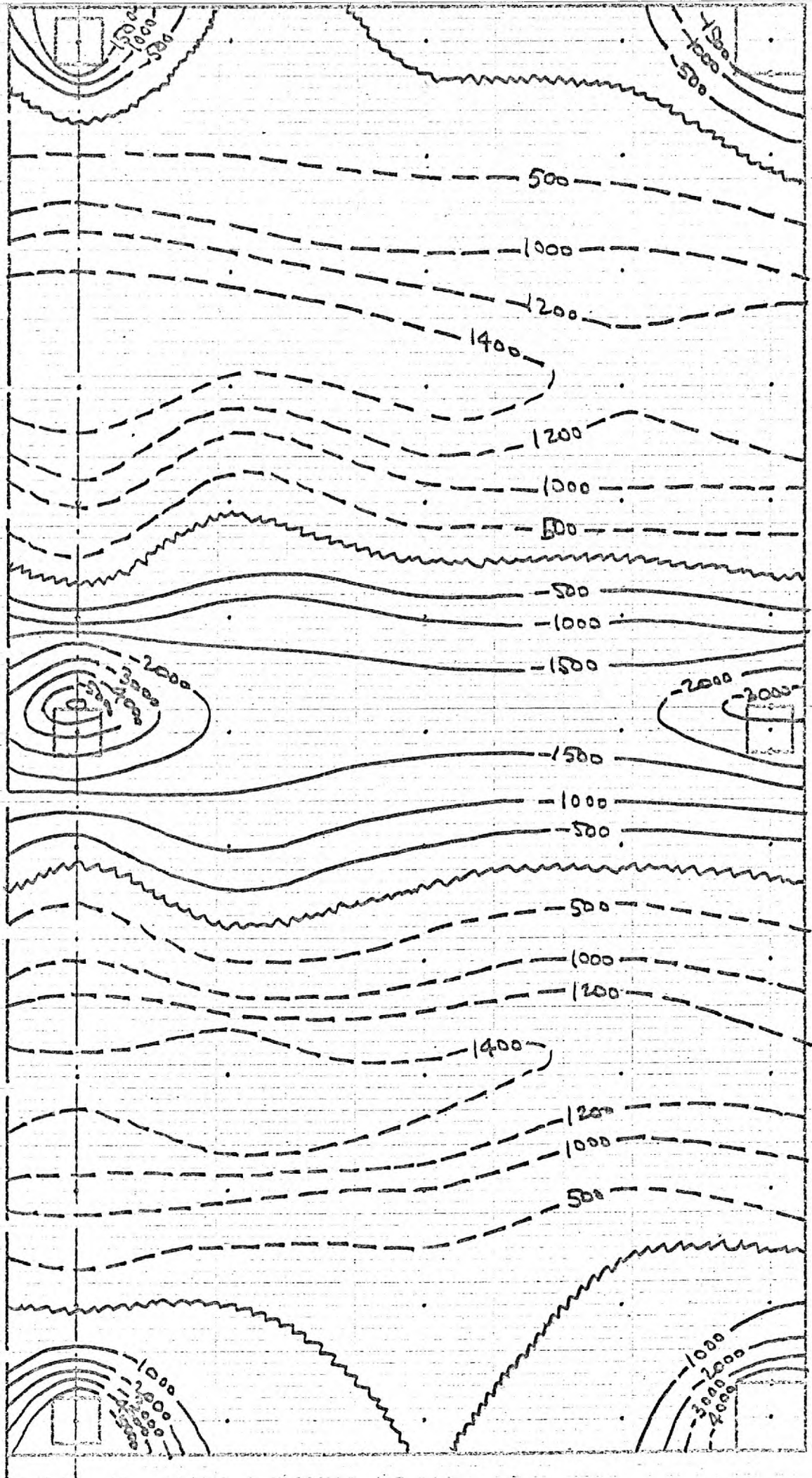


FIG. 69 - EQUAL MOMENT (M_y) CONTOURS FOR 1/4/7

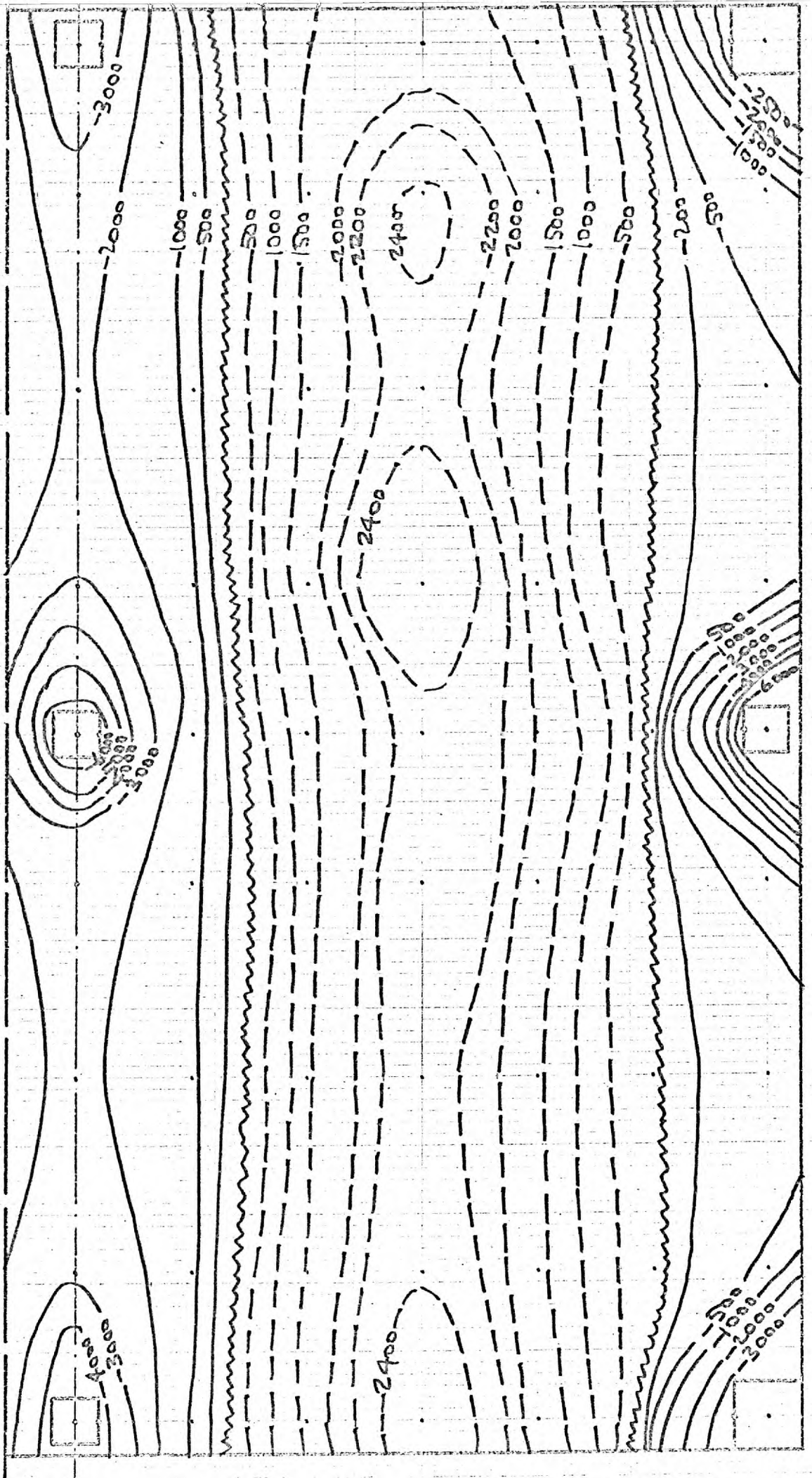


FIG. 70 - EQUAL MOMENT (M_x) CONTOURS FOR 1/41/11

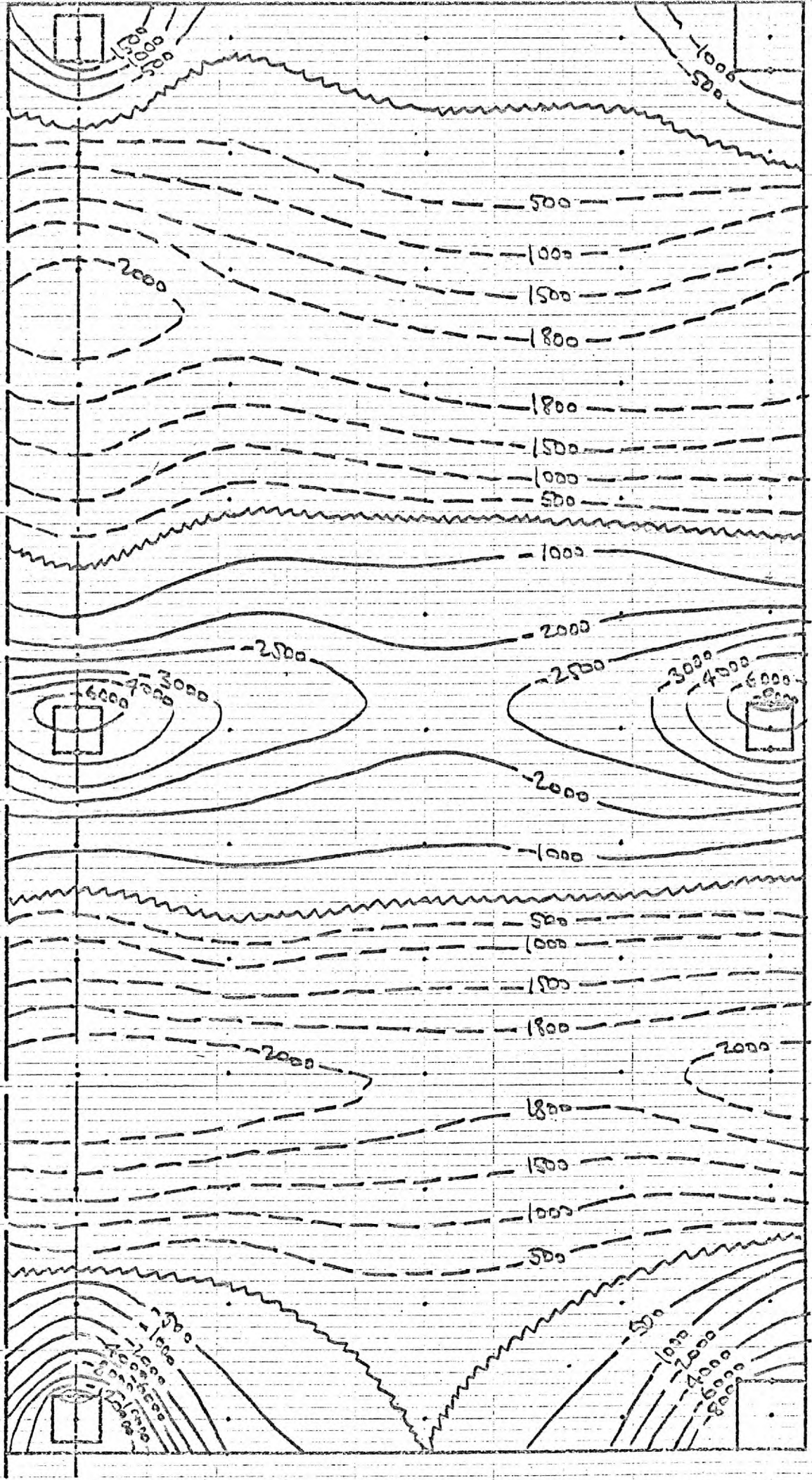


FIG. 71 - EQUAL MOMENT (M_y) CONTOURS FOR 1/41/11

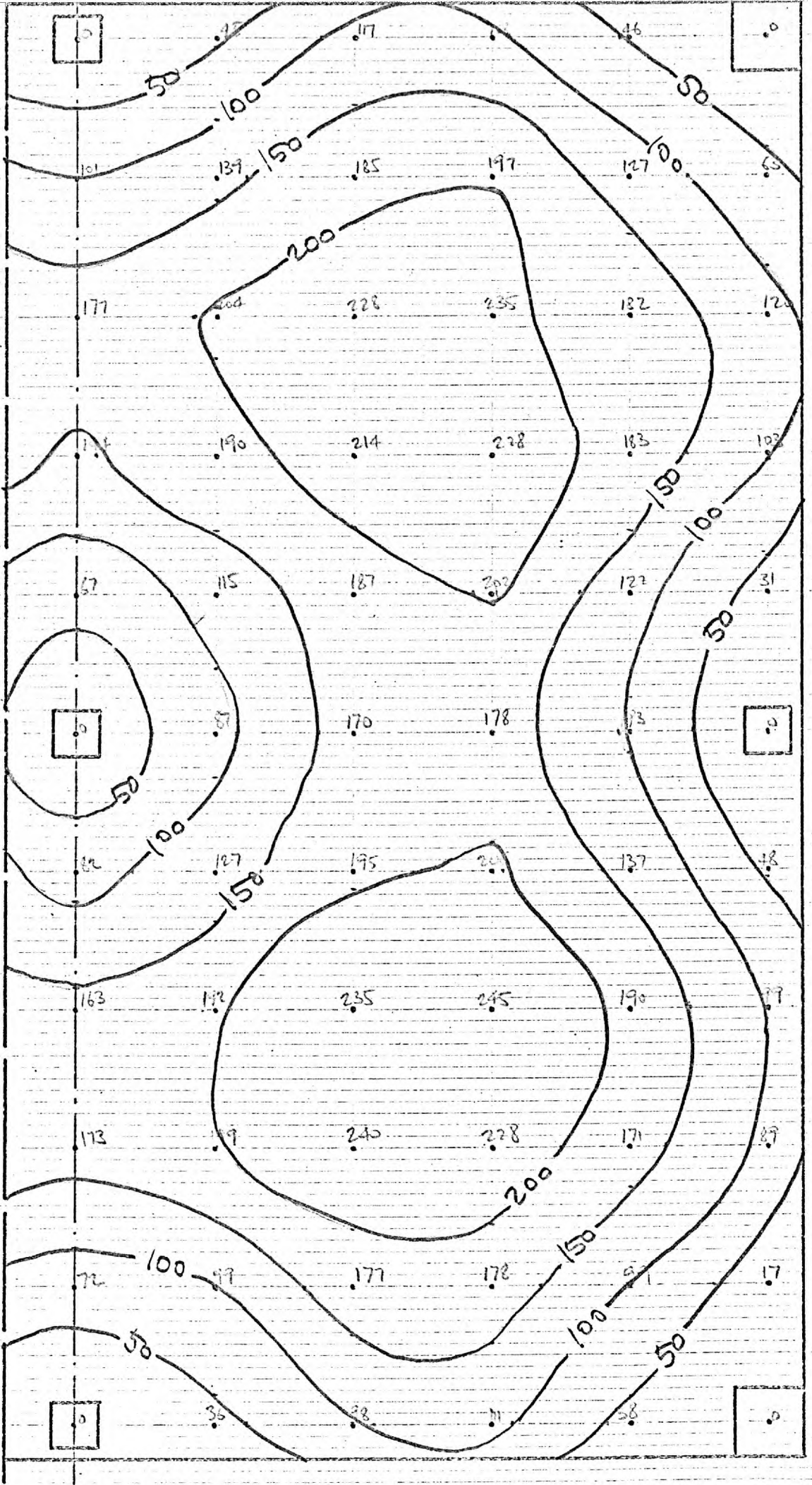


FIG. 72 - EQUAL DEFLECTION CONTOURS FOR 1/41/11

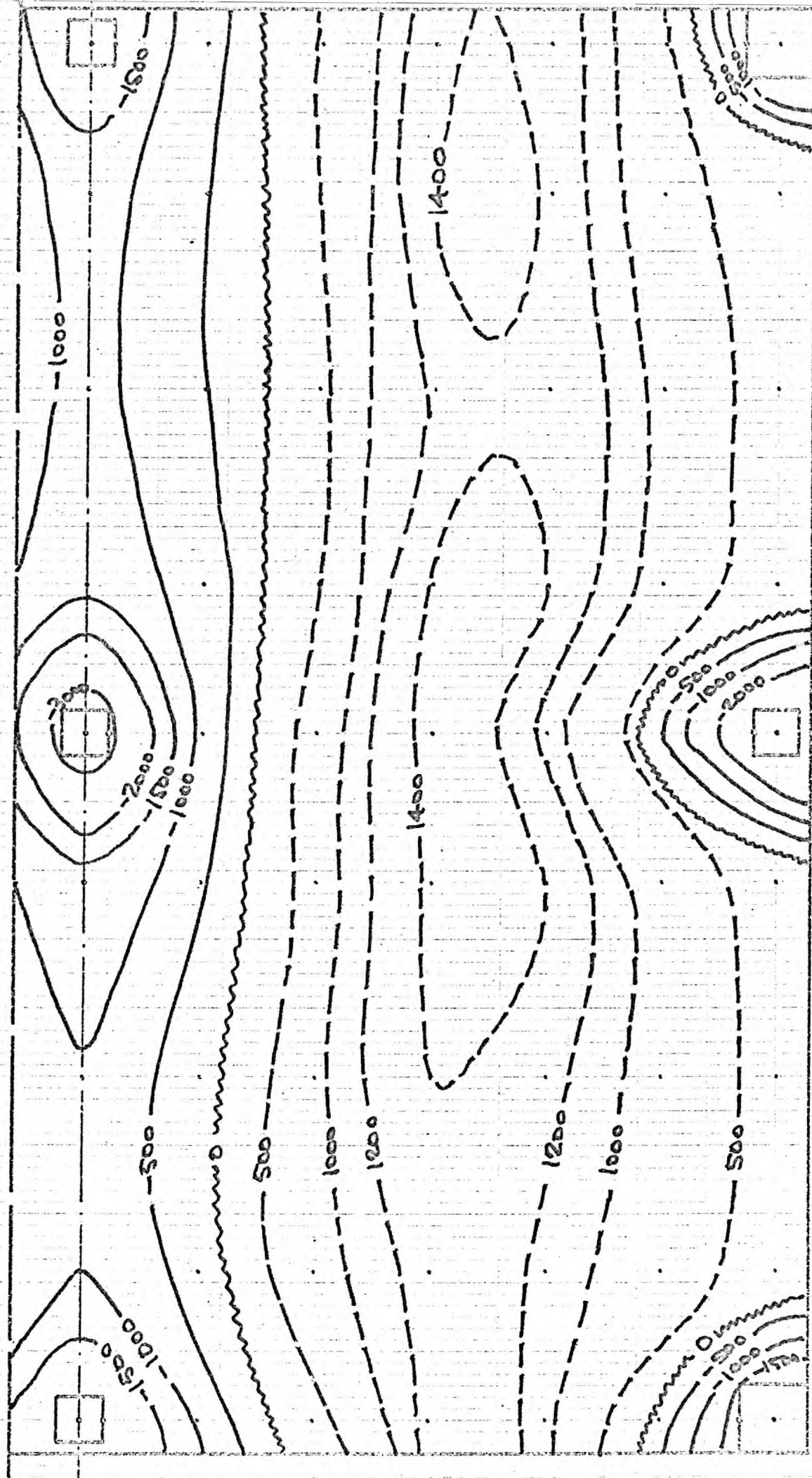


FIG. 73 - EQUAL MOMENT (M_x) CONTOURS FOR 2/11/7

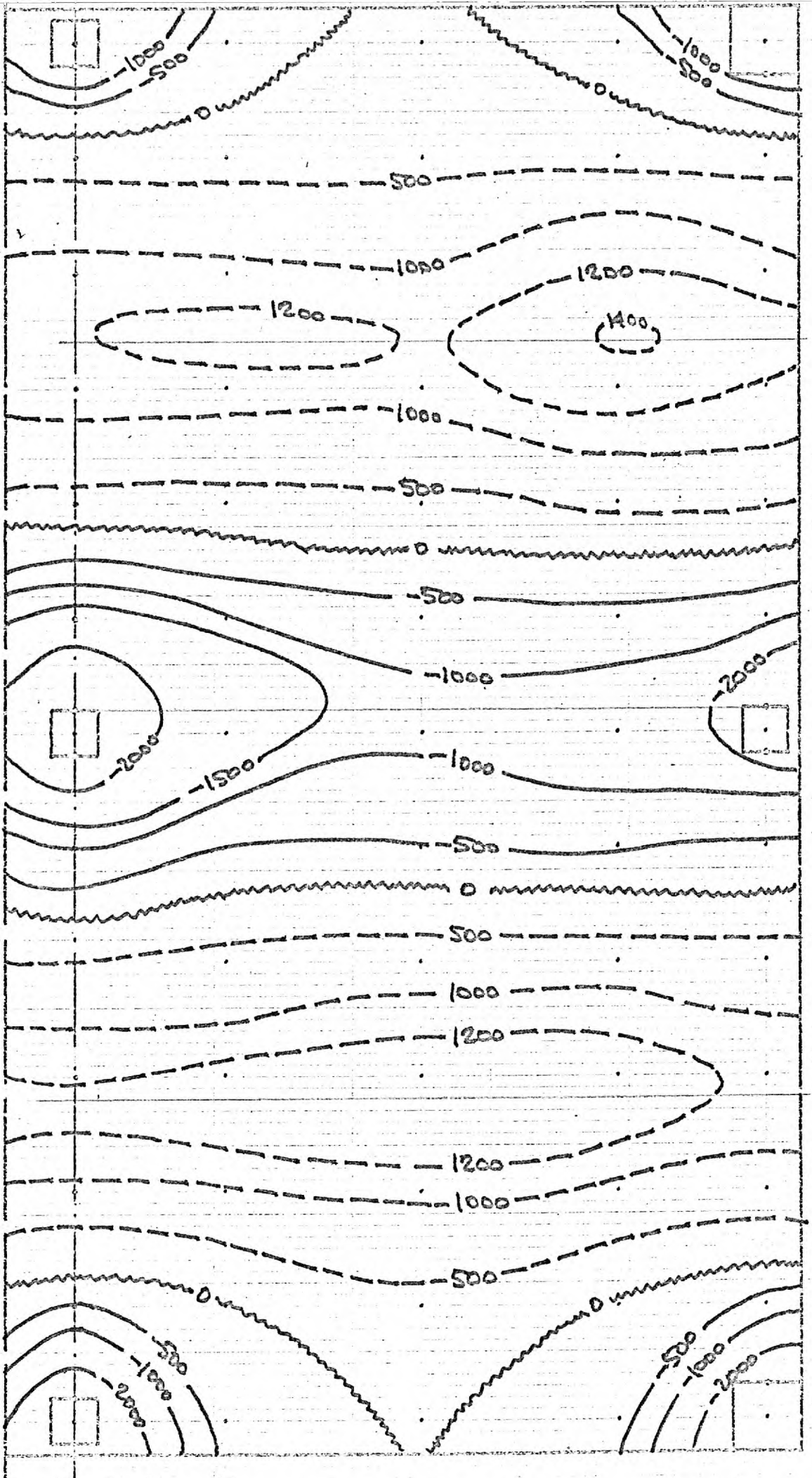


FIG. 74 - EQUAL MOMENT (M_y) CONTOURS FOR 2/11/7

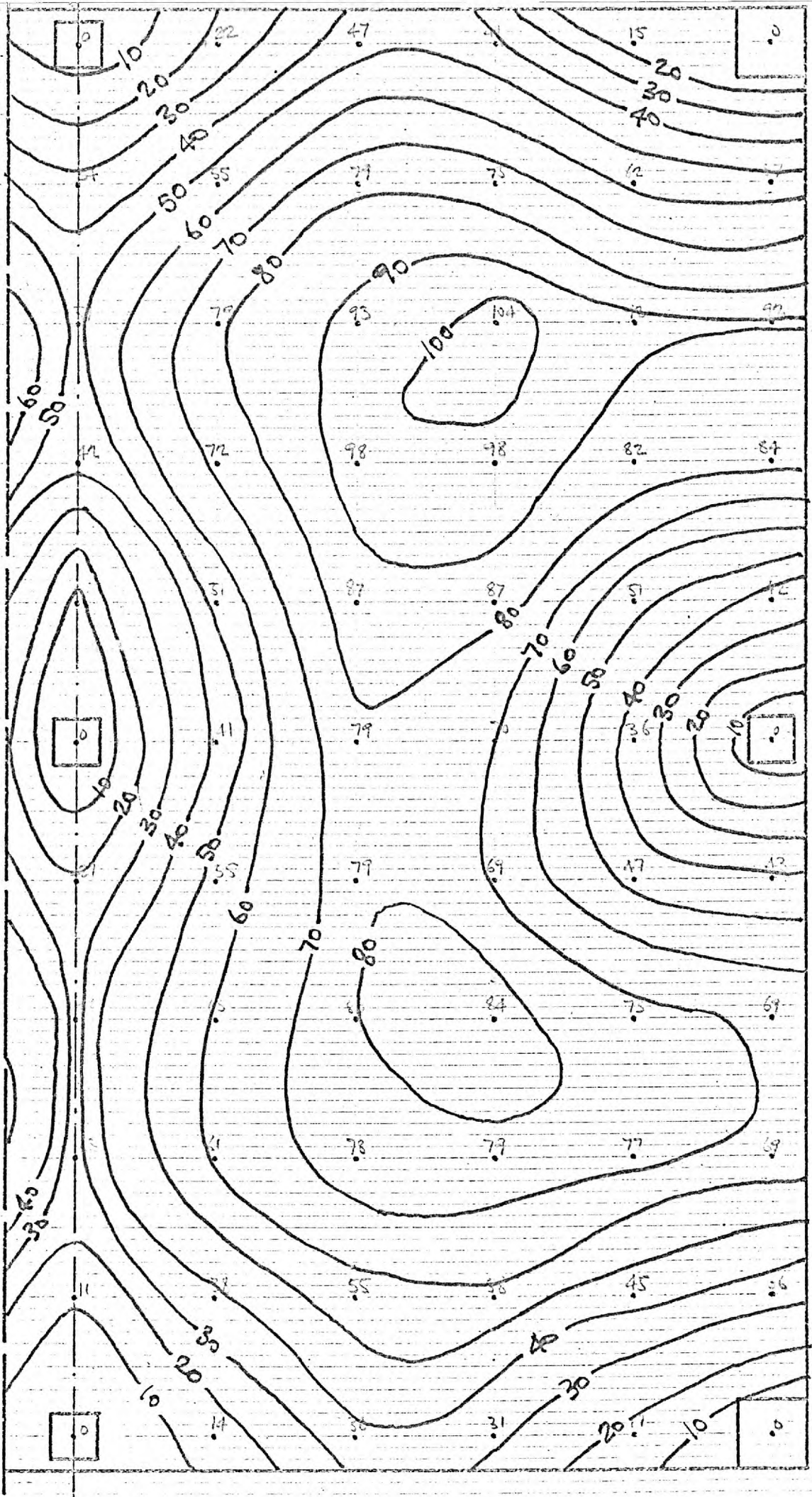


FIG. 75 - EQUAL DEFLECTION CONTOURS FOR 2/11/7

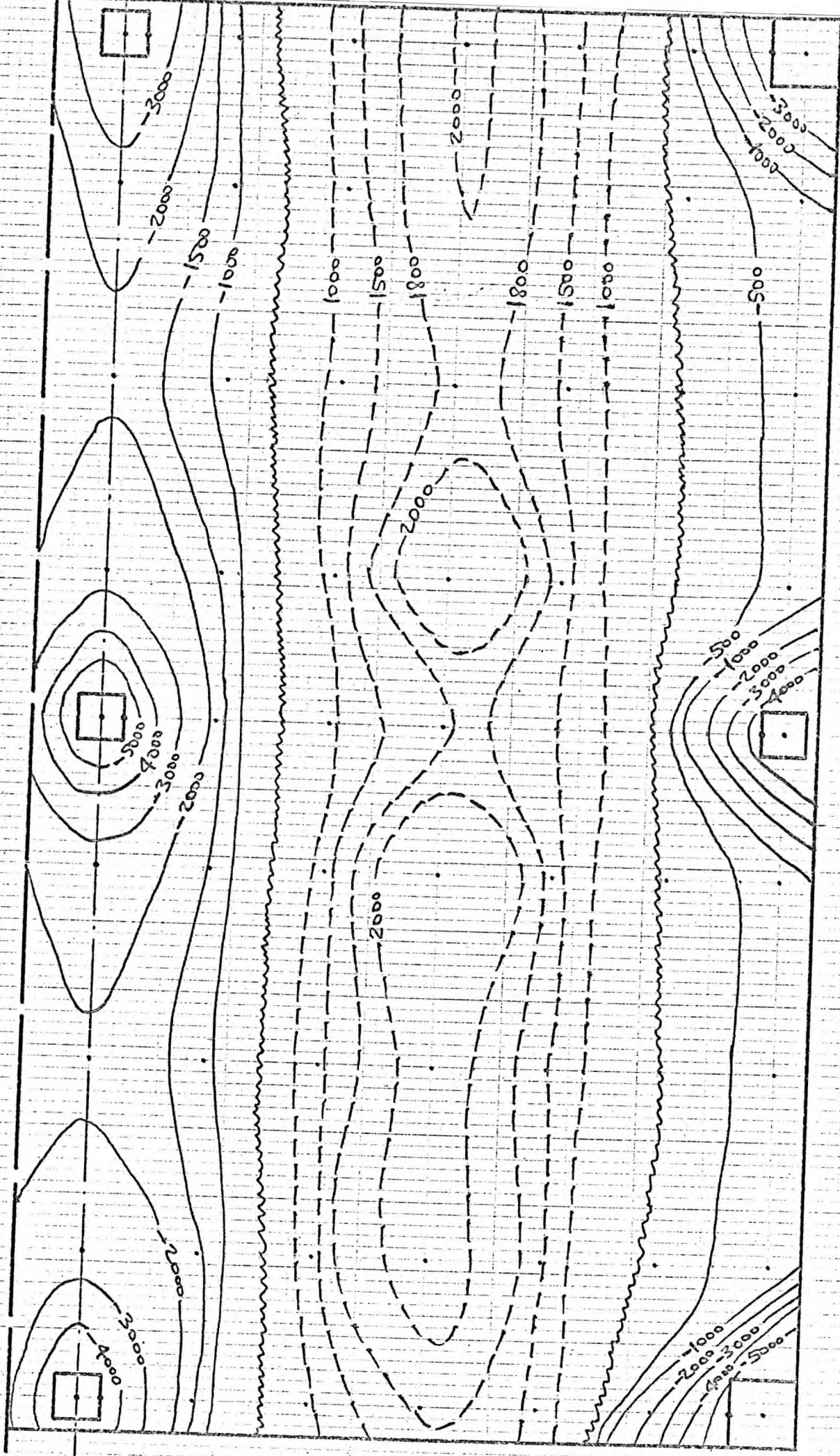


FIG. 76 - EQUAL MOMENT (M_x) CONTOURS FOR 2/31/11

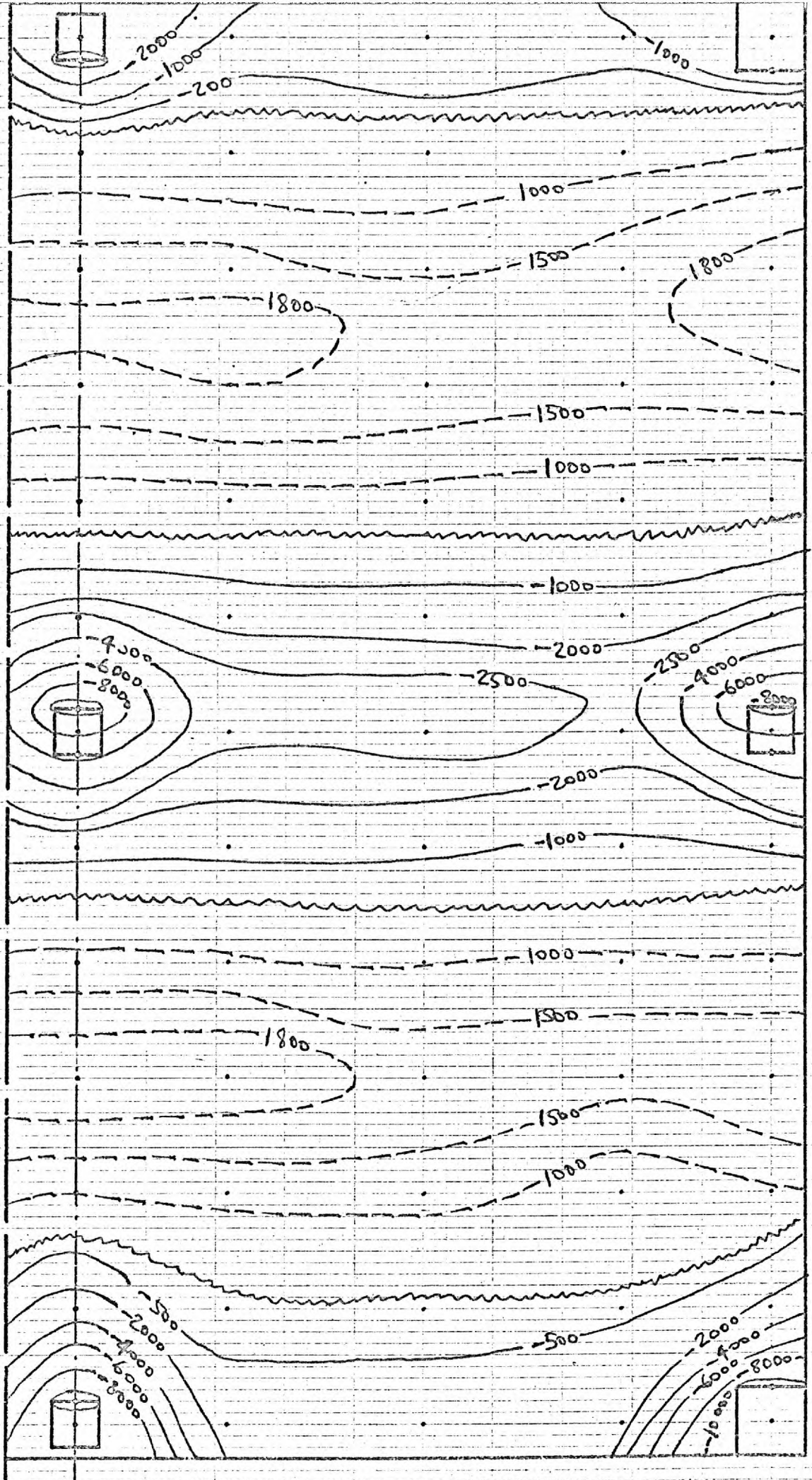


FIG. 77 - EQUAL MOMENT (M_j) CONTOURS FOR 2/31/11

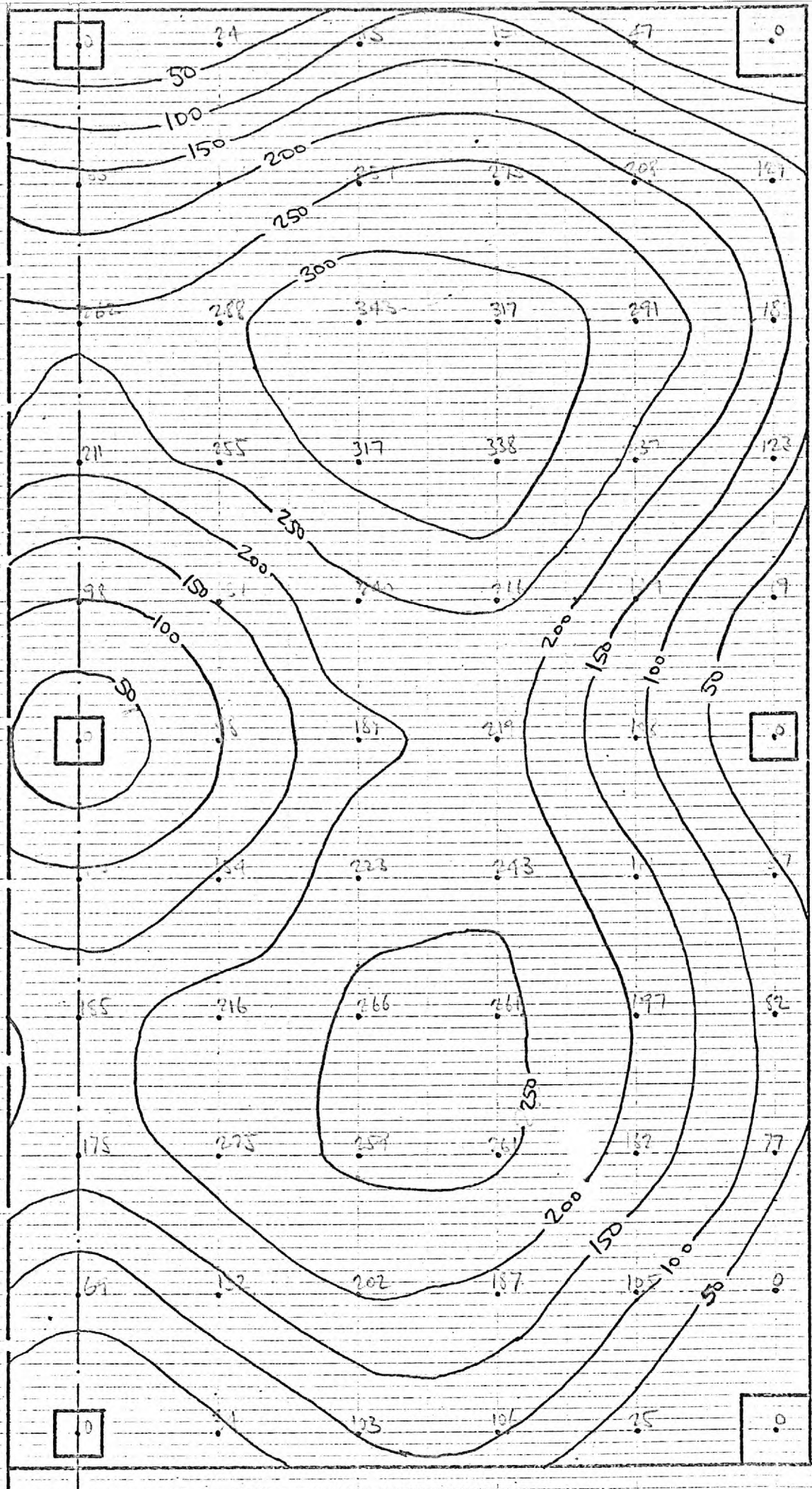


FIG. 78 - EQUAL DEFLECTION CONTOURS FOR 2/31/11

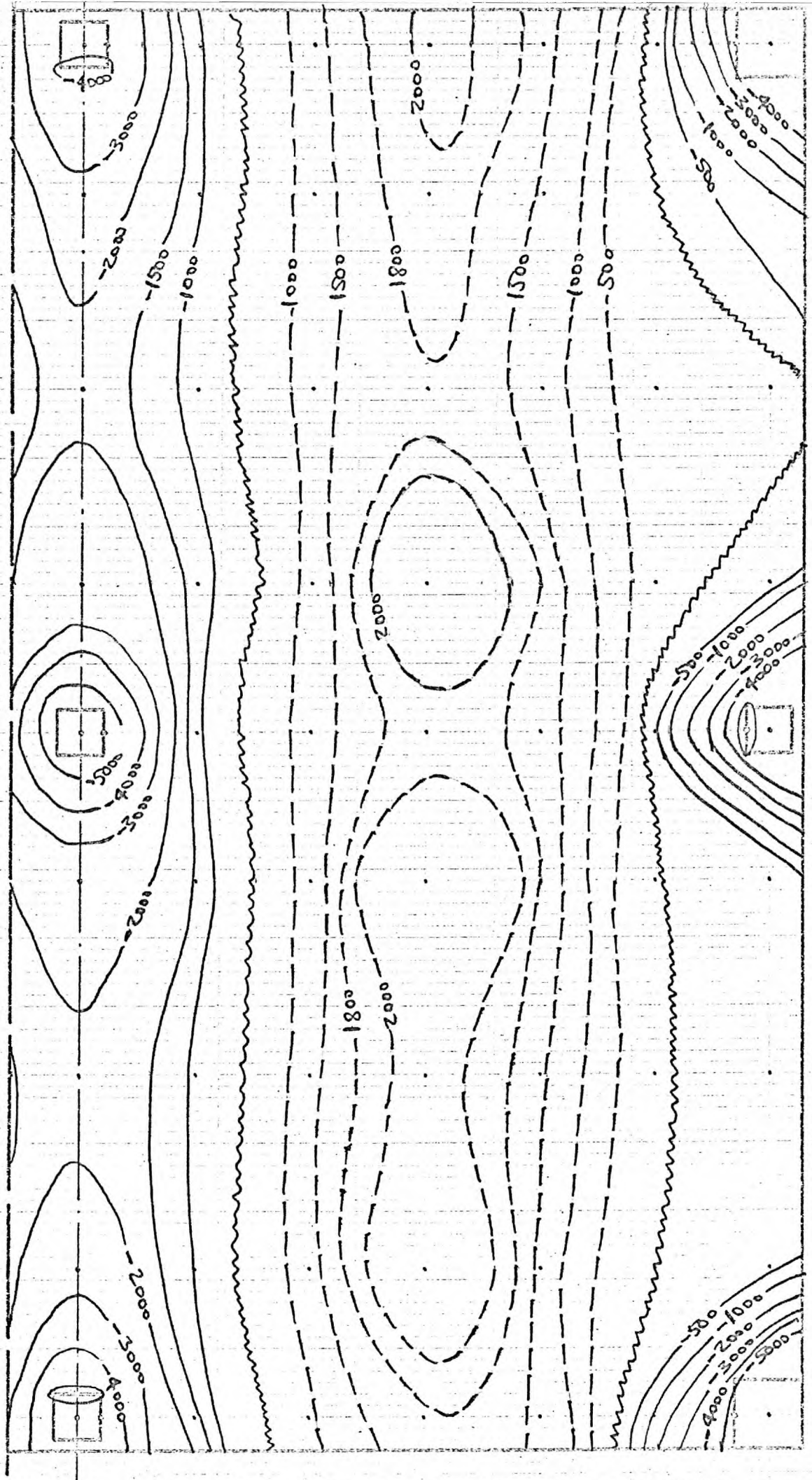


FIG. 79 - EQUAL MOMENT (M_2) CONTOURS FOR 2/32/2

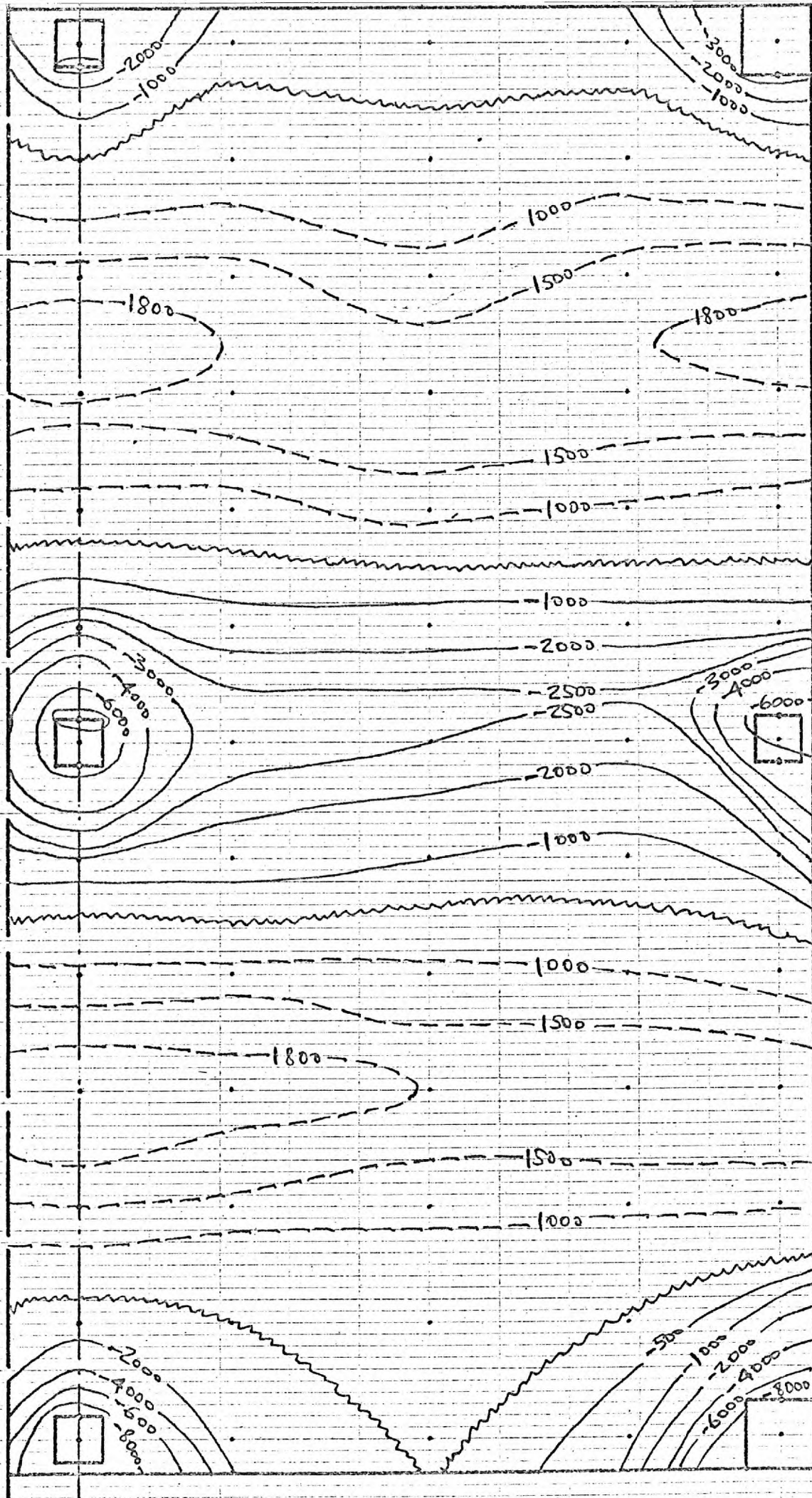


FIG. 80 - EQUAL MOMENT (M_y) CONTOURS FOR 2/32/2

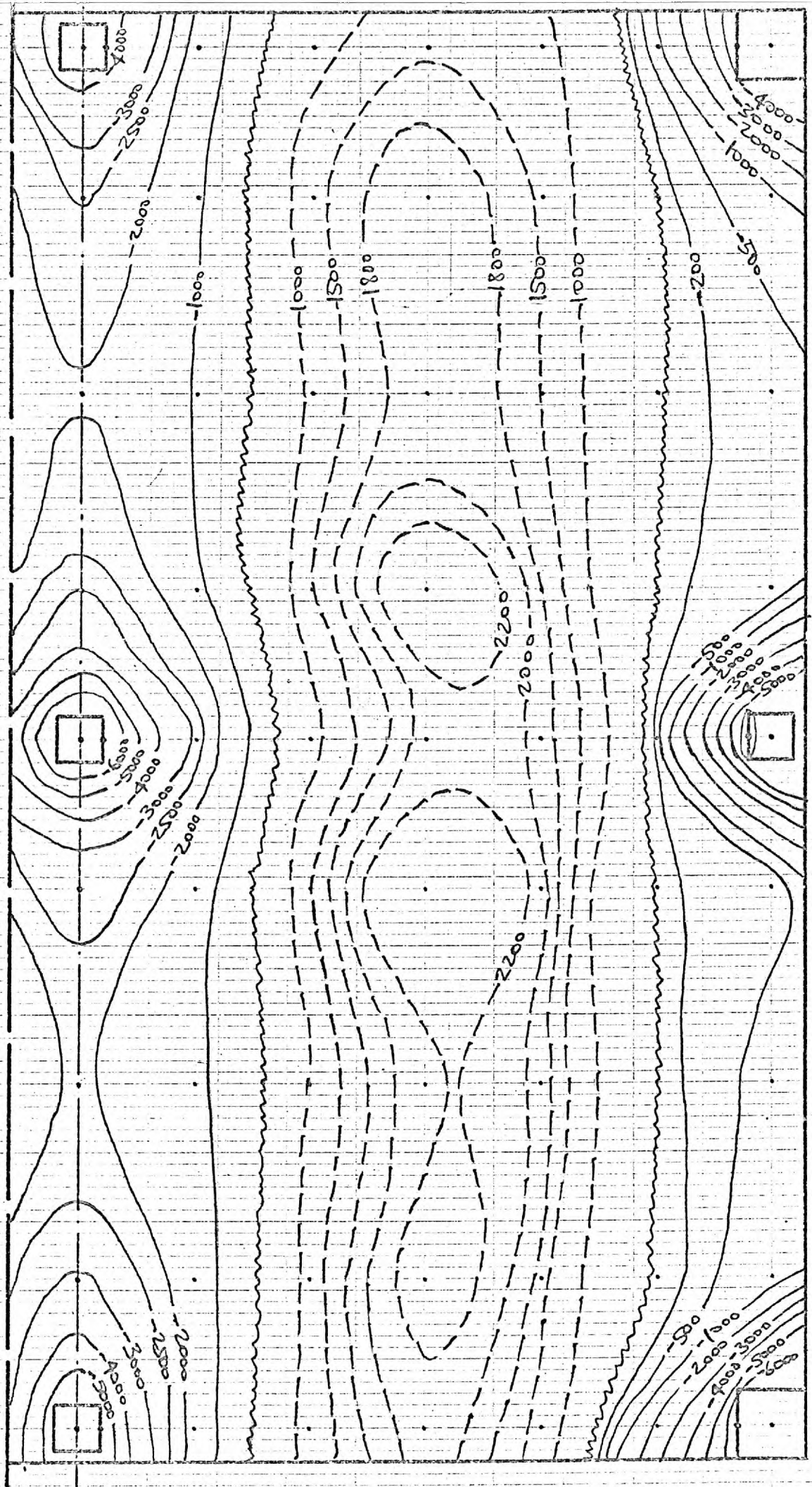


FIG. 82 - EQUAL MOMENT (M_x) CONTOURS FOR 2/32/8

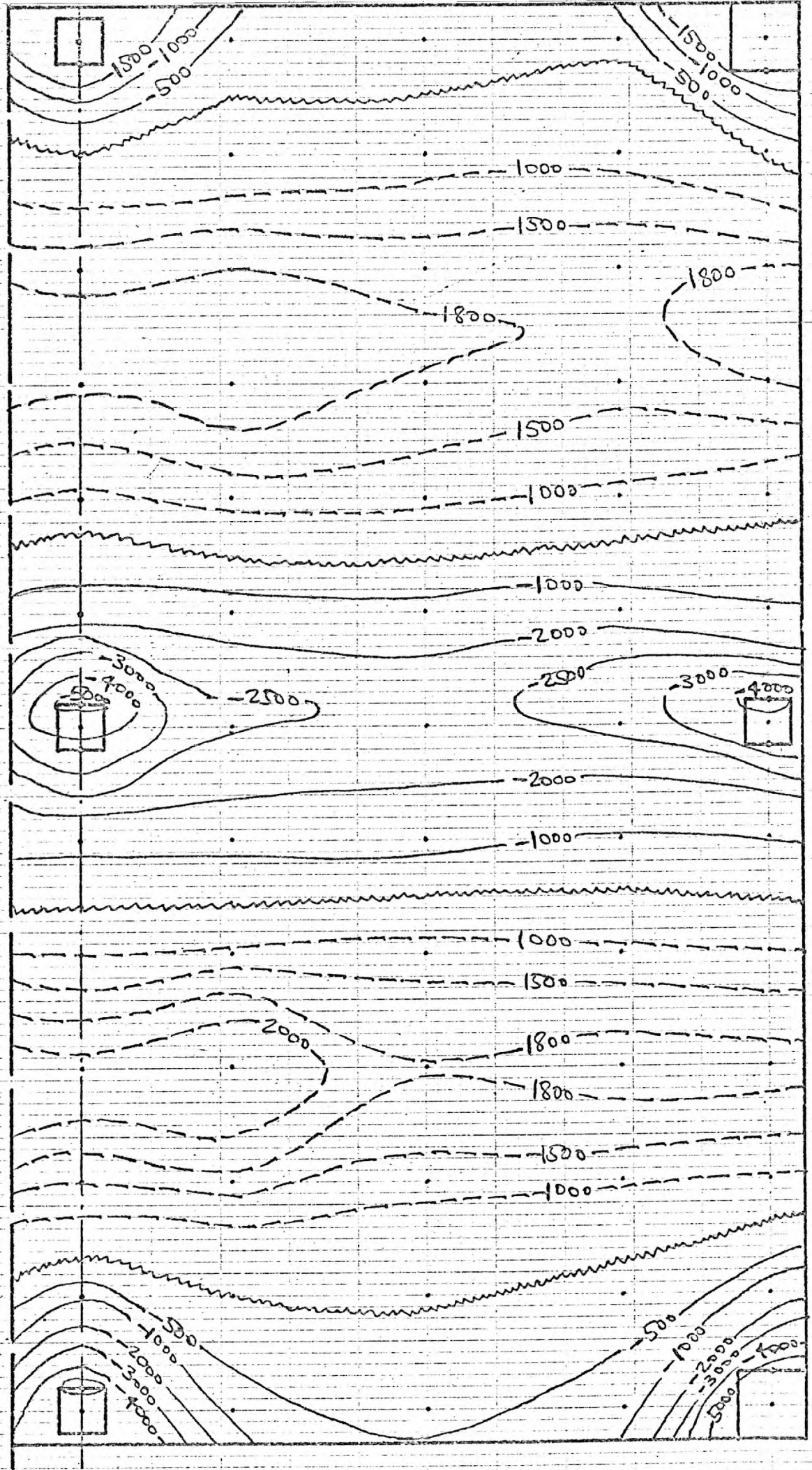


FIG. 83 - EQUAL MOMENT (M_j) CONTOURS FOR 2/32/8

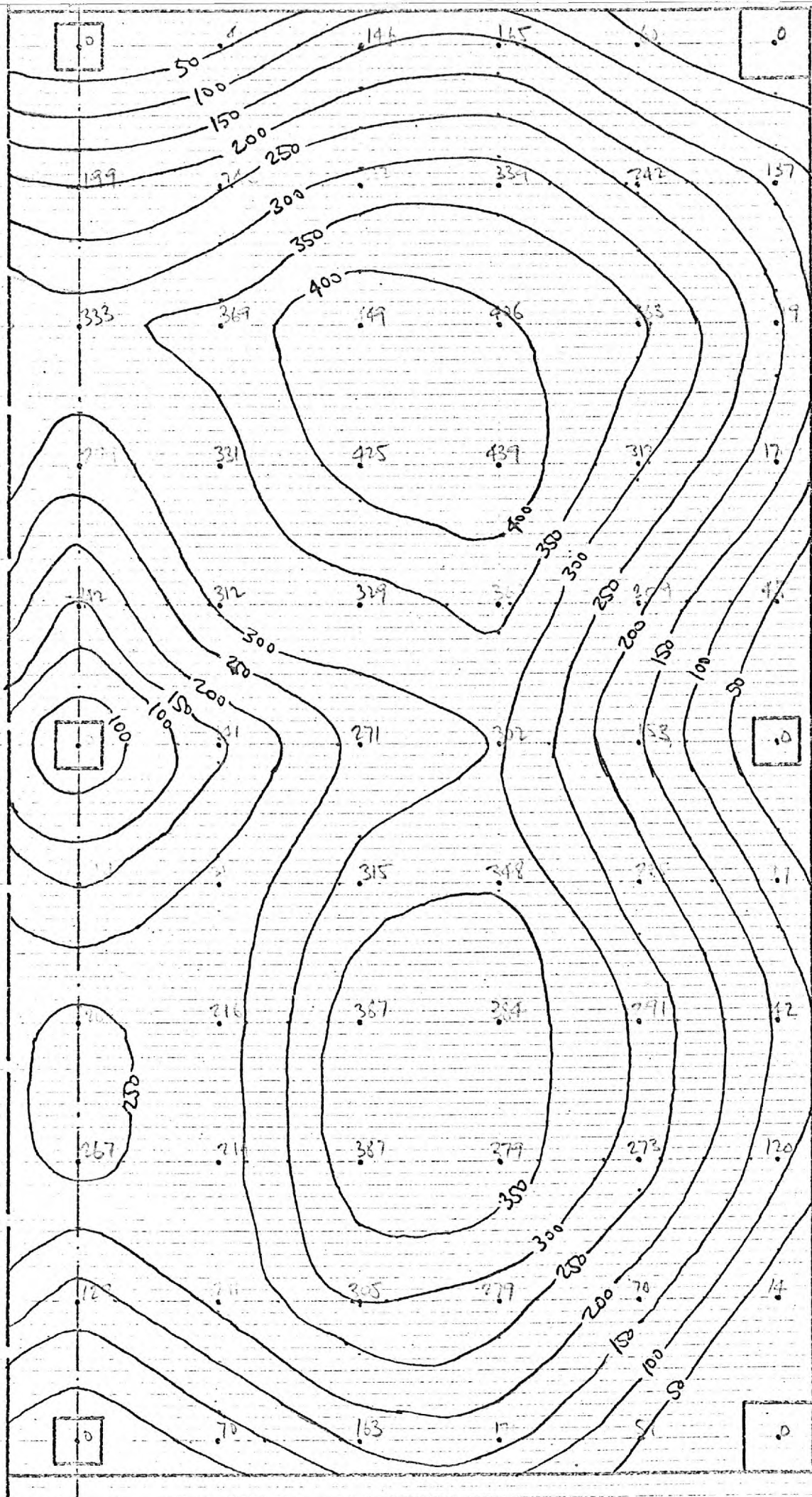


FIG. 84 - EQUAL DEFLECTION CONTOURS FOR 2/32/8

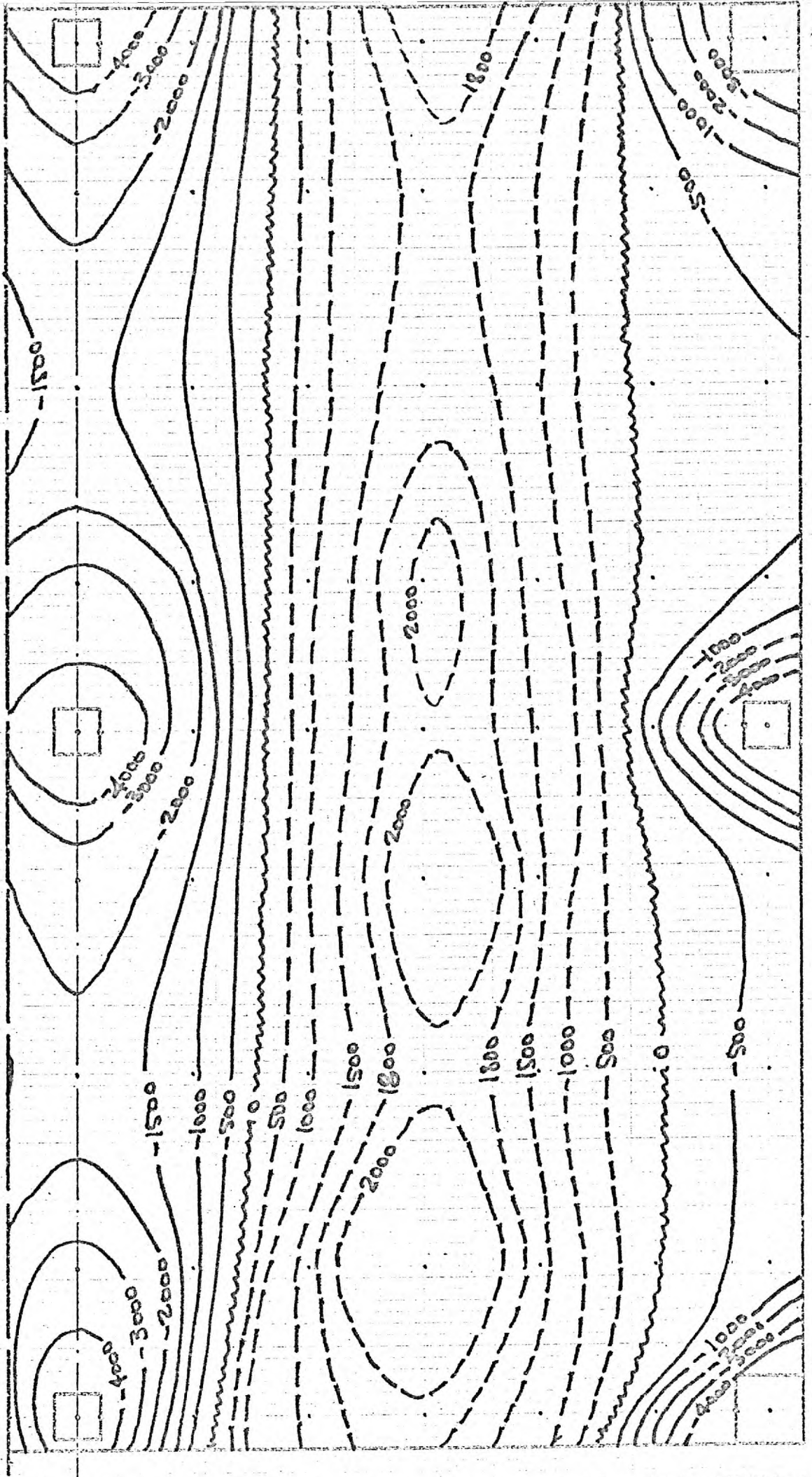


FIG. 85 - EQUAL MOMENT (M_z) CONTOURS FOR 2/32/11

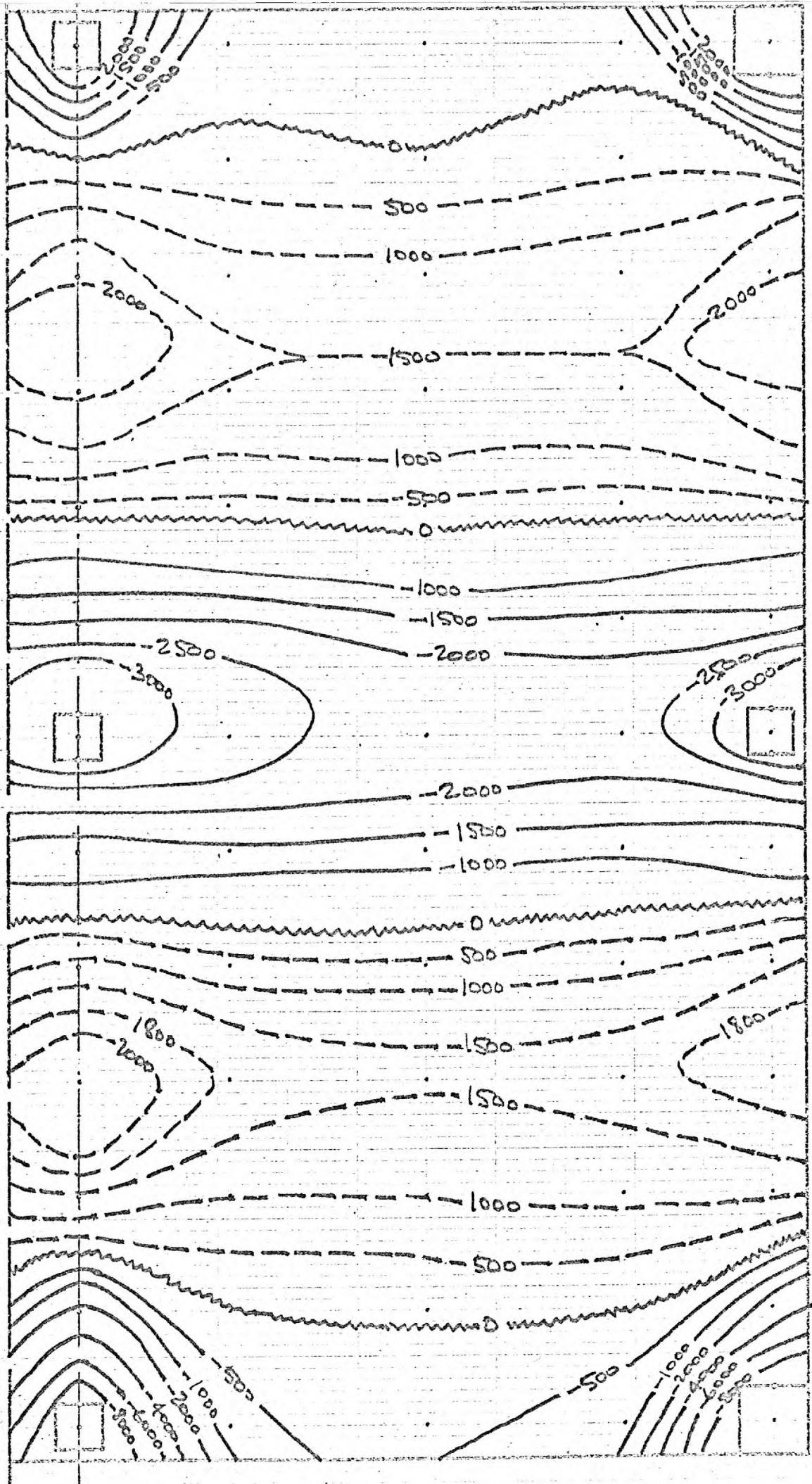


FIG. 86 - EQUAL MOMENT (M_y) CONTOURS FOR 2/32/11

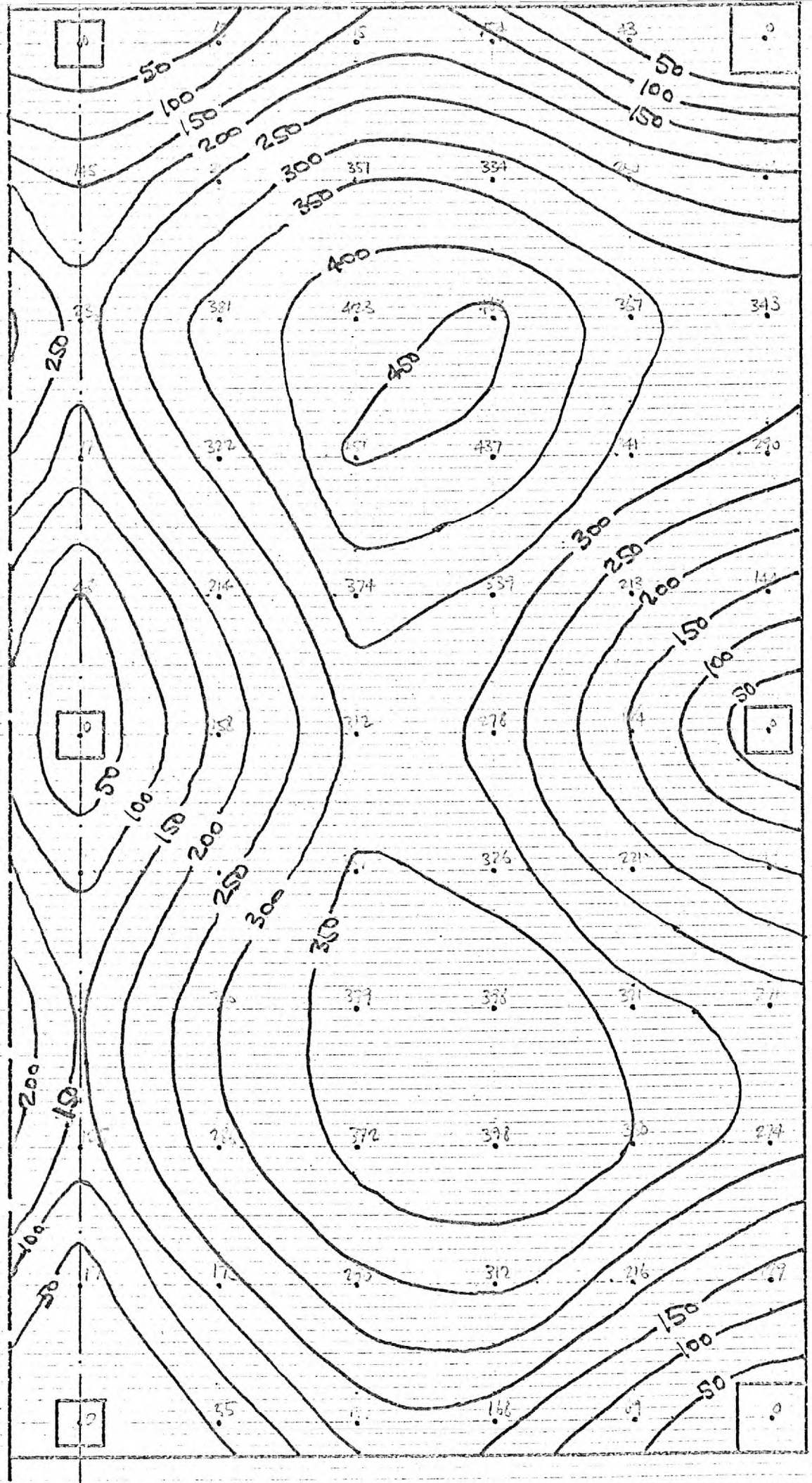


FIG. 87 - EQUAL DEFLECTION CONTOURS FOR 2/32/11

A P P E N D I X 2DETAILS OF THE STRIP BEAMS

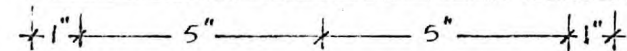
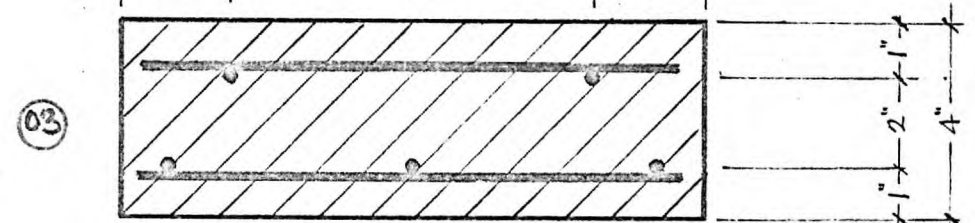
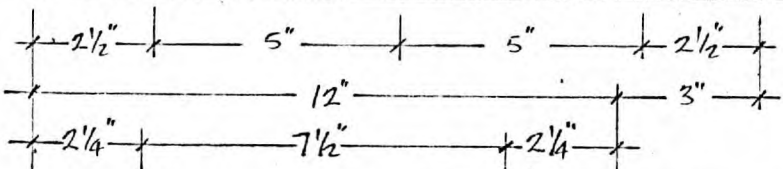
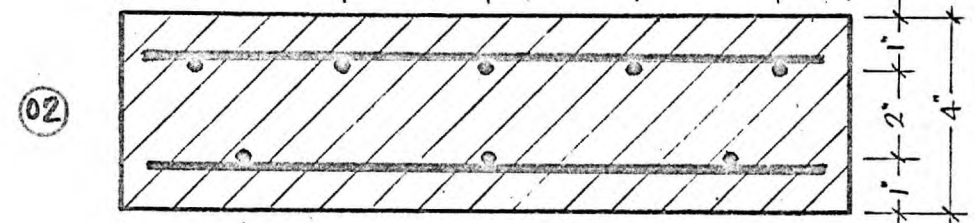
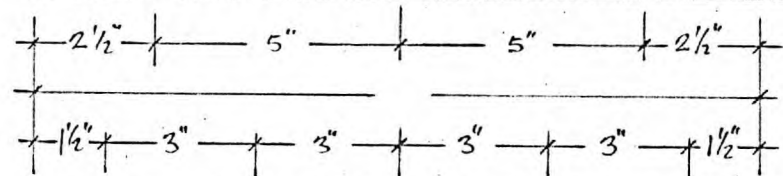
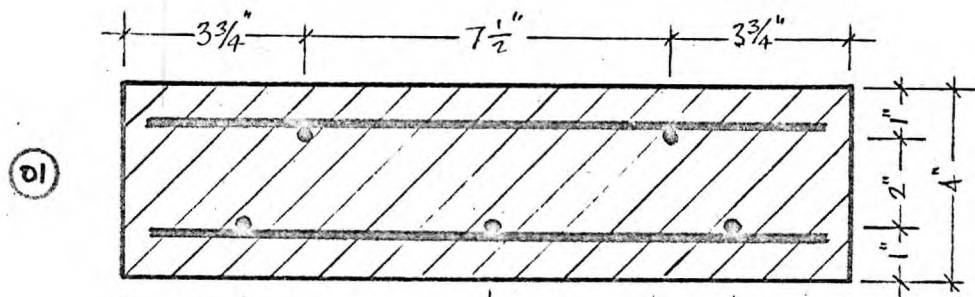
The use and the theory of strip beams are explained in Chapter 7. The related details are given in this appendix.

Altogether twenty strip beams were tested; two sets of three strip beams each served as preliminary investigation specimens, two sets of six were cast and tested with each test structure, and two odd ones which had been cast during the unsuccessful first trial of casting of the test structure 1. The sectional properties of each strip beam are given in Figs. 88, 89 and 90.

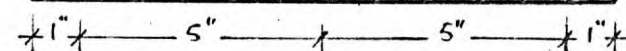
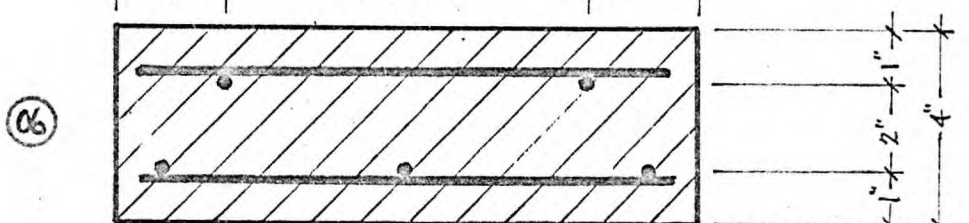
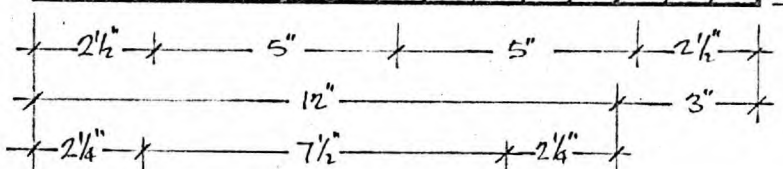
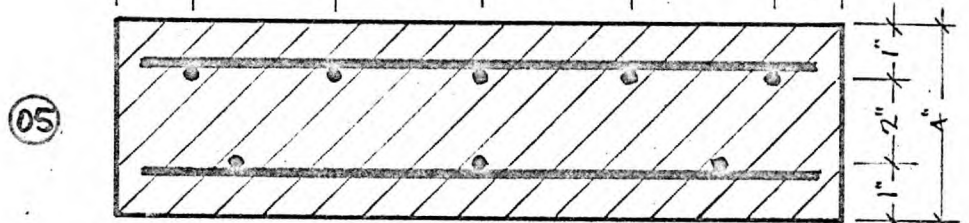
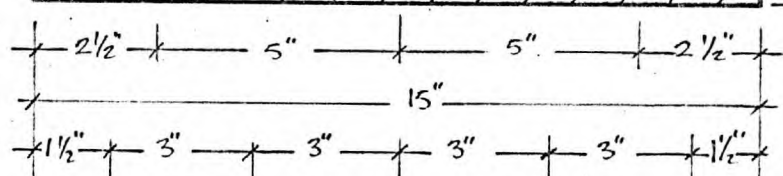
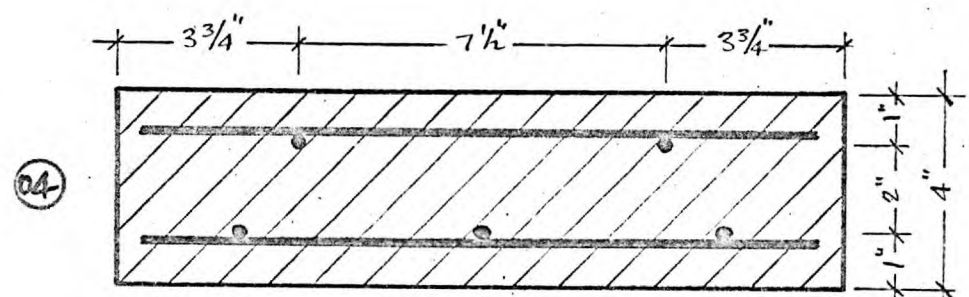
The first set of the preliminary beams were tested mainly to investigate the mechanical problems such as, the performance of the instruments used and the testing rig, the efficiency of the slot gauges in comparison with the conventional surface gauges, the rate of loading etc. The second set of preliminary strip beams were, on the other hand, used to study the behaviour of such beams; mainly the effect of compression reinforcement and the correction for beam width. To study the former problem, PB21 was compared with PB22, since they had the same sectional properties except the compression reinforcement. Similarly, the comparison of PB21 with PB23 served as a basis for the investigation of the latter; the only difference between these two beams was the beam width.

The variation of the compression reinforcement seemed to have very little effect on the general behaviour of the strip beam. A small correction was found useful for the strip beams which did not have the correct beam width corresponding to the reinforcement provided.

A typical set of (i) load-deflection, (ii) moment-steel strain, (iii) moment-curvature and (iv) moment-rotation relationship curves are given in Fig. 91. Table 24 summarizes the idealized moment-steel strain relationships for the beams used in the flexural analysis.



a. FIRST SET PRELIMINARY STRIP BEAMS



b. SECOND SET PRELIMINARY STRIP BEAMS

FIG. 88 - SECTIONAL PROPERTIES OF THE PRELIMINARY STRIP BEAMS

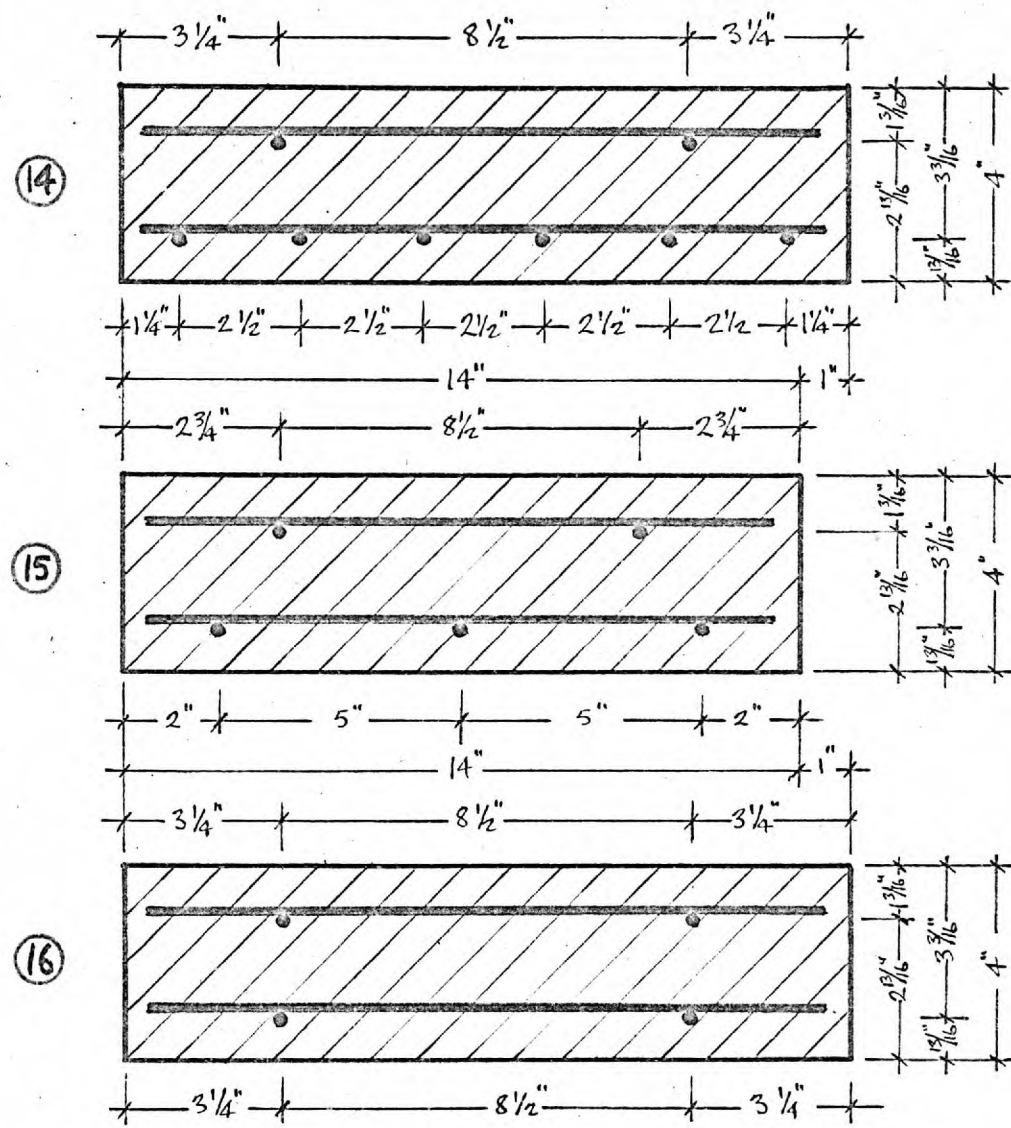
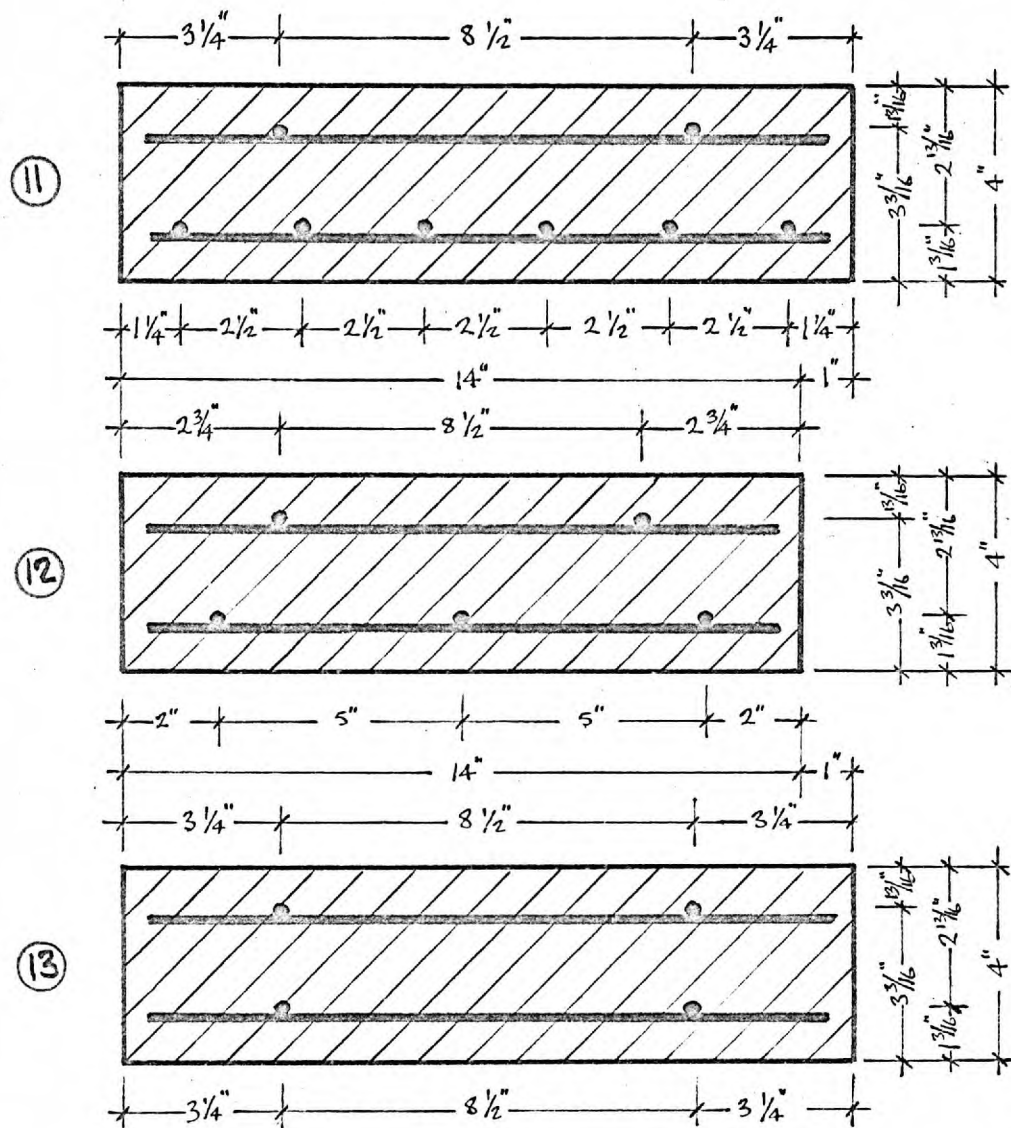


FIG. 89. SECTIONAL PROPERTIES OF THE STRIP BEAMS ACCOMPANYING THE TEST STRUCTURE I

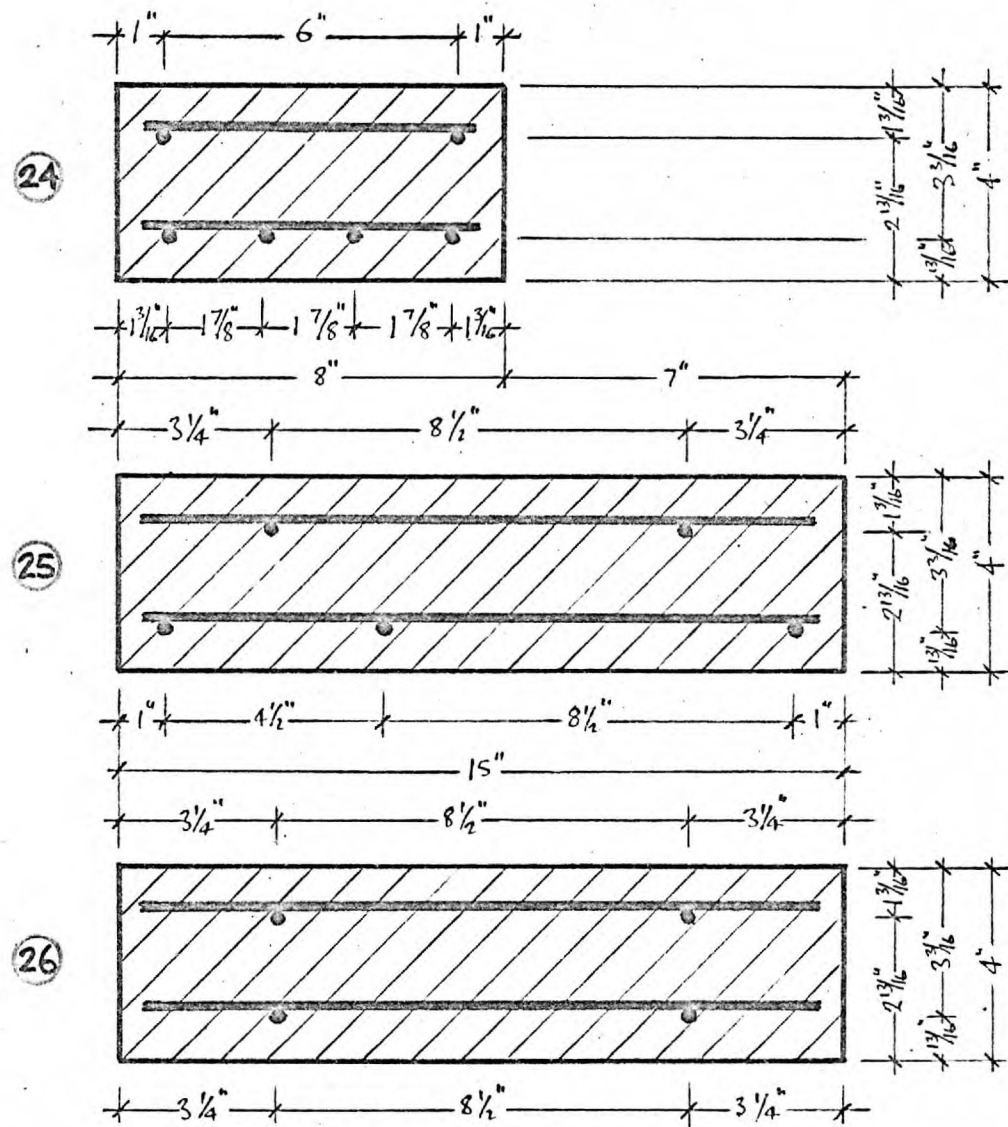
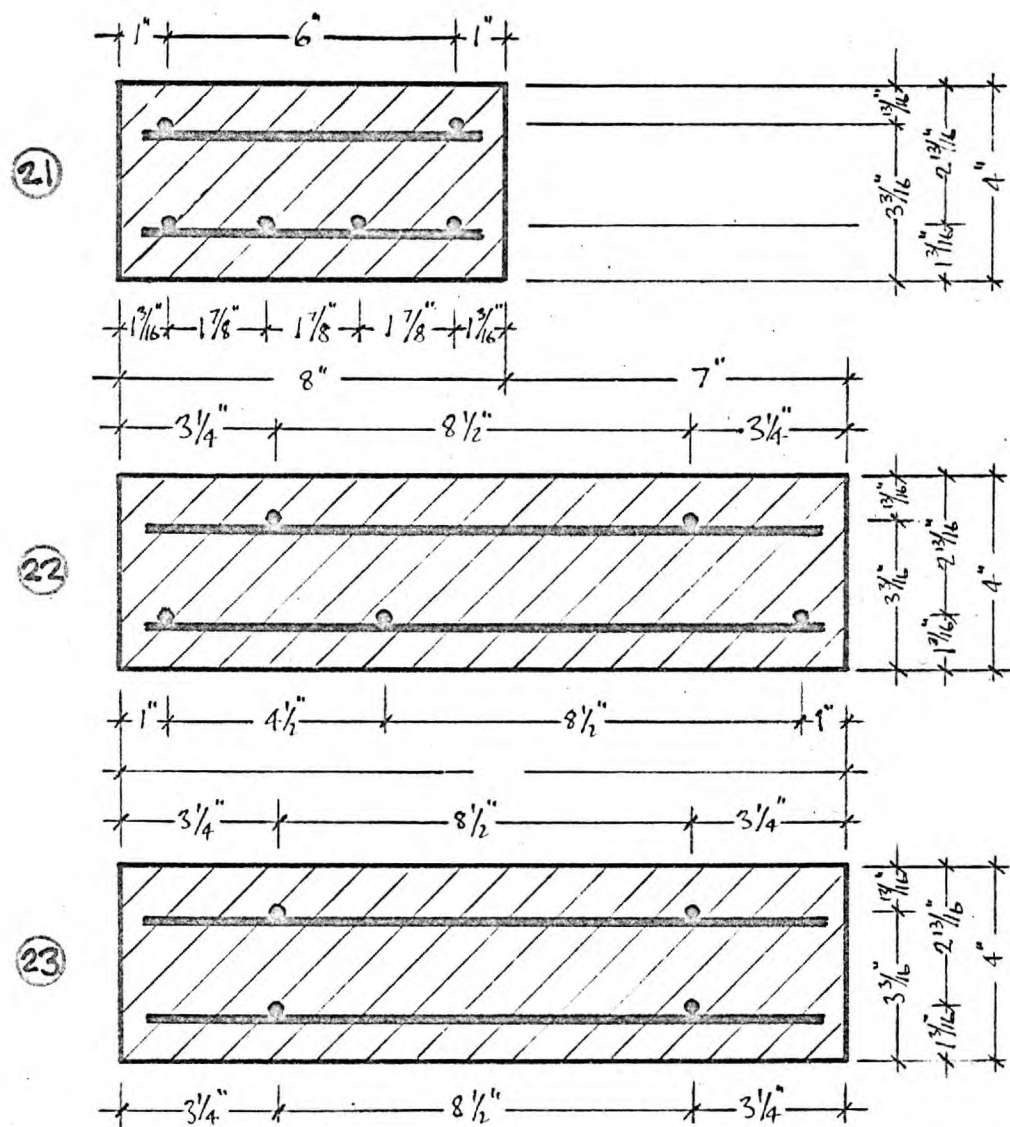


FIG. 90. SECTIONAL PROPERTIES OF THE STRIP BEAMS ACCOMPANYING THE TEST STRUCTURE 2

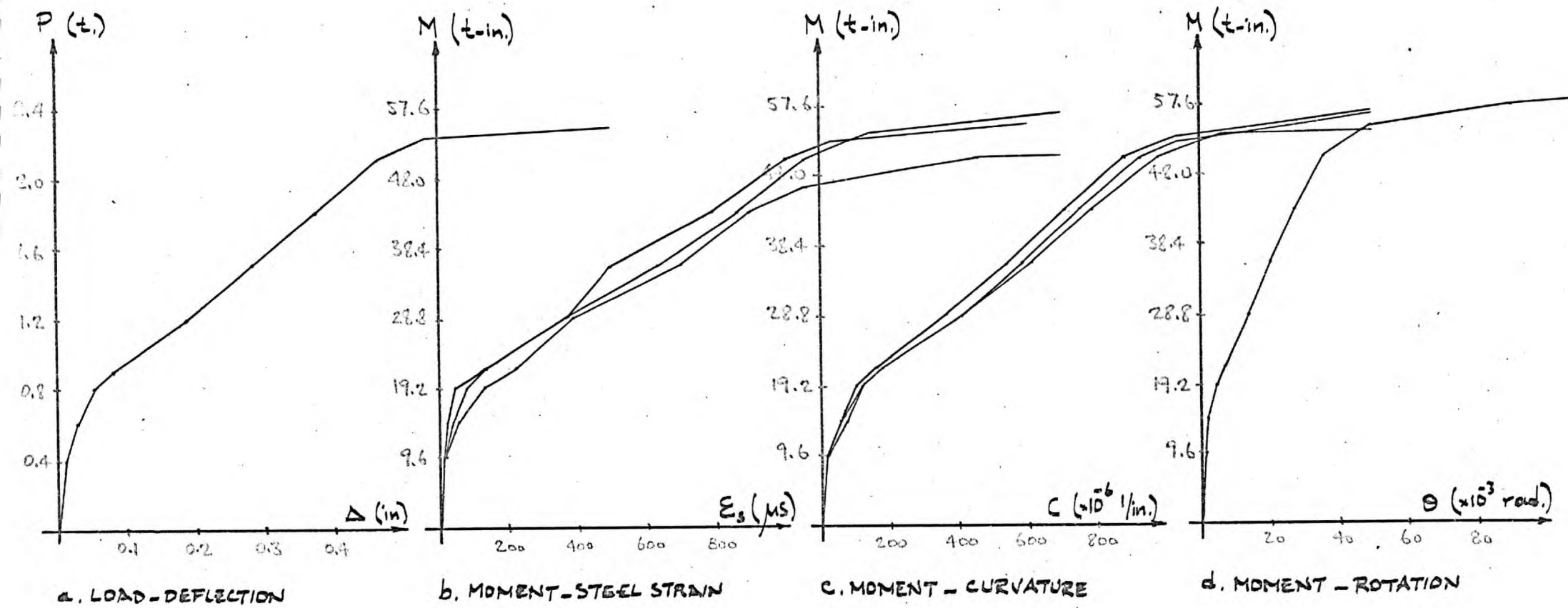


FIG. 91 - TYPICAL FLEXURAL RELATIONSHIPS FOR STRIP BEAMS (PB 21)

BEAM	STATE	$\epsilon_s \leq a$	a (μs)	$a \leq \epsilon_s \leq b$	b (μs)	$b \leq \epsilon_s$
11	UNCR'D	$M = 11.350 \epsilon_s$	125	$M = 896 + 4.18 \epsilon_s$	2360	$M = 10306 + 0.194 \epsilon_s$
	CRACKED	$M = 4.561 \epsilon_s$				
12	UNCR'D	$M = 22.080 \epsilon_s$	60	$M = 1209 + 1.936 \epsilon_s$	2500	$M = 5653 + 0.16 \epsilon_s$
	CRACKED	$M = 2.421 \epsilon_s$				
13	UNCR'D	$M = 14.635 \epsilon_s$	110	$M = 1480 + 1.183 \epsilon_s$	2985	$M = 4585 + 0.15 \epsilon_s$
	CRACKED	$M = 1.686 \epsilon_s$				
14	UNCR'D	$M = 21.355 \epsilon_s$	70	$M = 1075 + 5.973 \epsilon_s$	2165	$M = 13679 + 0.15 \epsilon_s$
	CRACKED	$M = 6.468 \epsilon_s$				
15	UNCR'D	$M = 24.000 \epsilon_s$	60	$M = 1285 + 2.56 \epsilon_s$	2750	$M = 7645 + 0.16 \epsilon_s$
	CRACKED	$M = 2.940 \epsilon_s$				
16	UNCR'D	$M = 23.744 \epsilon_s$	85	$M = 1895 + 1.445 \epsilon_s$	3100	$M = 5914 + 0.15 \epsilon_s$
	CRACKED	$M = 2.058 \epsilon_s$				
21	UNCR'D	$M = 52.00 \epsilon_s$	40	$M = 1838 + 6.04 \epsilon_s$	1400	$M = 8053 + 0.288 \epsilon_s$
	CRACKED	$M = 7.35 \epsilon_s$				
22	UNCR'D	$M = 53.67 \epsilon_s$	30	$M = 1564 + 1.55 \epsilon_s$	1300	$M = 3480 + 0.076 \epsilon_s$
	CRACKED	$M = 2.76 \epsilon_s$				
23	UNCR'D	$M = 50.34 \epsilon_s$	30	$M = 1482 + 0.94 \epsilon_s$	1565	$M = 2795 + 0.101 \epsilon_s$
	CRACKED	$M = 1.88 \epsilon_s$				
24	UNCR'D	$M = 32.35 \epsilon_s$	40	$M = 996 + 7.44 \epsilon_s$	1345	$M = 10232 + 0.573 \epsilon_s$
	CRACKED	$M = 8.18 \epsilon_s$				
25	UNCR'D	$M = 37.69 \epsilon_s$	40	$M = 1428 + 2.00 \epsilon_s$	1350	$M = 3973 + 0.115 \epsilon_s$
	CRACKED	$M = 3.05 \epsilon_s$				
26	UNCR'D	$M = 43.63 \epsilon_s$	35	$M = 1478 + 1.40 \epsilon_s$	1440	$M = 3353 + 0.098 \epsilon_s$
	CRACKED	$M = 2.43 \epsilon_s$				

TABLE 24. STRIP BEAM MOMENT-STEEL STRAIN RELATIONSHIPS

A P P E N D I X 3

PUNCHING SHEAR FORMULAE

As briefly explained in Chapter 7, the method suggested by J. Moe does not apply to the edge and corner columns as it is given in the text. It was therefore modified in its most general form, strictly on the same basis as the original derivation.

On the other hand, the method recommended by ACI-ASCE Joint Committee 426 suggests an expression for shear stress which considers column moment only in one direction. However, the method is based on the principle of superposition; therefore in the cases of moment in both directions, the formula had to be extended to cover them both, and the same value of the coefficient K was accepted for both moments. The polar moments of inertia of the critical sections were calculated for various types of columns and given in this appendix for easy reference.

3.1. GENERALIZED FORM OF MOE EQUATIONS - The ultimate punching strength of slab-column connections is given by

$$\bar{v} = \frac{15(1 - 0.075 \frac{r}{d}) \sqrt{f'_c}}{1 + 5.25 \frac{b_o d_1 \sqrt{f'_c}}{V_{flex}}} \quad \text{where}$$

r = equivalent column size

d_1 = effective depth of the slab

f'_c = cylinder strength of concrete

b_o = length of the critical section to be calculated at the column face

V_{flex} = shear force at ultimate flexural capacity

On the other hand, referring to Fig. 92, the shear stresses can be calculated as follows:

3.1.1. INTERNAL COLUMNS - The moment of inertia of the critical resisting section around its centroidal axis is given by

$$I_x = d_1 \left[2b \left(\frac{a}{2}\right)^2 + 2 \frac{a^3}{12} \right] = \frac{a^2 d_1}{6} (3b + a)$$

Then, the sectional modulus is

$$Z_x = \frac{I_x}{\frac{a}{2}} = \frac{ad_1}{3} (3b + a)$$

And similarly,

$$Z_y = \frac{bd_1}{3} (3a + b)$$

If the rule of superposition and the linear variation of shear stresses are assumed to hold true, then the maximum shear stress can be calculated as,

$$v = \frac{P}{2(a+b)d_1} + \frac{\beta M_x}{\frac{ad_1}{3} (3b+a)} + \frac{\beta M_y}{\frac{bd_1}{3} (3a+b)}$$

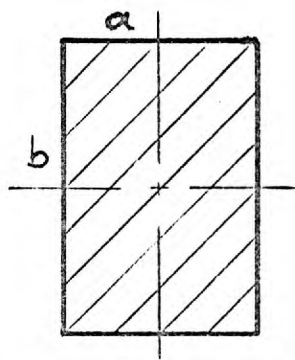
where β is the coefficient determining the amount of moment resisted by torsion. J. Moe recommends $\beta = \frac{1}{3}$, on the basis of data available.

Therefore,

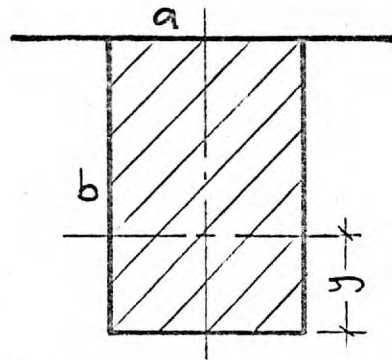
$$v = \frac{P}{2(a+b)d_1} \left[1 + \frac{2 e_x (a+b)}{a(3b+a)} + \frac{2 e_y (a+b)}{b(3a+b)} \right]$$

For the special case of square column,

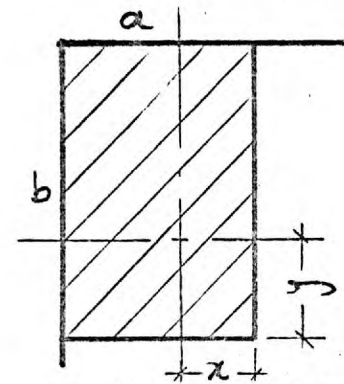
$$v = \frac{P}{4ad_1} \left[1 + \frac{e_x + e_y}{a} \right]$$



a. INTERNAL COLUMN

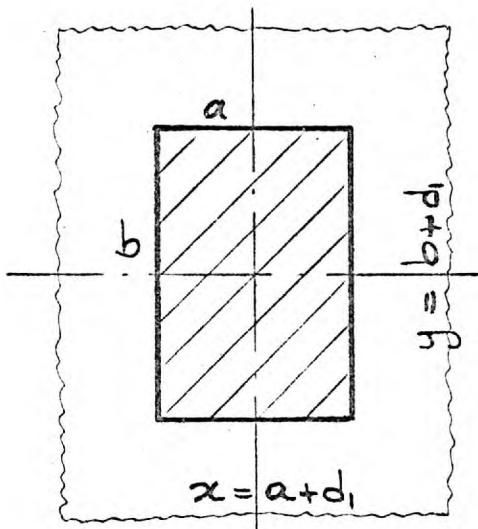


b. EDGE COLUMN

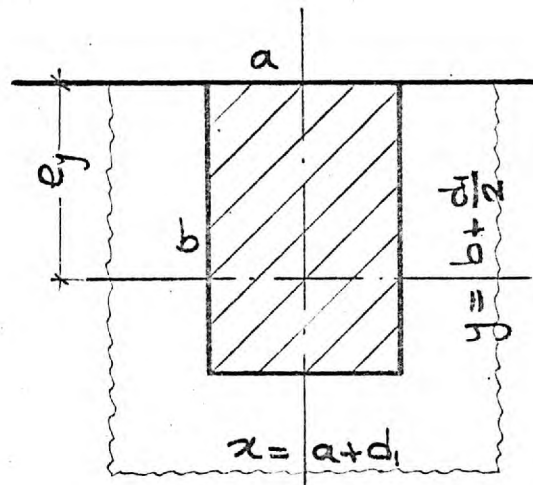


c. CORNER COLUMN

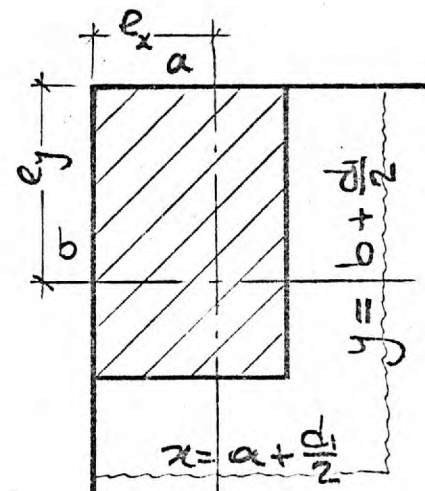
FIG. 92. CRITICAL SECTIONS FOR THE METHOD SUGGESTED BY J. MOE



a. INTERNAL COLUMN



b. EDGE COLUMN



c. CORNER COLUMN

FIG. 93. CRITICAL SECTIONS FOR THE ACI-ASCE JOINT COMMITTEE 426 METHOD

3.1.2. EDGE COLUMNS - For the moment acting parallel to the edge,

$$I_x = d_1 \left[2b \left(\frac{a}{2}\right)^2 + \frac{a^3}{12} \right] = \frac{a^2 d_1}{12} (6b + a)$$

$$\text{And } z_x = \frac{I_x}{\frac{a}{2}} = \frac{ad_1}{6} (6b + a)$$

For the moment acting perpendicular to the edge,

$$I_y = d_1 \left[2b \left(\frac{b}{2} - y\right)^2 + 2 \frac{b^3}{12} + ay^2 \right] \quad \text{where}$$

y is calculated as,

$$2b \frac{b}{2} = y(2b + a), \quad \text{or } y = \frac{b^2}{2b + a}$$

The sectional modulus then becomes,

$$z_y = \frac{I_y}{y} = \frac{bd_1}{3(2b + a)} \left[2b^2 + 2a^2 + 5ab \right]$$

Considering the same assumptions,

$$v = \frac{P}{(2b + a)d_1} + \frac{\gamma M_x}{\frac{ad_1}{6} (6b + a)} + \frac{\beta M_y}{\frac{bd_1}{3(2b + a)} [2b^2 + 2a^2 + 5ab]}$$

Due to the lack of any better information, it is assumed that $\gamma = \beta = \frac{1}{3}$.

Then

$$v = \frac{P}{(2b + a)d_1} \left[1 + \frac{2e_x (2b + a)}{a(6b + a)} + \frac{e_y (2b + a)^2}{b(2a^2 + 2b^2 + 5ab)} \right]$$

For $a = b$,

$$v = \frac{P}{3ad_1} \left[1 + \frac{e_y}{y} + \frac{6}{7} \frac{e_x}{a} \right]$$

3.1.3. CORNER COLUMNS - The location of centroidal axis of the resisting section is calculated by

$$x = \frac{a \frac{a}{2}}{a + b} = \frac{a^2}{2(a + b)}$$

Then, the moment of inertia and the sectional modulus respectively become,

$$I_x = d_1 \left[\frac{a^3}{12} + a\left(\frac{a}{2} - x\right)^2 + bx^2 \right] \quad \text{and}$$

$$Z_x = \frac{I_x}{x} = \frac{ad_1}{6} (4b + a)$$

Similarly, $Z_y = \frac{bd_1}{6} (4a + b)$

The maximum shear stress can then be expressed as,

$$v = \frac{P}{(a + b)d_1} + \frac{\delta M_x}{\frac{ad_1}{6} (4b + a)} + \frac{\delta M_y}{\frac{bd_1}{6} (4a + b)}$$

There is no reason why the assumption

$$\delta = \beta = \frac{1}{3}$$

should not be extended to this case. After this substitution the expression becomes,

$$v = \frac{P}{(a + b)d_1} \left[1 + \frac{2e_x (a + b)}{a(4b + a)} + \frac{2e_y (a + b)}{b(4a + b)} \right]$$

This can be simplified, for the case of square column, into

$$v = \frac{P}{2ad_1} \left[1 + \frac{4}{5} \cdot \frac{e_x + e_y}{a} \right]$$

3.2. FORMULAE FOR ACI-ASCE JOINT COMMITTEE 426 METHOD - The method is expressed in the following general form,

$$v = \frac{P}{b_o d_1} + K_x \frac{M_x}{J_x} C_x + K_y \frac{M_y}{J_y} C_y \leq 2\sqrt{f'_c}$$

where $K_x = K_y = 0.2$ or 0.4 as recommended by the committee itself and by Hanson and Hanson respectively. J_x , C_x , J_y and C_y can readily be calculated from the expressions presented in Table 25 with reference to Fig. 93. In this case e_x and e_y are not used to indicate the eccentricity $\frac{M}{P}$, but in the geometrical sense as illustrated in the figure.

COL. TYPE	VALUE	GIVEN BY
Z Z J J S S A A I I N T E R	x	$a+d_1$
	y	$b+d_1$
	b_0	$2(a+b+2d_1)$
	e_x	0
	e_y	0
	c_x	$\frac{1}{2}x$
	c_y	$\frac{1}{2}y$
	J_x	$\frac{1}{6}d_1x^3 + \frac{1}{6}yd_1^3 + \frac{1}{2}yd_1x^2$
	J_y	$\frac{1}{6}d_1y^3 + \frac{1}{6}xd_1^3 + \frac{1}{2}xd_1y^2$
	Z Z J J S S E D G E	x
y		$b+\frac{1}{2}d_1$
b_0		$2(b+d_1)+a$
e_x		0
e_y		$y(x+y)/(2y+x)$
c_x		$\frac{1}{2}x$
c_y		$y-e_y$
J_x		$\frac{1}{12}d_1x^3 + \frac{1}{6}yd_1^3 + \frac{1}{2}yd_1x^2$
J_y	$\frac{1}{6}d_1y^3 + \frac{1}{12}xd_1^3 + xd_1(y-e_y)^2 + 2yd_1(\frac{1}{2}y-e_y)^2$	
Z Z J J S S C O R N E R	x	$a+\frac{1}{2}d_1$
	y	$b+\frac{1}{2}d_1$
	b_0	$a+b+d_1$
	e_x	$x(2y+x)/2(x+y)$
	e_y	$y(2x+y)/2(x+y)$
	c_x	$x-e_x$
	c_y	$y-e_y$
	J_x	$\frac{1}{12}yd_1^3 + \frac{1}{12}d_1x^3 + yd_1(x-e_x)^2 + xd_1(\frac{1}{2}x-e_x)^2$
	J_y	$\frac{1}{12}xd_1^3 + \frac{1}{12}d_1y^3 + xd_1(y-e_y)^2 + yd_1(\frac{1}{2}y-e_y)^2$

TABLE 25 - EXPRESSIONS FOR THE TERMS REQUIRED FOR ACI-ASCE 426 METHOD